USGS
science for a changing world

Spatial and Stratigraphic Distribution of Water in Oil Shale of the Green River Formation Using Fischer Assay, Piceance Basin, Northwestern Colorado

Scientific Investigations Report 2013–5241

U.S. Department of the Interior
U.S. Geological Survey

Spatial and Stratigraphic Distribution of Water in Oil Shale of the Green River Formation Using Fischer Assay, Piceance Basin, Northwestern Colorado

By Ronald C. Johnson, Tracey J. Mercier, and Michael E. Brownfield

Scientific Investigations Report 2013–5241

U.S. Department of the Interior
U.S. Geological Survey

U.S. Department of the Interior
SALLY JEWELL, Secretary

U.S. Geological Survey
Suzette M. Kimball, Acting Director

U.S. Geological Survey, Reston, Virginia: 2014

Suggested citation:
Johnson, R.C., Mercier, T.J., and Brownfield, M.E., 2014, Spatial and stratigraphic distribution of water in oil shale of the Green River Formation using Fischer assay, Piceance Basin, northwestern Colorado: U.S. Geological Survey Scientific Investigations Report 2013–5241, 108 p., 1 pl., *http://dx.doi.org/10.3133/sir20135241*.

ISSN 2328-0328 (online)

Contents

Plate

Figures

Table

Spatial and Stratigraphic Distribution of Water in Oil Shale of the Green River Formation Using Fischer Assay, Piceance Basin, Northwestern Colorado

By Ronald C. Johnson, Tracey J. Mercier, and Michael E. Brownfield

Abstract

The spatial and stratigraphic distribution of water in oil shale of the Eocene Green River Formation in the Piceance Basin of northwestern Colorado was studied in detail using some 321,000 Fischer assay analyses in the U.S. Geological Survey oil-shale database. The oil-shale section was subdivided into 17 roughly time-stratigraphic intervals, and the distribution of water in each interval was assessed separately. This study was conducted in part to determine whether water produced during retorting of oil shale could provide a significant amount of the water needed for an oil-shale industry. Recent estimates of water requirements vary from 1 to 10 barrels of water per barrel of oil produced, depending on the type of retort process used. Sources of water in Green River oil shale include (1) free water within clay minerals; (2) water from the hydrated minerals nahcolite ($NaHCO_3$), dawsonite ($NaAl(OH)_2CO_3$), and analcime ($NaAlSi_2O_6{\cdot}H_20$); and (3) minor water produced from the breakdown of organic matter in oil shale during retorting. The amounts represented by each of these sources vary both stratigraphically and areally within the basin. Clay is the most important source of water in the lower part of the oil-shale interval and in many basin-margin areas. Nahcolite and dawsonite are the dominant sources of water in the oil-shale and saline-mineral depocenter, and analcime is important in the upper part of the formation. Organic matter does not appear to be a major source of water. The ratio of water to oil generated with retorting is significantly less than 1:1 for most areas of the basin and for most stratigraphic intervals; thus water within oil shale can provide only a fraction of the water needed for an oil-shale industry.

Introduction

The Eocene Green River Formation in the Piceance Basin of northwestern Colorado (fig. 1) contains the largest and most concentrated oil-shale deposit in the world, recently estimated at 1.525 trillion barrels of oil in place (Johnson and others, 2010). It is one of three basins in Colorado, Utah, and Wyoming that contains large deposits of oil shale in the Eocene Green River Formation (fig. 2). The Piceance Basin is a structural and sedimentary basin that formed during the Laramide orogeny from Late Cretaceous through Eocene time with the structurally deepest part of the basin in the north-central part (fig. 3).

Two methods currently are being developed for the extraction of oil from oil shale: (1) conventional methods where the oil shale is mined and processed in surface retorts, and (2) in situ methods where the oil shale is heated in place, typically with electric heaters. A conventional surface retort industry would require water for site preparation, mining, crushing, dust suppression, retorting, shale-oil upgrading, reclamation, drilling, and generation of electricity. In-situ retorting requires water for construction, drilling, dust suppression, reclamation, and power generation used to run the electric heaters. Recent estimates of water needs for conventional mining and surface retorting include (1) from 1 to 3 barrels of water per barrel [1 barrel = 42 gallons] of oil produced (Cameron and others, 2006), and (2) from 2 to 5 barrels of water per barrel of oil (Bartis and others, 2005). Water requirements for the in situ processes at present are not well known. Boak and Mattson (2009) estimated that these processes could require any amount from 1 to 10 barrels of water for each barrel of oil produced. Additional water would be required to support the increase in population related to oil-shale development.

The Piceance Basin largely is a semiarid region with limited local surface water and groundwater supplies, and water resources in many of the major nearby river basins, including those of the Colorado, Gunnison, and White Rivers, are "over-appropriated" (Crawford and others, 2009). This shortage of water long has been a concern to developing an oil-shale industry in the basin. Green River oil shales contain water locked up in organic matter, minerals, and pore spaces that is released upon retorting, and it has been suggested that such water could help ease some of the water concerns. Produced water contains contaminants including carbon dioxide (CO_2), hydrogen sulfide (H_2S), and various organic compounds; recent experiments have tested the feasibility of upgrading that water so it could be used for oil-shale extraction and possibly in the electric power industry (Ryan and others, 2009).

Here, we present a comprehensive study of the amount of water that is locked up in the oil shale in the Piceance Basin. This study uses some 321,000 Fischer assay analyses available for the basin in the U.S. Geological Survey (USGS) oil-shale database. The Fischer assay method, a standardized laboratory test for

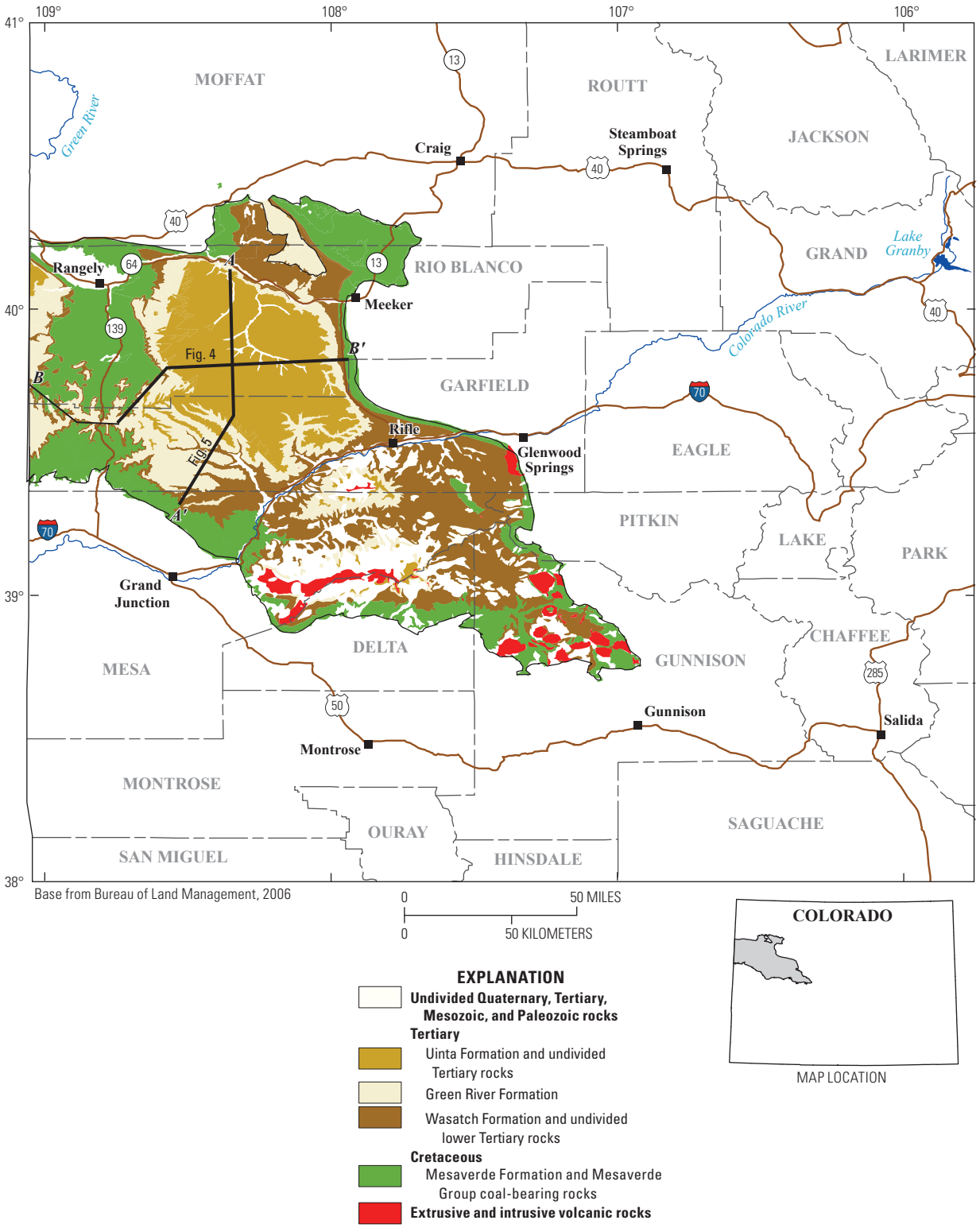

Figure 1. Piceance Basin, northwestern Colorado, showing Upper Cretaceous and lower Tertiary stratigraphic units. Extent of the Piceance Basin is the same as the Uinta-Piceance Province boundary (USGS Uinta-Piceance Assessment Team, 2003). Locations of cross sections of figures 4 and 5 are shown. Modified after Tweto (1979).

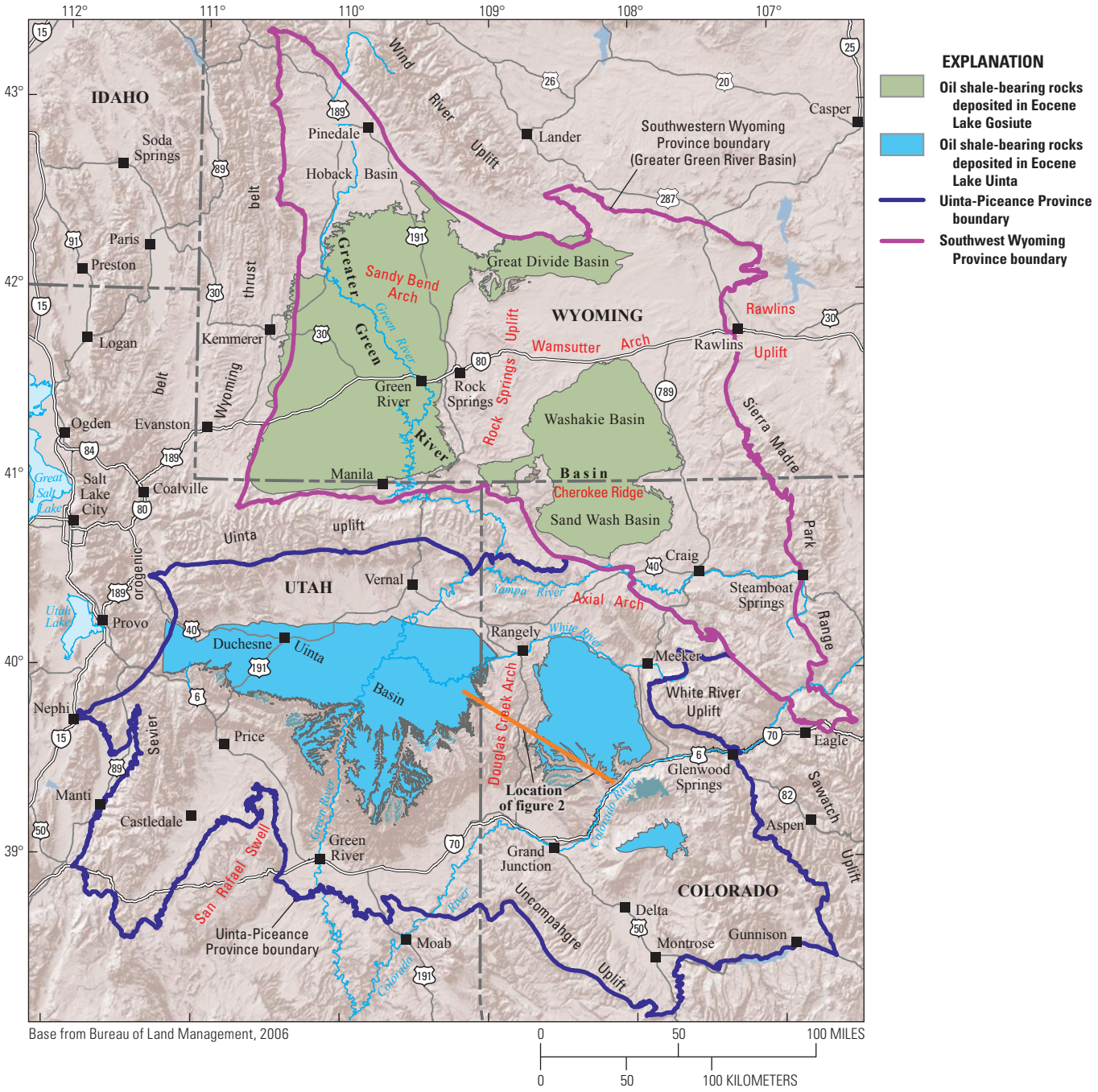

Figure 2. Extent of Uinta (Utah) and Piceance Basins (Colo.), the Greater Green River Basin (Wyo.), and approximate extent of oil shale in the Green River Formation. Extent of the Uinta and Piceance Basins is the same as the Uinta-Piceance Province boundary (USGS Uinta-Piceance Assessment Team, 2003). Extent of the Greater Green River Basin is the same as the Southwestern Wyoming Province boundary (USGS Southwestern Wyoming Province Assessment Team, 2005). For the extent of oil shale in the Piceance Basin, the base of the Parachute Creek Member of the Green River Formation as mapped by Tweto (1979) was used for all but the northwestern part of the basin, where the base of the lower member of the Green River Formation was used. For the extent of oil shale in the eastern part of the Uinta Basin, the base of the Parachute Creek Member of the Green River Formation, as mapped by Cashion (1973) and Rowley and others (1985), was used. In the western part of the basin, the top of the Mahogany oil-shale bed as mapped by Witkind (1995) was used. In the northern part of the Uinta Basin, only those areas where oil shale occurs at a depth of 6,000 ft or less are shown. This area was determined using a structure contour map of the top of the Mahogany oil-shale bed compiled by Johnson and Roberts (2003). For the Sand Wash, Washakie, Great Divide, and southeastern parts of the Green River Basin, the base of the Tipton Shale Member of the Green River Formation as mapped by Tweto (1979) and Love and Christiansen (1985) was used as the extent of oil shale. For the western part of the Green River Basin, the base of the Wilkins Peak Member of the Green River Formation, and for the northern part of the Green River Basin, the base of the Laney Shale Member of the Green River Formation as mapped by Love and Christiansen (1985) were used.

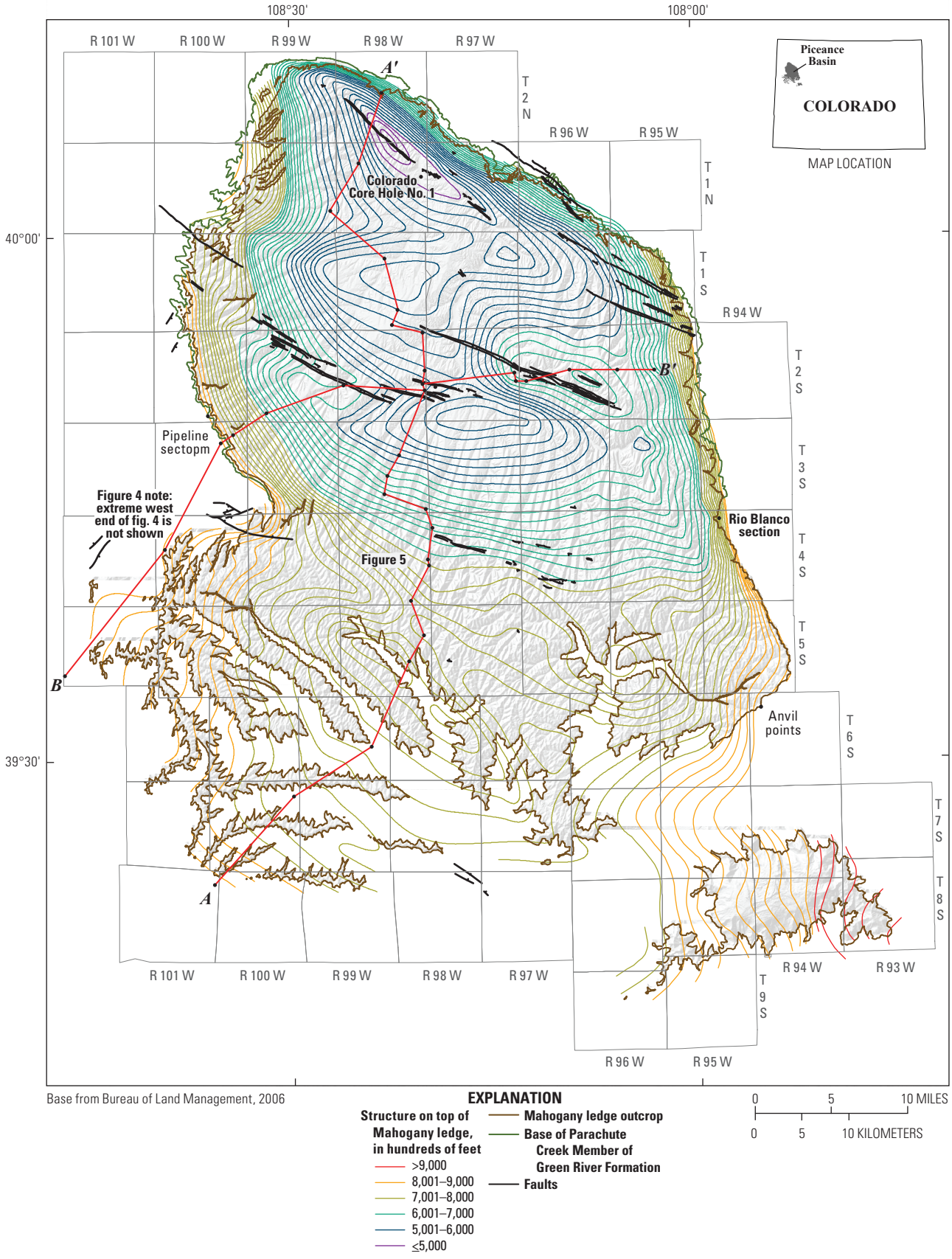

Figure 3. Top of the Mahogany oil-shale zone, Piceance Basin, Colo. Digitized from Hail and Smith (1994, 1997). Locations of cross sections of figures 4 and 5, as well as some surface localities mentioned in text, are shown.

determining the oil yield from oil shale, has been used almost universally to determine oil yields for Green River Formation oil shales (Stanfield and Frost, 1949; American Society for Testing Materials [ASTM], 1984). The standard Fischer assay method consists of heating a crushed and screened –8 (2.38-mm)-mesh, 100-gram sample in a small aluminum retort to 500 °C at a rate of 12 °C per minute and then holding the sample at that temperature for 40 minutes. The volatile vapors of shale oil, gas, and water pass through a condenser cooled (to about 5 °C) with ice water and are collected in a graduated centrifuge tube. The oil and water are then separated by centrifuging and weighed. Quantities reported for the original sample are the weight percentages of shale oil, water, shale residue (contains carbon char), and "gas plus loss" (noncondensable gas yield) by difference. The specific gravity of the shale oil is measured and used to calculate the oil yield in gallons per ton (GPT).

Johnson and others (2010) recently assessed the in-place oil-shale resources of the Piceance Basin from this Fischer assay database using the Radial Basis Function (RBF) method to generate resource maps and to estimate resources. Due to the number of data records and the complexity of the spatial data involved in the assessment, Microsoft Access database-management software and Esri ArcGIS software were used to combine, store, and analyze the raw data. (A complete description of that database and how to use it is presented in Mercier and others, 2010.) Johnson and others (2010) generated four maps for each of the 17 oil-shale zones that they assessed: (1) an isopach map, (2) a map showing variations in oil yield in GPT, (3) a map showing variations in barrels of oil per acre (BPA), and (4) a map showing total in-place oil in each township in the basin. As both oil and water contents from Fischer assays were included in the Access table, it was a fairly straightforward process to substitute water for oil in the queries that produced the resource maps and resource calculations. Table 1 lists the average gallons of water per ton of oil shale (GPTW) and gallons of water per acre (GPAW) for each of the 17 oil-shale zones in all the core holes used in the assessment using the same methodology and calculations described in Johnson and others (2010) and Mercier and others (2010). Two additional sets of maps are presented here for each of the 17 oil-shale zones assessed by Johnson and others (2010): (1) variations in GPTW, and (2) variations in GPAW. The GPTW also displays a bubble at each control point, sized proportionally to the ratio of water-to-oil generated. As previously discussed, the ratio is commonly used when estimating water requirements for an oil-shale industry.

Geology of the Oil-Shale Deposit in the Piceance Basin

The Green River Formation was deposited in Eocene Lake Uinta, a large, internally drained saline lake that extended across the Piceance Basin, the Uinta Basin to the west, and the intervening Douglas Creek arch (fig. 4). Large amounts of oil shale also were deposited in the Green River Formation in another largely contemporary saline lake, Lake Gosiute in the Greater Green River Basin to the north (fig. 2). The term oil shale is somewhat of a misnomer in that it does not contain oil but rather kerogen, a hydrogen-rich type of organic matter that will convert to oil at high temperatures. Although the Piceance Basin is much smaller than the Uinta Basin to the west and the Greater Green River Basin to the north, it contains the largest in-place resource of oil shale and thus is a much more concentrated deposit. A nearly continuous oil-shale section about 2,000 ft thick is present in the central part of the basin (figs. 4 and 5). This contrasts with the oil-shale intervals in the Uinta Basin to the west and the Greater Green River Basin to the north where much of the oil-shale interval is interbedded with kerogen-poor sandstone, siltstone, claystone, and limestone even in the central parts of those basins.

Lake Uinta formed when two smaller fresh-water lakes, one in the Piceance Basin and one in the Uinta Basin, expanded and coalesced across the Douglas Creek arch to form one large saline lake (Johnson, 1985). Salinity appears to have increased throughout the early history of the lake, first killing off the fresh-water molluscan fauna present in the previous fresh-water lakes and ultimately leading to precipitation of vast quantities of the sodium bicarbonate mineral nahcolite ($NaHCO_3$), the sodium-aluminum-carbonate mineral dawsonite ($NaAl(OH)_2CO_3$), and halite (NaCl). Nahcolite precipitated due to the high partial pressure of CO_2 in the lake and interstitial waters (Bradley and Eugster, 1969), and dawsonite, an authigenic mineral, probably formed as a result of the dissolution of silicate minerals in the highly alkaline interstitial waters (Hite and Dyni, 1967; Dyni, 1981). Nahcolite, dawsonite, and halite were deposited in the saline depocenter (fig. 6) of Lake Uinta in the north-central part of the basin, and that depocenter remained in approximately the same place throughout saline-mineral deposition (Brownfield and others, 2010). Nahcolite is used as a raw material in the manufacture of a variety of basic industrial chemicals, such as baking soda, and in the removal of sulfur dioxide from power-plant emissions; dawsonite can be used as a source of aluminum. Overall, the saline depocenter corresponds closely with the area containing maximum in-place oil-shale resources (fig. 6) near the structurally deepest part of the basin (fig. 3). The area where maximum oil-shale resources were being deposited, however, shifted with time. During saline-mineral deposition, the oil-shale depocenter occupied roughly the same area as the saline-mineral depocenter, but for some periods prior to saline-mineral deposition the oil-shale depocenter was farther to the south. After the end of saline-mineral deposition, the oil-shale depocenter occupied a much larger area than the saline depocenter, extending well into the southeastern part of the basin (Johnson and others, 2010). Illite-rich oil shale was deposited in offshore areas during the early, less saline period, whereas dolomite-rich oil shale dominated once saline-mineral precipitation began. The name Garden Gulch Member is applied to the illitic oil shales, and the name Parachute Creek Member is applied to the dolomitic oil shales. The oil-shale interval grades towards the basin margins into marginal lacustrine rocks of the Anvil Points and Douglas Creek Members of the Green River Formation (figs. 4 and 5). The relation between the marginal and offshore lacustrine facies is complex; for a more complete discussion see Johnson and others (2010).

Table 1. Total oil in place, water in place, and water-to-oil ratios for each of the 17 oil-shale zones in the Piceance Basin, Colo. Water in nahcolite for each zone (from Brownfield and others, 2010) also is listed, and water-to-oil ratios were calculated for nahcolite-free oil shale.

[The R-5 and L-5 zones (shaded red) have thick nahcolite beds that were not assessed with Fischer assay, and the water content is underestimated in those zones]

Oil shale zone	Oil in place (barrels)	Total water (gallons)	Total water (barrels)	Water to oil ratio	Tons nahcolite	Tons water in nahcolite	Gallons water in nahcolite	Gallons water not from nahcolite	Barrels water not from nahcolite	Water to oil ratio exc. nahcolite	Percent water from nahcolite
Top A-groove-top bed 44	186,467,922,130	1,998,106,673,820	47,573,968,424	0.26				1,998,106,673,820	47,573,968,424	0.26	
A-groove	6,283,095,737	82,625,917,016	1,967,283,738	0.31				82,625,917,016	1,967,283,738	0.31	
Mahogany zone	191,716,681,060	1,041,608,945,649	24,800,212,992	0.13				1,041,608,945,649	24,800,212,992	0.13	
B-groove	7,819,053,970	180,017,089,140	4,286,121,170	0.55				180,017,089,140	4,286,121,170	0.55	
R-6	185,366,007,632	1,483,898,265,214	35,330,911,077	0.19				1,483,898,265,214	35,330,911,077	0.19	
L-5	66,063,806,739	925,448,082,043	22,034,478,144	0.33	851,799,000	91,142,493	21,864,577,865	903,583,504,178	21,513,892,957	0.33	2.36
R-5	198,239,468,346	2,171,609,181,340	51,704,980,508	0.26	12,901,712,000	1,380,483,184	331,170,248,638	1,840,438,932,702	43,819,974,588	0.22	15.25
L-4	69,126,949,762	1,110,976,025,839	26,451,810,139	0.38	10,100,180,000	1,080,719,260	259,258,548,159	851,717,477,679	20,278,987,564	0.29	23.34
R-4	127,150,178,615	1,344,462,390,313	32,011,009,293	0.25	6,856,834,000	733,681,238	176,006,054,131	1,168,456,336,182	27,820,388,957	0.22	13.09
L-3	22,504,056,571	460,854,193,170	10,972,718,885	0.49	2,327,123,000	249,002,161	59,734,235,466	401,119,957,704	9,550,475,183	0.42	12.96
R-3	68,084,658,284	796,058,728,967	18,953,779,261	0.28	10,042,472,000	1,074,544,504	257,777,258,489	538,281,470,477	12,816,225,488	0.19	32.38
L-2	24,216,677,409	470,305,000,205	11,197,738,100	0.46	2,754,151,000	294,694,157	70,695,491,533	399,609,508,672	9,514,512,111	0.39	15.03
R-2	66,768,689,056	897,236,803,448	21,362,781,034	0.32	385,966,000	41,298,362	9,907,247,673	887,329,555,775	21,126,894,185	0.32	1.10
L-1	15,066,851,989	1,462,550,104,275	34,822,621,530	2.31				1,462,550,104,275	34,822,621,530	2.31	
R-1	195,372,090,899	4,645,047,388,502	110,596,366,393	0.57				4,645,047,388,502	110,596,366,393	0.57	
L-0	8,265,472,203	351,526,505,881	8,369,678,711	1.01				351,526,505,881	8,369,678,711	1.01	
R-0	83,416,642,063	2,110,984,168,748	50,261,527,827	0.60				2,110,984,168,748	50,261,527,827	0.60	
Total this assessment:	1,521,928,302,462	21,533,315,463,568	512,697,987,228	0.34	46,220,237,000	4,945,565,359	1,186,413,661,954	20,346,901,801,614	484,450,042,896	0.32	
Percent water from Nahcolite: 5.51											

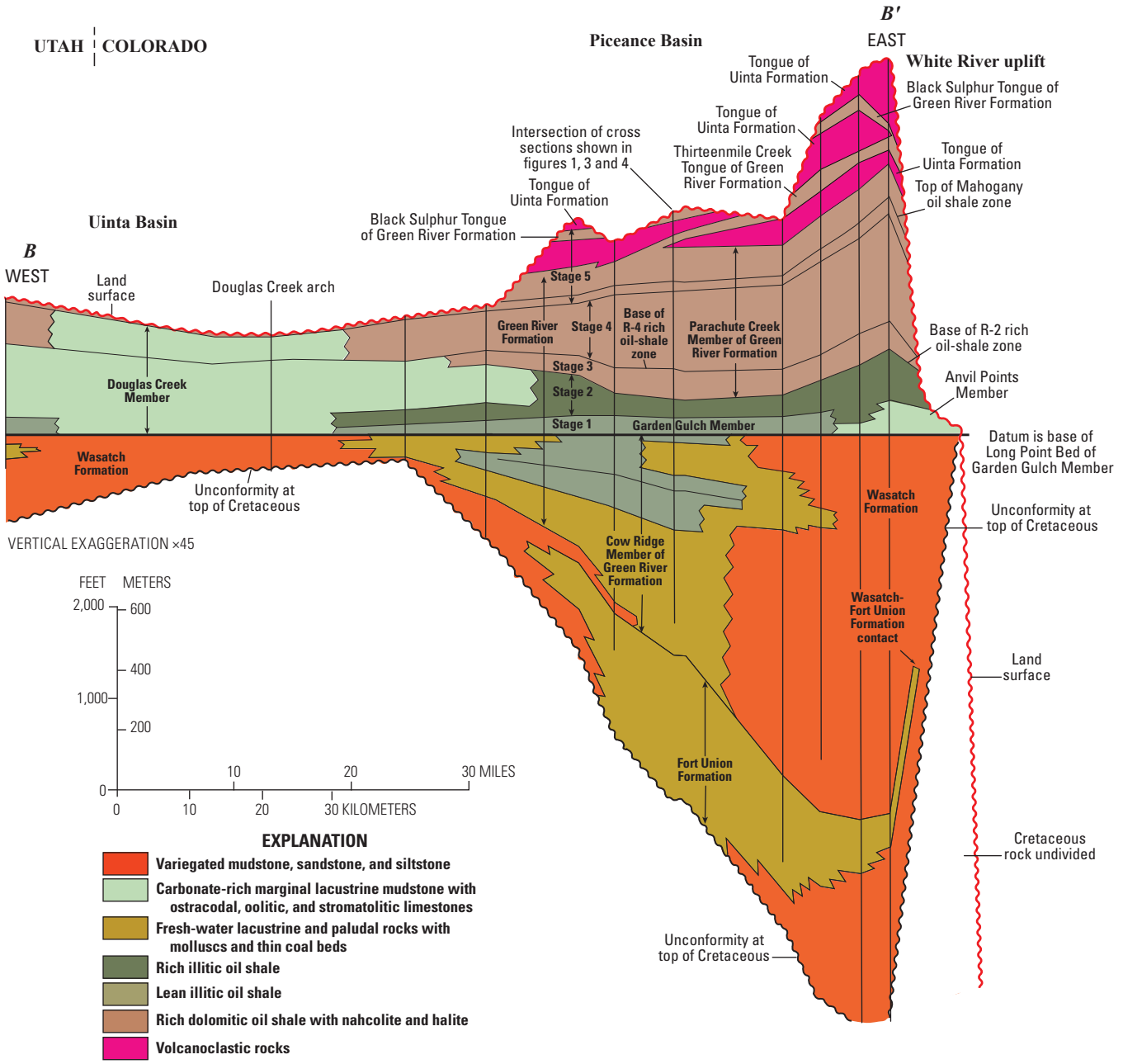

Figure 4. West-to-east cross section through the Piceance Basin and the Douglas Creek arch, Colorado, and the eastern part of the Uinta Basin, Utah, showing member subdivisions, stages of Lake Uinta as defined by Johnson (1985), and some of the rich and lean zones defined by Cashion and Donnell (1972). Location is shown on figures 1 and 3.

Cashion and Donnell (1972) recognized that the Parachute Creek and Garden Gulch Members in the oil-shale depocenter could be subdivided into a sequence of oil-rich zones (the R-zones) and oil-lean zones (L-zones) that could be recognized throughout much of the rich oil-shale area in the central part of the Piceance Basin and in the eastern part of the Uinta Basin (fig. 7). Most of these zones grade into marginal lacustrine rocks towards the basin margins, and the approximate marginal lacustrine equivalents of many of the R-zones have been identified in some areas (see for example, Johnson and others, 1988). These zones appear to approximate time-stratigraphic units that record changing rates of organic-matter production and preservation that occurred simultaneously throughout Lake Uinta. The rich- and lean-zone stratigraphy formed the basis of the most recent USGS Piceance Basin assessment (Johnson and others, 2010; see also earlier USGS assessments including Pitman and Johnson, 1978; Pitman, 1979; and Pitman and others, 1989) with each rich and lean zone assessed separately. In these assessments four maps were generated for each zone: (1) an isopach map, (2) a map showing variations in gallons per ton of oil, (3) a map showing variations in barrels of oil per acre, and (4) a map showing total oil in each 6-mile by 6-mile township. Similarly, the water content of each R-zone is estimated separately in this report.

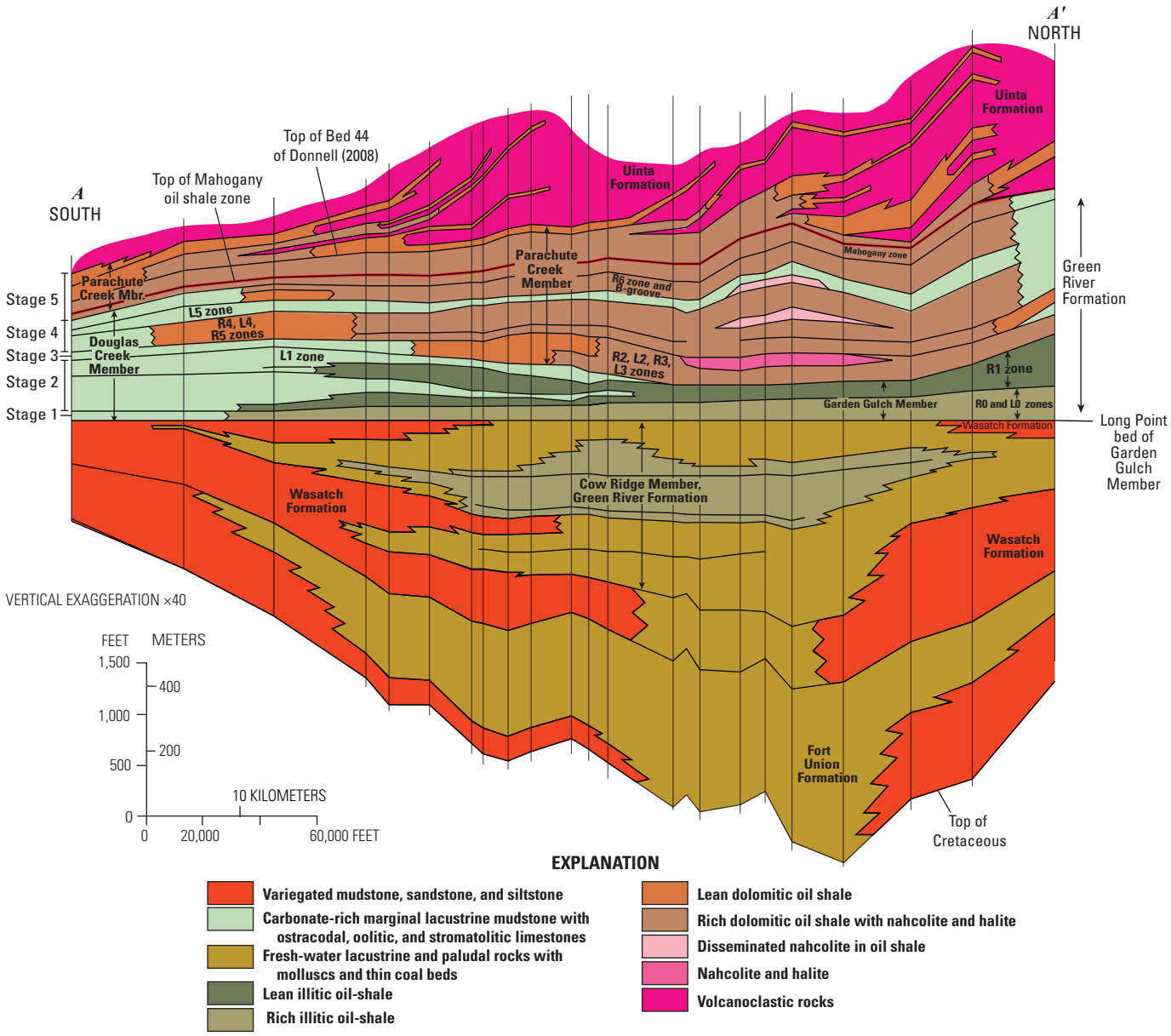

Figure 5. South-to-north cross section through the Piceance Basin, northwestern Colorado, showing member subdivisions, stages of Lake Uinta as defined by Johnson (1985), and some of the rich and lean zones defined by Cashion and Donnell (1972). Location is shown on figures 1 and 3.

Sources and Distribution of Water in Oil Shale

Colburn and others (1989) in their study of samples from the Mahogany oil-shale zone (fig. 7) in the Piceance Basin identified five possible sources of water released during retorting of Green River Formation oil shale: (1) free water within clay minerals, (2) water from the hydrated minerals nahcolite, dawsonite, and analcime, (3) water from reaction of iron compounds with hydrogen sulfide (H_2S), (4) water from elimination of organic oxygen in kerogen, and (5) equilibrated water. They (Colburn and others, 1989) determined that dehydration of kerogen, a significant source of water in the Devonian oil shales of the eastern United States that they also studied, was only a minor source of water in Green River oil shales, contributing about 0.2 g of water per 100 g of oil shale. Water from reaction of iron compounds with H_2S and from equilibrated water, which can form above 550 °C from reactions such as carbon dioxide and hydrogen forming water and carbon monoxide, were also determined by Colburn and others (1989) not to be major sources of water in oil shales of the Green River Formation. It is unlikely that a significant amount of water is lost due to dehydration of clay minerals between oil-shale core collection and when it is assayed. Only the Garden Gulch Member contains significant clay in the form of illite, which loses only a small fraction of its water at temperatures of less than 100 °C (R.M. Pollastro, U.S. Geological Survey, written commun., January 5, 2011).

Figure 8 plots GPT oil versus water in GPTW to see if there is a relationship between oil yield and water yield. A positive correlation between these two factors would indicate that the breakdown of kerogen is a major source of water produced from Fischer assay. The three core holes are from areas where the oil shale does not contain nahcolite, a major source of water in the Green River oil shales (discussed later in this report). The extreme scatter suggests that there is no relation between GPT oil and GPTW. Interestingly, the scatter in GPTW values decreases as oil yields increase, settling on a water value of about 3–5 GPT for the richest oil shale. Assuming a weight of 8.345 pounds per gallon for fresh water, then 25 to 42 pounds or 1.3 to 2.1 percent of the weight of raw oil shale is given off as water at high oil yields. It is unclear at present what this possible relation might mean.

Plate 1 is a generally south-to-north stratigraphic cross section that extends from outcrops at Long Point in the south, through the oil-shale and saline-mineral depocenter, to outcrops along lower Piceance Creek in the north. The section is based on eight cored holes and two measured surface sections. The measured section at Long Point is from Johnson (1975), but the measured section along lower Piceance Creek is new to this report, although sections were previously described at that locality by Brobst and Tucker (1973) and Pipiringos and Johnson (1976). The core-hole columns graphically display both oil and water contents based on Fischer assay. The cross section also shows the approximate limits of mineral phases that produce water with Fischer assay. Mineral data for the lower Piceance Creek section are from Brobst and Tucker (1973), and mineral data for the Colorado Core Hole No. 1 are from Robb and Smith (1974). Limits of nahcolite and dawsonite in the Shell Greno 1–4 core hole are from Beard and others (1974). No mineral data have been published for the Pan American Peterson No. 1 core hole, but data are available for another core hole in the same section, the Juhan No. 4–1 core hole (Beard and others, 1974). There also are no published mineral data for the 31–1 (fig. 4) and Fawn Creek No. 2 core holes. However, nahcolite and dawsonite data are available for the Equity Ebler No. 1 core hole located about 3 miles east of the Fawn Creek core hole (Beard and others, 1974), and those data were used as a guide. No mineral data are available for the three southernmost core holes nor for the measured section at Long Point. Based on work on outcrops in basin-margin areas in other parts of the basin (Brobst and Tucker, 1973), however, it is assumed that clay, predominantly illite, is the major water-bearing phase in the Garden Gulch Member (fig. 6), and that both clay and analcime are the major water-bearing phases in the Parachute Creek Member (fig. 6).

Clay Minerals

Clay minerals contribute a significant amount of water in Green River oil shale, particularly the illitic zone of the Garden Gulch Member, which extends from the base of the R-0 zone into the R-2 zone (fig. 7, pl. 1). The amount of water in clay will vary depending on how well the sample was dried prior to retorting (Colburn and others, 1989). Robb and Smith (1974), in their study using X-ray diffraction of the U.S Bureau of Mines/Atomic Energy Commission (AEC) Colorado Core Hole No. 1 in the oil-shale and saline-mineral depocenter, estimated that illite [$K_{0.65}Al_{2.0}\square Al_{0.65}Si_{3.35}O_{10}(OH)_2$] (Mandarino and Back, 2004) comprises about two-thirds of all mineral content in that interval. A reexamination of the original X-ray traces used in the study by Robb and Smith (1974) found that most of the Garden Gulch Member samples were run twice, the second time after glycolation to look for evidence of expandable clays such as montmorillonite [$(Na,Ca)_{0.3}(Al,Mg)_2Si_4O_{10}(OH)_2 \cdot nH_2O$] (Mandarino and Back, 2004). Although illite is clearly the dominant clay, expandable clays were detected in the majority of analyzed oil-shale samples as well. Illite content decreases upwards in the R-2 zone and is not a major phase in the overlying dolomitic oil shale of the Parachute Creek Member, detected in only 20 percent of the analyzed samples from that core hole. Analyses of the Mahogany zone of the Parachute Creek Member (fig. 7), on samples taken from Anvil Points along the southeastern margin of the Piceance Basin (fig. 1) by Colburn and others (1989), also indicated very little water released from clay minerals. Smith (1974) believed that illite formed from the hydrolysis of silicate and aluminosilicate minerals in the highly alkaline waters of Lake Uinta.

Analysis by X-ray of surface sections from marginal areas of the basin indicates that clay is at least a minor component throughout much of the Parachute Creek Member in those areas. Brobst and Tucker (1973) studied the mineralogy of three measured sections of the Parachute Creek Member around the margins of the basin using X-ray diffraction. Those sections extend stratigraphically from significantly above the Mahogany zone to as low as the R-2 zone in the lower part of the Parachute Creek Member (fig. 7). Clay was detected in most of the analyzed samples. The clay mostly is illite, based on the position of the dominant X-ray peak for clay. Thus it appears that illite and possibly some minor expandable clays, confined largely to the Garden Gulch Member or to the R-0 through R-2 oil-shale zones in the central part of the basin, become widespread throughout much if not all of the overlying Parachute Creek Member toward the basin margins (pl. 1).

Nahcolite

The sodium-bicarbonate mineral nahcolite ($NaHCO_3$) decomposes to natrite (Na_2CO_3) or soda ash, carbon dioxide, and water at temperatures near 100 °C and contains about 10.7 percent by weight water. Nahcolite forms disseminated aggregates, nodules, bedded units of disseminated brown crystals, and white crystalline beds associated with dawsonite ($NaAl(CO_3)(OH)_2$ and halite (NaCl) minerals (Dyni, 1981; Brownfield and others, 2010). Beard and others (1974) and Dyni (1974) estimated nahcolite content using 14 and 10 boreholes, respectively, whereas Brownfield and others (2010) used 58 boreholes as part of their recent assessment of in-place

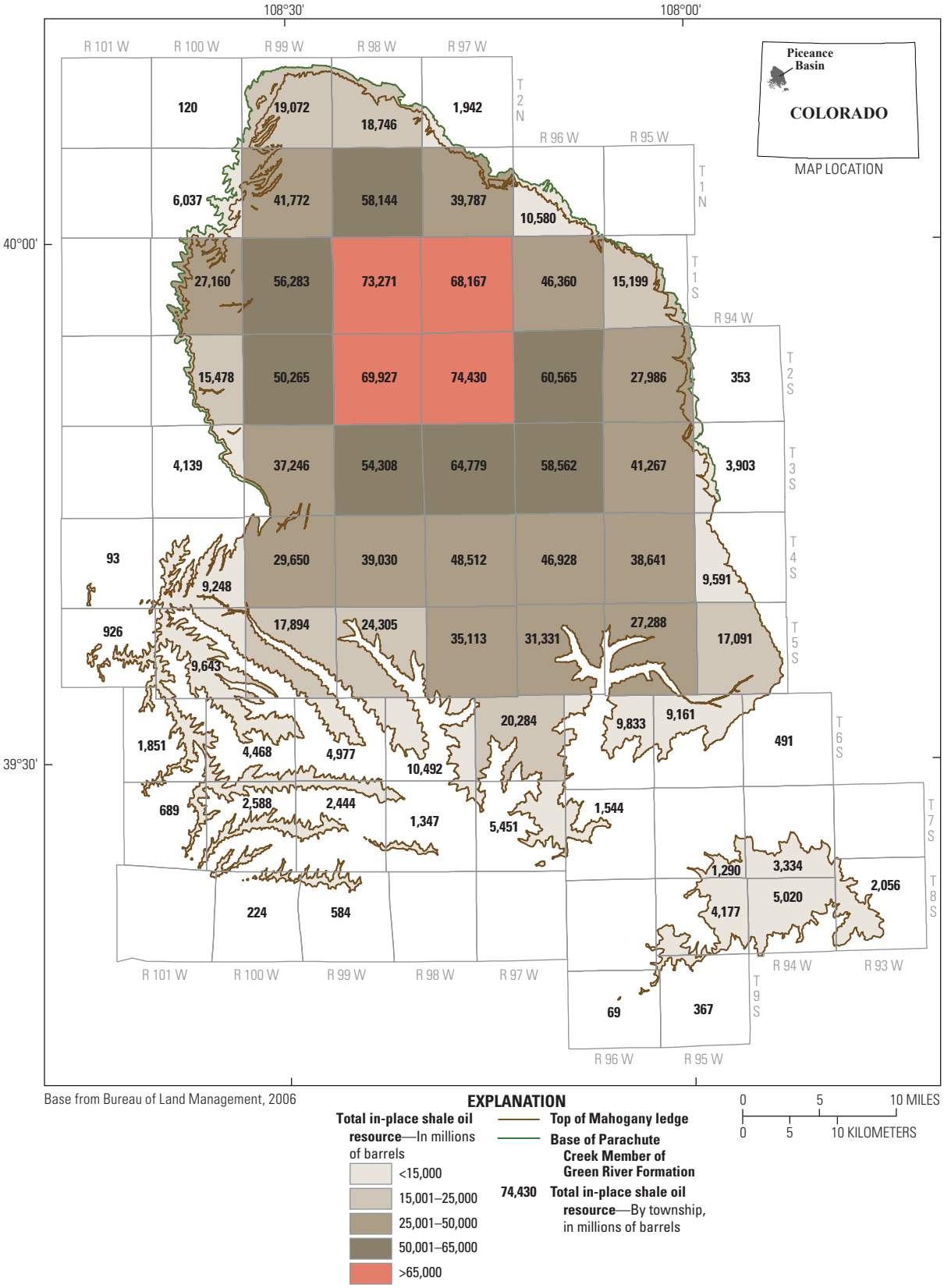

Figure 6. Comparing total in-place oil and nahcolite, respectively, in the Piceance Basin, Colo. Oil amount (in millions of barrels per township) is from Johnson and others (2010). Nahcolite in tons per acre is from Brownfield and others (2010).

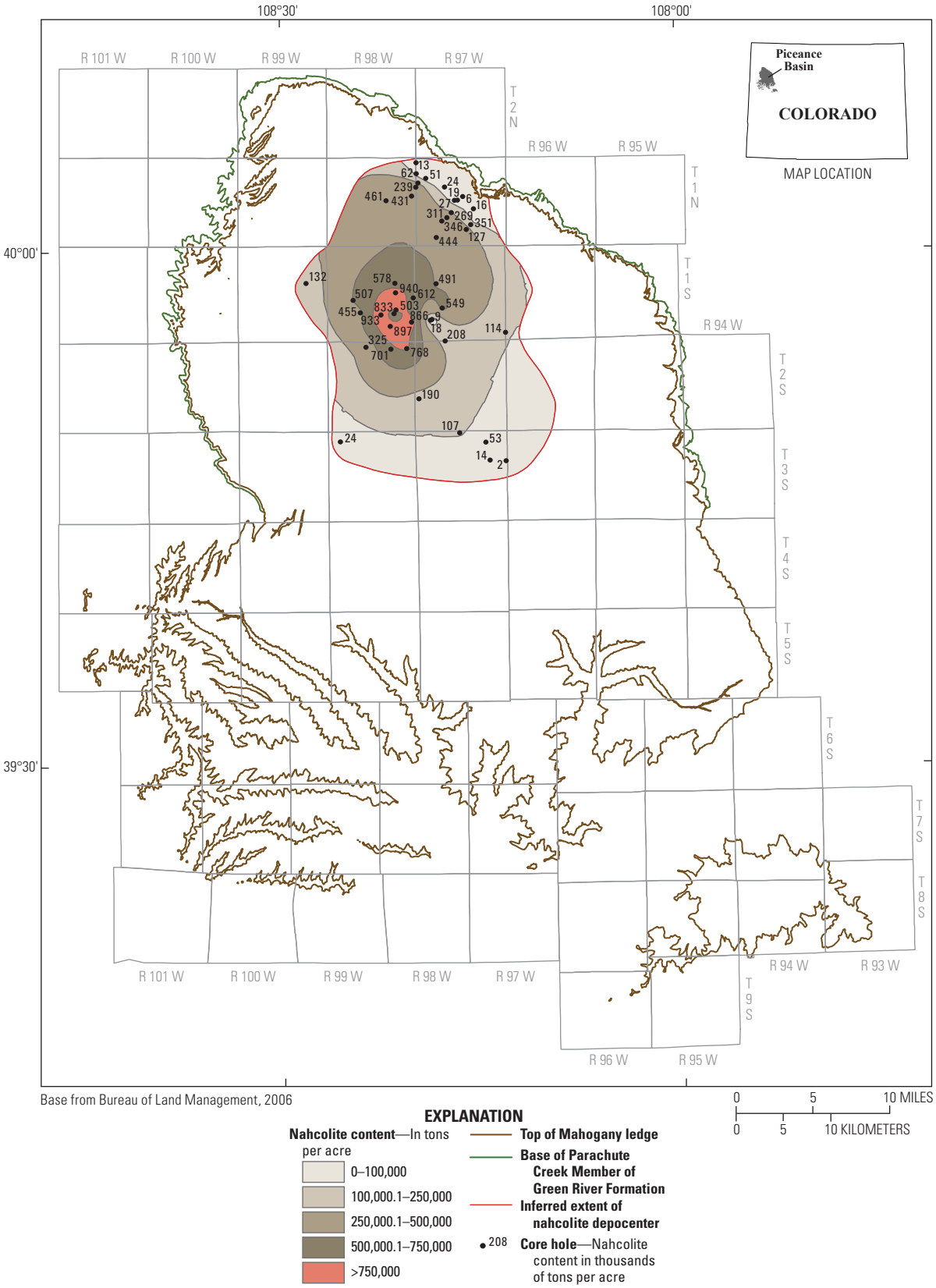

Figure 6. Comparing total in-place oil and nahcolite, respectively, in the Piceance Basin, Colo. Oil amount (in millions of barrels per township) is from Johnson and others (2010). Nahcolite in tons per acre is from Brownfield and others (2010). —Continued

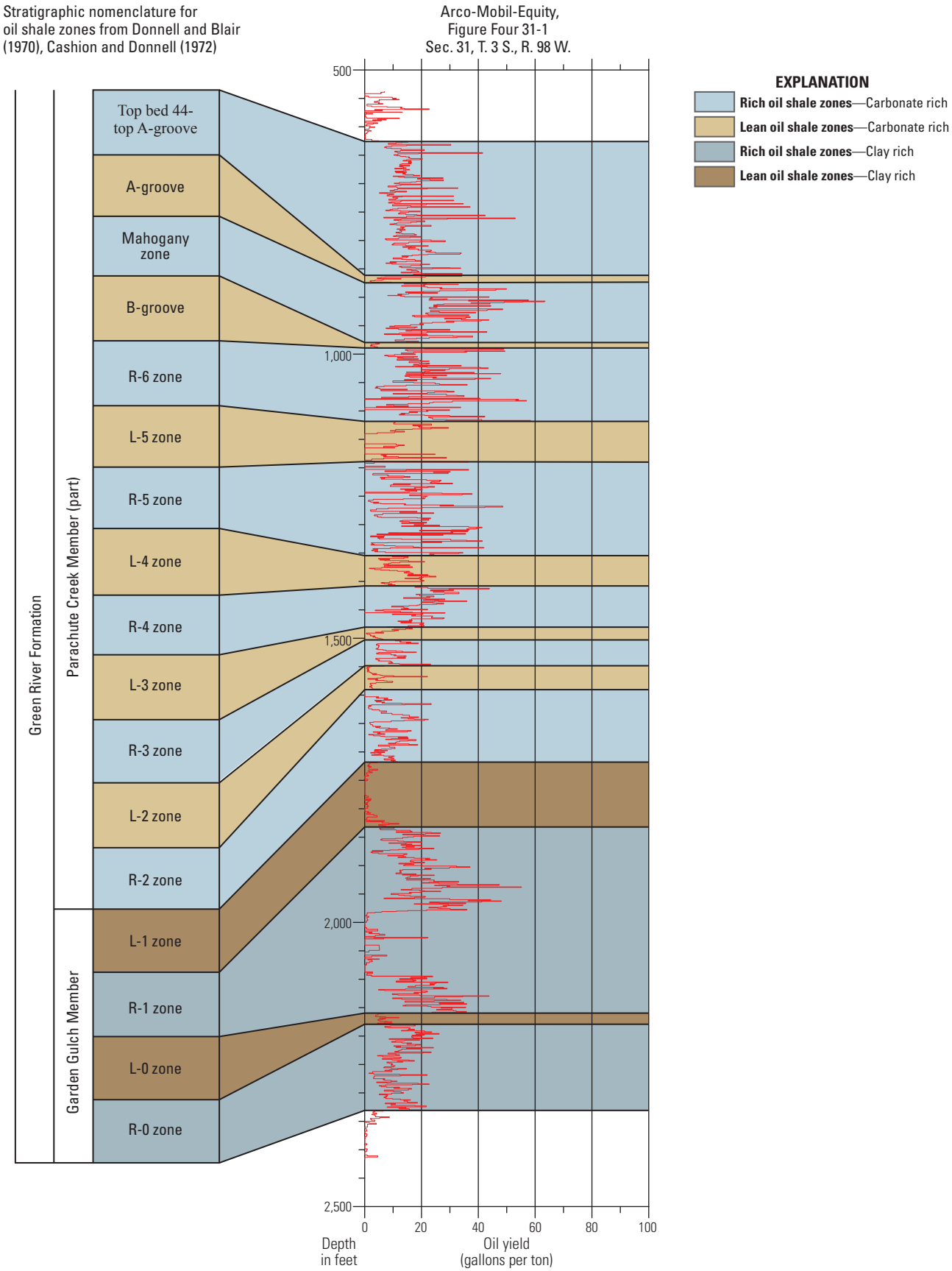

Figure 7. Rich and lean zones for the Green River Formation, originally defined by Cashion and Donnell (1972) for the Piceance Basin, western Colorado, and the Uinta Basin of eastern Utah and western Colorado. Graph shows oil in gallons per ton (red trace).

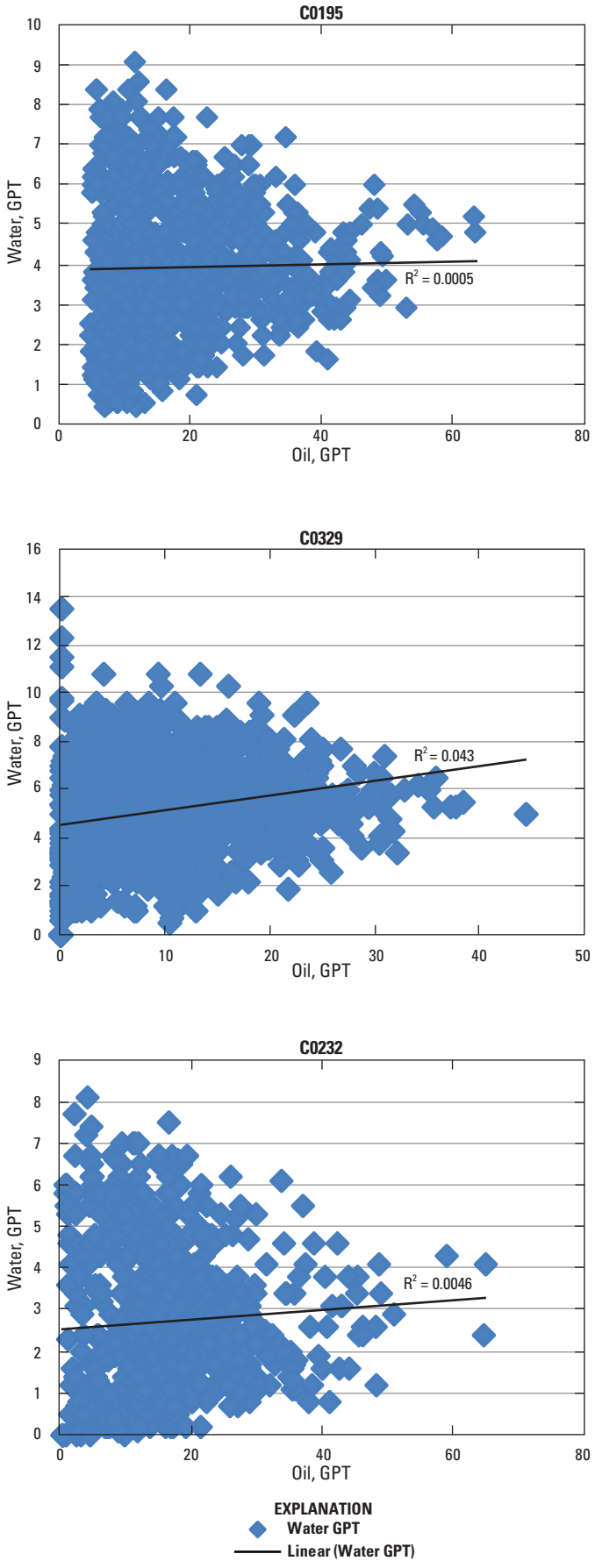

Figure 8. Gallons per ton oil (GPT) in relation to gallons per ton water (GPTW) for three core holes outside the nahcolite area, Piceance Basin, Colo. Core hole C0195 is the Arco-Mobil-Equity Figure Four 31–1 core hole in sec. 31, T. 3 S., R. 98 W.; core hole C0232 is the Humble Oil and Refining 1 East Willow Creek in sec. 28, T. 4 S., R. 97 W.; and core hole 329 is the Carter Oil 2 Opportunity core hole in sec. 28, T. 1 N., R. 96 W.

nahcolite. Nahcolite is confined to the saline depocenter where it generally extends from the lower part of the L-2 zone to the lower part of the L-5 zone, although Dyni (1974) found minor nahcolite as low as the upper part of the R-2 zone. Figure 9 charts the water content for the U.S Bureau of Mines/Atomic Energy Commission (AEC) Colorado Core Hole No. 1 in sec. 13, T. 1 N., R. 98 W.; water content clearly is related to nahcolite content as it increases markedly in all nahcolite-bearing intervals from 1,735 ft to 2,510 ft. All of the high-water intervals correspond very closely to nahcolite-rich intervals identified by Dyni (1974) and Robb and Smith (1974).The Colorado Core Hole No. 1 is included on the cross section (pl. 1) along with another core hole that contains nahcolite, the Shell Greno No. 1–4 core hole in sec. 4, T. 3 S., R. 97 W. The nahcolite-bearing interval in the Shell Greno core hole is also easily discernible from the water-content data, although the interval is more restricted stratigraphically in that core hole than in the Colorado Core Hole No. 1.

Nahcolite has been leached out around the margins of the saline depocenter by groundwater movement, creating what is referred to as the leached zone (Hite and Dyni, 1967; Dyni and others, 1970; Dyni, 1974). The exact lateral and vertical extent of nahcolite-bearing rock prior to leaching has not been determined, but collapse breccias related to that leaching are found stratigraphically as high as the middle part of the L-5 zone (Dyni, 1974), and vugs that likely were once filled with nahcolite are present in the lower part of the Mahogany zone along lower Piceance Creek (Brobst and Tucker, 1973). The stratigraphic position of the vugs is shown on the lower Piceance Creek section on plate 1.

Dawsonite

Dawsonite, a hydrated sodium-aluminum-carbonate mineral ($NaAl(CO_3)(OH)_2$), thermally breaks down at temperatures of 200 °C to 370 °C—below retort temperatures—into soda ash (Al_2O_3), water, and CO_2. It contains about 12.5 weight percent water. Dawsonite forms minute crystals, 5 µm or less in size, disseminated throughout the oil-shale matrix (Dyni, 1974; 1981). It may compose as much as 25 percent of the rock over short intervals (Smith and Milton, 1966) but commonly is less than 10 percent (Young and Smith, 1970). Dawsonite appears for the first time in the lower part of the R-2 zone, about 65–75 ft below the first occurrence of nahcolite, and increases in abundance upwards (Dyni, 1981). Robb and Smith (1974), in their study of the Colorado

Core Hole No. 1 in the oil-shale and saline-mineral depocenter (fig. 1), found significant dawsonite in virtually every analyzed sample starting in the L-1 zone and extending upwards to near the top of the R-5 zone (pl. 1). Scattered samples in the R-6 zone also contained minor dawsonite, but dawsonite was not detected in any samples of the Mahogany zone and above. It should be noted that the R-zone stratigraphy for the Colorado Core Hole No. 1 was added in this report, as the R-zones were not identified by Robb and Smith (1974). Dyni (1981, his table 4) published quantitative estimates of mineral phases in the Juhan 4–1 core hole in sec. 4, T. 2 S., R. 98 W., but only for that part of the core that contains nahcolite, from near the top of the R-4 zone to the middle of the R-2 zone. Dawsonite was detected in every sample with a maximum value of 23.8 weight percent.

Dawsonite-bearing oil shale extends considerably beyond the maximum extent of nahcolite largely because it is not water-soluble and thus has not been leached by groundwater (Beard and others, 1974). The exact limits of dawsonite-bearing rocks are not well-defined, but the limits of dawsonite-bearing rock become more restricted stratigraphically toward the basin margins, and ultimately dawsonite disappears altogether. Dawsonite was not detected in the pipeline or Rio Blanco surface sections (fig. 3) sampled by Beard and others (1974). Beard and others (1974) estimated the amount of dawsonite in 22 wells in the central part of the basin using water and gas measurements from Fischer assay and found significant dawsonite as far as 4.5 mi south and east of the present limit of nahcolite shown in figure 6. There were insufficient data to determine extent of dawsonite in the northernmost part of the basin. Average weight percent dawsonite in the 22 wells varied from 1.9 to 5.7 percent (Beard and others, 1974). Again, the R-zone stratigraphy was added to these holes in this report. The top of the dawsonite interval in these wells extends from near the top of the R-5 zone to near the top of the R-1 zone in the saline depocenter, but the base climbs stratigraphically as high as the R-3 zone toward the basin margins (pl. 1). Along lower Piceance Creek, dawsonite is restricted (pl. 1) to the interval from the lower part of the L-4 zone to the uppermost part of the R-5 zone (Brobst and Tucker, 1973).

Analcime

Analcime ($NaAlSi_2O_6{\cdot}H_20$) is a zeolite mineral formed from altered ash beds and volcanic detritus. Colburn and others (1989) determined that water was released from analcime in Colorado oil shales at a temperature of about 300 °C. Analcime contains about 8.2 percent water by weight. In the oil-shale and saline-mineral depocenter, analcime is most common in the interval in the lower part of the R-6 zone and above. Robb and Smith (1974) detected analcime in most of the samples that they analyzed from the Colorado Core Hole No. 1 in sec. 13, T. 1 N., R. 98 W. (fig. 3, pl. 1) starting in the lower part of the R-6 zone and extending to the top of the Mahogany zone, the highest cored zone. Robb and Smith (1974) found that analcime was nearly absent in the oil-shale interval below, an interval that extends down to the lower part of the R-0 oil-shale zone or very close to the base of the Green River oil-shale section.

Brobst and Tucker (1973) detected analcime in most of the oil shale and marlstone samples analyzed in three surface sections around the margins of the basin. Those sections extend stratigraphically from 412 ft above the Mahogany Bed at the Rio Blanco section along the eastern margin to as low as the R-2 zone at their pipeline section along the western margin of the basin (fig. 3). Thus, the entire Parachute Creek Member contains analcime in basin-margin areas away from the oil-shale and saline-mineral depocenter. Analcime in the Green River Formation probably forms from clays and zeolites derived from volcanic glass, although zeolite precursors have not been found in the Piceance Basin (Brobst and Tucker, 1973). Analcime can convert to feldspar or dawsonite in environments of high salinity (Hay, 1966; Sheppard and Gude, 1968, 1969; Brobst and Tucker, 1973). Colburn and others (1989) determined that analcime provided most of the water released during retorting of samples of the Mahogany zone from Anvil Points (fig. 3). They (Colburn and others, 1989) determined that about 15 percent analcime could account for all the water released. Robb and Smith (1974) found that analcime and dawsonite in general do not coexist in Colorado Core Hole No. 1. Brobst and Tucker (1973) suggested that analcime alters to dawsonite and quartz at pH greater than 9. Brobst and Tucker (1973), however, did find both analcime and dawsonite in some samples along lower Piceance Creek but also cited evidence that analcime may have been altered to form dawsonite and quartz**.**

According to Lee (L.-J. Lee, Texas Technical University, 1979, written commun.) analcime expels all zeolitic water between 80 °C to 400 °C, or below maximum retort temperatures, but will readsorb water upon rehydration at temperatures below 400 °C. At higher temperatures, the mineral structure breaks down, and rehydration will not occur. This may be important for in-situ extraction processes to extract shale oil, as the retorted oil-shale interval is treated with steam at the end of the retort process to scavenge remaining toxic organic compounds, and presumably, the analcime would become rehydrated during that process.

Distribution of Water in the Green River Formation

Two sets of maps were generated for each of the 17 oil-shale zones assessed by Johnson and others (2010): (1) variations in gallons of water per ton of oil shale (GPTW); and (2) variations in gallons of water per acre (GPAW). The GPTW map displays variations in *average* water content for each of the 17 zones, whereas the GPAW map displays variations in *total*

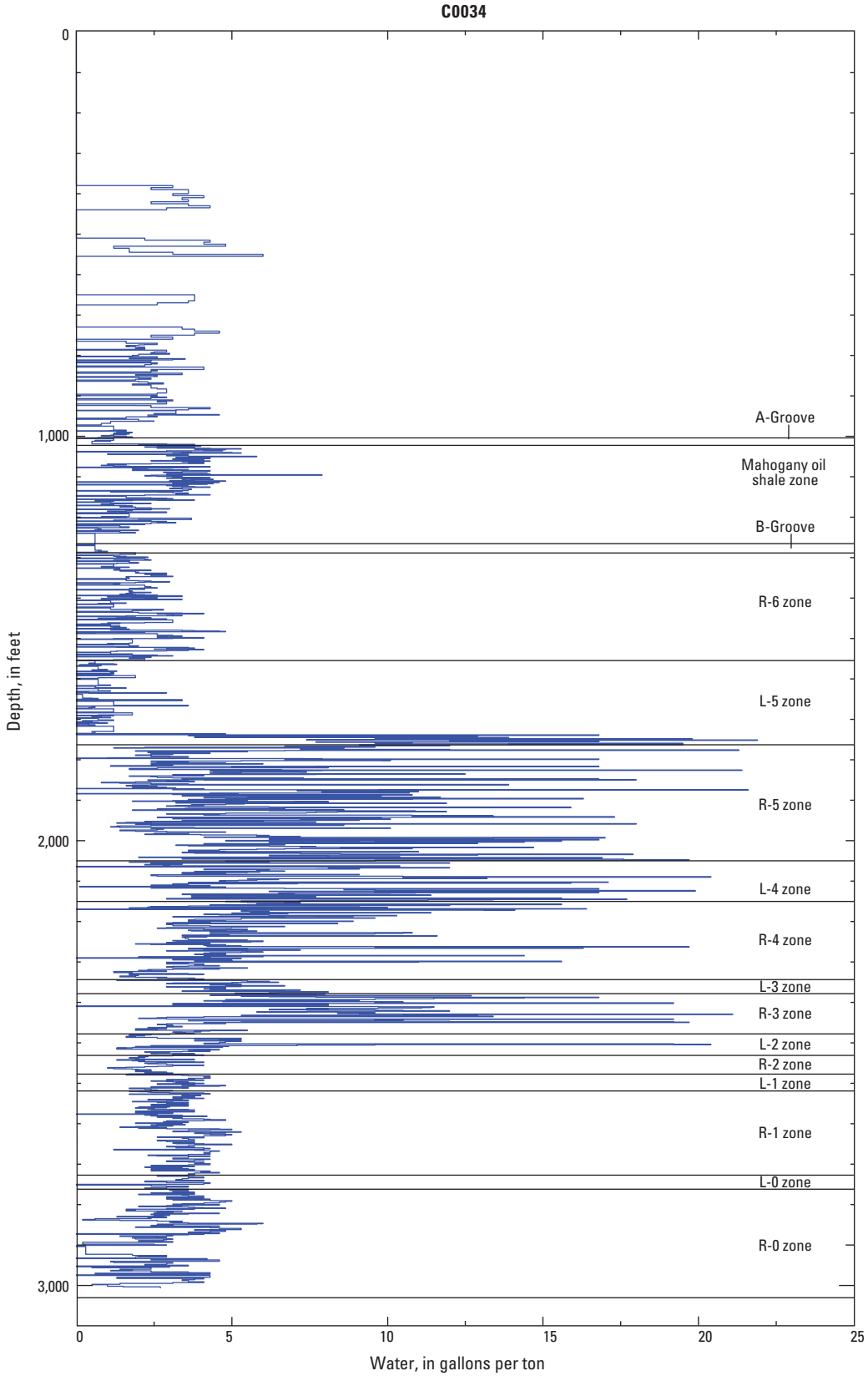

Figure 9. Variations in water content (gallons per ton) with depth for the U.S. Bureau of Mines/AEC Colorado Core borehole No. 1 in sec. 13, T. 1 N., R. 98 W., Piceance Basin, Colo.

water within each zone. The GPTW map also displays a bubble at each control point of size proportional to the generated ratio of water to oil. As previously discussed, that ratio is commonly used when estimating water requirements for an oil-shale industry. Isopach maps and maps showing gallons per ton of oil (GPT) and barrels per acre of oil (BPA) by Johnson and others (2010) are included for many of the oil-shale zones.

The process used to generate these maps and the in-place water estimates is identical to the process used to estimate in-place oil, except that water volumes commonly are expressed in gallons (that is, gallons of water per acre, GPAW) rather than in barrels (Johnson and others, 2010; Mercier and others, 2010). Variations in GPTW were estimated for each oil-shale zone at each control point by calculating a weighted average of water content from all the Fischer assay analyses available for that zone. The data then were contoured using the Radial Basis Function (RBF) method. Calculating gallons of oil and gallons of water per acre requires that the specific gravity and thus volume of the original pre-assayed oil-shale sample be known—a measurement that is not routinely made during Fischer assay. Stanfield and others (1954), however, reported volume-weight/oil-yield relations from about 20,500 Green River Formation oil-yield analyses, and based on those data, Johnson and others (2010) and Mercier and others (2010) generated a third-order trend line relating oil yield to specific gravity of Green River oil shale with an R^2 regression value of 0.9997. Using the data, Johnson and others (2010) and Mercier and others (2010) determined the average density of the oil shale in each assessed zone at each control point used in the assessment of in-place oil. Those densities then were used to calculate barrels of oil per acre (BPA) and ultimately total in-place oil (in barrels). Those same average densities for each oil-shale zone at each control point, determined from oil content, were used to calculate GPAW. All maps were created by applying a hillshade function to the Esri GeoStatistical models instead of the Esri GRIDs to visually enhance displayed contours, creating the illusion that the maps are three-dimensional. The hillshade function was not used for display of in-place oil (Johnson and others, 2010).

The R-5 and L-5 zones in the central part of the basin contain thick beds of nahcolite and halite (Dyni, 1974, 1981; Brownfield and others, 2010) that commonly are not assessed using Fischer assay. As a result, there are no data on water content of those beds, and the total water estimated for the R-5 and L-5 zones is underestimated in the area where the nahcolite and halite beds are present.

The R-0 zone was the first oil-shale zone deposited in Lake Uinta. The upper part of the R-0 zone is marked in the central part of the basin by a distinctive increase in resistivity, known informally on electric logs as the orange marker, named for the color of pen used to mark it on geophysical logs (Chancellor and others, 1974; Ziemba, 1974). The orange marker, which comprises about the upper 30 ft of the R-0 zone, is caused by a slight increase in carbonate in illitic sediments. The orange marker is equivalent to the carbonate marker in the Uinta Basin part of Lake Uinta, which also represents a temporary increase in carbonate precipitation (Johnson, 1985). The R-0 zone thickens gradually from a minimum of 75 ft thick near the Douglas Creek arch to about 200 ft in the east-central part of the basin (fig. 10). From there eastward, the R-0 zone thickens markedly to more than 500 ft along the northeastern and southeastern margins of the basin where it grades predominantly into sandstone, siltstone and mudstone (fig. 4, pl. 1). Both GPT of oil and BPA of oil increase towards the central part of the basin (figs. 11 and 12). The gallons of water per ton values are highest along the western and southwestern margins of the basin with values greater than 8 in some areas (fig. 13). Those GPTW values decrease to less than 3 in an area extending from the central part of the basin northeastward to approximately the mouth of Piceance Creek (fig. 13). Well control, however, is sparse to nonexistent in the southern and eastern parts of the basin. Variations in GPAW follow a similar trend (fig. 14). This water trend, however, generally is opposite the trend for gallons per ton (GPT) of oil and barrels per acre (BPA) of oil, both of which increase towards the central part of the basin (figs. 11 and 12). The water-to-oil ratio is significantly less than 1:1 except for one core hole in the extreme western part of the basin that has a ratio of 1.28:1 (fig. 13).

The L-0 zone is a thin interval varying from 13 to 35 ft throughout most of the basin and thickening markedly to 90 ft along the eastern basin margin where it grades into sandstone (fig. 15, pl. 1). Oil GPT and BPA of oil increase towards the same central basin area as the underlying R-0 zone (figs. 16 and 17). As with the R-0 zone, control is sparse to nonexistent in the southern and eastern parts of the basin (fig. 15). Water GPTW generally decreases from about 9 around the western and southern basin margins to about 3 in the basin center and its eastern extent (fig. 18). The GPAW is greatest in the northeastern and northwestern basin margins where it reaches 700,000, decreasing to less than 200,000 in the central and southern parts (fig. 19). Water-to-oil ratios are significantly less than 1:1 throughout most of the central part of the basin, increasing to as much as 2.60:1 in some core holes in marginal areas (fig. 18), largely because oil yields are very low there—less than 10 GPT oil (fig. 16).

The R-1 zone probably is the stratigraphically lowest oil-shale zone that has the potential to be exploited and is the target of an in-situ process currently being developed (Day, 2009). It is thickest around the margins of the basin and thins towards the oil-shale and saline depocenter (fig. 20). It contains some of the richest oil shale in the basin with GPT oil values from 20 to 30 GPT in the oil-shale depocenter (fig. 21). Total in-place oil, however, is greatest south of the depocenter due to a combination of greater thickness and comparatively high oil yields (fig. 22). The GPTW for the R-1 zone ranges to greater than 9 along the northwestern and northeastern margins, decreasing markedly towards the central

kerogen-rich area to less than 3 (fig. 23). The GPAW is greater than 7,000,000 in most marginal areas, decreasing to less than 1,000,000 where the interval is thinnest and oil yields are greatest (fig. 24). The area of maximum in-place oil is plotted on the map of in-place water (fig. 24), and there appears to be no relationship between the two. Water-to-oil ratio is significantly less than 1:1 in all but the extreme marginal areas, where ratios for three core holes are as high as 1.18:1, largely because oil yields are low there—6.5 to 7 GPT oil (fig. 21).

The L-1 zone thickens from less than 20 ft along the northern margin of the basin to a maximum of 80 ft to the northeast and to as much as 168 ft in the southwest (fig. 25). Both GPT oil and BPA oil are greatest in the north-central part of the basin (figs. 26 and 27). The GPTW reaches 10 in some marginal areas, decreasing to less than 3 in the central part (fig. 28). The GPAW can reach 4,000,000 along the southwestern basin margin, where the interval is thickest, decreasing to less than 200,000 in the north-central part of the basin (fig. 29). Water-to-oil ratios range from much less than 1:1 to as high as 14.66:1 in areas with very low oil yields (fig. 28). Oil yields in those core holes with high ratios are all significantly less than 10 GPT (fig. 26).

The R-2 zone represents the transition from illite-rich oil shales to carbonate-rich oil shales. Illite correspondingly decreases in abundance upwards through the R-2 zone (Dyni, 1974; 1981; Robb and Smith, 1974). The zone is thickest along an east-to-northeast-trending belt across the south-central and northeastern parts of the basin, where it ranges from about 90 to 155 ft thick (fig. 30). Oil in both GPT and BPA increases toward the saline depocenter in the north-central part of the basin (figs. 31 and 32), although the R-2 zone contains comparatively minor amounts of nahcolite (Dyni, 1974; Brownfield and others, 2010). The GPTW is lowest, less than 3, in a generally north-south area from the oil-shale and saline-mineral depocenter south to the southern margin of the basin (fig. 33). The GPAW is lowest, to as low as 310,000, in the saline and oil-shale depocenter, increasing to 1,800,000 in some marginal areas (fig. 34). An area of high water content extends around the southern and eastern margins of the depocenter in the same area where the R-2 zone is thickest (figs. 30 and 34). The area where nahcolite occurs in the R-2 zone is plotted on figure 33. The limited amount of nahcolite in that zone, however, does not appear to have greatly impacted either average water or total water, as both decrease towards the central part of the basin (figs. 33 and 34) in similar fashion to the illite-rich zones below and in sharp contrast to overlying zones in the nahcolite interval. The R-2 zone contains substantial clay and far less nahcolite than any of the overlying zones in the saline interval (Brownfield and others, 2010). Water-to-oil ratios are significantly less than 1:1 except in marginal areas where oil yields are 4.3 GPT or less (fig. 33).

The L-2 zone is the first zone that contains little clay and consists mainly of carbonate-rich oil shale. In addition, it is the stratigraphically lowest zone that contains significant nahcolite (Dyni, 1974, 1981; Brownfield, 2010). As previously discussed, saline-mineral deposition is centered in the north-central part of the basin (fig. 6). In all zones that do not contain nahcolite, the GPTW deceases inward from the basin margins. That general trend also can be discerned for nahcolite-bearing zones. However, there is a major increase in GPTW values in the nahcolite area.

Similar to the R-2 zone, the L-2 zone is thickest around the southern and eastern margins of the saline depocenter, more than 100 ft thick in some areas south of the depocenter (fig. 35), whereas GPT and BPA oil increase toward that depocenter (figs. 36 and 37). The GPTW reaches a maximum of more than 17 in the area with high nahcolite, decreasing to a minimum less than 2 just outside the nahcolite area (fig. 38). From there, water values increase toward the basin margins to greater than 6 in some marginal areas. The GPAW in the L-2 zone displays a complex pattern that is strongly influenced by both nahcolite content and thickness, as there are high values both in the area of high nahcolite and the area of maximum thickness south and east of the nahcolite depocenter (figs. 35 and 39). In addition, GPAW increases towards the southeastern basin margin (fig. 39). Water-to-oil ratios are significantly less than 1:1 except in some core holes near the basin margin where the ratio is as high as 5.96:1 in areas with low oil yields (fig. 38).

The R-3 zone thickens from as little as 30 ft in basin-margin areas to as much as 153 ft toward the area with maximum nahcolite (fig. 40). Some of that thickening is due to large amounts of nahcolite; Brownfield and others (2010) estimated as much as 135,000 tons per acre in the R-3 zone. Both GPT and BPA oil also increase towards the saline depocenter (figs. 41 and 42). The GPTW reaches a maximum greater than 11 in the area with the most nahcolite, decreasing to less than 2 just south of the nahcolite area (fig. 43). Note that GPTW generally is in the range from 3 to 5 in basin-margin areas (fig. 43). Water-to-oil ratios generally are less than 1:1 even in the area with the most nahcolite (fig. 43). The GPAW reaches a maximum of greater than 5,000,000 in the center of the nahcolite area, decreasing to less than 200,000 around the margins of that area (fig. 44).

The L-3 zone, a comparatively thin zone (just more than 70 ft thick), reaches a maximum thickness south of the saline depocenter (fig. 45). It thickens towards the south-central part of the basin and towards the eastern margin (fig. 45). Both GPT and BPA of oil increase towards the saline depocenter (figs. 46 and 47). The zone contains little nahcolite, both because the zone is thin and because there are few nahcolite-rich intervals within the zone (Dyni, 1974; Brownfield and others, 2010). Despite the scarcity of nahcolite, GPTW reaches a maximum of about 10 in the nahcolite area, decreasing to less than 2 around the southern margin of that area (fig. 48). The GPT of water generally ranges between 4 and 5 in basin-margin areas (fig. 48). The GPAW ranges from a minimum near 100,000 just south of the nahcolite area to more than 1,300,000 in the center of that area (fig. 49).

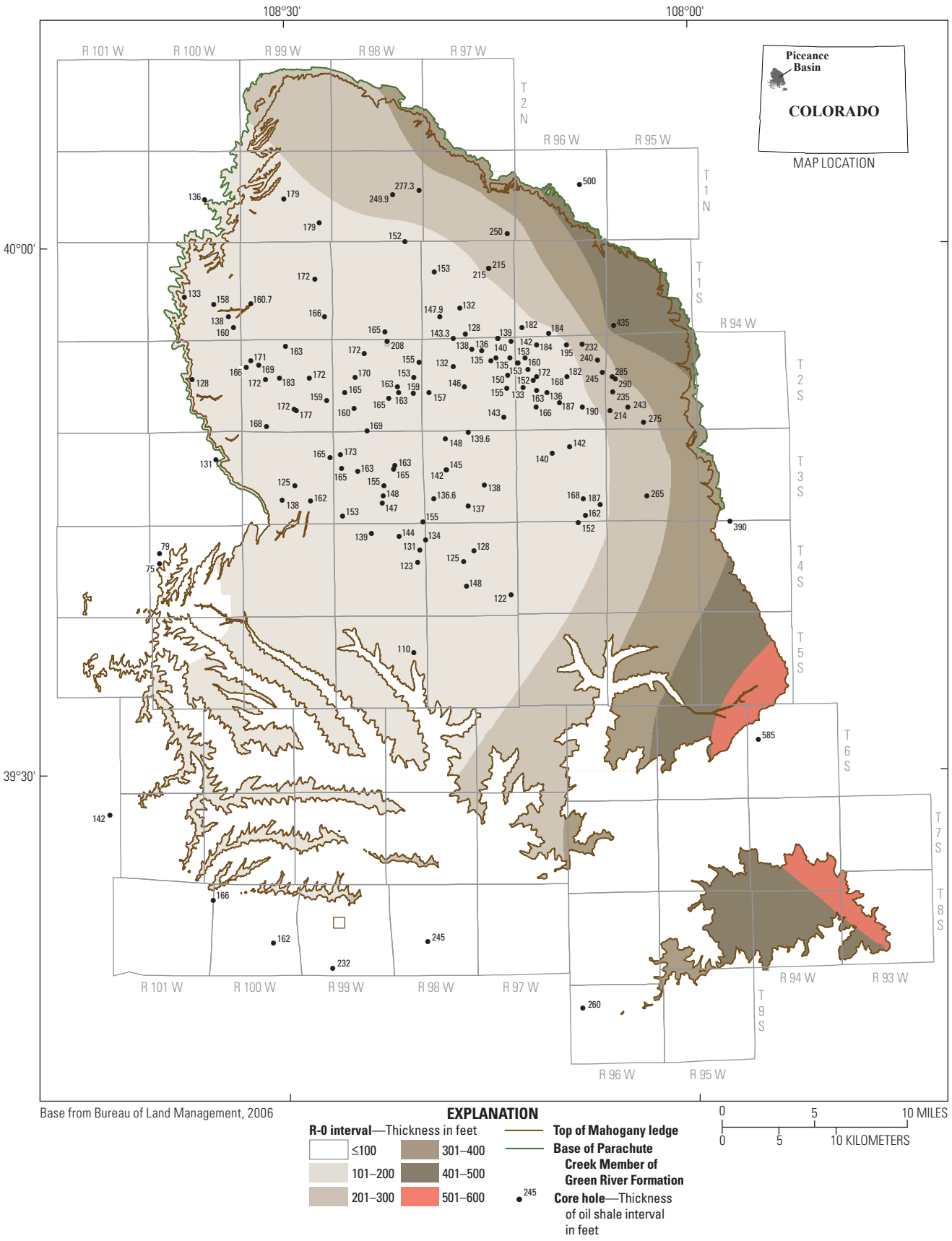

Figure 10. R-0 zone, Piceance Basin, Colo., using both core-hole and rotary-hole data. The Radial Basis Function Method (RBF) was used for contouring.

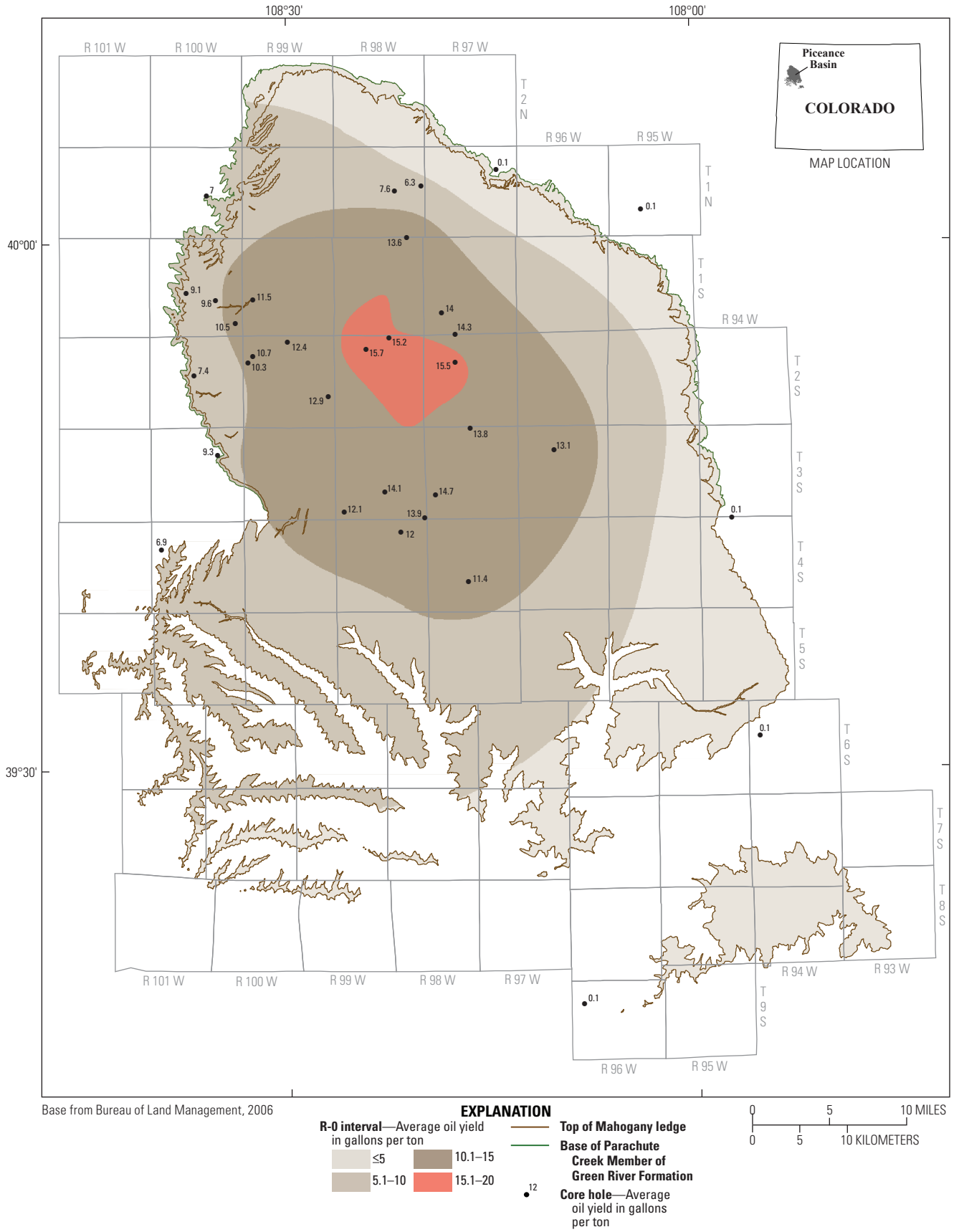

Figure 11. R-0 zone, Piceance Basin, Colo., showing the oil yield in gallons per ton (GPT). The Radial Basis Function Method (RBF) was used for contouring.

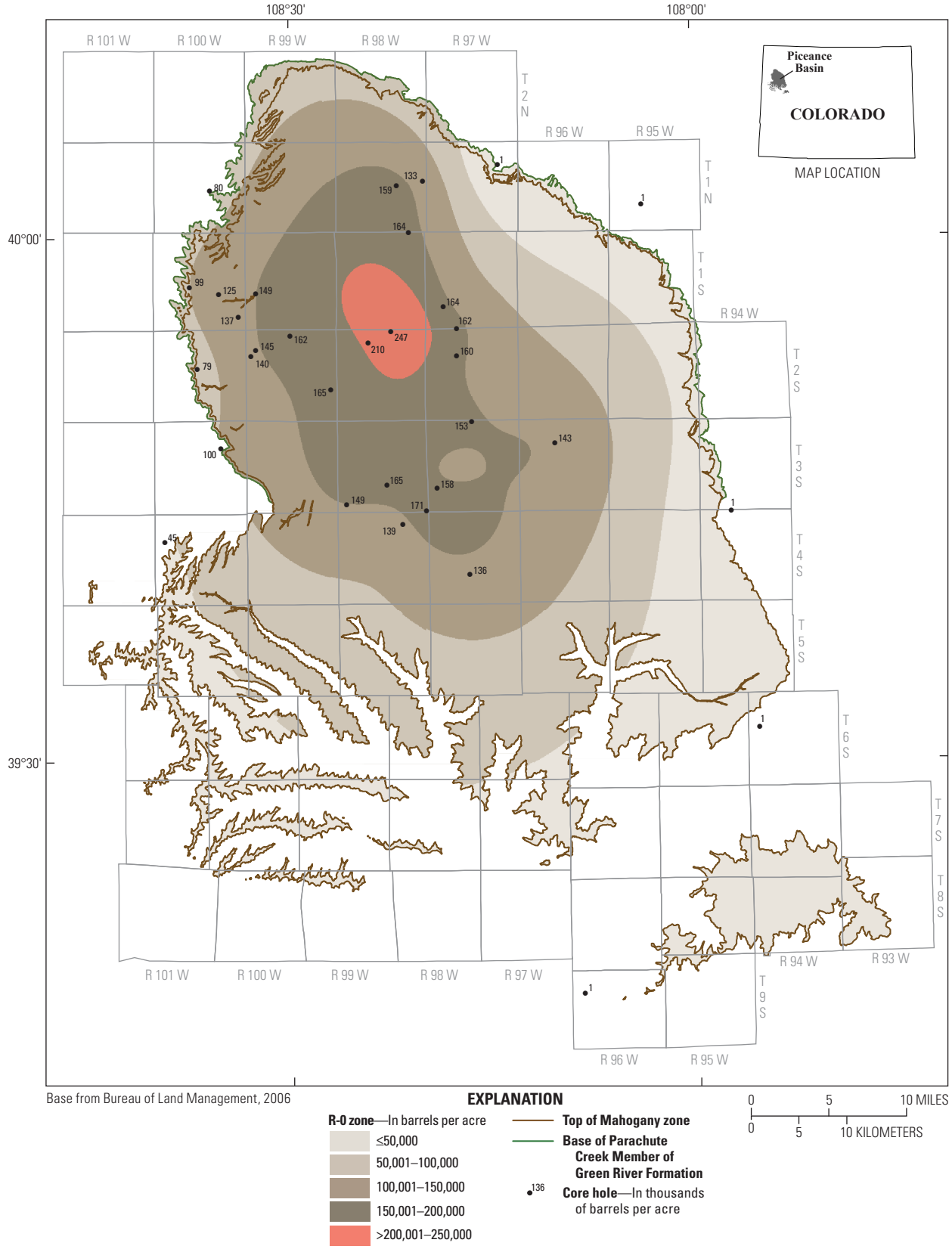

Figure 12. R-0 zone, Piceance Basin, Colo., showing oil yields in barrels per acre (BPA). The Radial Basis Function Method (RBF) was used for contouring.

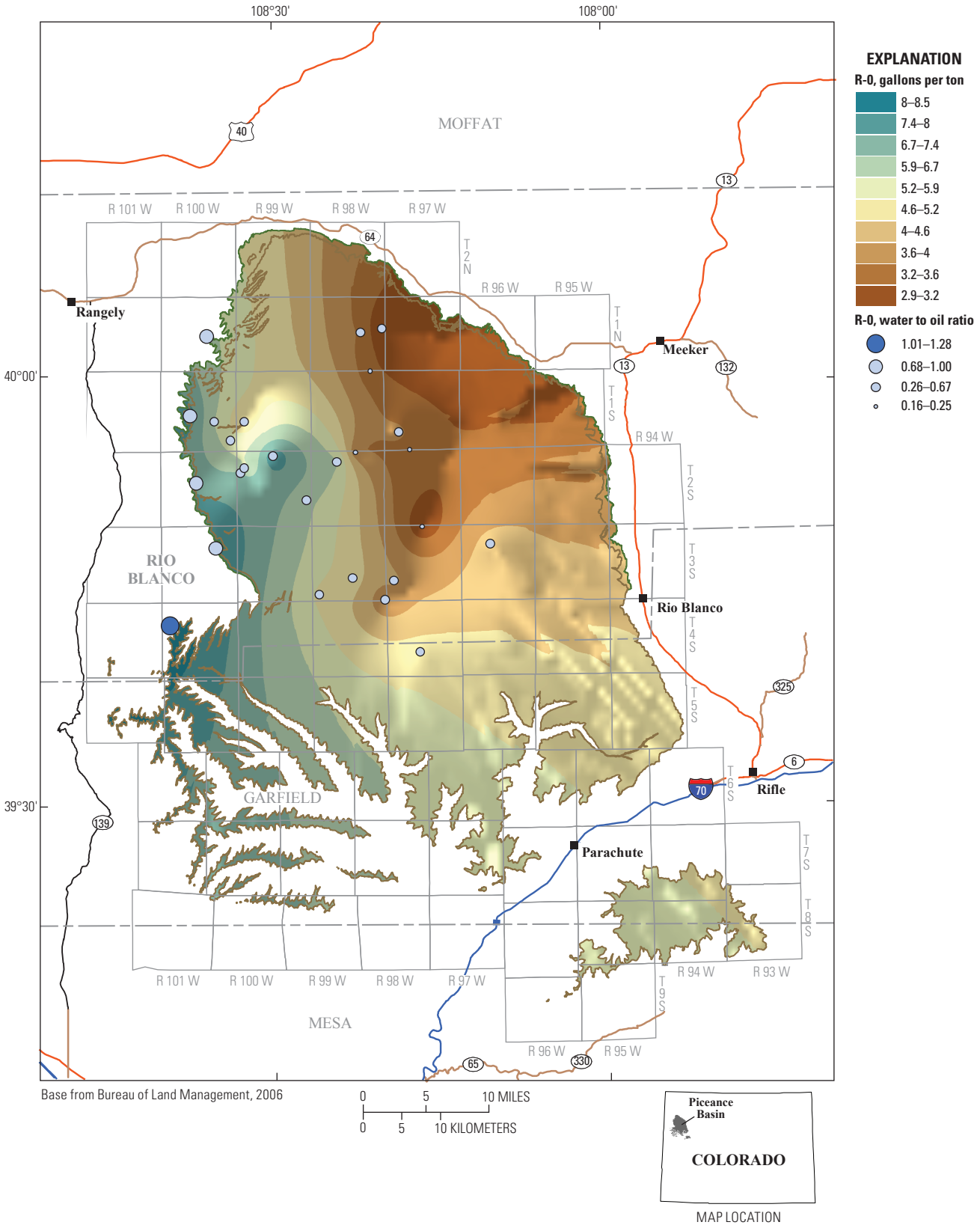

Figure 13. Variation in gallons of water per ton of oil shale (GPTW) for the R-0 oil-shale zone, Piceance Basin, Colo. A hillshade function was applied to visually enhance the displayed contours, creating the illusion that the map is three dimensional. Bubbles indicate the ratio of water to oil produced for the R-0 zone at each of the utilized control points.

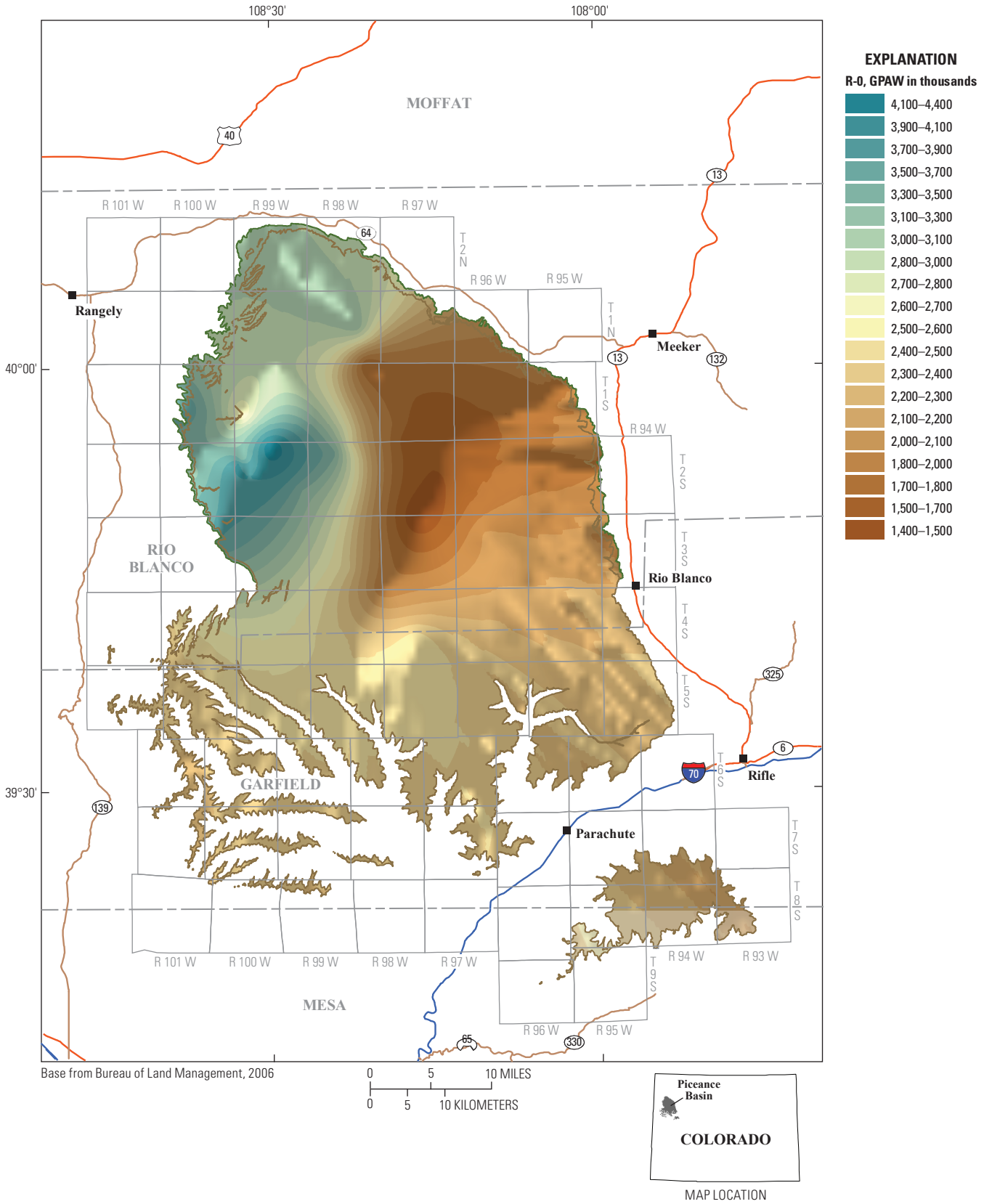

Figure 14. Variations in gallons of water per acre (GPAW) for the R-0 oil-shale zone, Piceance Basin, Colo. A hillshade function was applied to visually enhance the displayed contours, creating the illusion that the maps are three dimensional.

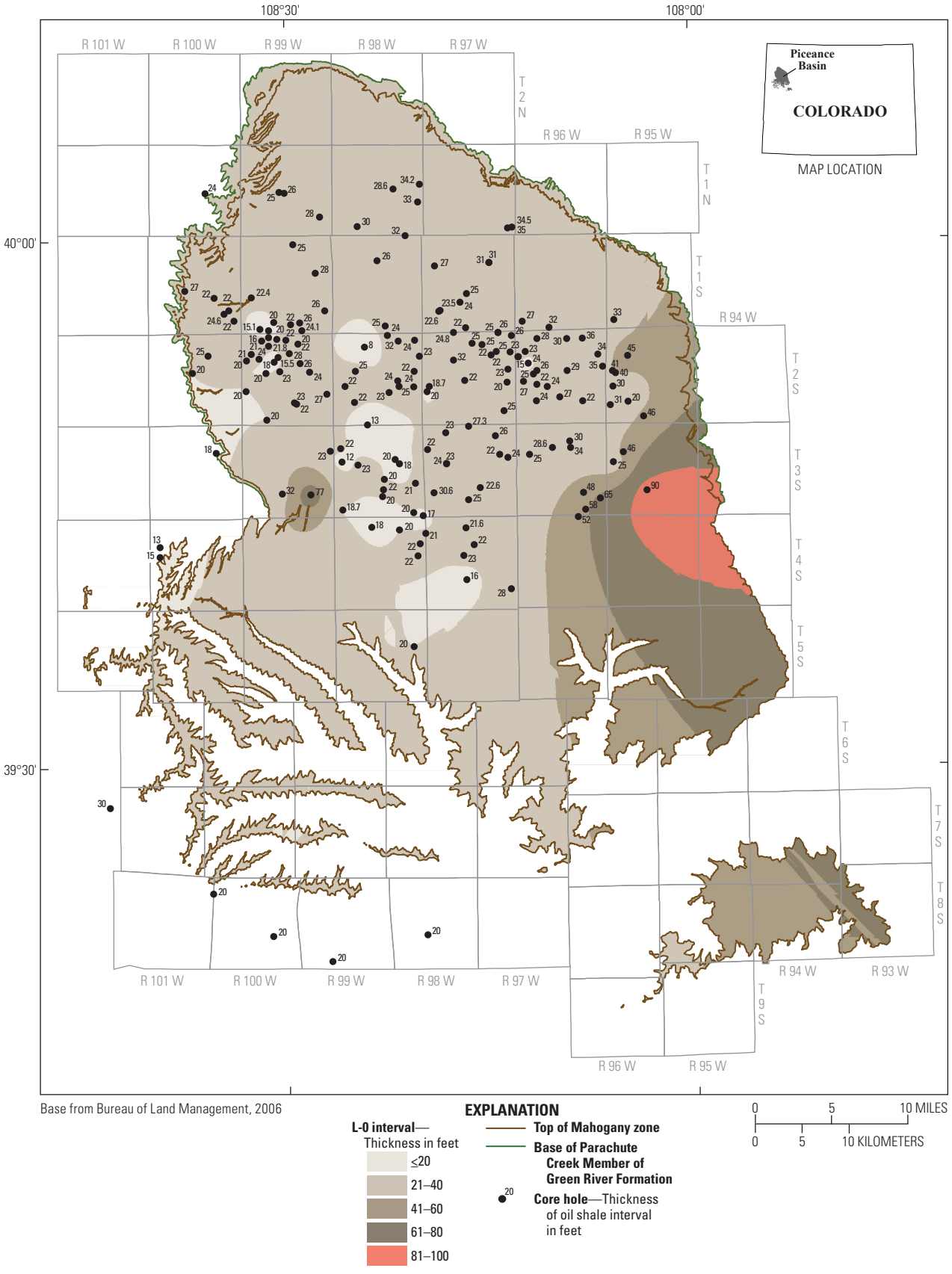

Figure 15. L-0 zone, Piceance Basin, Colo., using both core-hole and rotary-hole data. The Radial Basis Function Method (RBF) was used for contouring.

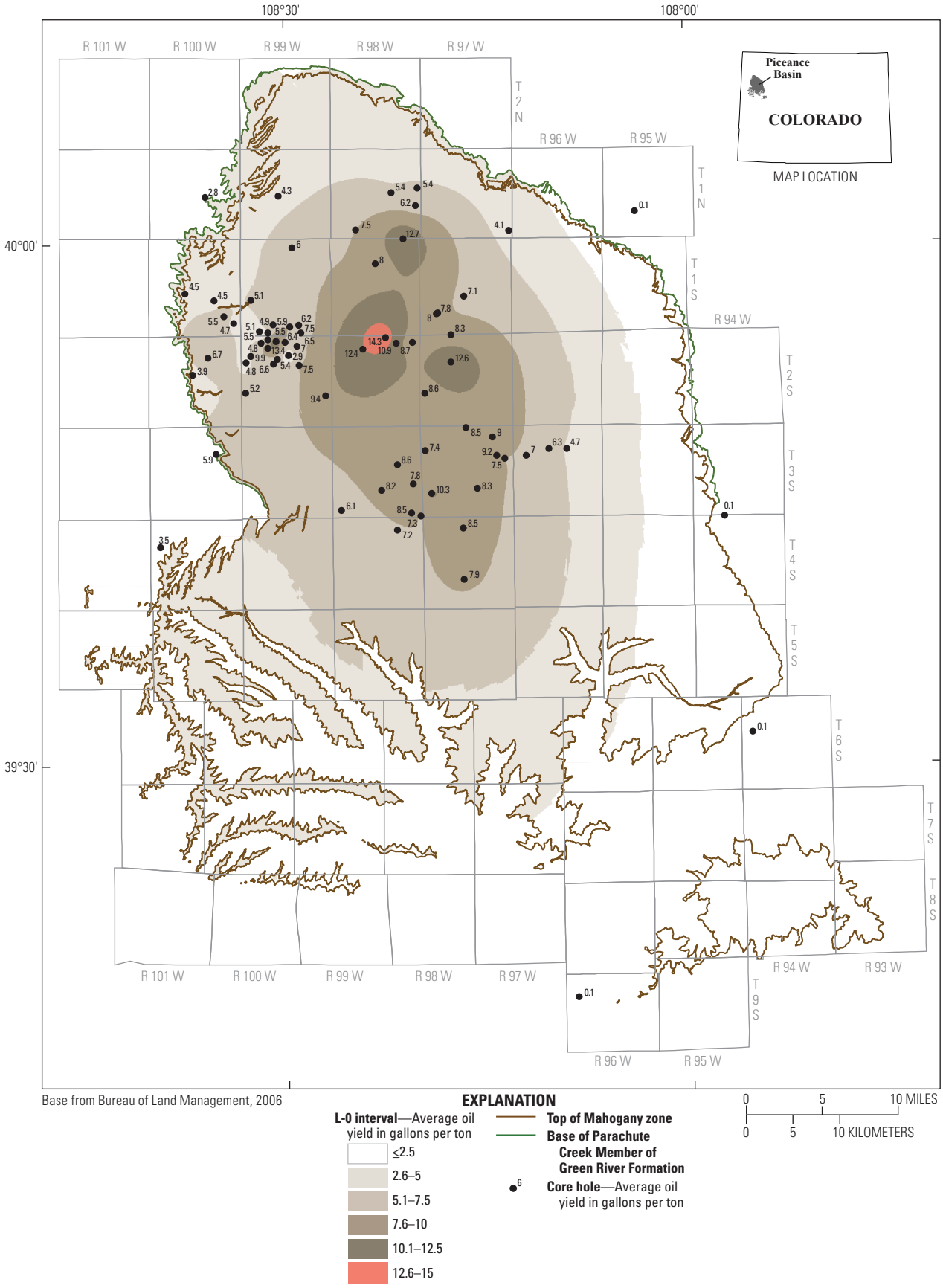

Figure 16. L-0 zone, Piceance Basin, Colo., showing the oil yield in gallons per ton (GPT). The Radial Basis Function Method (RBF) was used for contouring.

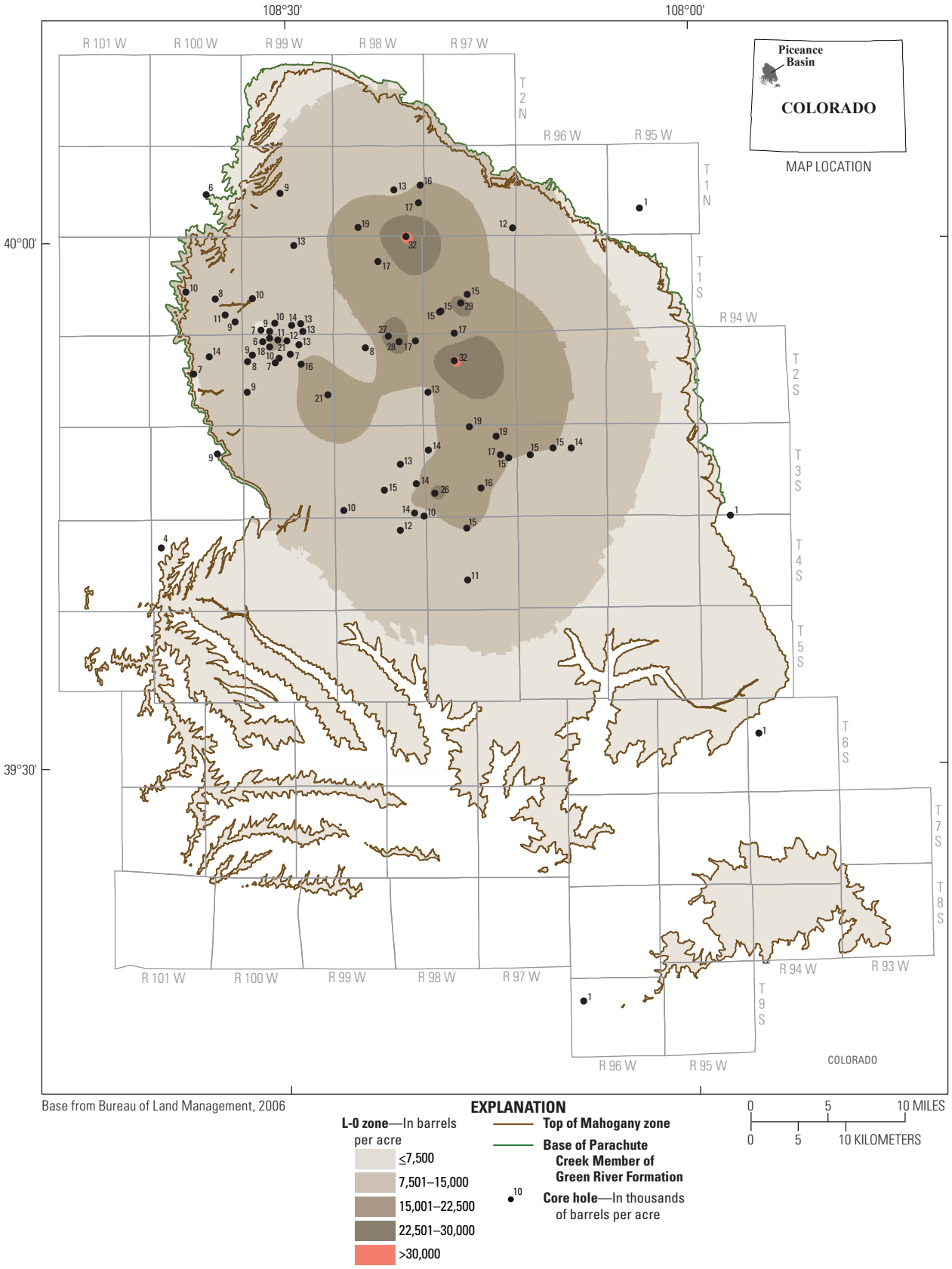

Figure 17. L-0 zone, Piceance Basin, Colo., showing oil yields in barrels per acre (BPA). The Radial Basis Function Method (RBF) was used for contouring.

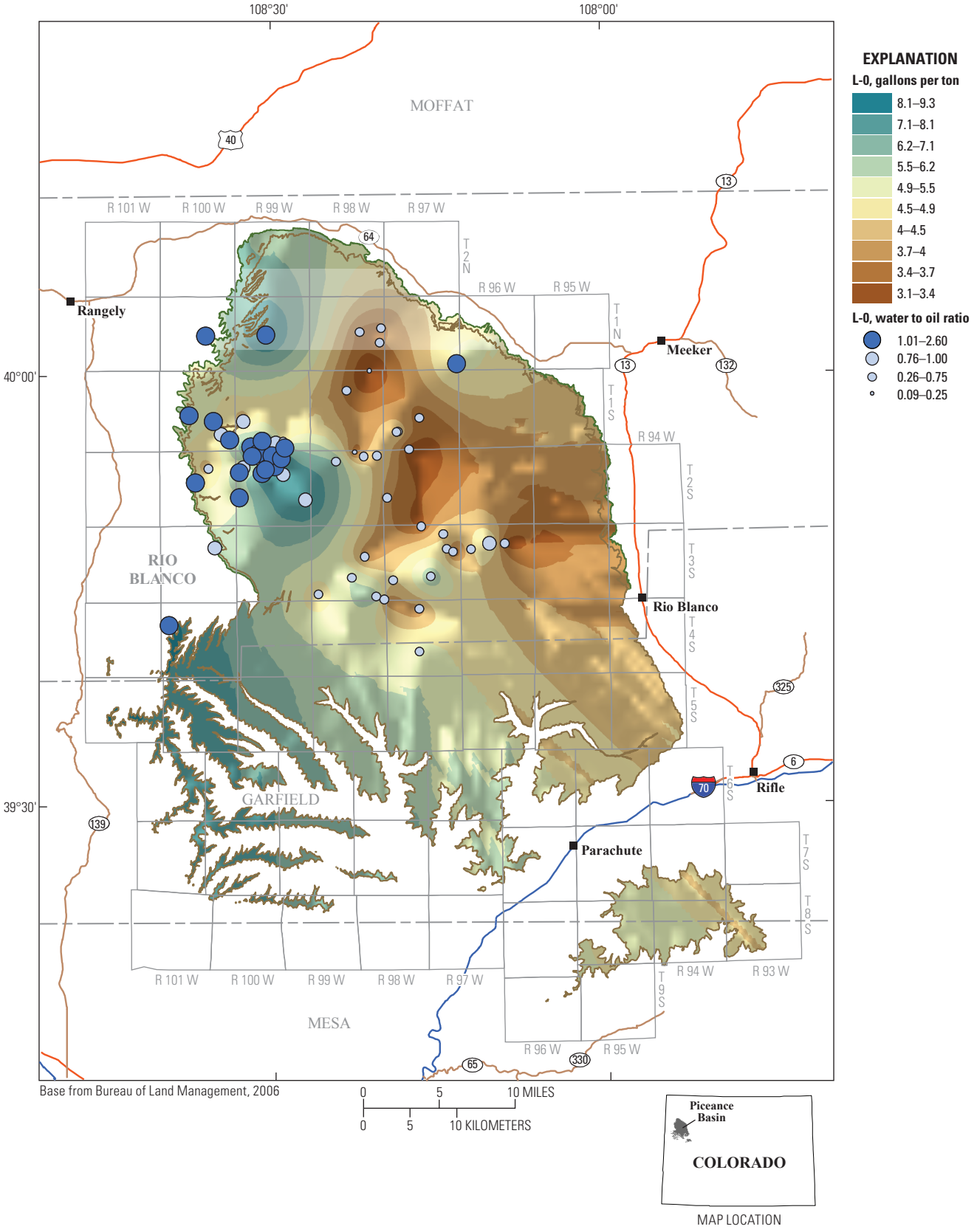

Figure 18. Variation in gallons of water per ton of oil shale (GPTW) for the L-0 oil-shale zone, Piceance Basin, Colo. A hillshade function was applied to visually enhance the displayed contours, creating the illusion that the maps are three dimensional. Bubbles indicate the ratio of water to oil produced for the L-0 zone at each of the utilized control points.

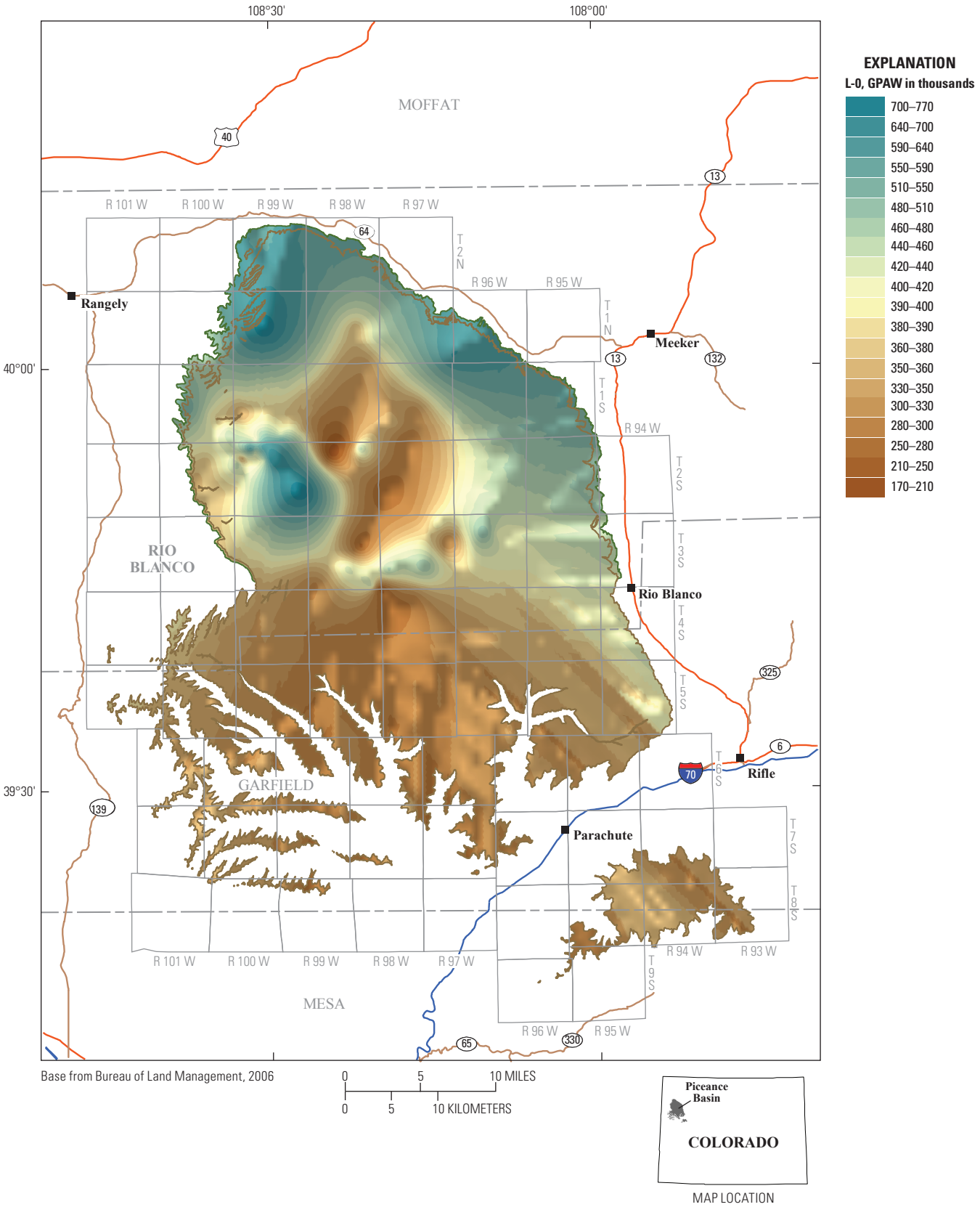

Figure 19. Variations in gallons of water per acre (GPAW) for the L-0 oil-shale zone, Piceance Basin, Colo. A hillshade function was applied to visually enhance the displayed contours, creating the illusion that the maps are three dimensional.

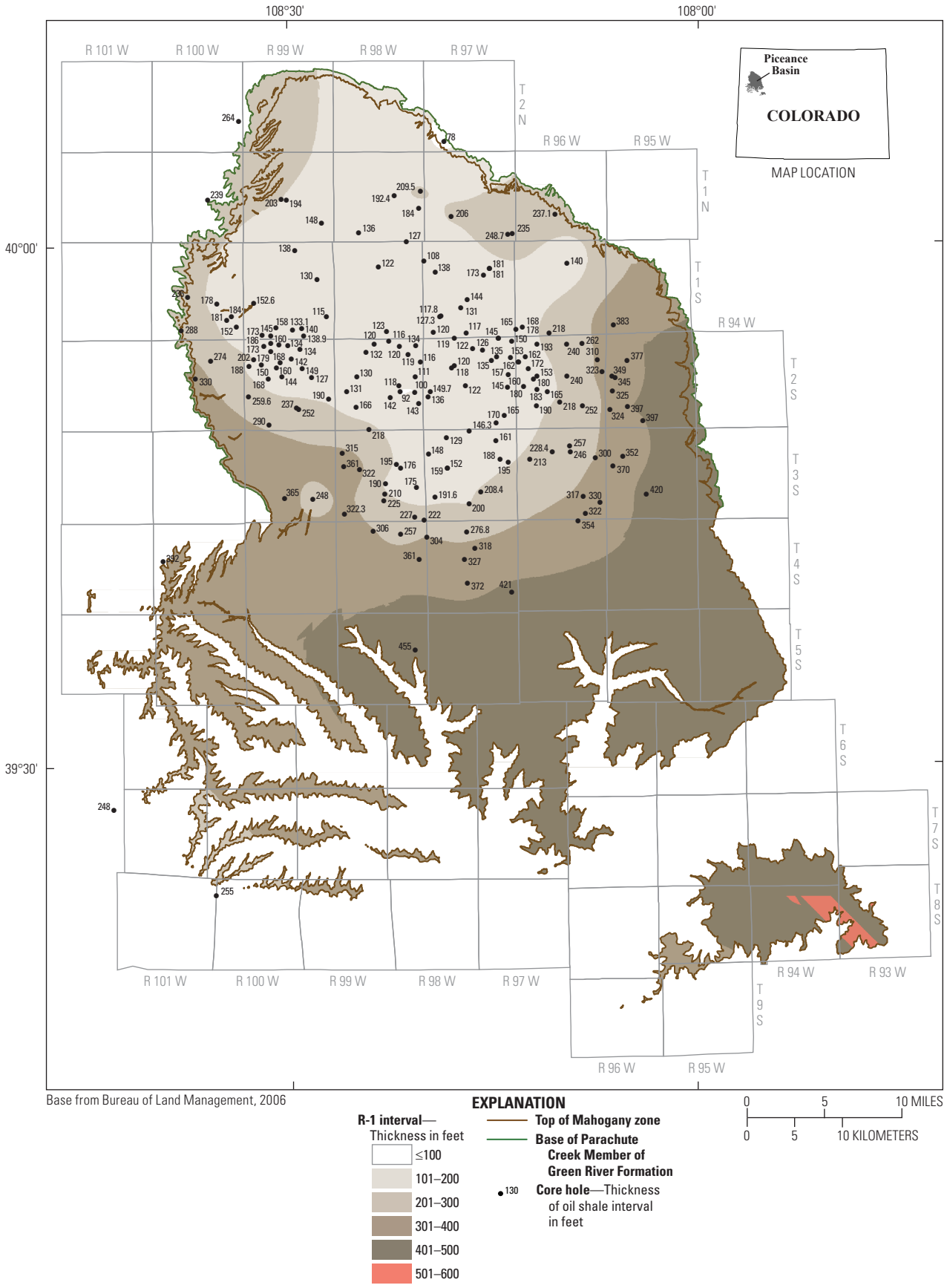

Figure 20. R-1 zone, Piceance Basin, Colo., using both core-hole and rotary-hole data. The Radial Basis Function Method (RBF) was used for contouring.

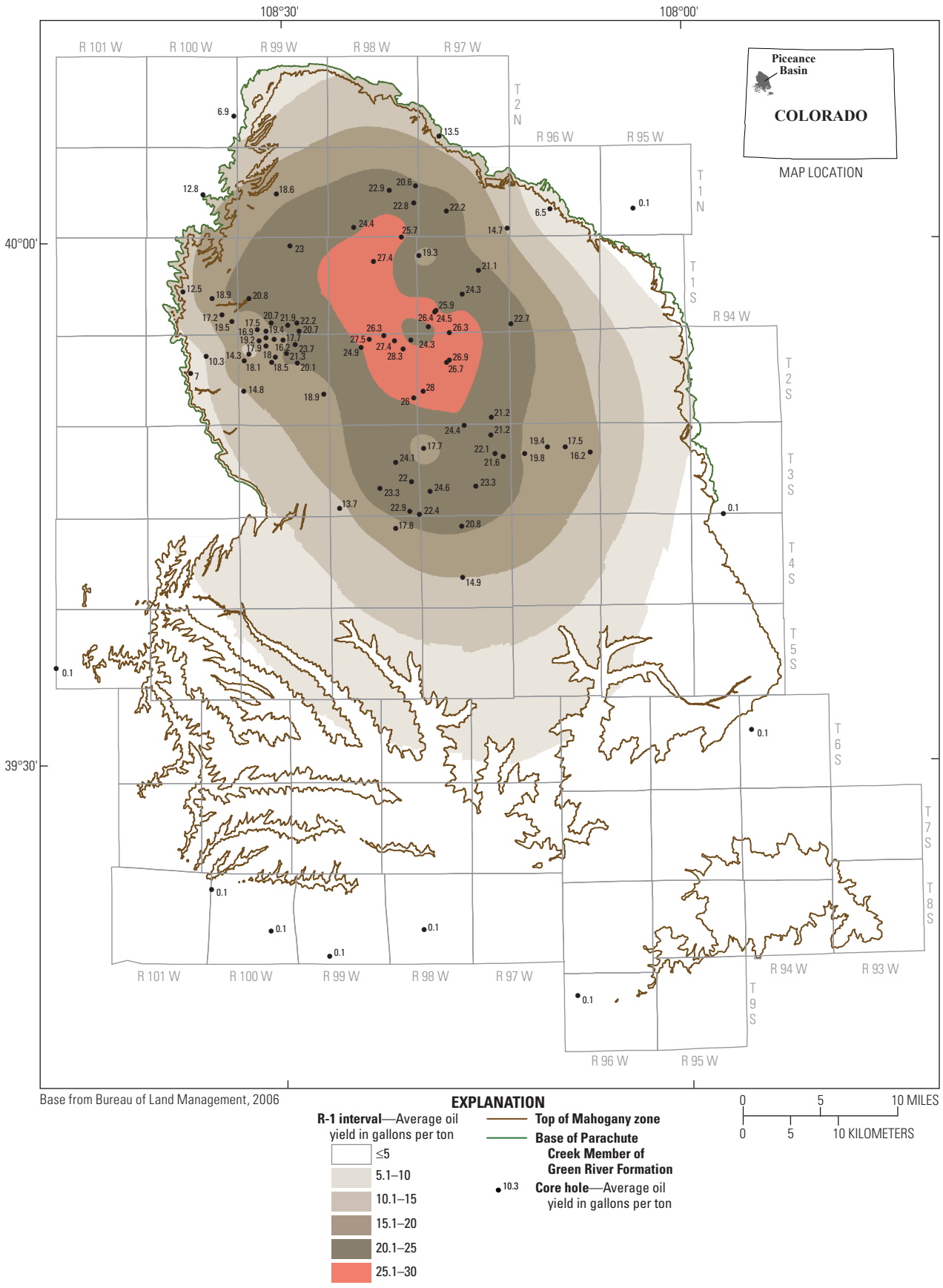

Figure 21. R-1 zone, Piceance Basin, Colo., showing the oil yield in gallons per ton (GPT). The Radial Basis Function Method (RBF) was used for contouring.

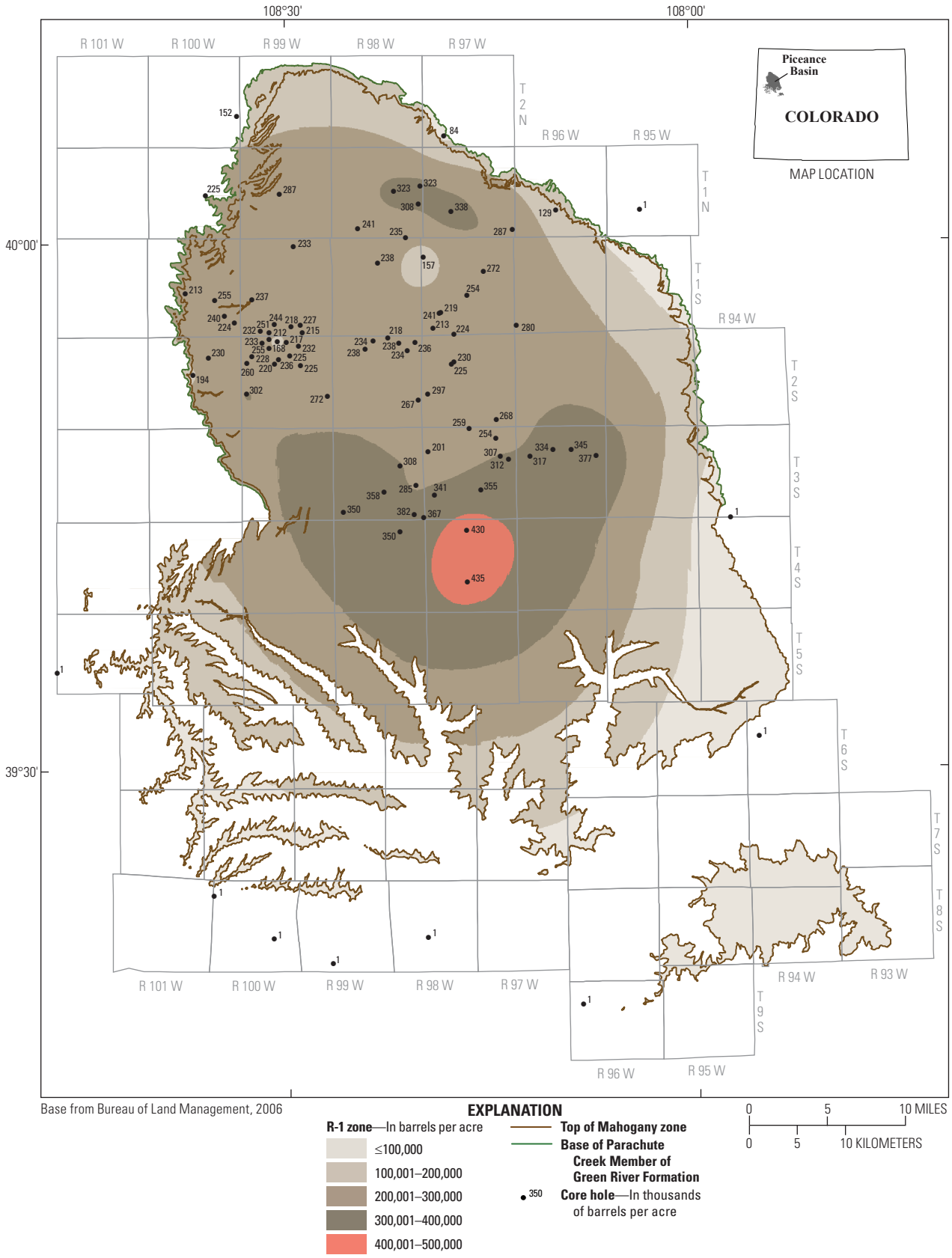

Figure 22. R-1 zone, Piceance Basin, Colo., showing oil yields in barrels per acre (BPA). The Radial Basis Function Method (RBF) was used for contouring.

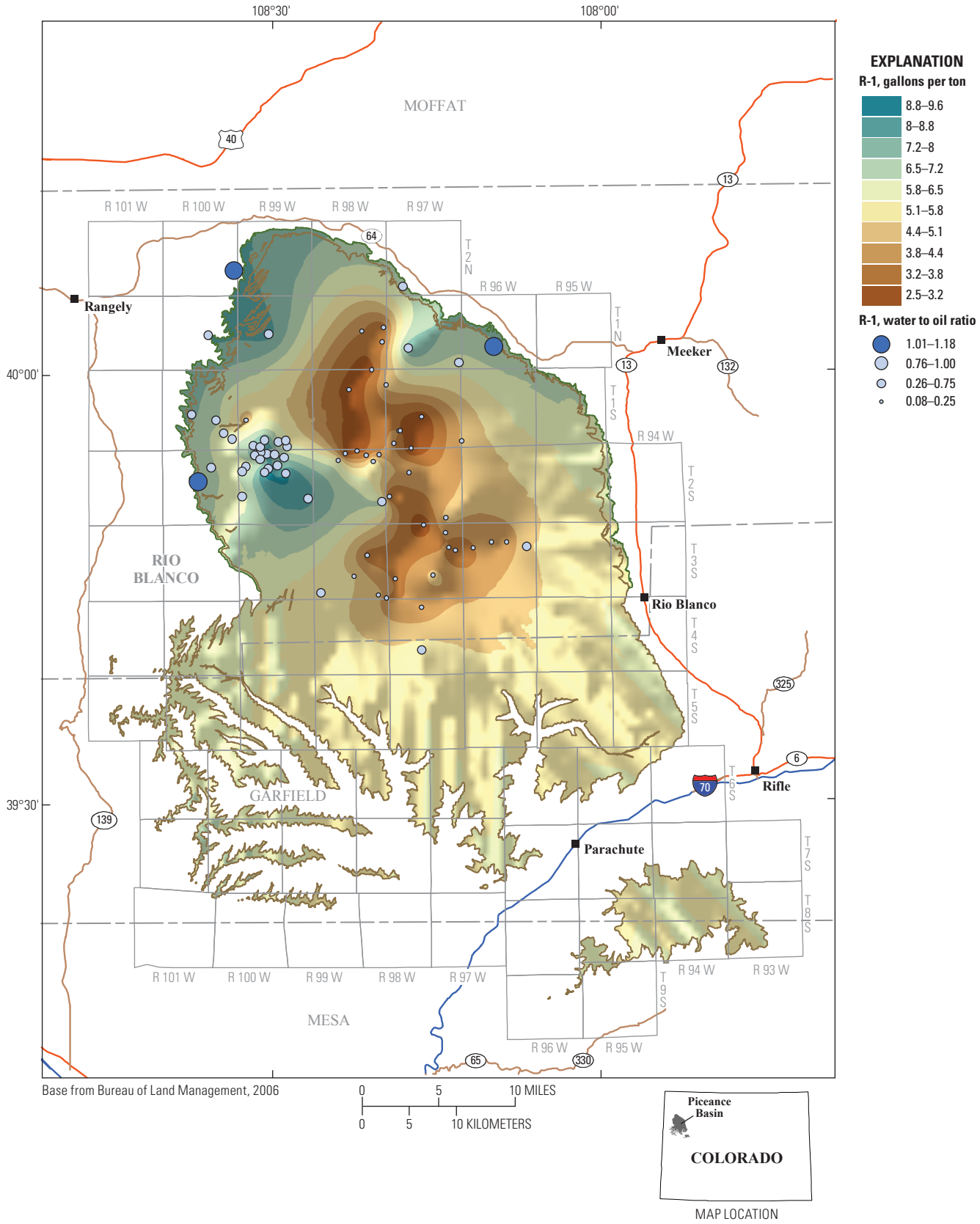

Figure 23. Variation in gallons of water per ton of oil shale (GPTW) for the R-1 oil-shale zone, Piceance Basin, Colo. A hillshade function was applied to visually enhance the displayed contours, creating the illusion that the maps are three dimensional. Bubbles indicate the ratio of water to oil produced for the R-1 zone at each of the utilized control points.

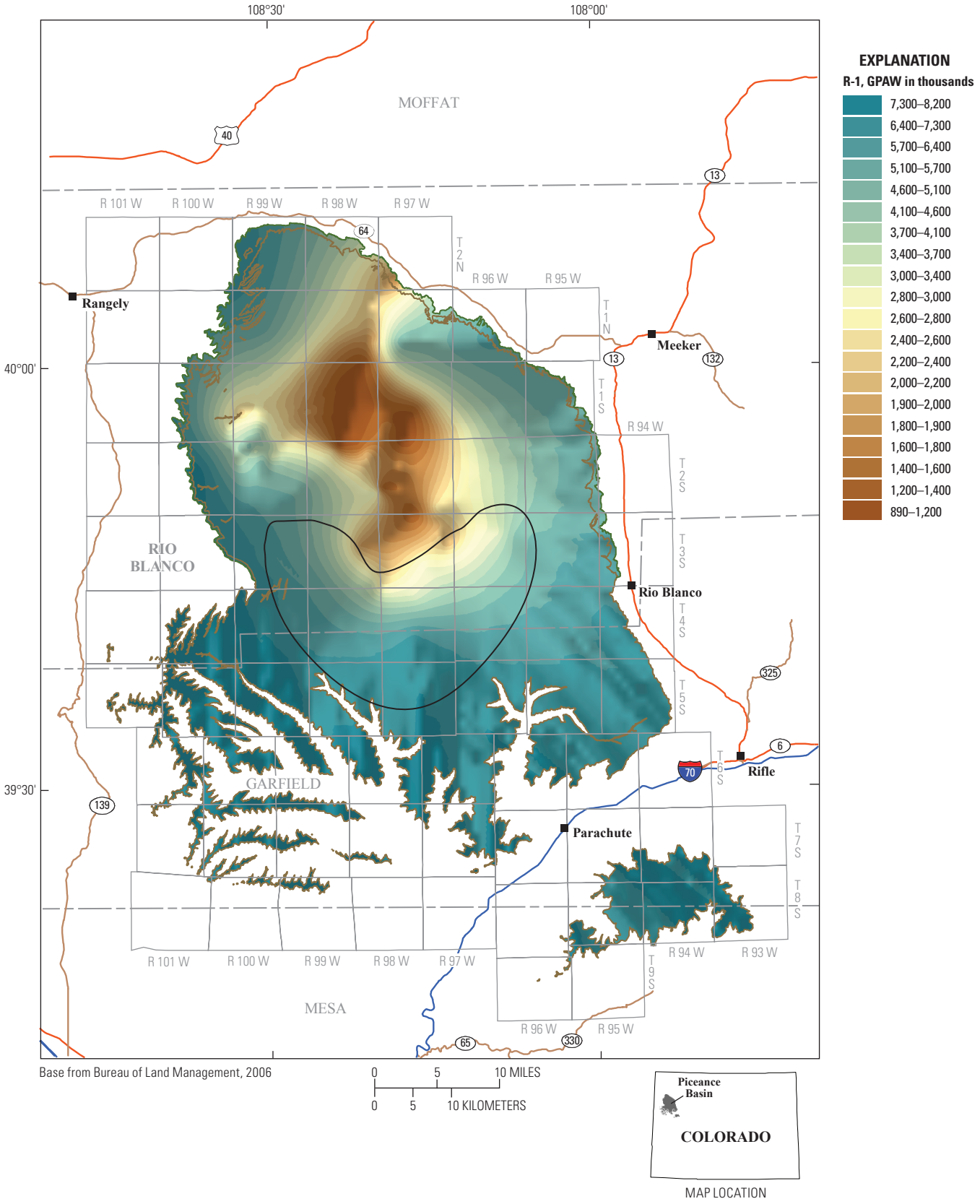

Figure 24. Variations in gallons of water per acre (GPAW) for the R-1 oil shale zone, Piceance Basin, Colo. A hillshade function was applied to visually enhance the displayed contours, creating the illusion that the maps are three dimensional. Outlined area indicates maximum in-place oil shown on figure 22.

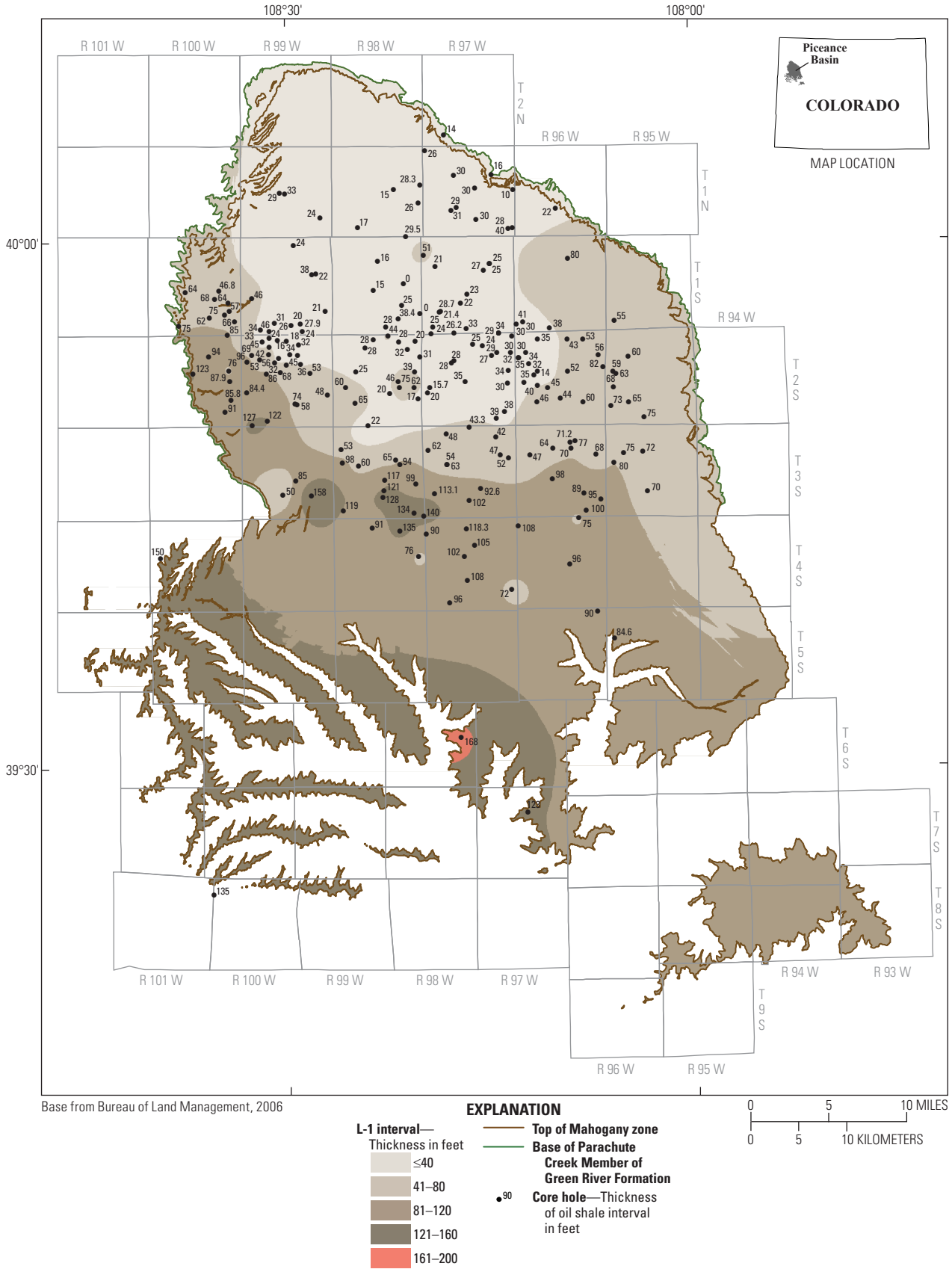

Figure 25. L-1 zone, Piceance Basin, Colo., using both core-hole and rotary-hole data. The Radial Basis Function Method (RBF) was used for contouring.

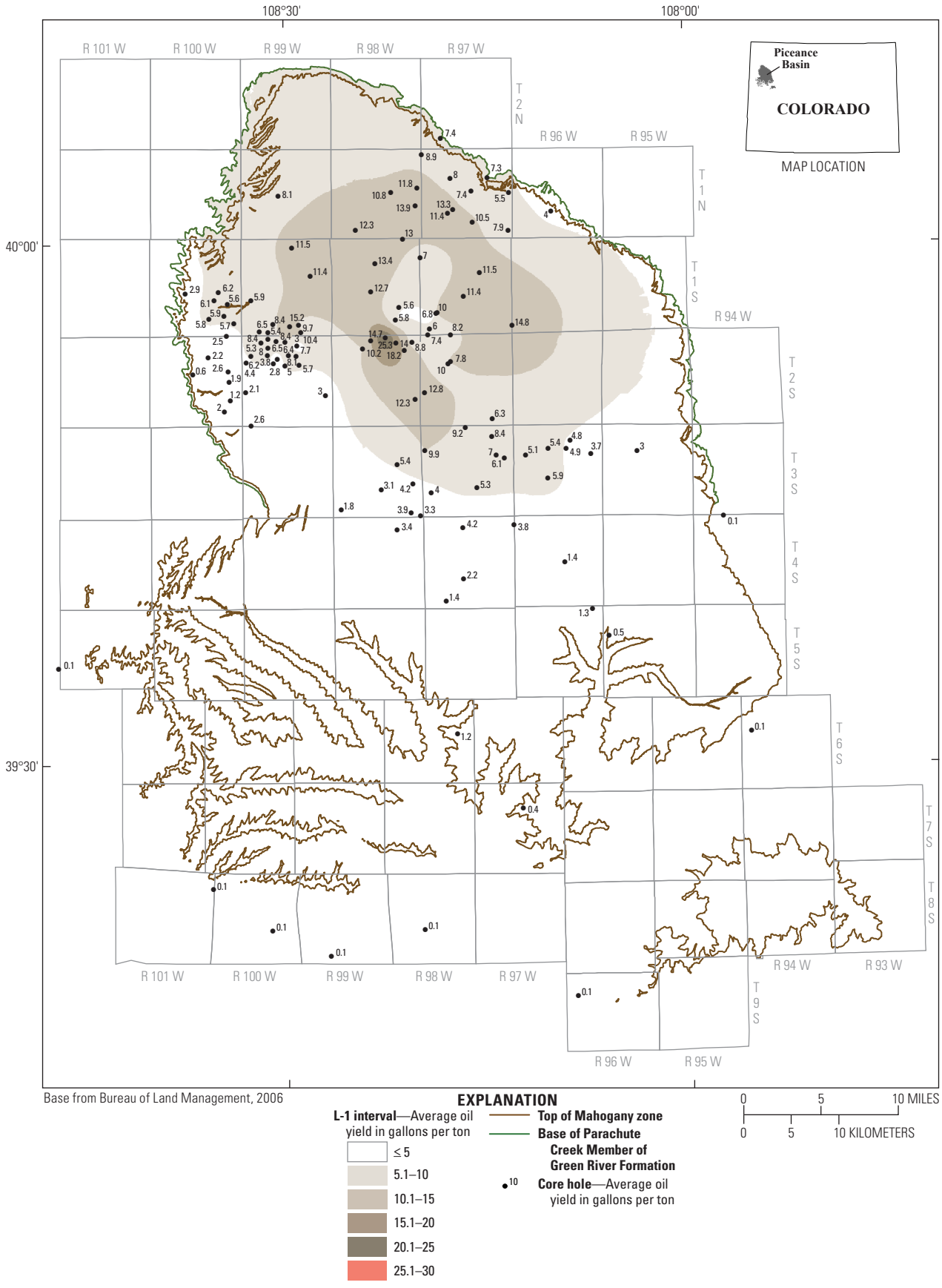

Figure 26. L-1 zone, Piceance Basin, Colo., showing the oil yield in gallons per ton (GPT). The Radial Basis Function Method (RBF) was used for contouring.

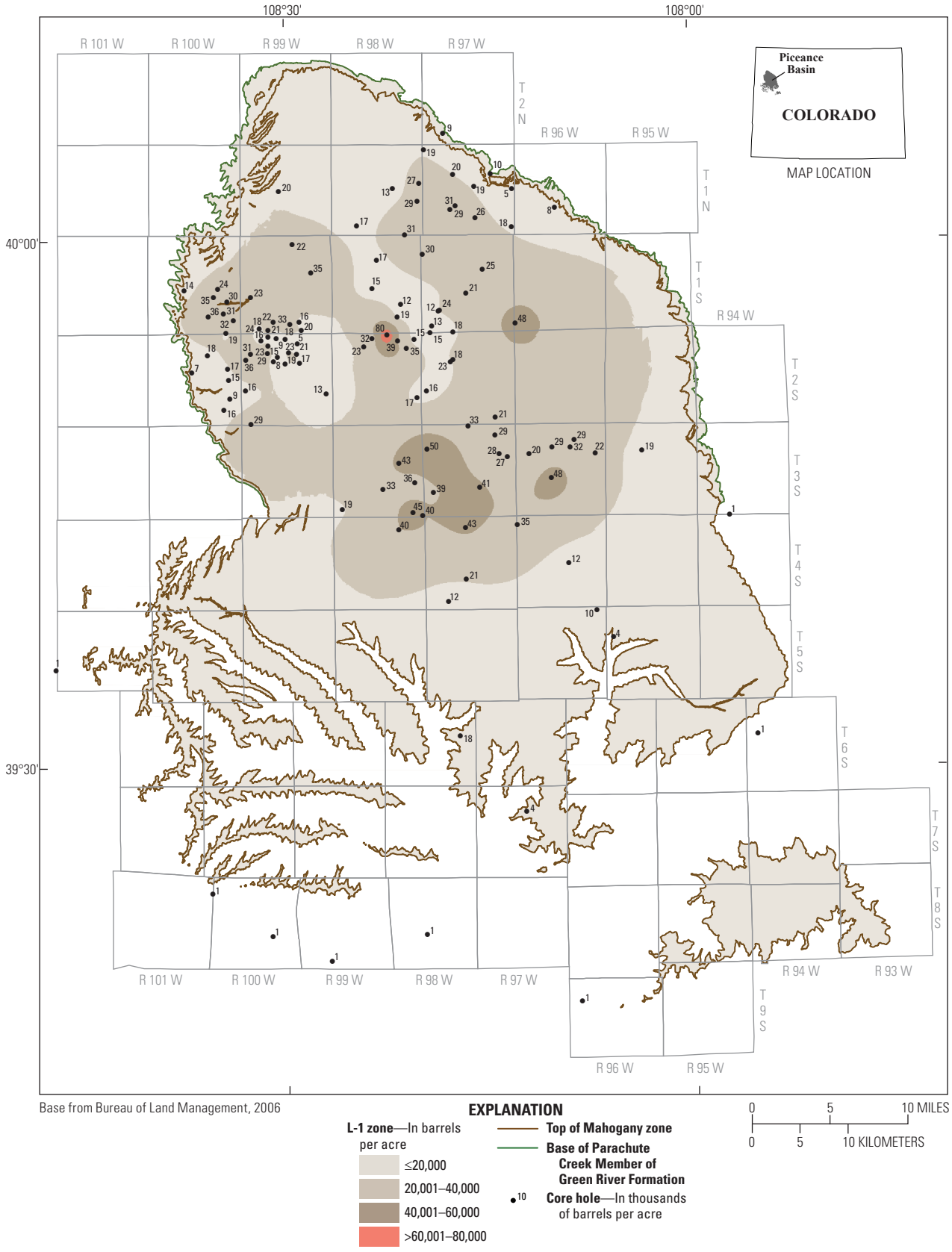

Figure 27. L-1 zone, Piceance Basin, Colo., showing oil yields in barrels per acre (BPA). The Radial Basis Function Method (RBF) was used for contouring.

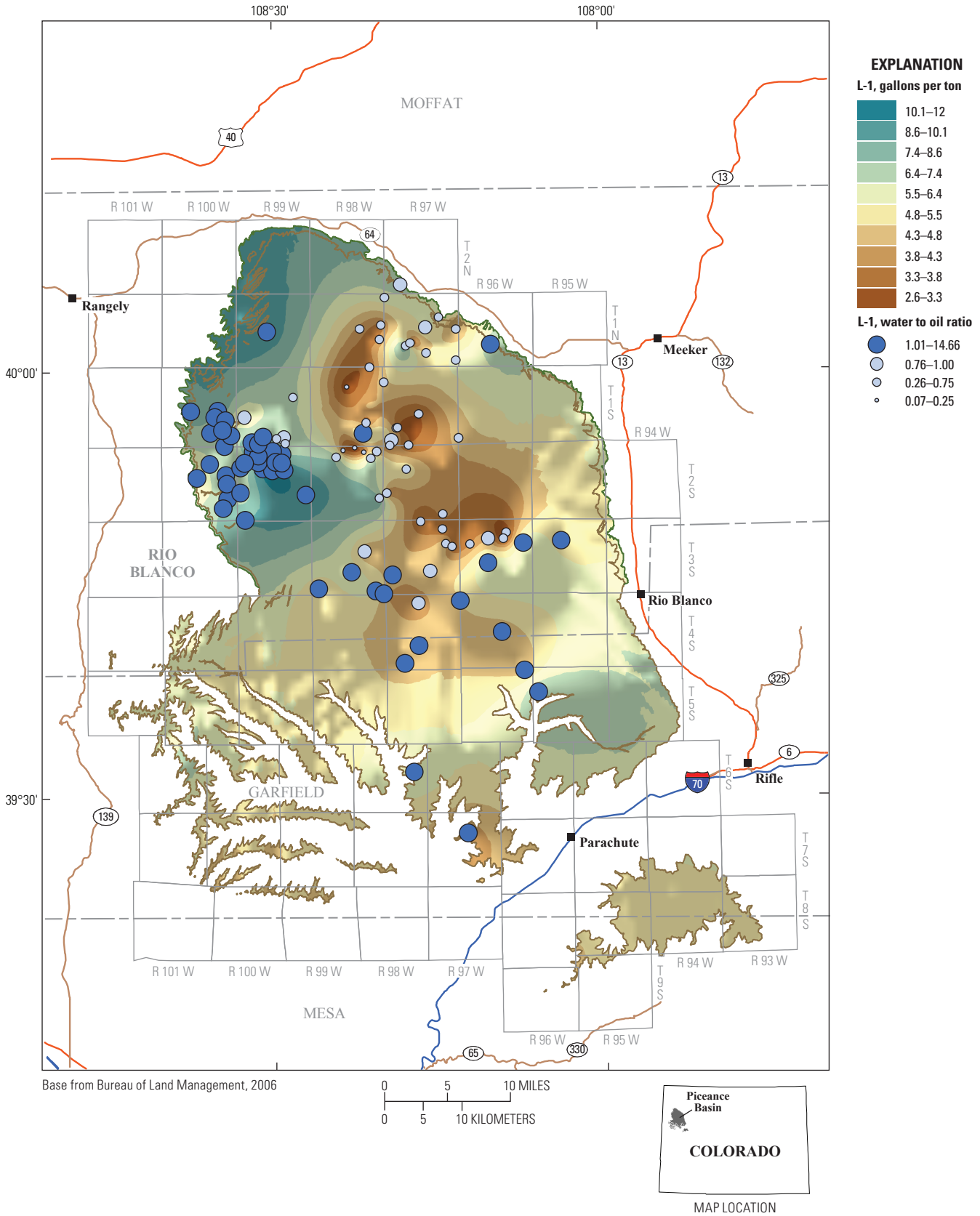

Figure 28. Variation in gallons of water per ton of oil shale (GPTW) for the L-1 oil-shale zone, Piceance Basin, Colo. A hillshade function was applied to visually enhance the displayed contours, creating the illusion that the maps are three dimensional. Bubbles indicate the ratio of water to oil produced for the L-1 zone at each of the utilized control points.

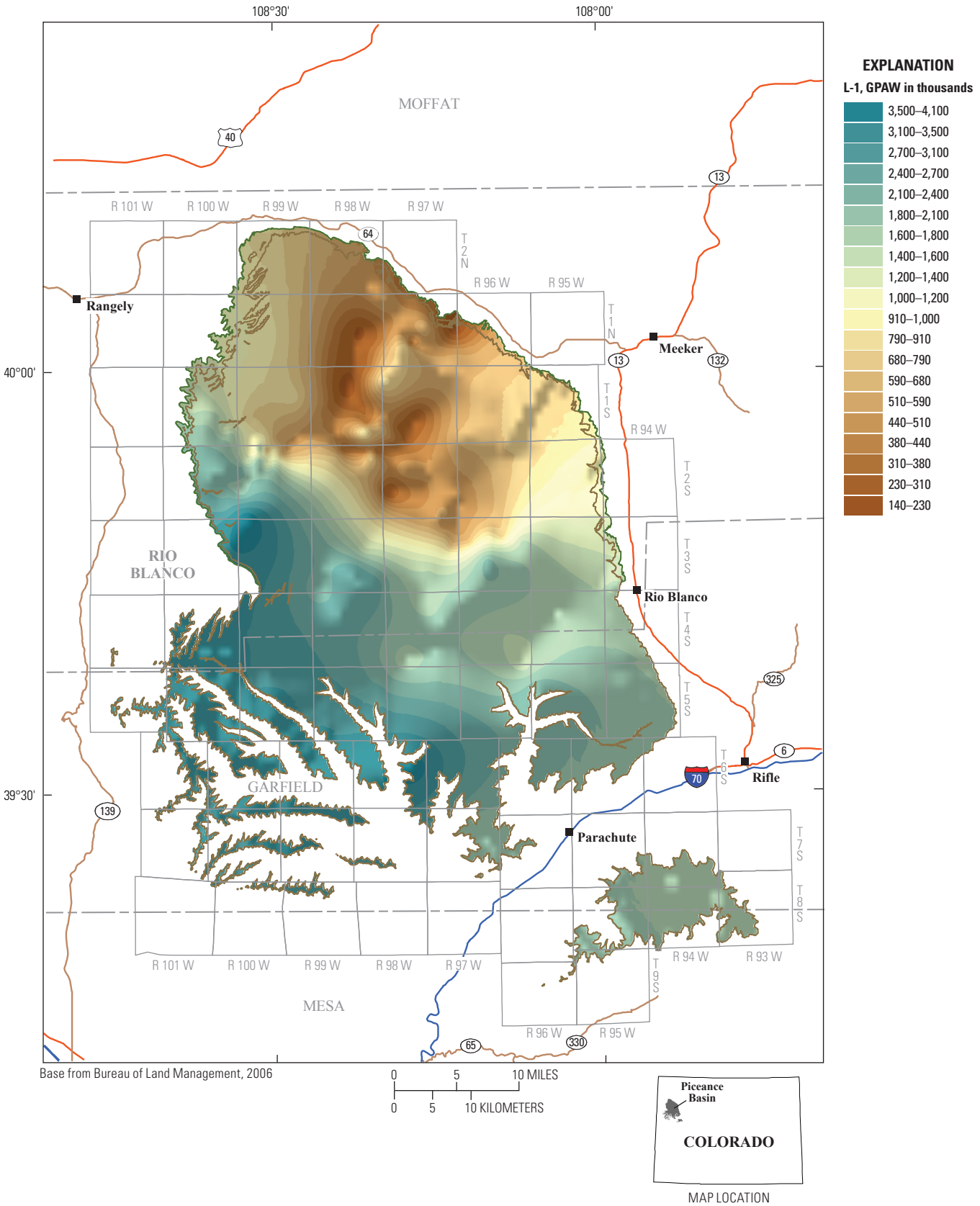

Figure 29. Variations in gallons of water per acre (GPAW) for the L-1 oil-shale zone, Piceance Basin, Colo. A hillshade function was applied to visually enhance the displayed contours, creating the illusion that the maps are three dimensional.

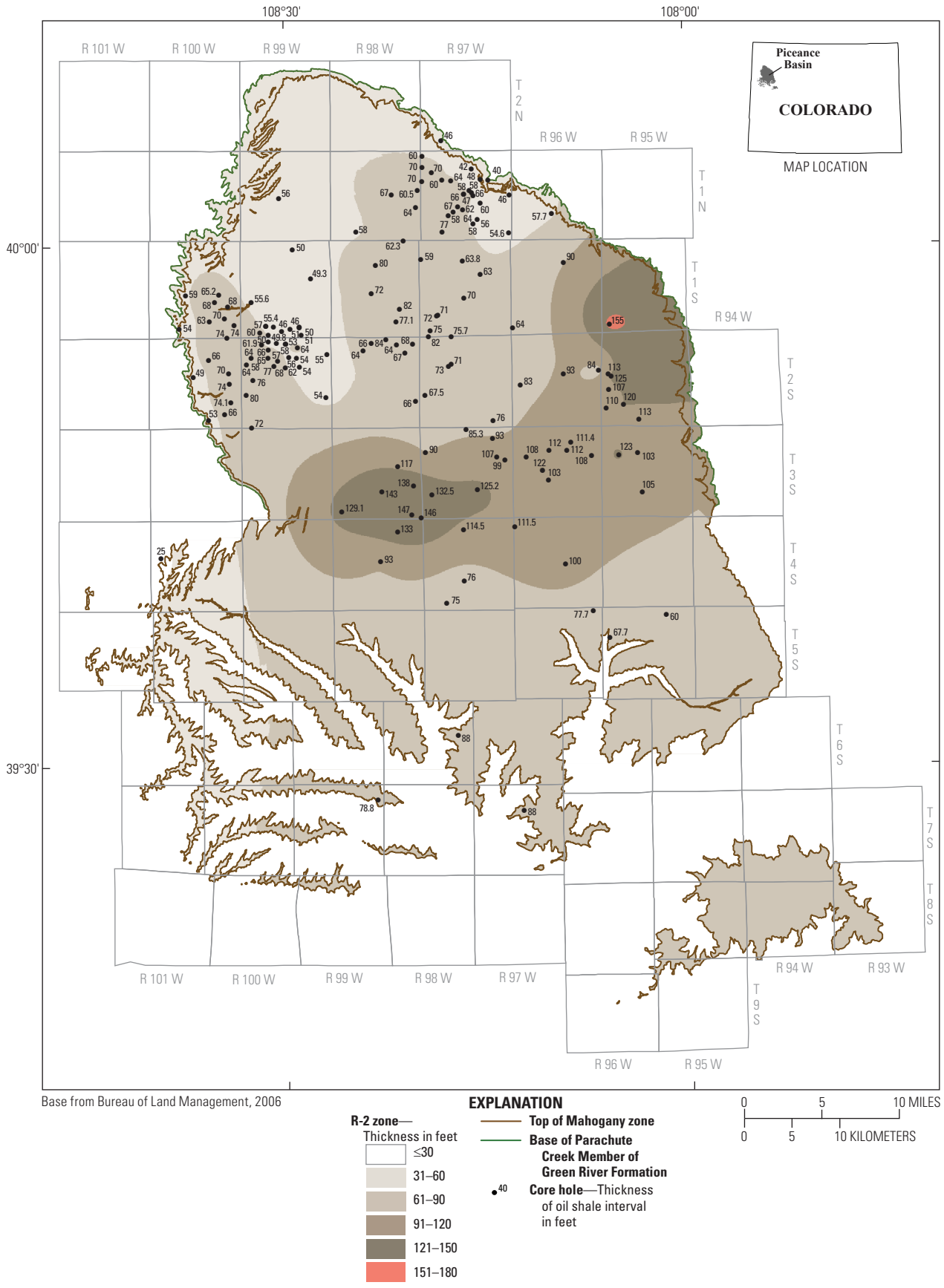

Figure 30. R-2 zone, Piceance Basin, Colo., using both core-hole and rotary-hole data. The Radial Basis Function Method (RBF) was used for contouring.

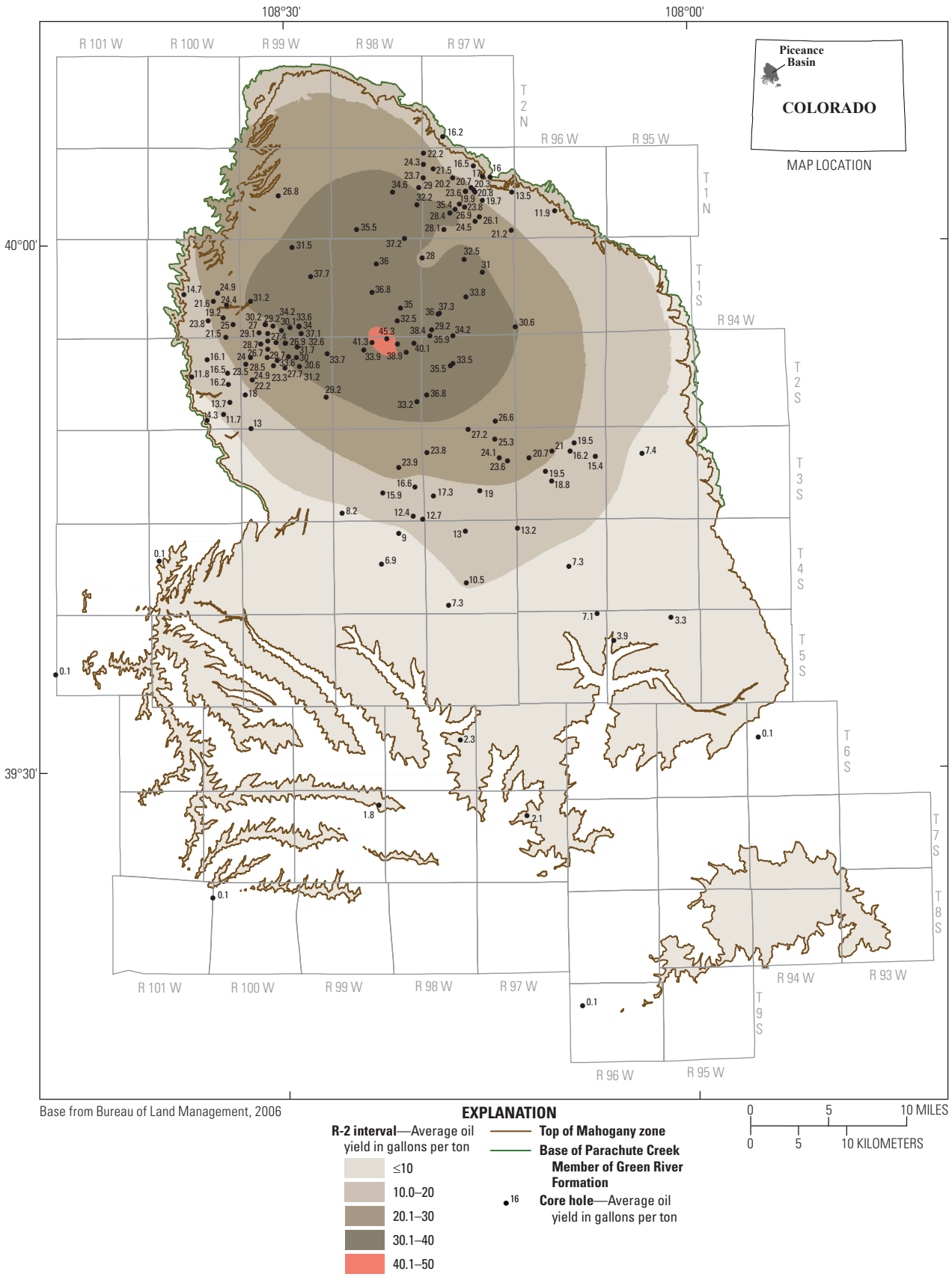

Figure 31. R-2 zone, Piceance Basin, Colo., showing the oil yield in gallons per ton (GPT) using only core-hole data. The Radial Basis Function Method (RBF) was used for contouring.

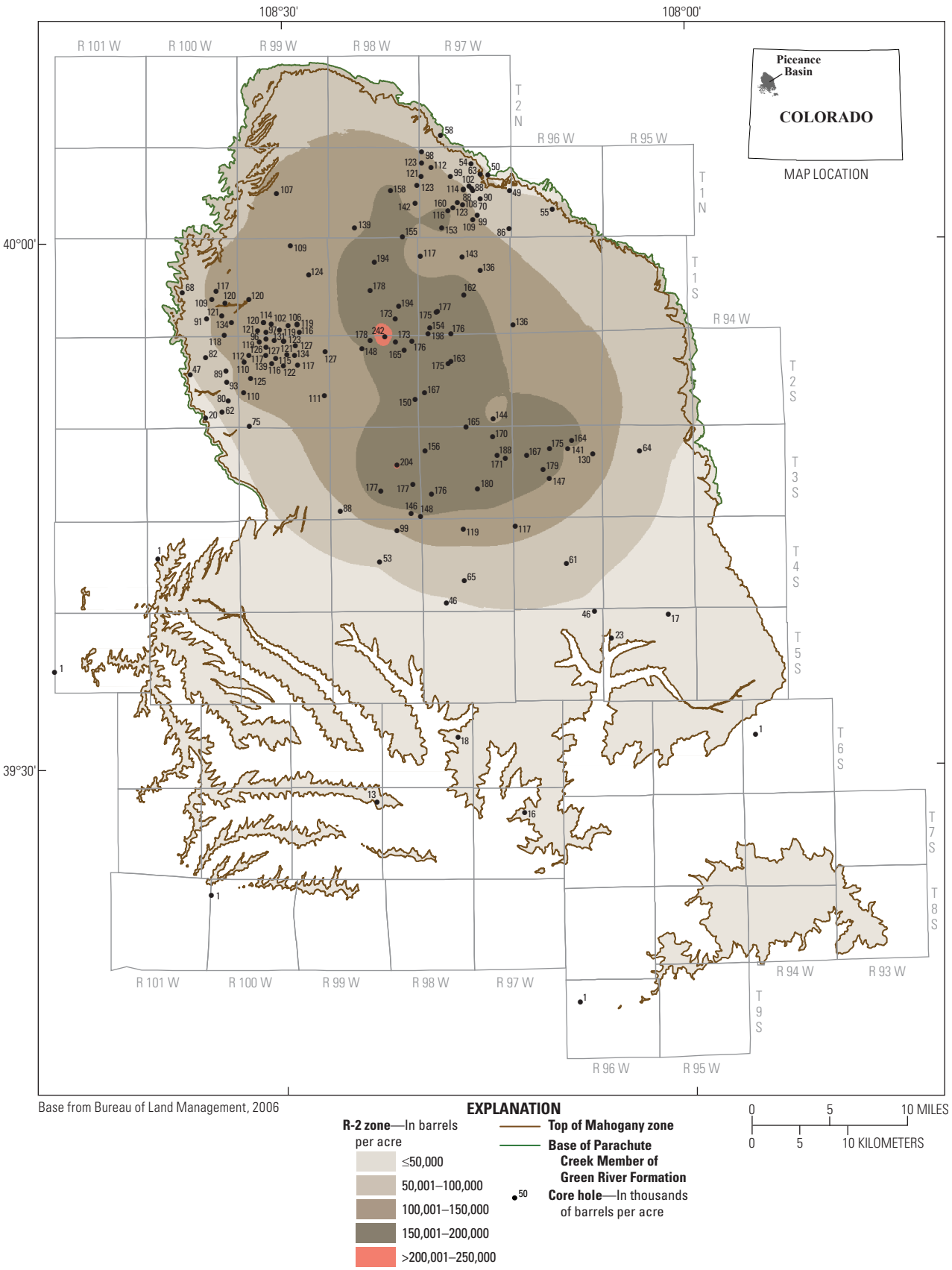

Figure 32. R-2 zone, Piceance Basin, Colo., showing oil yields in barrels per acre (BPA) using only core-hole data. The Radial Basis Function Method (RBF) was used for contouring.

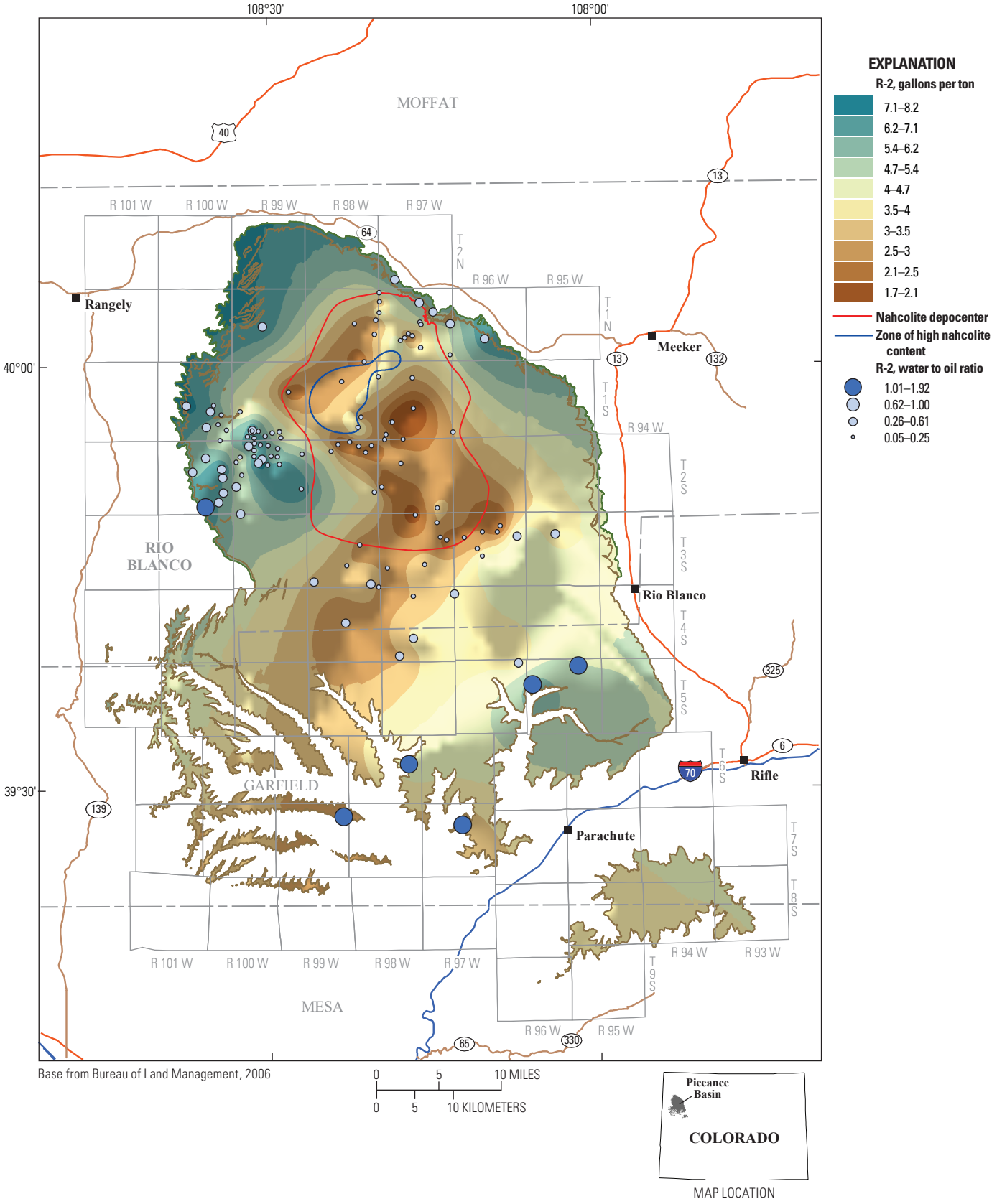

Figure 33. Variation in gallons of water per ton of oil shale (GPTW) for the R-2 oil-shale zone, Piceance Basin, Colo. A hillshade function was applied to visually enhance the displayed contours, creating the illusion that the maps are three dimensional. Bubbles indicate the ratio of water to oil produced for the R-0 zone at each of the utilized control points.

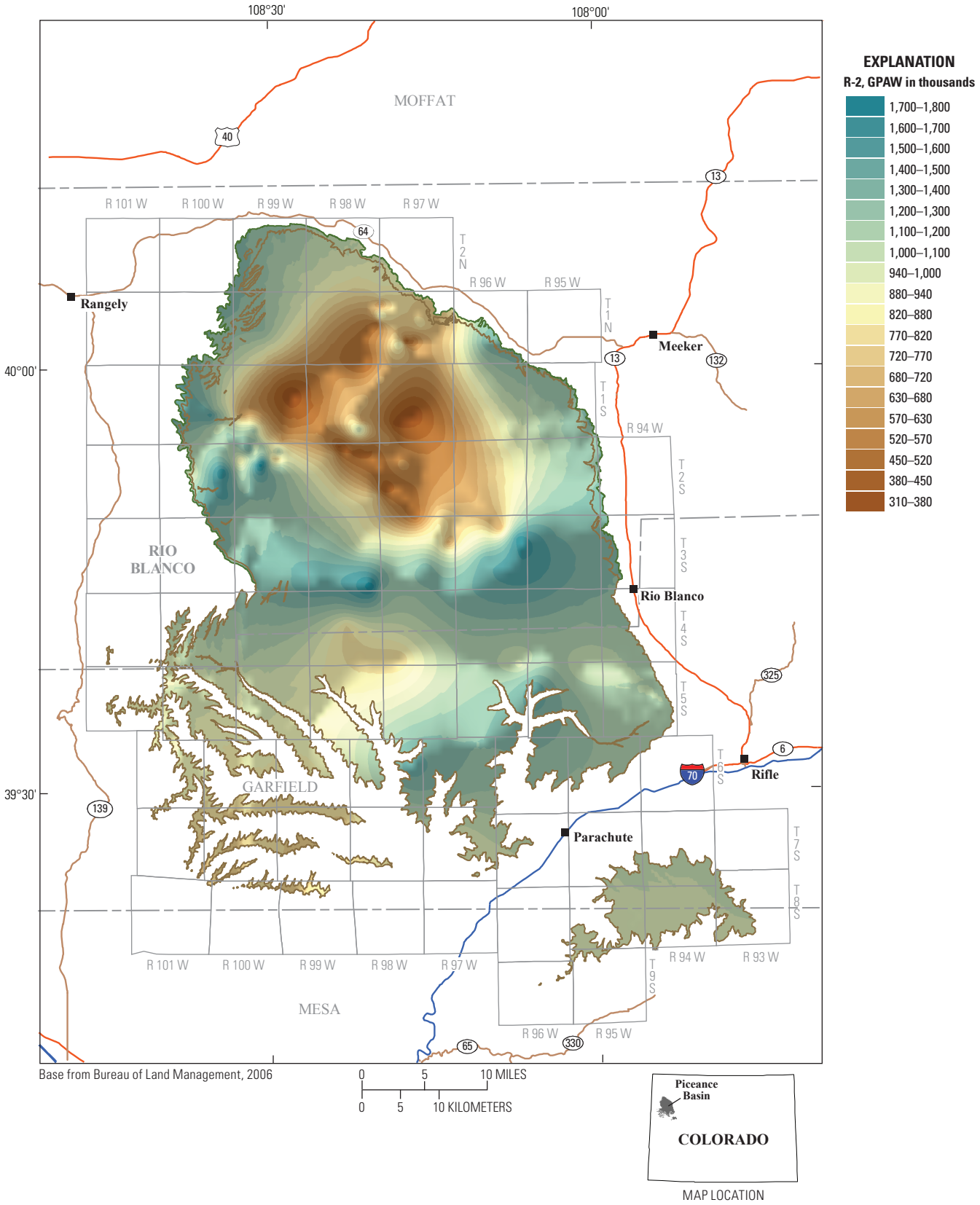

Figure 34. Variations in gallons of water per acre (GPAW) for the R-2 oil-shale zone, Piceance Basin, Colo. A hillshade function was applied to visually enhance the displayed contours, creating the illusion that the maps are three dimensional.

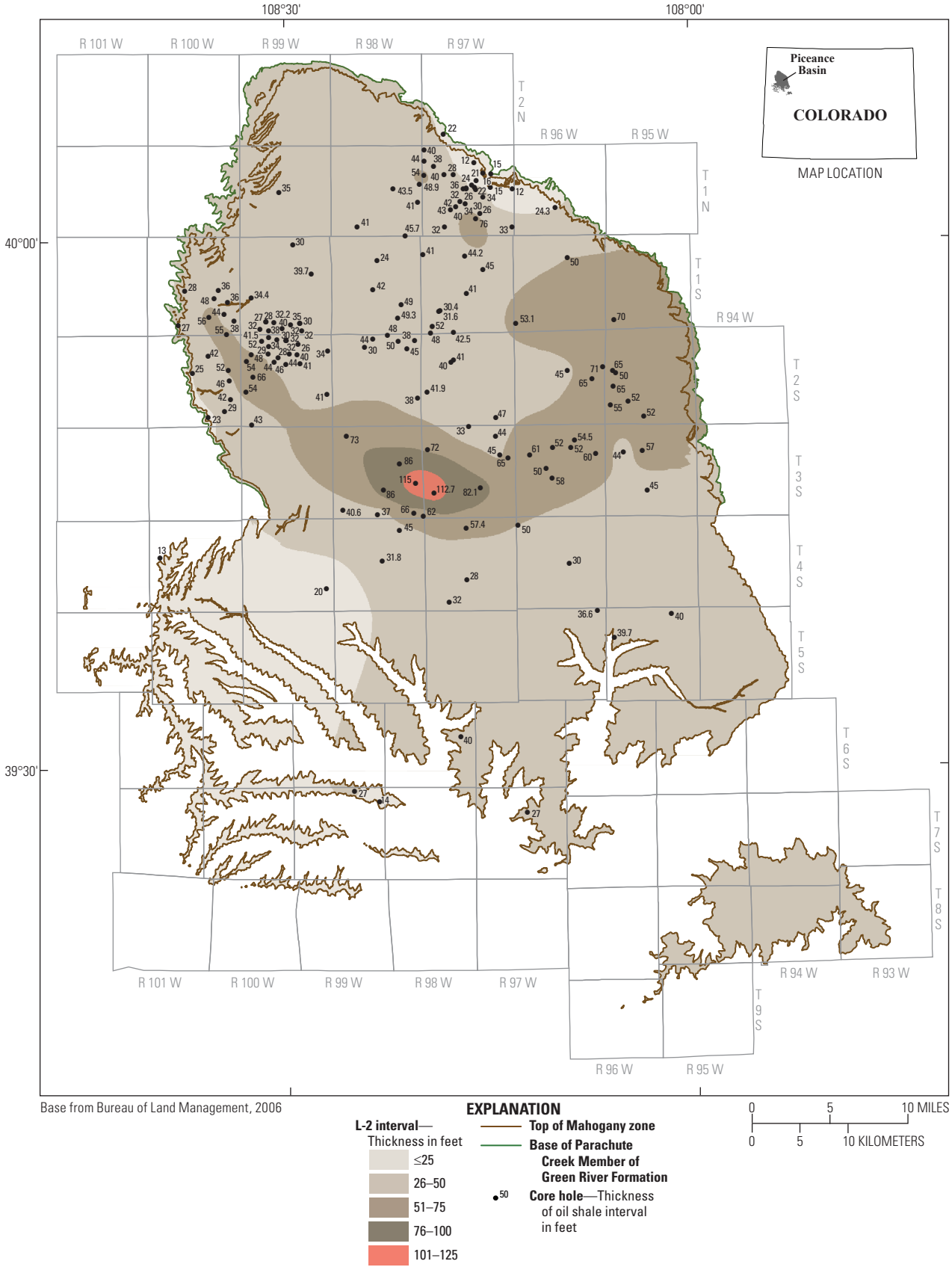

Figure 35. L-2 zone, Piceance Basin, Colo., constructed using the Radial Basis Function Method (RBF) for contouring.

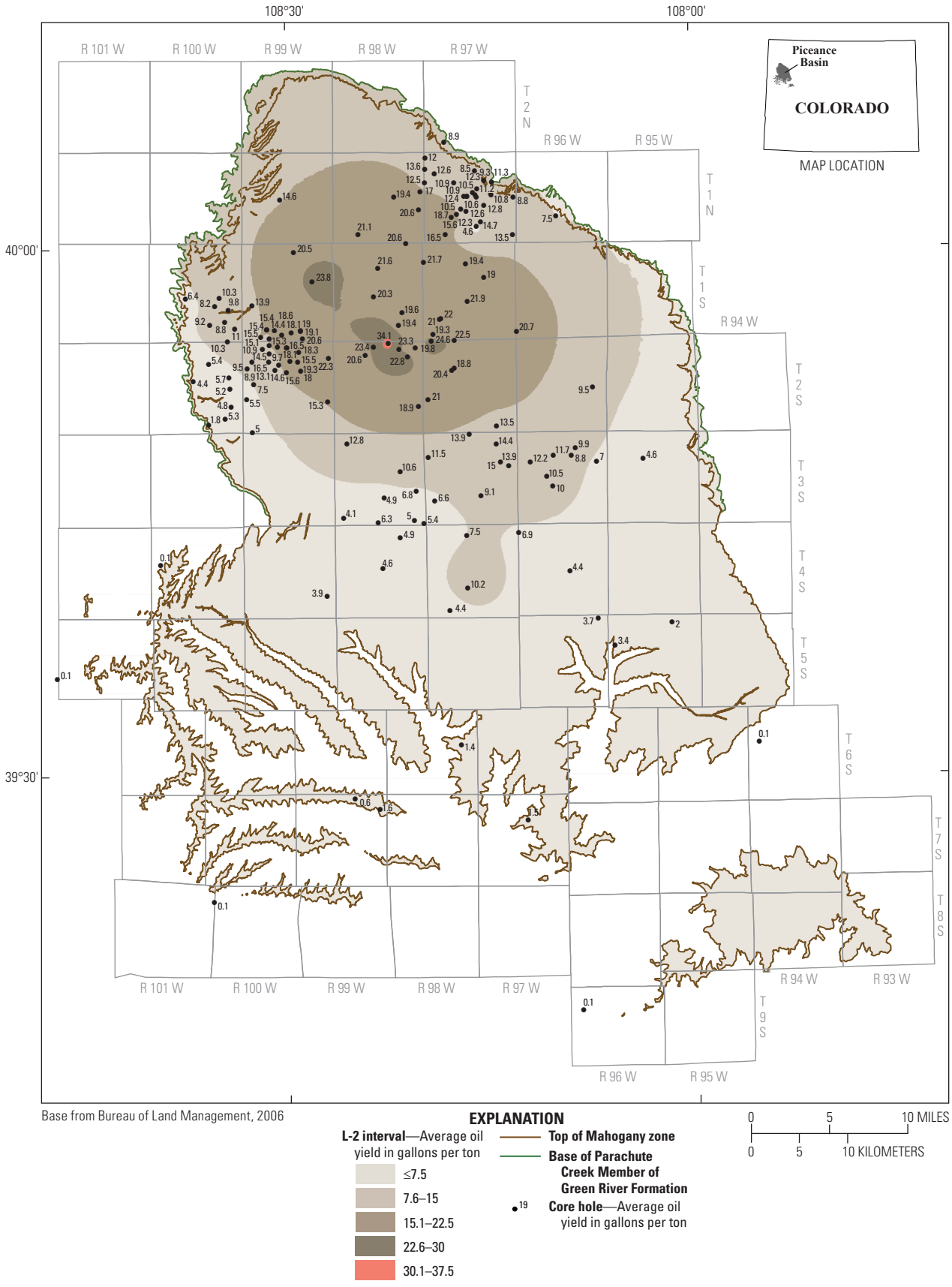

Figure 36. L-2 zone, Piceance Basin, Colo., showing oil yields in gallons per ton (GPT), using both core-hole and rotary-hole data. The Radial Basis Function Method (RBF) was used for contouring.

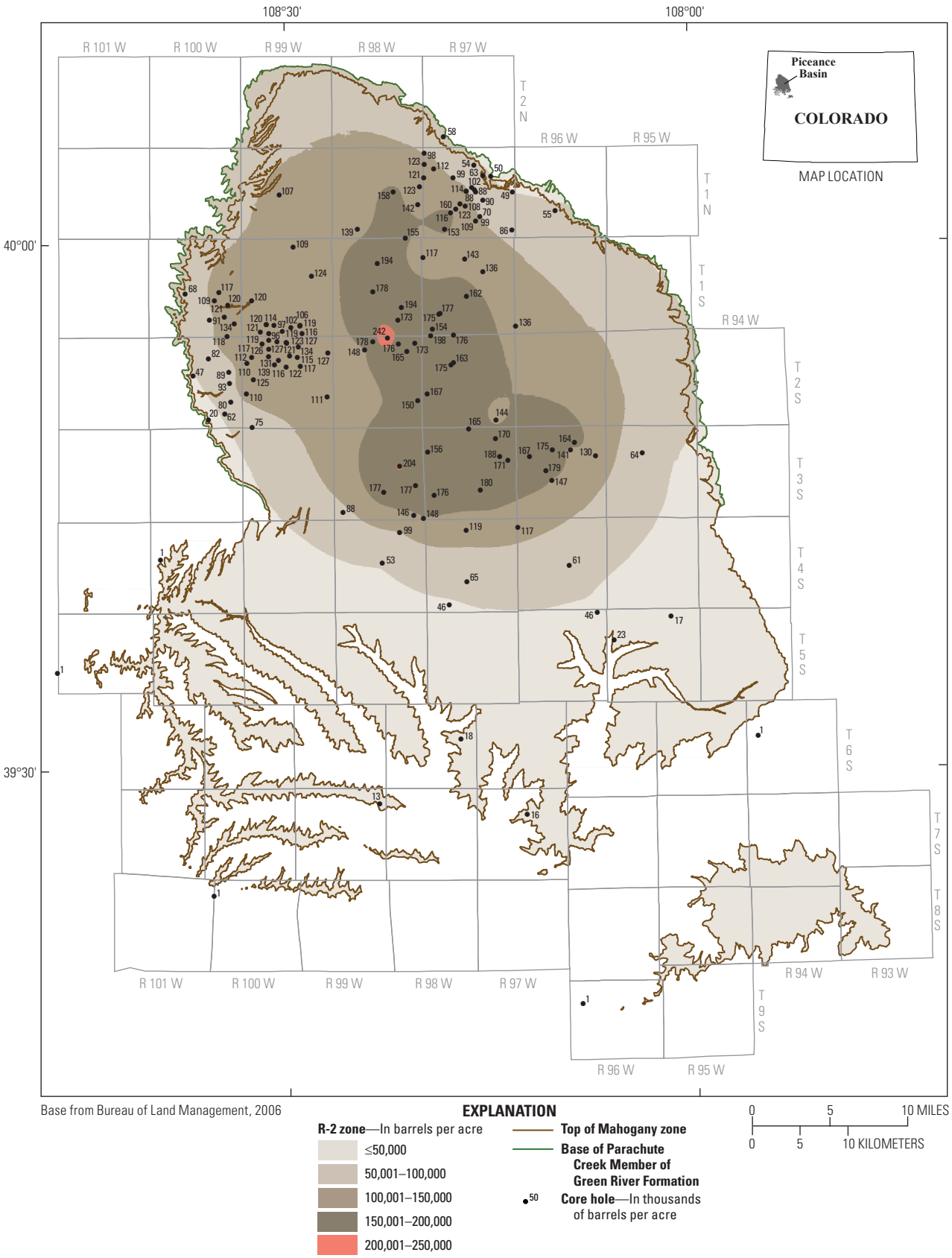

Figure 37. L-2 zone, Piceance Basin, Colo., showing oil yields in barrels per acre (BPA) using only core-hole data. The Radial Basis Function Method (RBF) was used for contouring.

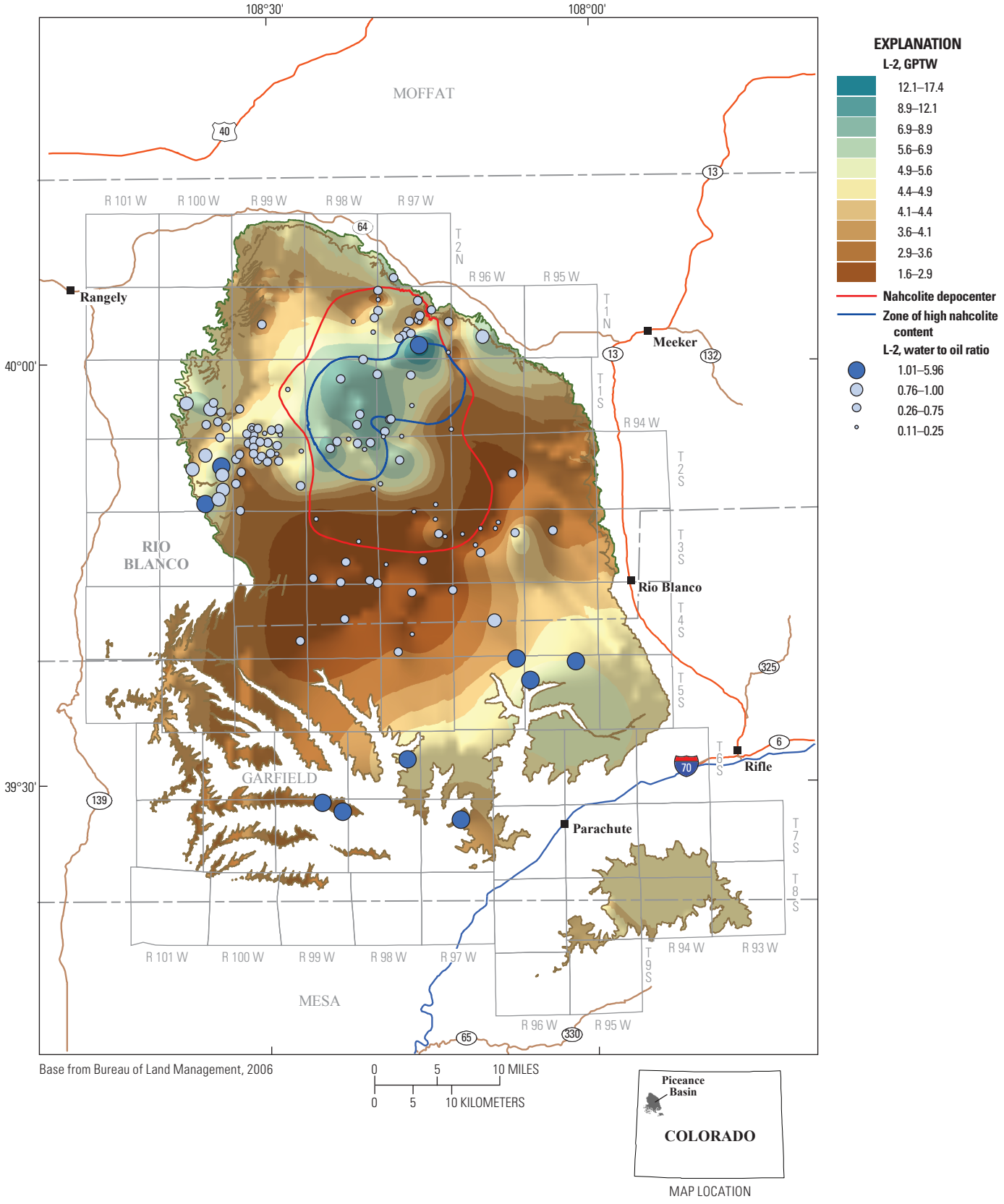

Figure 38. Variation in gallons of water per ton of oil shale (GPTW) for the L-2 oil-shale zone, Piceance Basin, Colo. A hillshade function was applied to visually enhance the displayed contours, creating the illusion that the maps are three dimensional. Bubbles indicate the ratio of water to oil produced for the L-2 zone at each of the utilized control points.

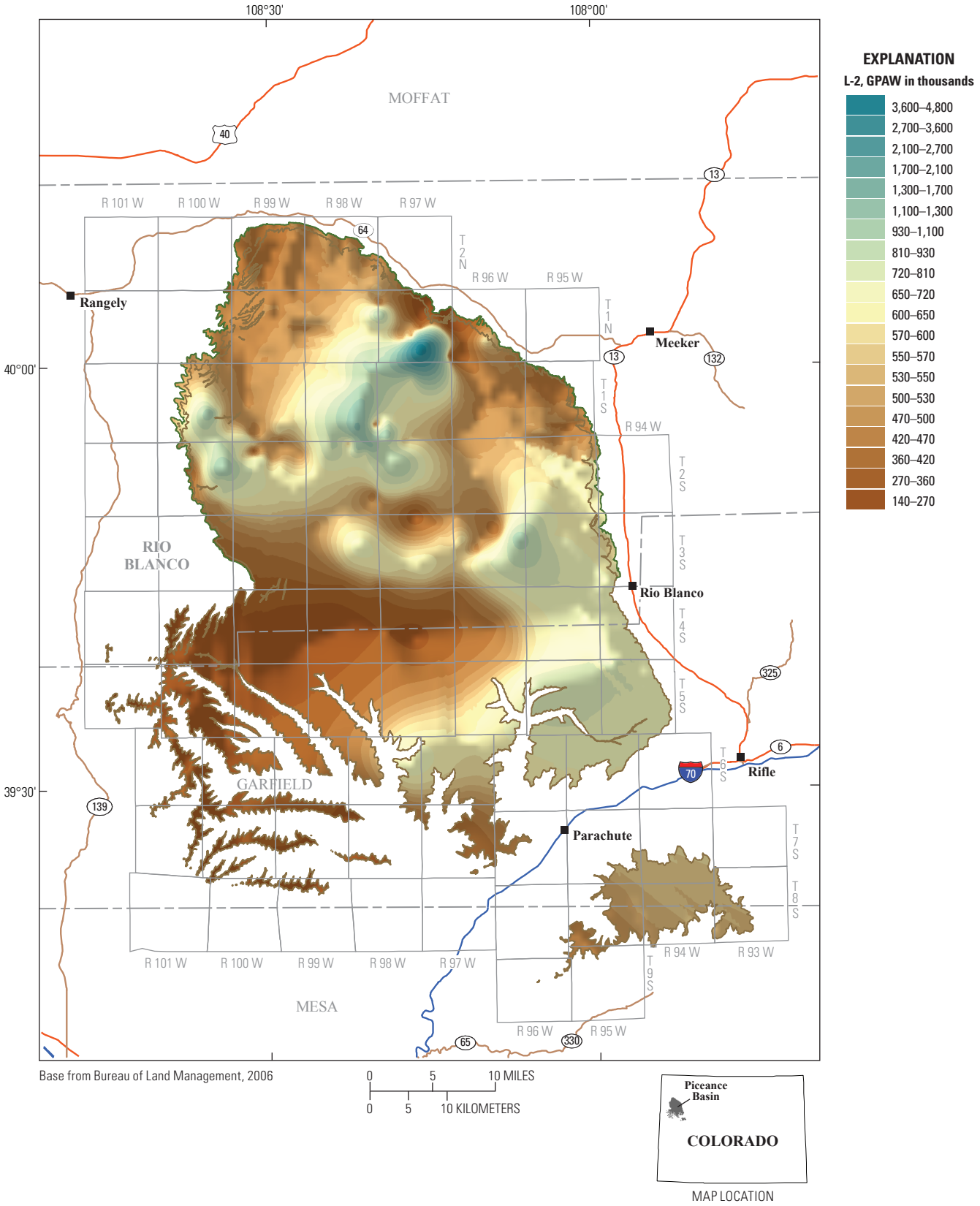

Figure 39. Variations in gallons of water per acre (GPAW) for the L-2 oil-shale zone, Piceance Basin, Colo. A hillshade function was applied to visually enhance the displayed contours, creating the illusion that the maps are three dimensional.

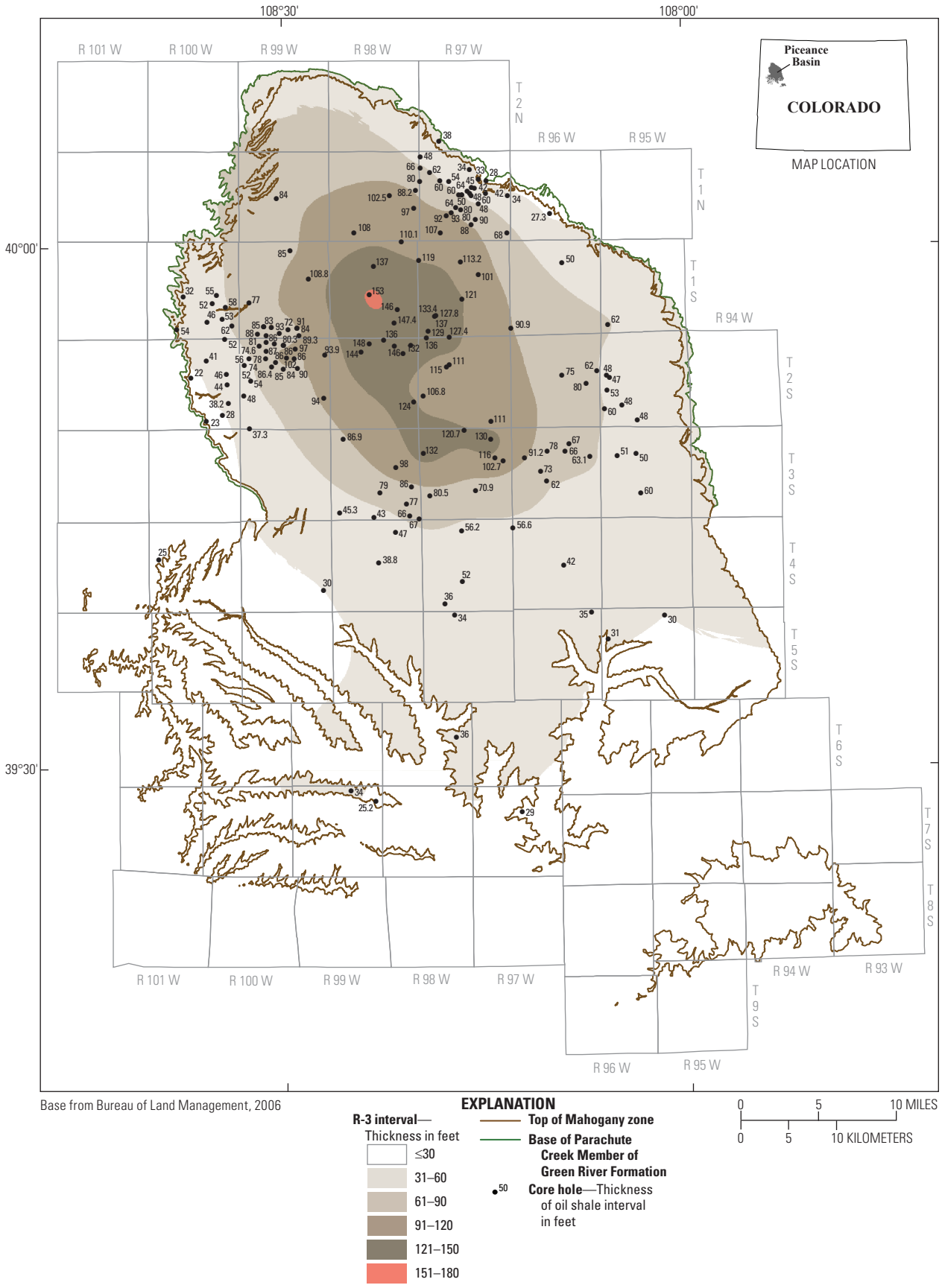

Figure 40. R-3 zone, Piceance Basin, Colo., using both core-hole and rotary-hole data. The Radial Basis Function Method (RBF) was used for contouring.

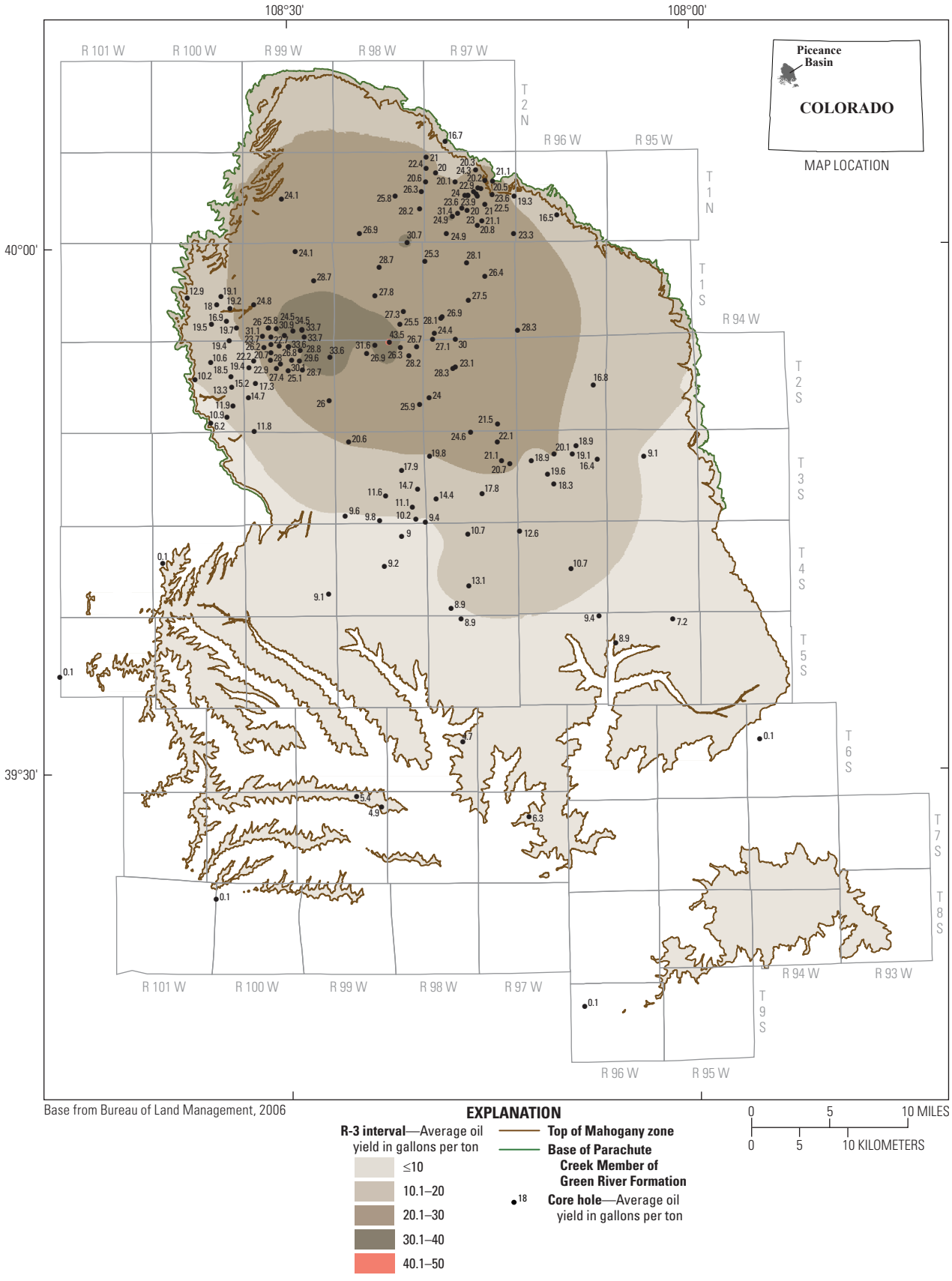

Figure 41. R-3 zone, Piceance Basin, Colo., showing the oil yield in gallons per ton (GPT) using only core-hole data. The Radial Basis Function Method (RBF) was used for contouring.

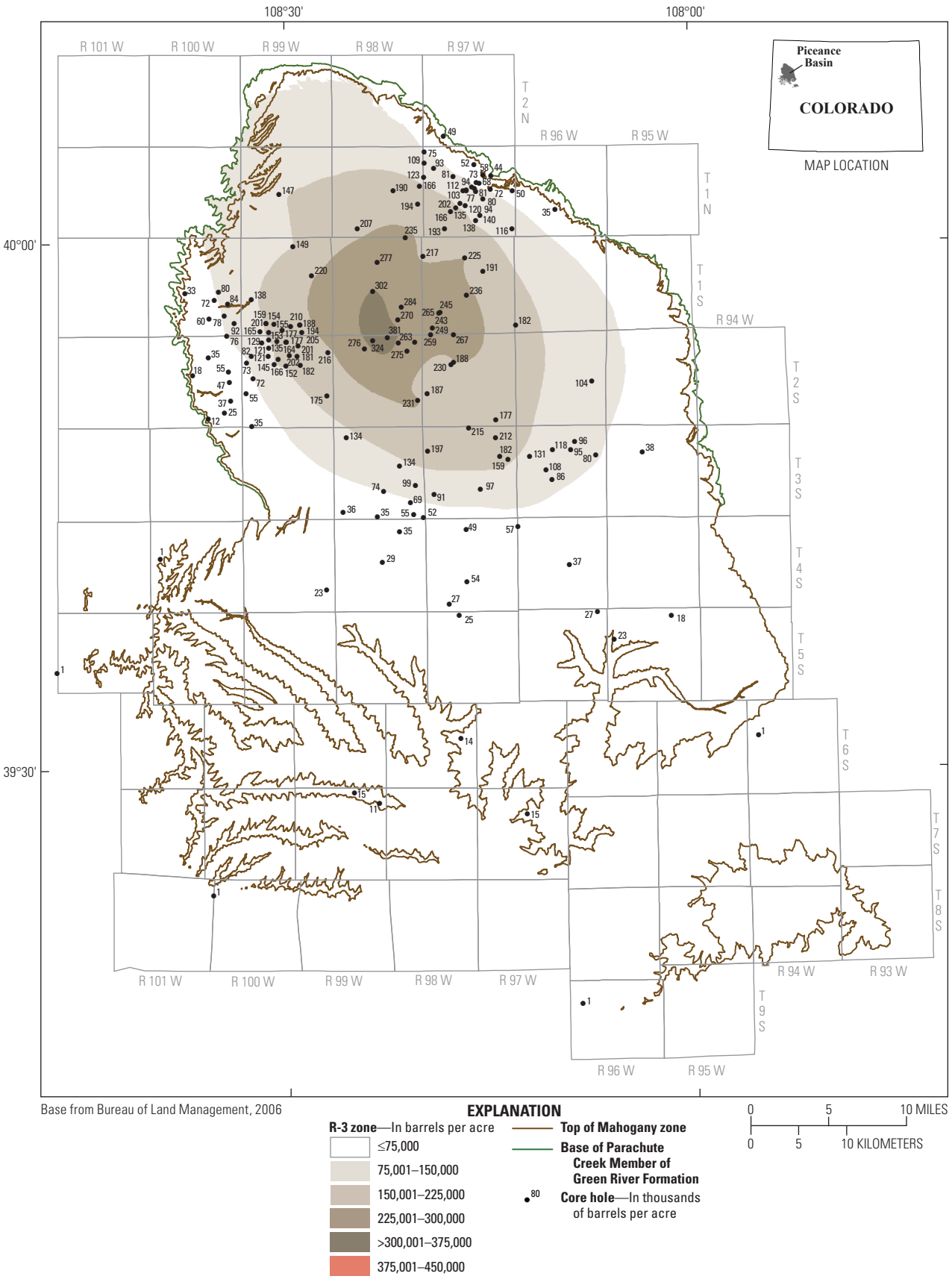

Figure 42. R-3 zone, Piceance Basin, Colo., showing oil yields in barrels per acre (BPA) using only core-hole data. The Radial Basis Function Method (RBF) was used for contouring.

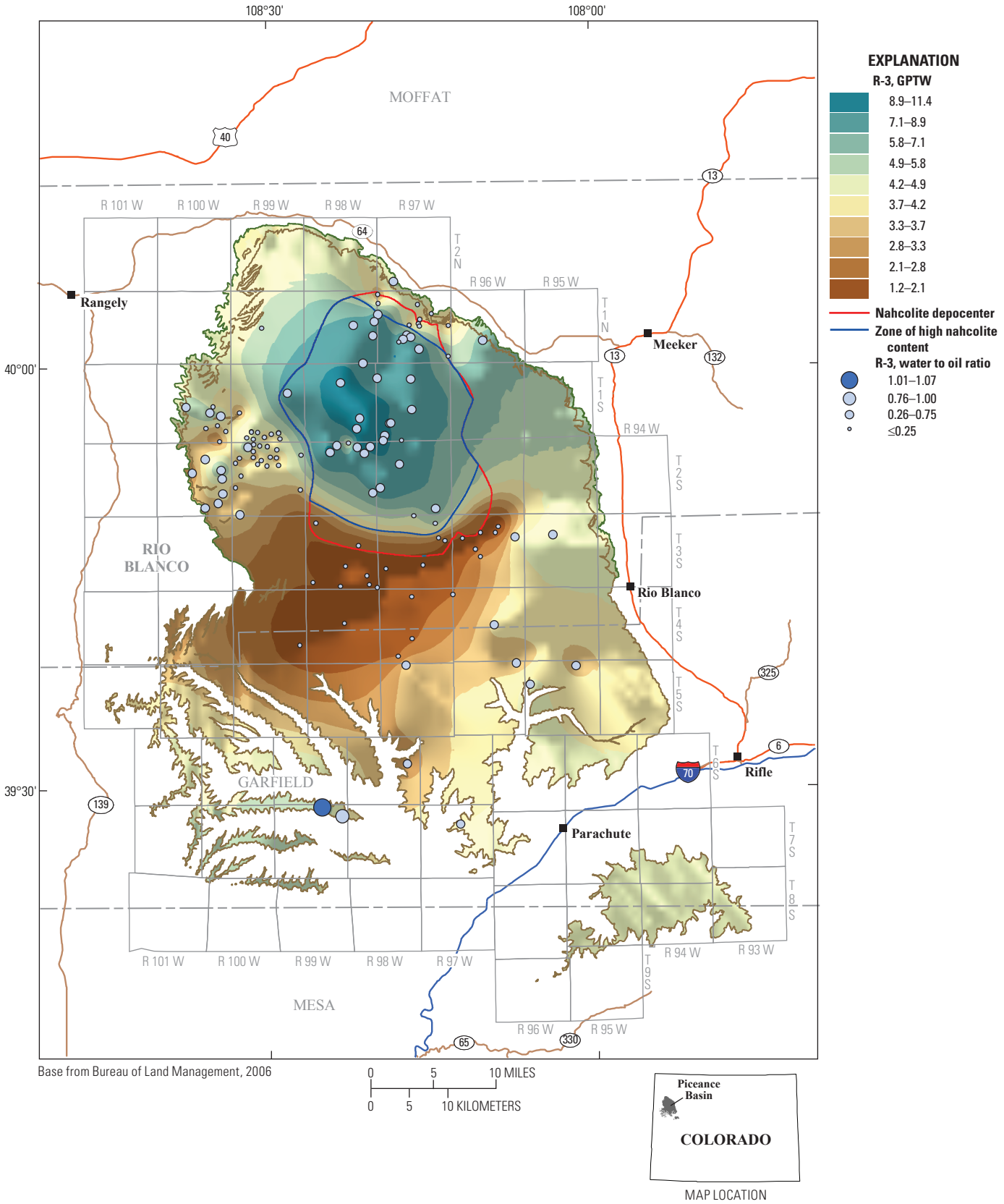

Figure 43. Variation in gallons of water per ton of oil shale (GPTW) for the R-3 oil-shale zone, Piceance Basin, Colo. A hillshade function was applied to visually enhance the displayed contours, creating the illusion that the maps are three dimensional. Bubbles indicate the ratio of water to oil produced for the R-3 zone at each of the utilized control points.

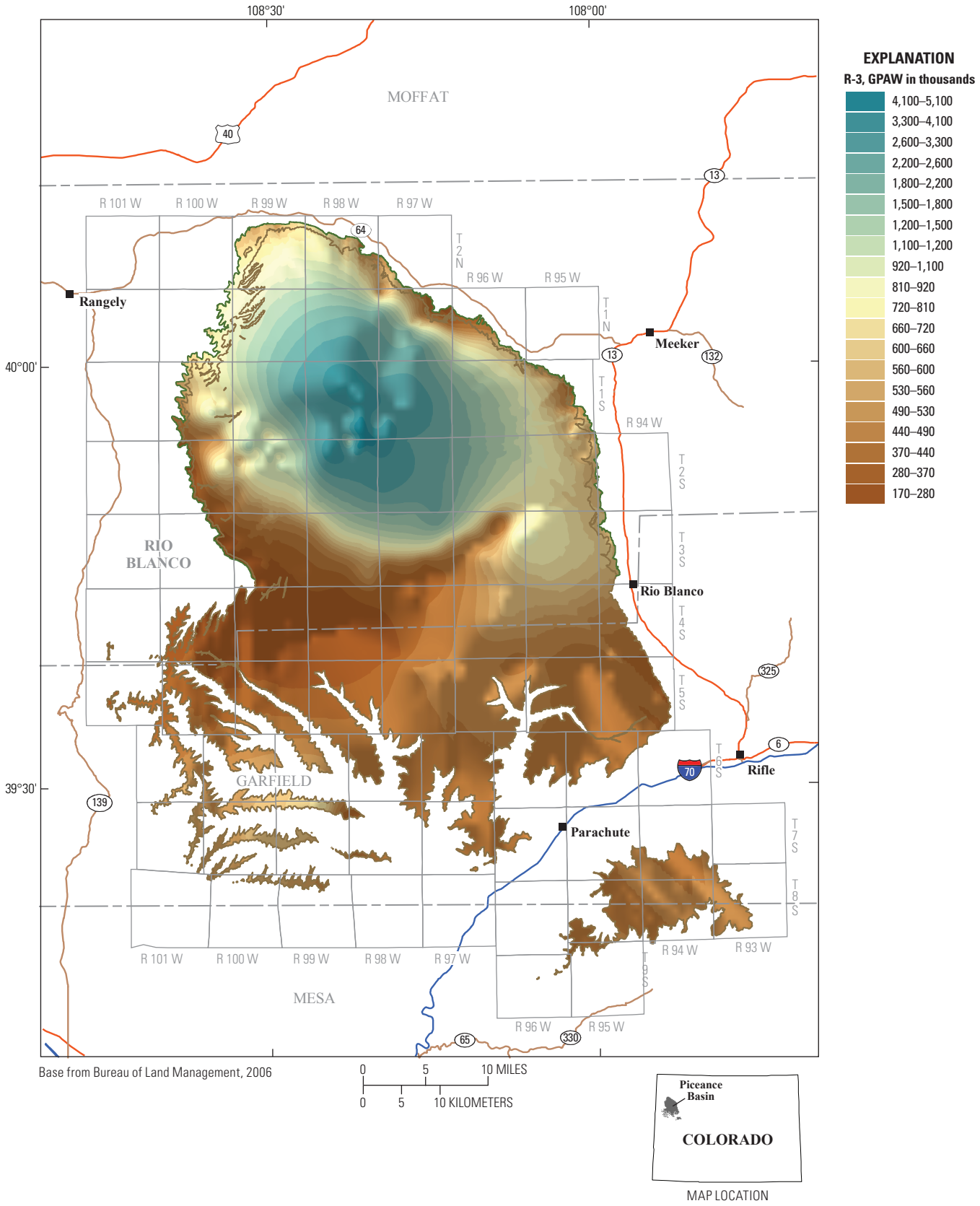

Figure 44. Variations in gallons of water per acre (GPAW) for the R-3 oil-shale zone, Piceance Basin, Colo. A hillshade function was applied to visually enhance the displayed contours, creating the illusion that the maps are three dimensional.

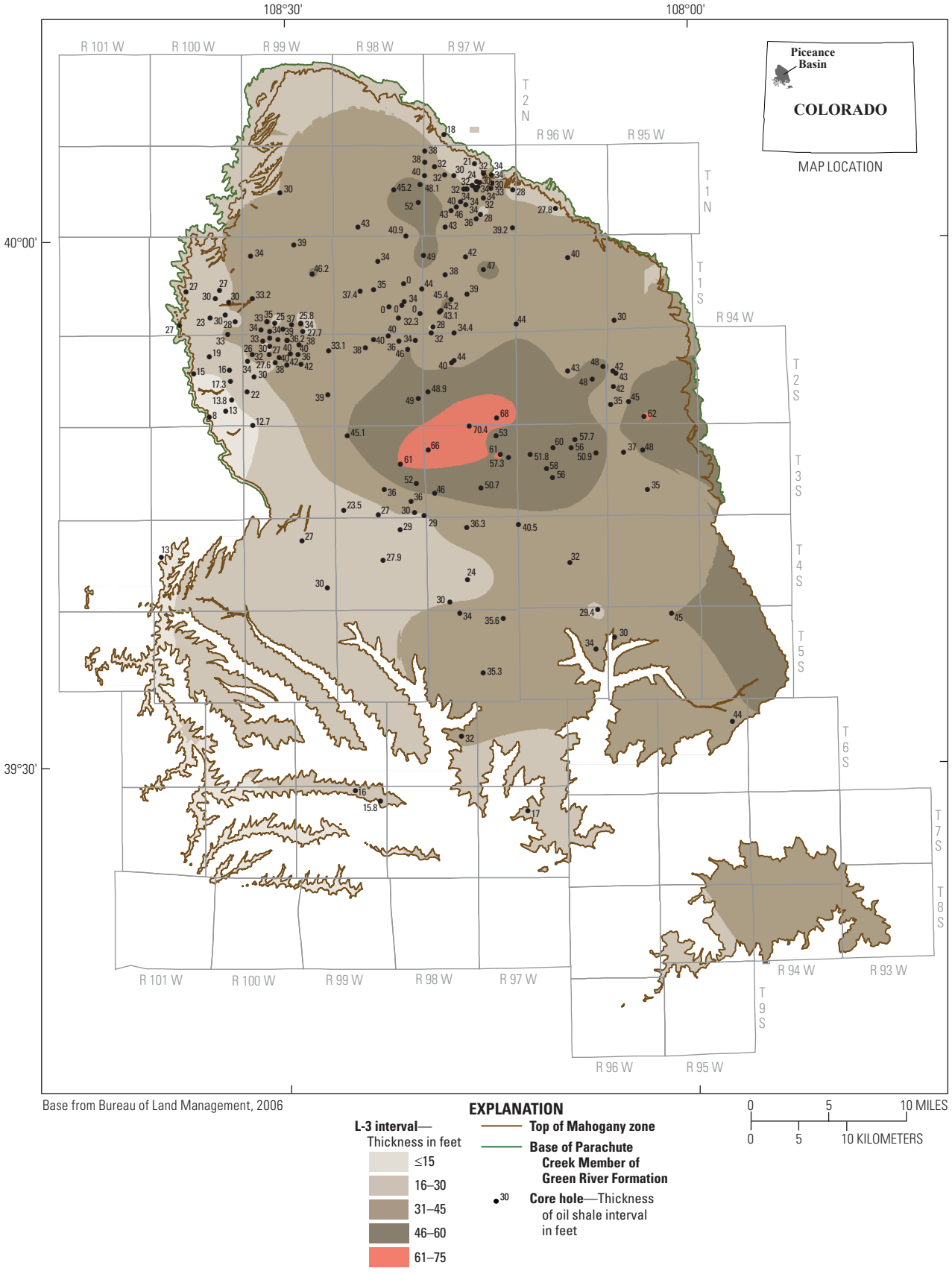

Figure 45. L-3 zone, Piceance Basin, Colo., using both core-hole and rotary-hole data. The Radial Basis Function Method (RBF) was used for contouring.

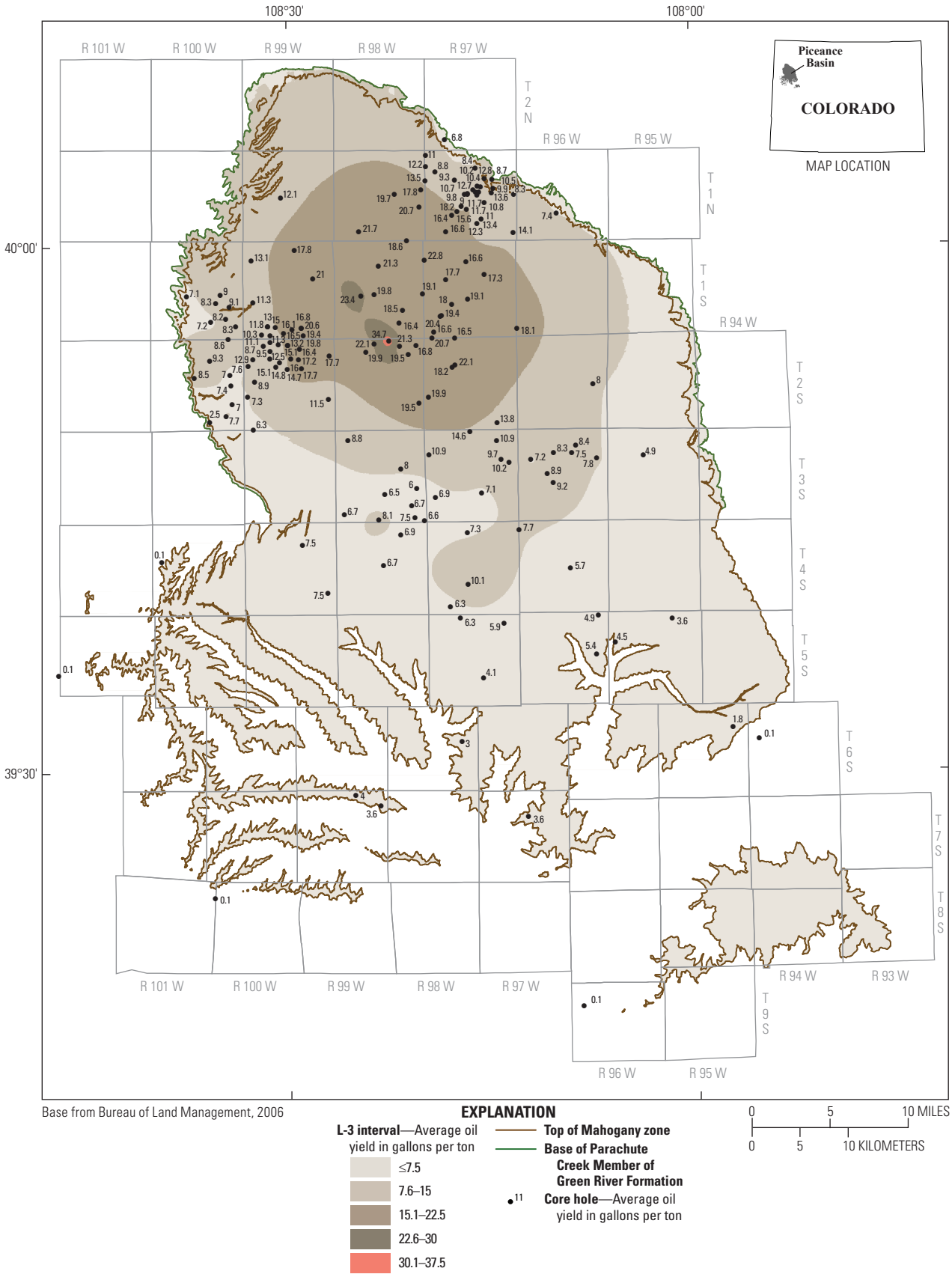

Figure 46. L-3 zone, Piceance Basin, Colo., showing the oil yield in gallons per ton (GPT) using only core-hole data. The Radial Basis Function Method (RBF) was used for contouring.

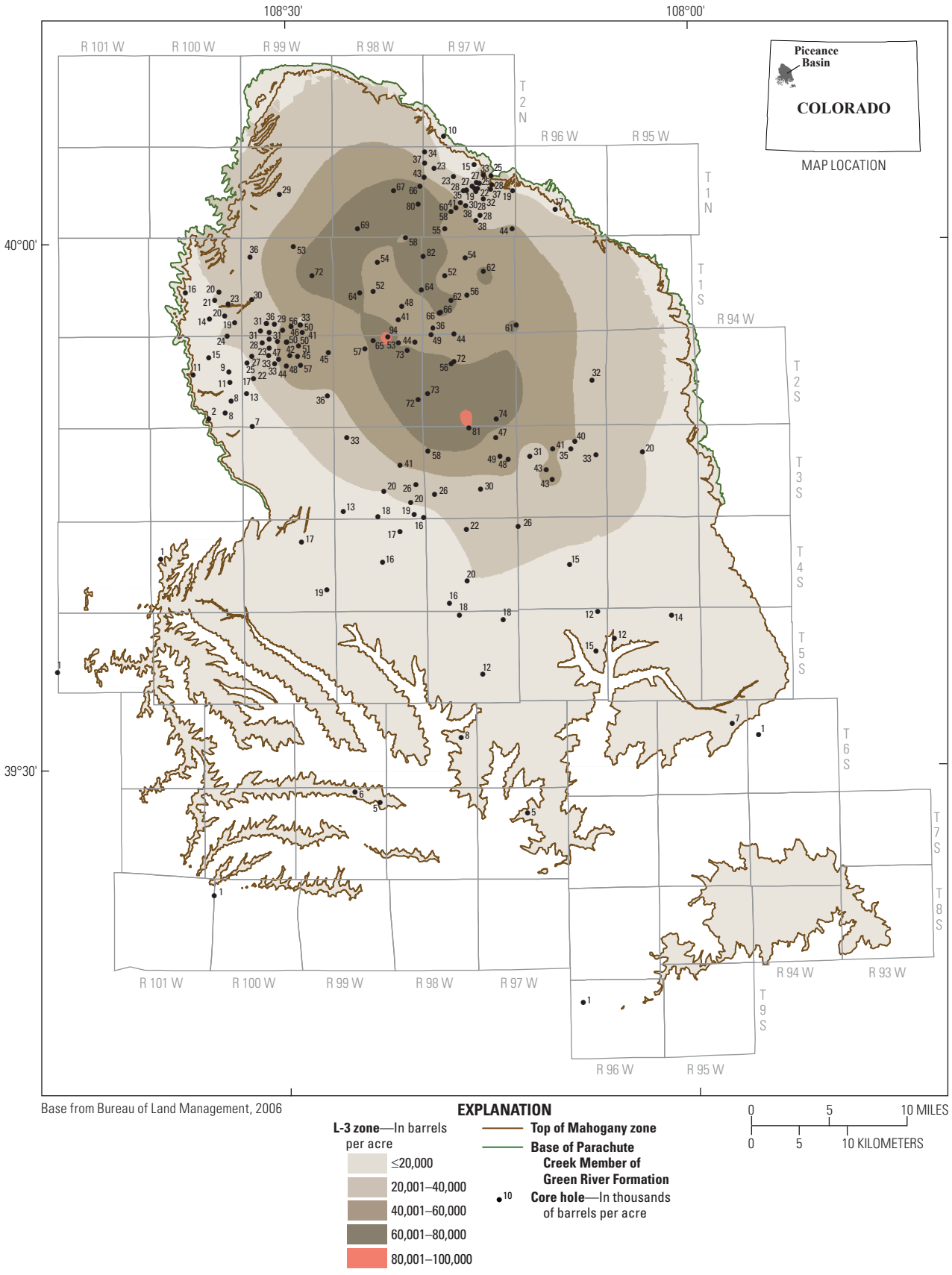

Figure 47. L-3 zone, Piceance Basin, Colo., showing oil yields in barrels per acre (BPA) using only core-hole data. The Radial Basis Function Method (RBF) was used for contouring.

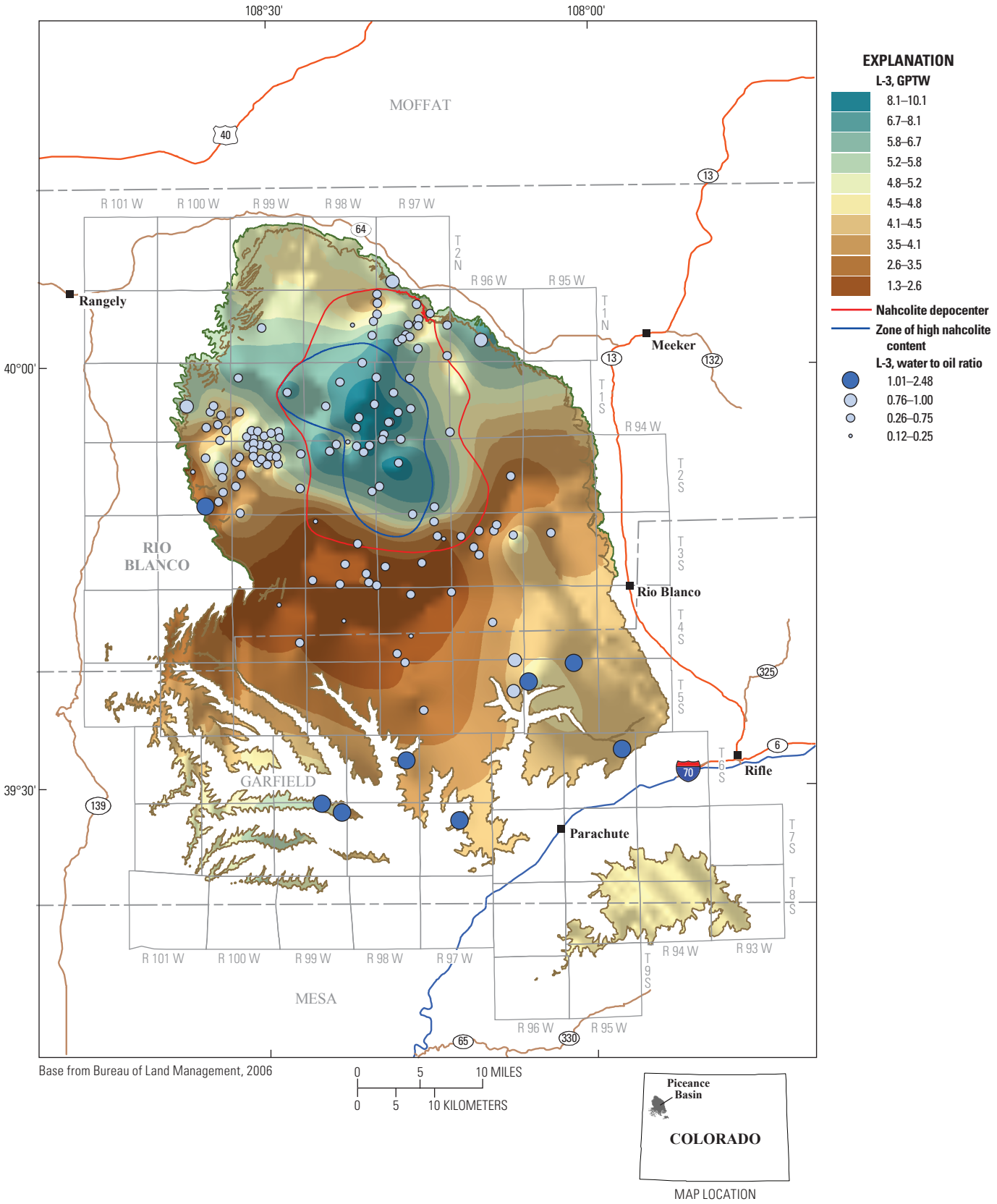

Figure 48. Variation in gallons of water per ton of oil shale (GPTW) for the L-3 oil-shale zone, Piceance Basin, Colo. A hillshade function was applied to visually enhance the displayed contours, creating the illusion that the maps are three dimensional. Bubbles indicate the ratio of water to oil produced for the R-3 zone at each utilized control point.

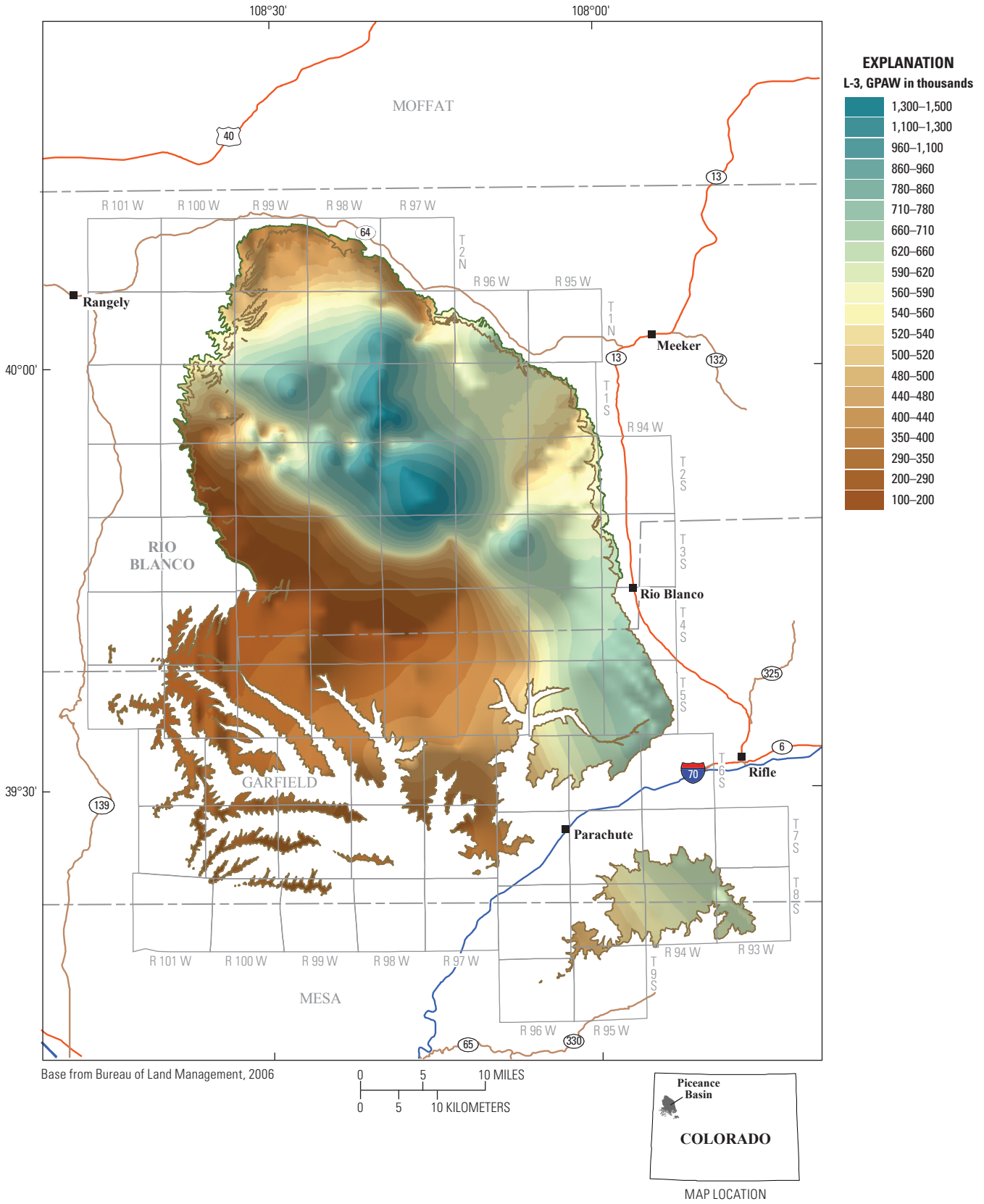

Figure 49. Variations in gallons of water per acre (GPAW) for the L-3 oil-shale zone, Piceance Basin, Colo. A hillshade function was applied to visually enhance the displayed contours, creating the illusion that the maps are three dimensional.

The R-4 zone thickens toward both the oil-shale and saline-mineral depocenter to a maximum of about 165 ft and toward the eastern margin of the basin where it reaches a maximum of about 150 ft (fig. 50). It thins to about 5 to 80 ft along the northern, western, and southern margins (fig. 50). The base of the R-4 zone approximately marks the onset of overall expansion of Lake Uinta that enlarged the area of rich oil-shale deposition (Johnson, 1985; Johnson and others, 2010). Although there were many contractions of the lake after that expansion, on average the area of rich oil-shale deposition remained larger after the expansion than before. This can be seen by comparing the GPT of oil and BPA of oil maps for the R-3 and R-4 zones (figs. 46, 47, 51, and 52). All these maps show an increase towards the oil-shale and saline-mineral depocenter, but the area of high oil-yield values is significantly larger for the R-4 zone than for R-3 (figs. 46 and 51). There are fewer nahcolite-rich zones in the R-4 zone than in the underlying R-3 zone (Dyni, 1974, his figs. 2 and 3; Brownfield and others, 2010, their pls. 1 and 2), possibly because the lake water freshened somewhat during that expansion. The GPTW reaches a maximum of about 9 in the area with highest nahcolite, decreasing to less than 3 just south of that area (fig. 53), but GPTW reaches a maximum of nearly 6 along the northern and western margins of the basin and in an area in the southeastern part of the basin (fig. 53). Water-to-oil ratios are substantially less than 1:1 for all but one cored hole near the southeastern margin of the basin (fig. 53). The GPAW reaches a maximum of nearly 4,000,000 in the center of the high-nahcolite area, decreasing to about 400,000 just south of that area (fig. 54); GPAW increases toward most but not all basin-margin areas (fig. 54).

Similar to the R-4 zone, the L-4 zone thickens both toward the oil-shale and saline depocenter *and* toward the east, reaching maximum thicknesses greater than 170 ft in that depocenter and more than 100 ft along the eastern basin margin (fig. 55), although the thickening towards the east is less conspicuous on the isopach map due to the isopach interval. The interval is thinnest along the southwestern margin of the basin where in places it is less than 30 ft thick (fig. 55). The GPT oil and BPA oil maps indicate a retreat of rich oil-shale deposition to the approximate area of rich deposition prior to the expansion at the base of the underlying R-4 zone (figs. 56 and 57). The L-4 zone includes far more nahcolite-rich zones than does the underlying R-4 zone (Dyni, 1974; 1981; Brownfield and others, 2010), indicating a return to highly saline conditions. The GPTW reaches a maximum greater than 11 in the high-nahcolite area, decreasing to less than 2 south of that area (fig. 58). Other GPTW values are in the range of 5 to 8, around the western and southwestern margins of the basin (fig. 58). The GPA water values increase markedly toward the area of maximum nahcolite deposition from less than 300,000 south of that area to greater than 5,000,000 in the area of highest nahcolite abundance (figs. 58 and 59).

The R-5 zone thickens to a maximum of nearly 375 ft in the oil-shale and saline-mineral depocenter and to greater than 250 ft along the eastern margin of the basin (fig. 60). The zone is thinner to the north, west, and southwest, reaching a minimum of 60 ft along the western basin margin (fig. 60). Rich oil-shale deposition during R-5 time covered approximately the same area as during deposition of the R-4 zone. For example, the area of 10 GPT oil or greater is virtually identical for the two zones (figs. 51 and 61); overall oil shale, however, is somewhat richer in the depocenter during R-4 time than during deposition of the R-5 zone (figs. 52 and 62). Thick beds of nahcolite and halite first occur in the lower part of the R-5 zone (Dyni, 1974, 1981; Brownfield and others, 2010). The GPTW reaches a maximum of more than 11 in the area with those thick beds, decreasing to less than 2 south of the nahcolite area (fig. 63). As previously discussed, thick nahcolite and halite beds are not always assessed with Fischer assay. Thus, there are no water values for those beds in many of the core holes where they are present, and the GPTW and GPAW are underestimated in that area. The GPAW increases to a maximum near 12,000,000 toward the area with greatest nahcolite content, decreasing to a minimum of about 220,000 south of that area (fig. 64).

Halite and nahcolite deposition culminated in the lower part of the L-5 zone, where two nahcolite and halite beds, reaching a maximum thickness of 60 to 65 ft, are present (Dyni, 1974; 1981). Those two beds are preserved only in the central part of the oil-shale and saline depocenter, having been leached by relatively recent groundwater movement away from that area. The L-5 zone reaches a maximum thickness of 186 ft where the two beds are preserved, decreasing to just more than 90 ft in nearby core holes where those beds have been leached (fig. 65). The R-5 interval also thickens to nearly 160 ft along the eastern and northern margin of the basin and to more than 250 ft near the mouth of Yellow Creek along the basin's northern margin (fig. 65), due in part to an influx of sediments from the north. The northward thickening may be related to inflow from Lake Gosiute to the north (Johnson, 1985, 2007). Oil yields increase toward the oil-shale and saline depocenter but are significantly lower than in the underlying R-5 zone (figs. 61 and 66). Total oil in place also increases toward that depocenter (fig. 67). The effect of nahcolite on the GPTW is confined to the small area in the north-central part of the basin where nahcolite is preserved, with GPTW reaching a maximum of about 8 in that area (fig. 68). Outside that limited area, GPTW trends are similar to zones that contain no nahcolite, reaching a minimum about 1 in the central part of the basin and increasing to more than 8 around the basin margins (fig. 68). Water-to-oil ratios are less than 1:1 except in some marginal areas. The BPAW reaches a minimum of about 200,000 in the south-central part of the basin, increasing to more than 4,500,000 in some marginal areas (fig. 69).

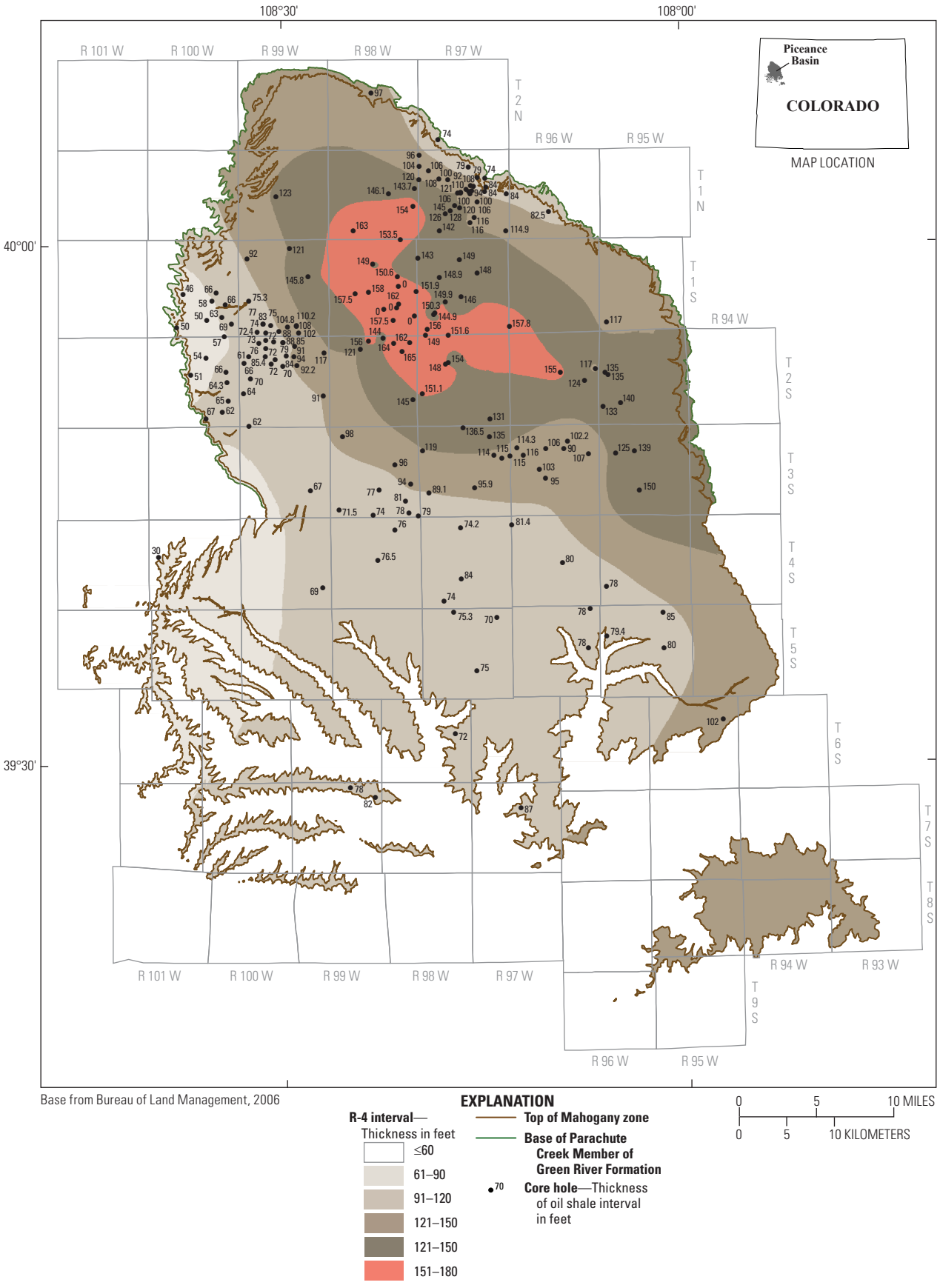

Figure 50. R-4 zone, Piceance Basin, Colo., using both core-hole and rotary-hole data. The Radial Basis Function Method (RBF) of contouring was used.

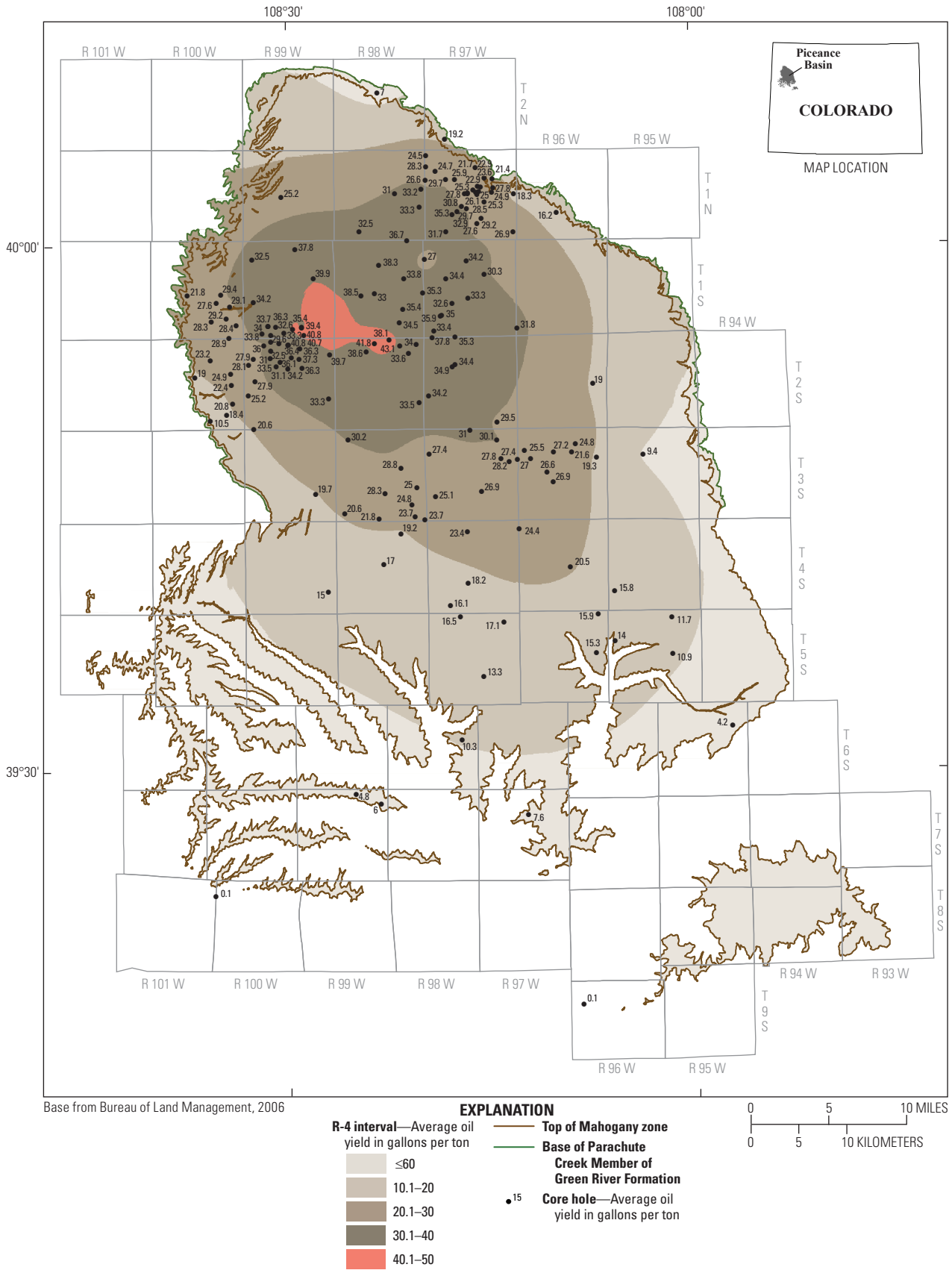

Figure 51. R-4 zone, Piceance Basin, Colo., showing the oil yield in gallons per ton (GPT) using only core-hole data. The Radial Basis Function Method (RBF) was used for contouring.

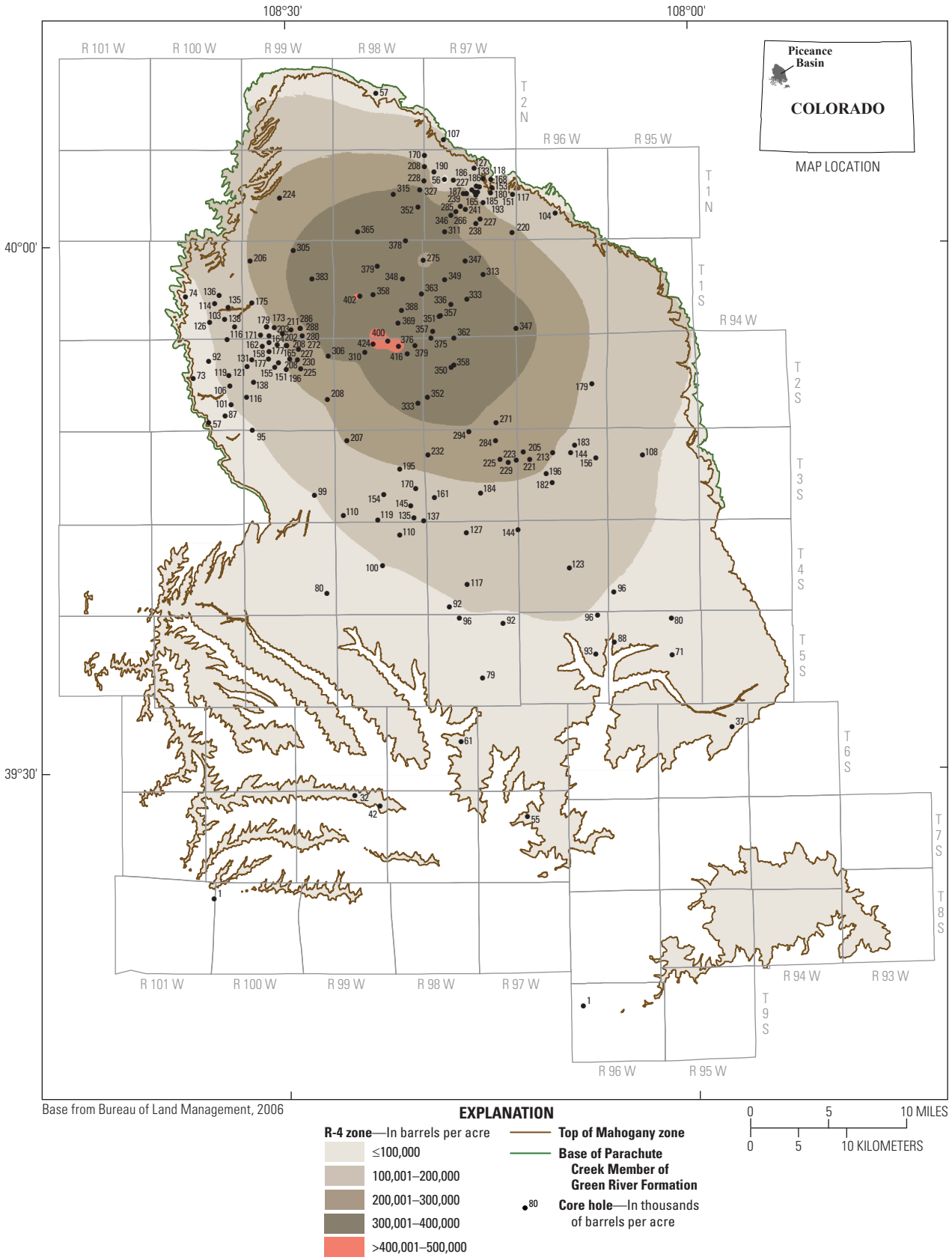

Figure 52. R-4 zone, Piceance Basin, Colo., showing oil yields in barrels per acre (BPA) using only core-hole data. The Radial Basis Function Method (RBF) was used for contouring.

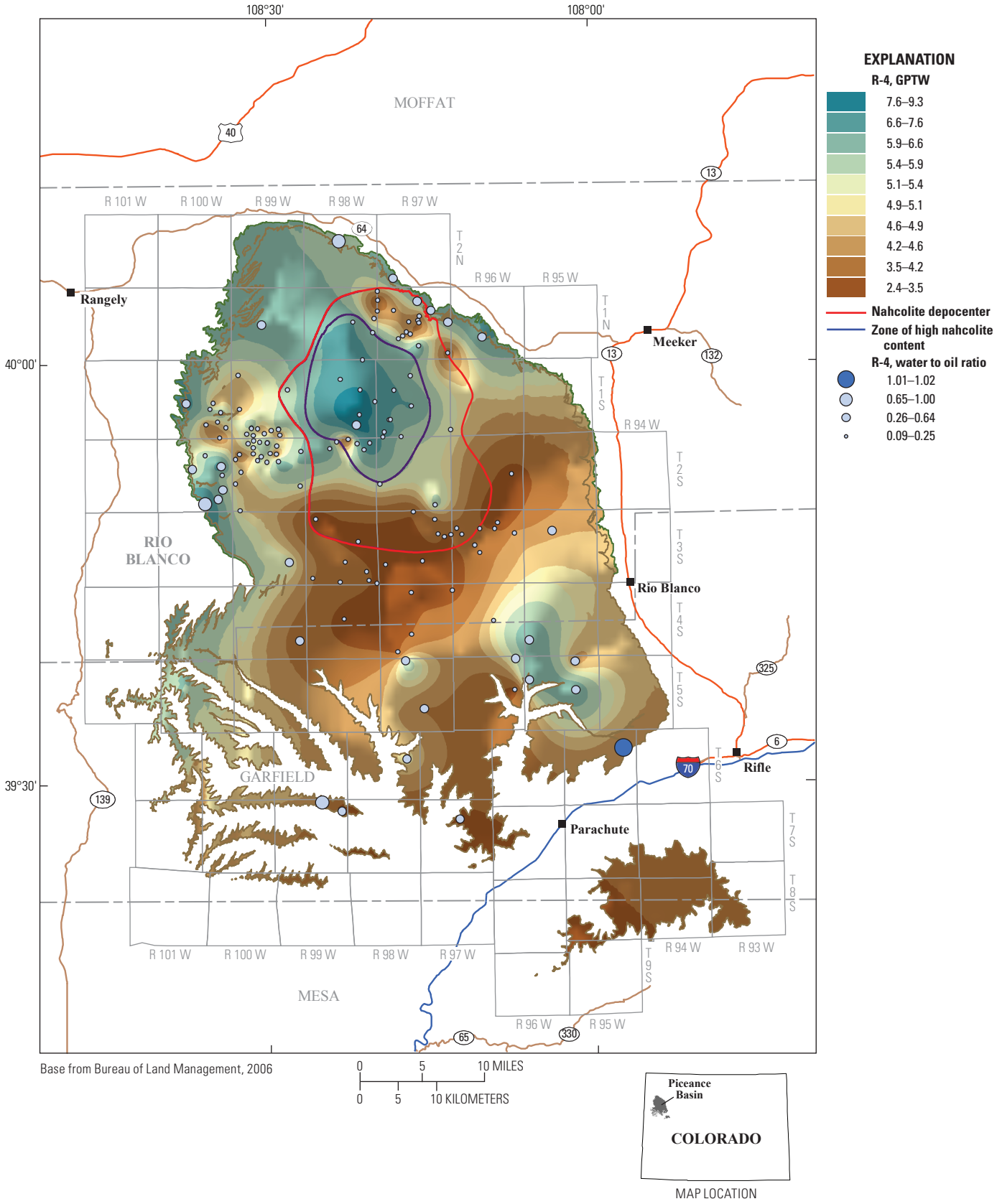

Figure 53. Variation in gallons of water per ton of oil shale (GPTW) for the R-4 oil-shale zone, Piceance Basin, Colo. A hillshade function was applied to visually enhance the displayed contours, creating the illusion that the maps are three dimensional. Bubbles indicate the ratio of water to oil produced for the R-4 zone at each of the utilized control points.

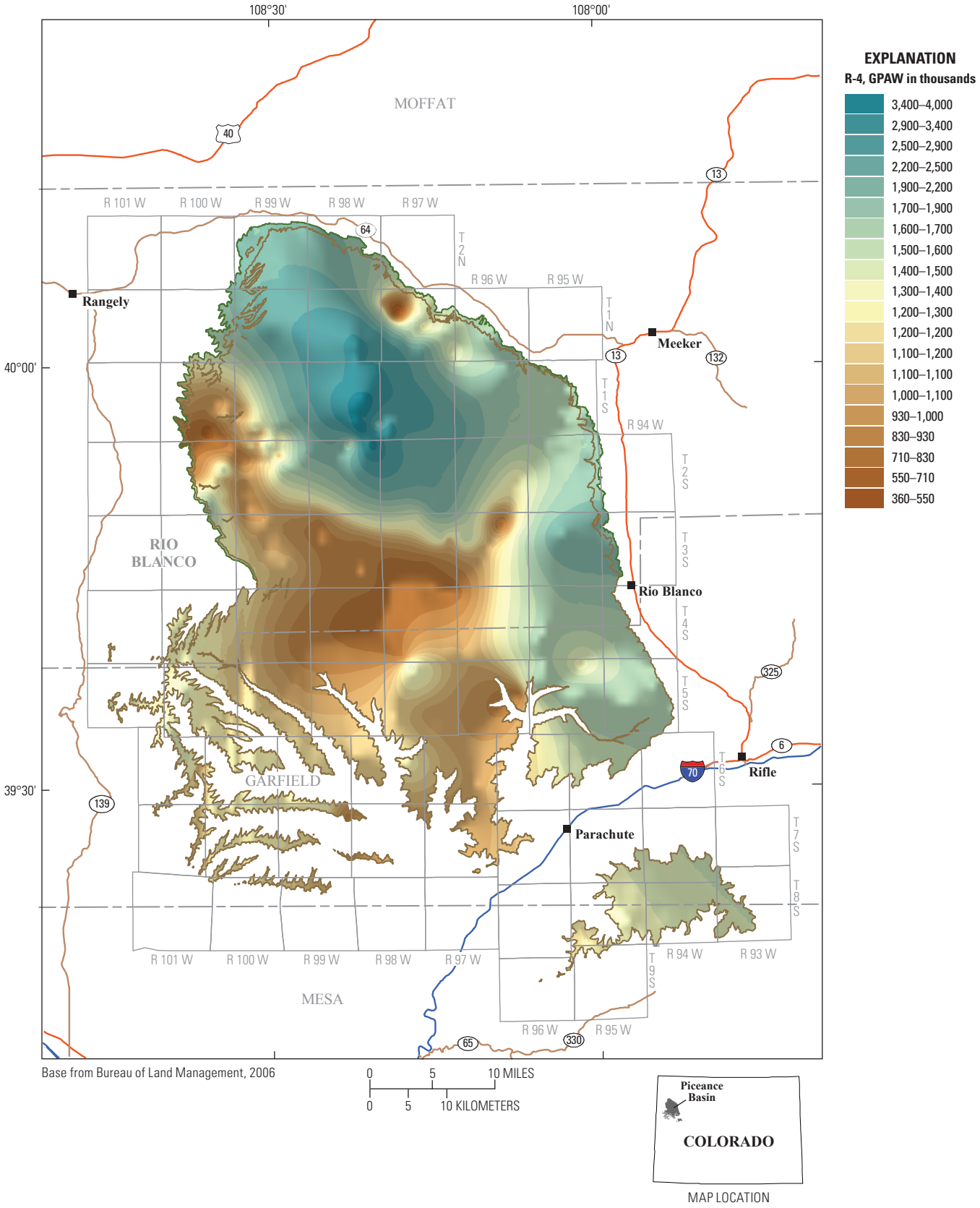

Figure 54. Variations in gallons of water per acre (GPAW) for the R-4 oil-shale zone, Piceance Basin, Colo. A hillshade function was applied to visually enhance the displayed contours, creating the illusion that the maps are three dimensional.

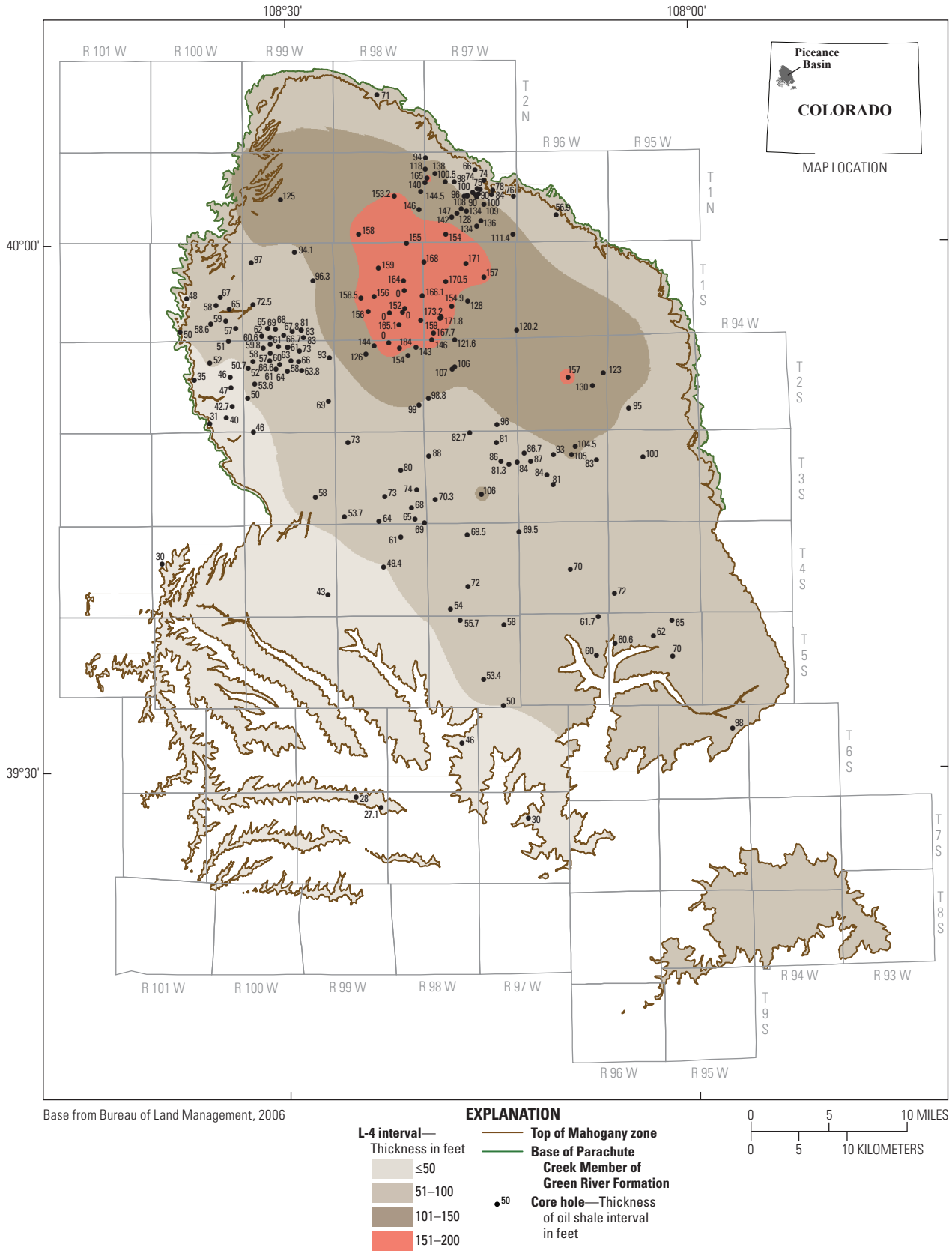

Figure 55. L-4 zone, Piceance Basin, Colo., using both core-hole and rotary-hole data. The Radial Basis Function Method (RBF) was used for contouring.

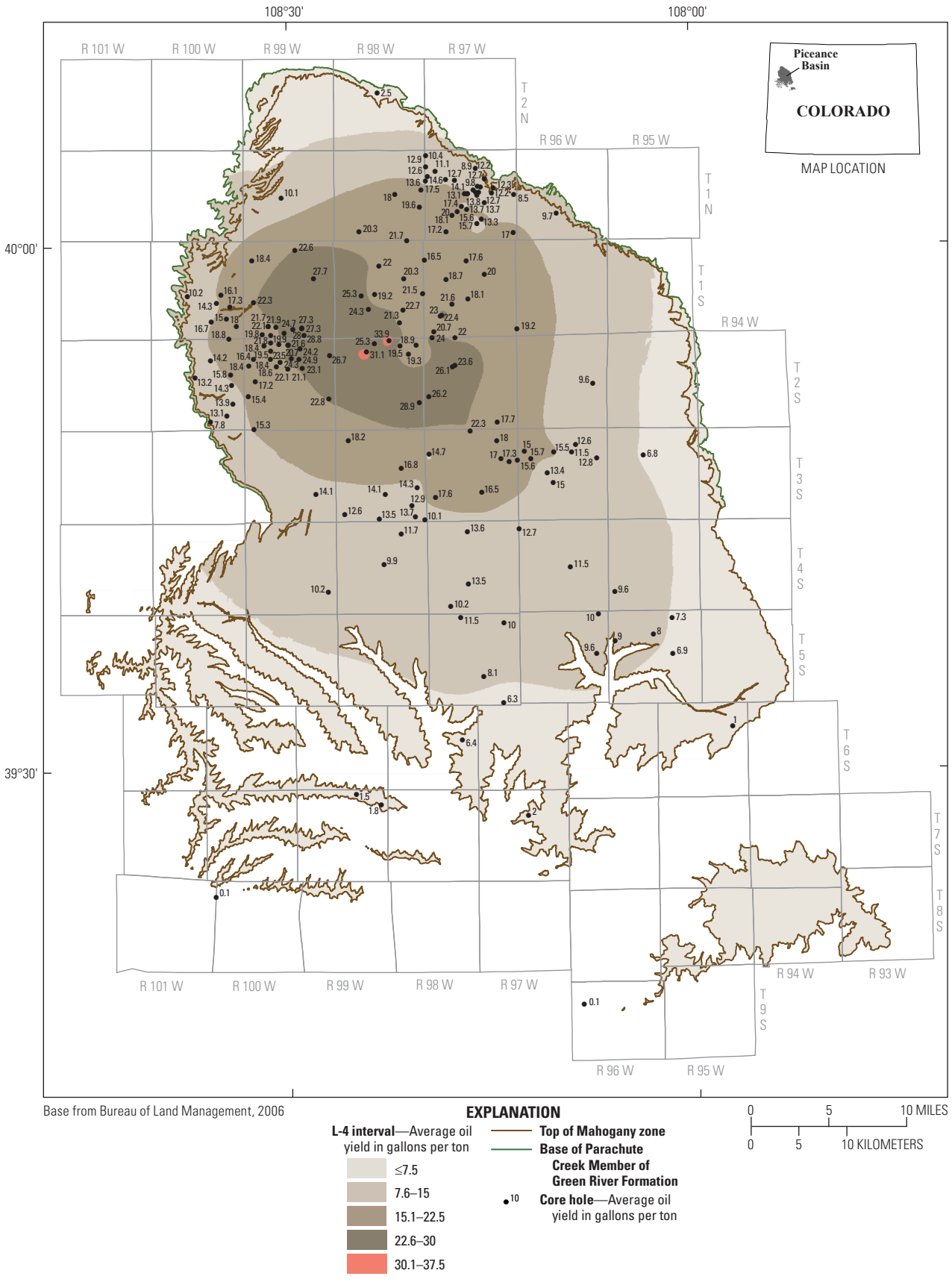

Figure 56. L-4 zone, Piceance Basin, Colo., showing the oil yield in gallons per ton (GPT) using only core-hole data. The Radial Basis Function Method (RBF) was used for contouring.

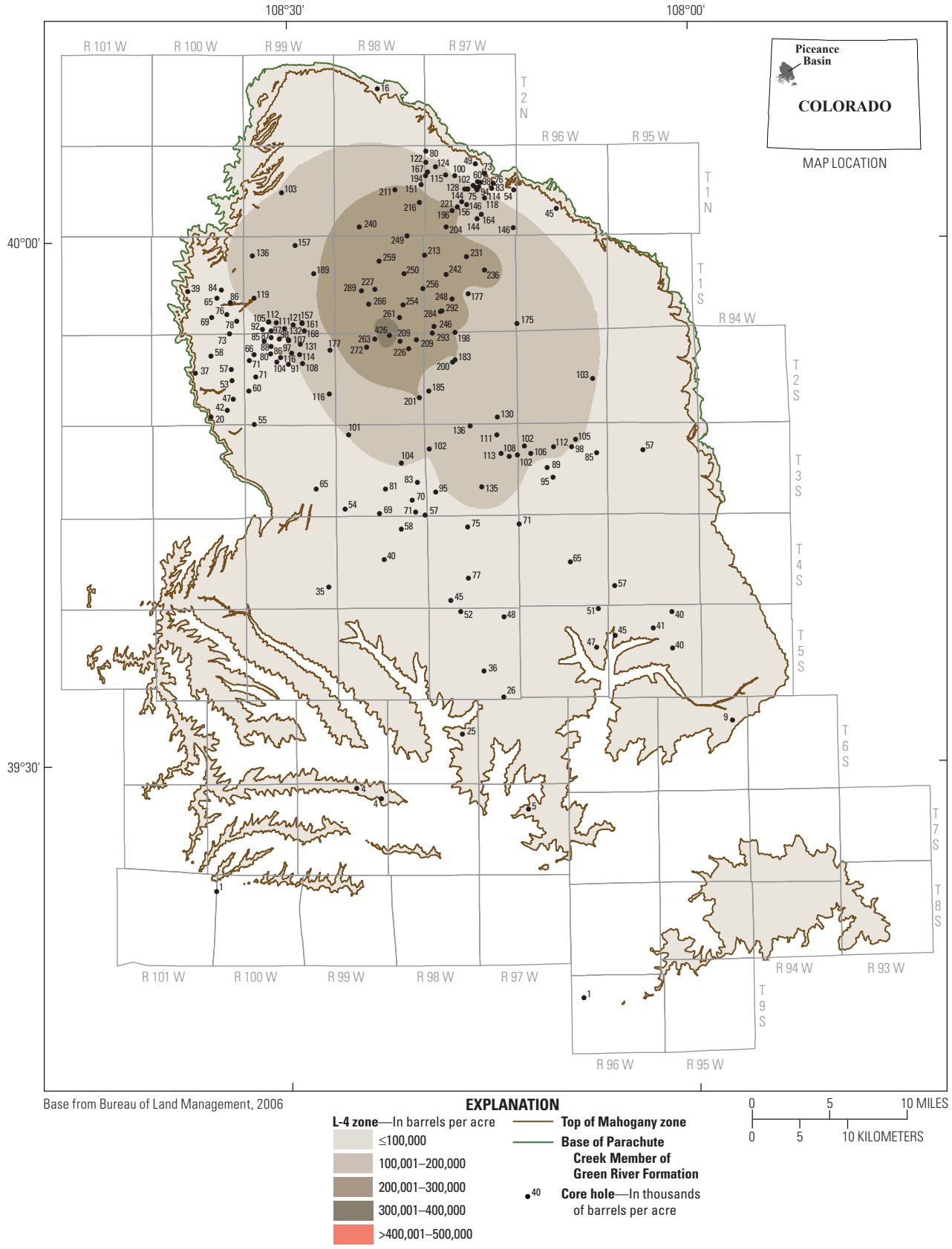

Figure 57. L-4 zone, Piceance Basin, Colo., showing oil yields in barrels per acre (BPA) using only core-hole data. The Radial Basis Function Method (RBF) was used for contouring.

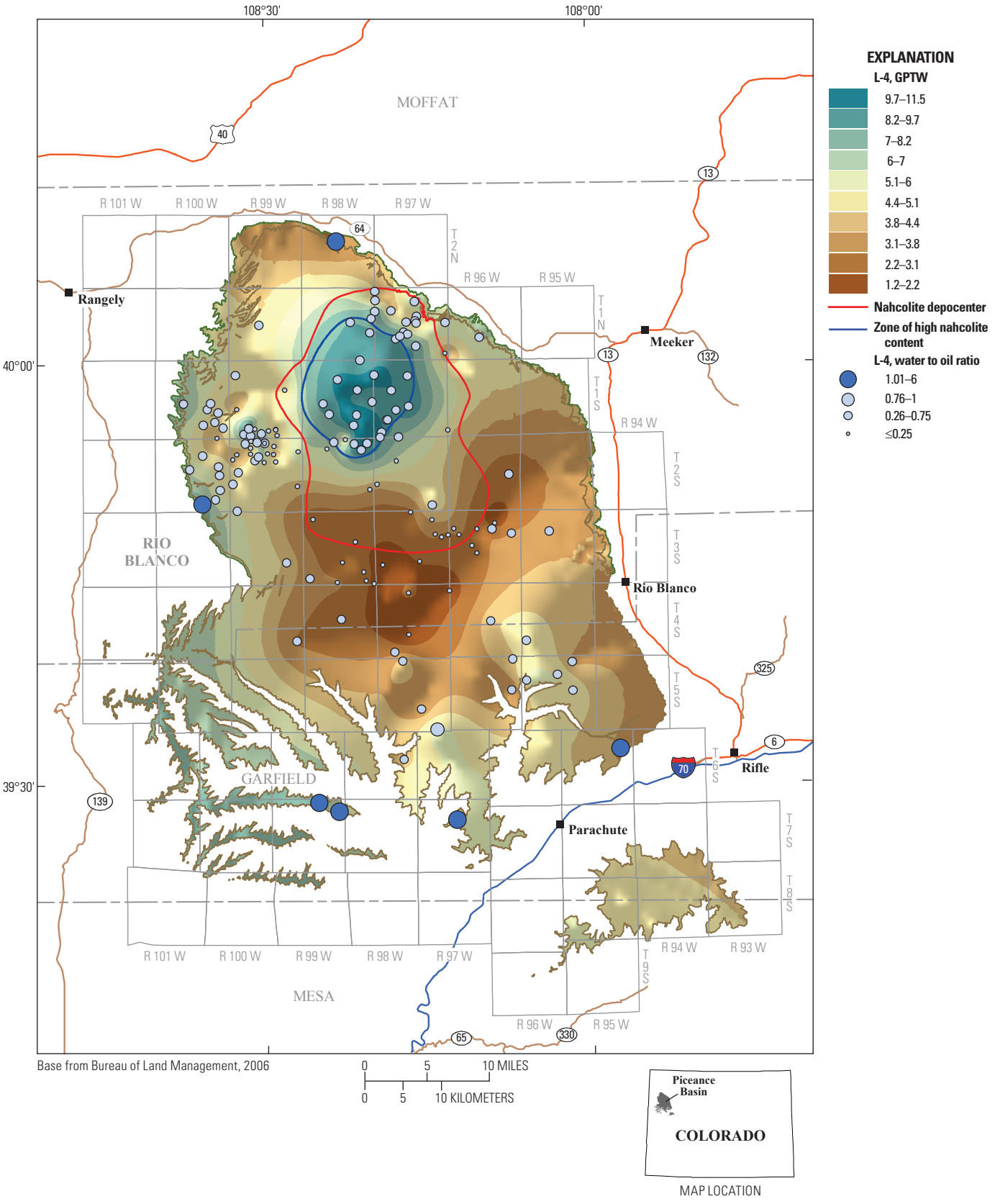

Figure 58. Variation in gallons of water per ton of oil shale (GPTW) for the L-4 oil-shale zone, Piceance Basin, Colo. A hillshade function was applied to visually enhance the displayed contours, creating the illusion that the maps are three dimensional. Bubbles indicate the ratio of water to oil produced for the L-4 zone at each of the utilized control points.

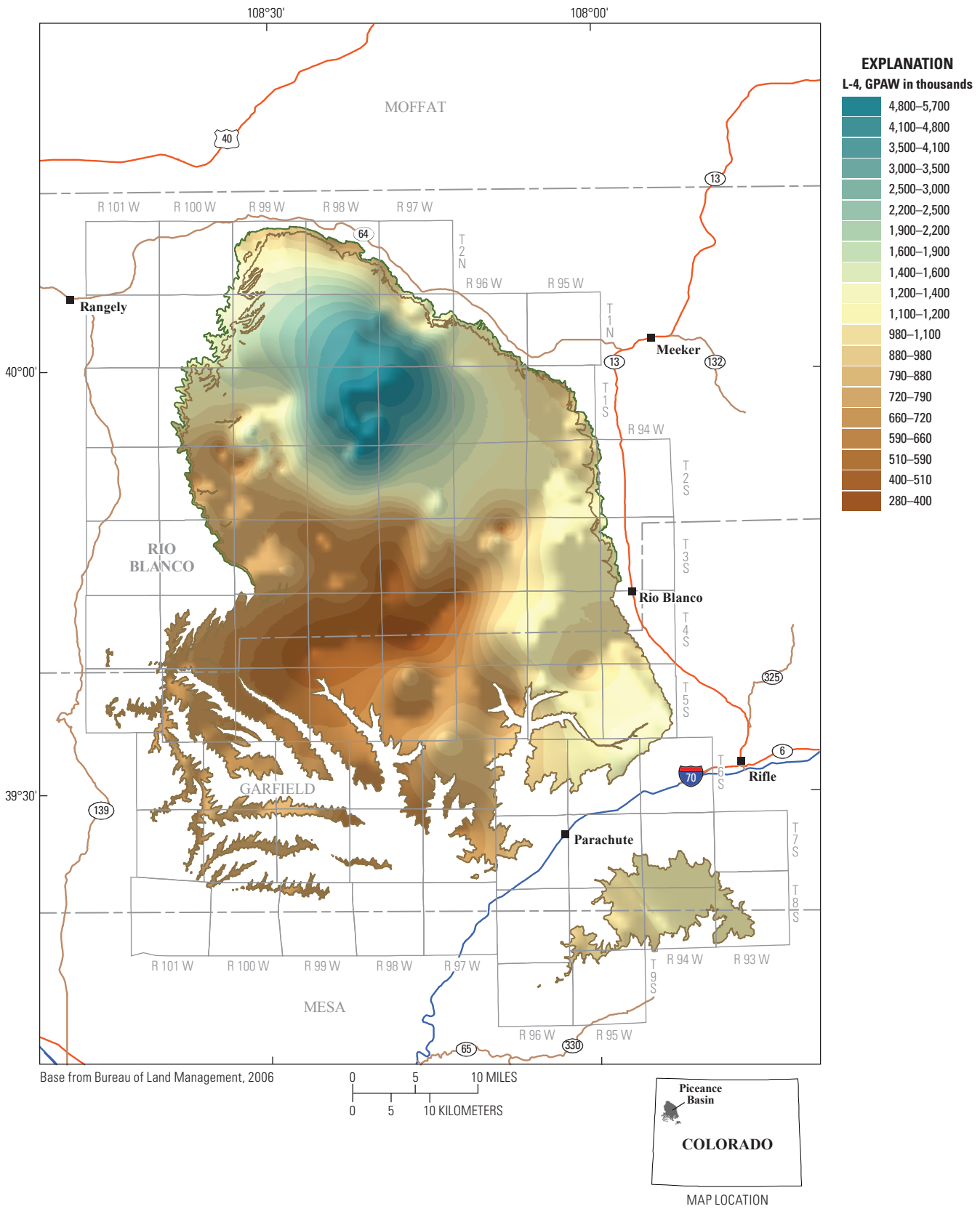

Figure 59. Variations in gallons of water per acre (GPAW) for the L-4 oil-shale zone, Piceance Basin, Colo. A hillshade function was applied to visually enhance the displayed contours, creating the illusion that the maps are three dimensional.

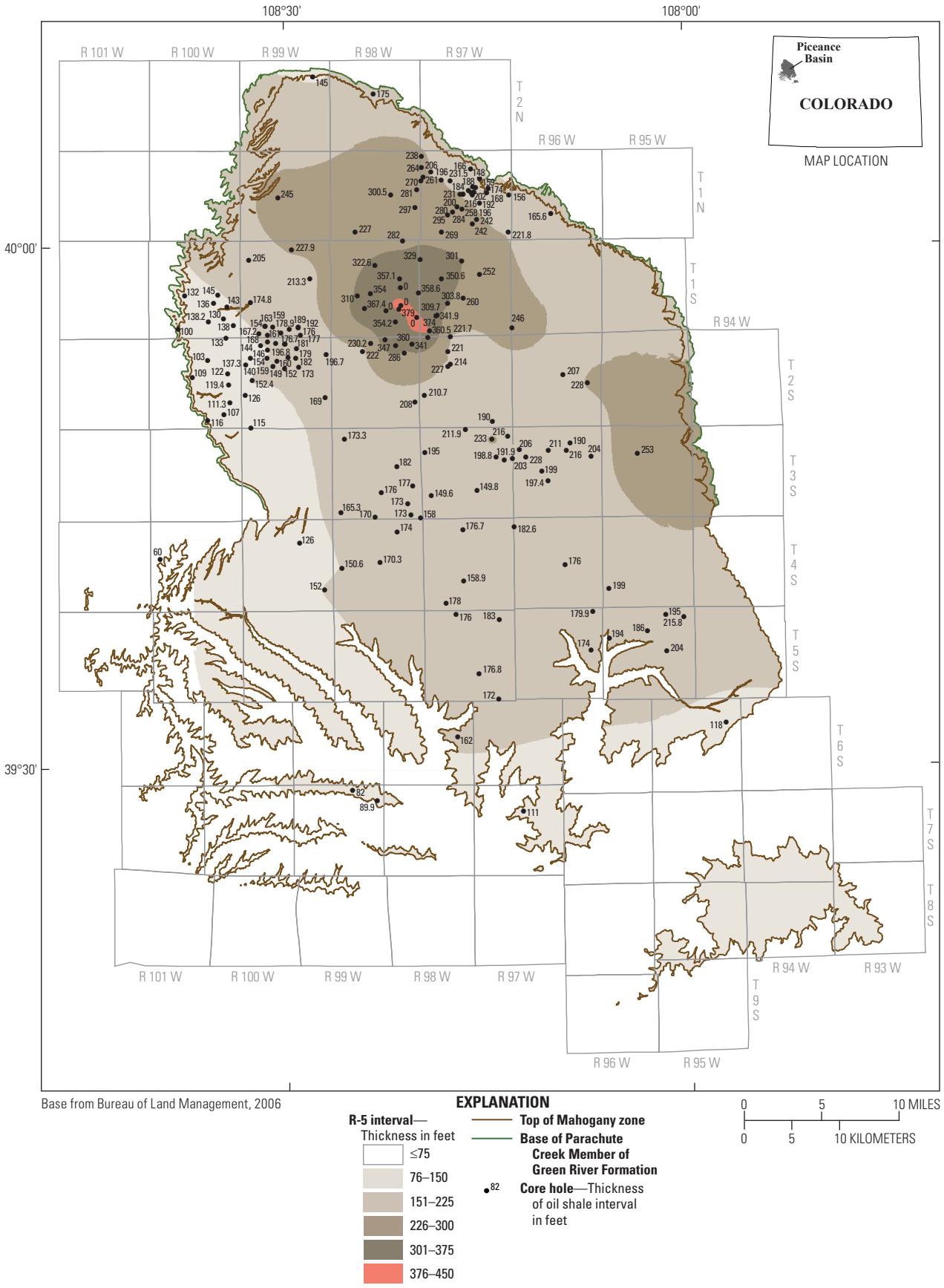

Figure 60. R-5 zone, Piceance Basin, Colo., using both core-hole and rotary-hole data. The Radial Basis Function Method (RBF) was used for contouring.

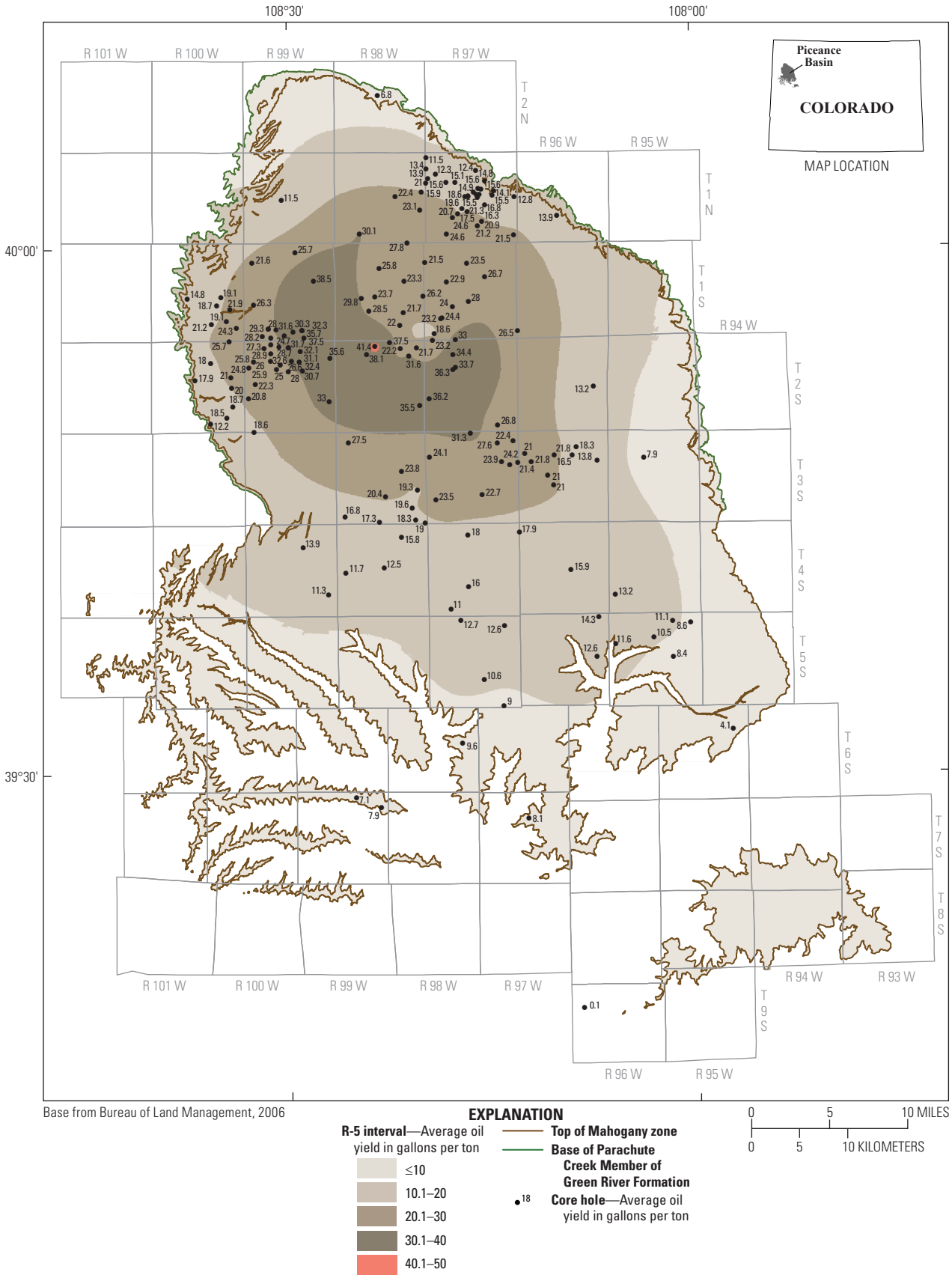

Figure 61. R-5 zone, Piceance Basin, Colo., showing the oil yield in gallons per ton (GPT) using only core-hole data. The Radial Basis Function Method (RBF) was used for contouring.

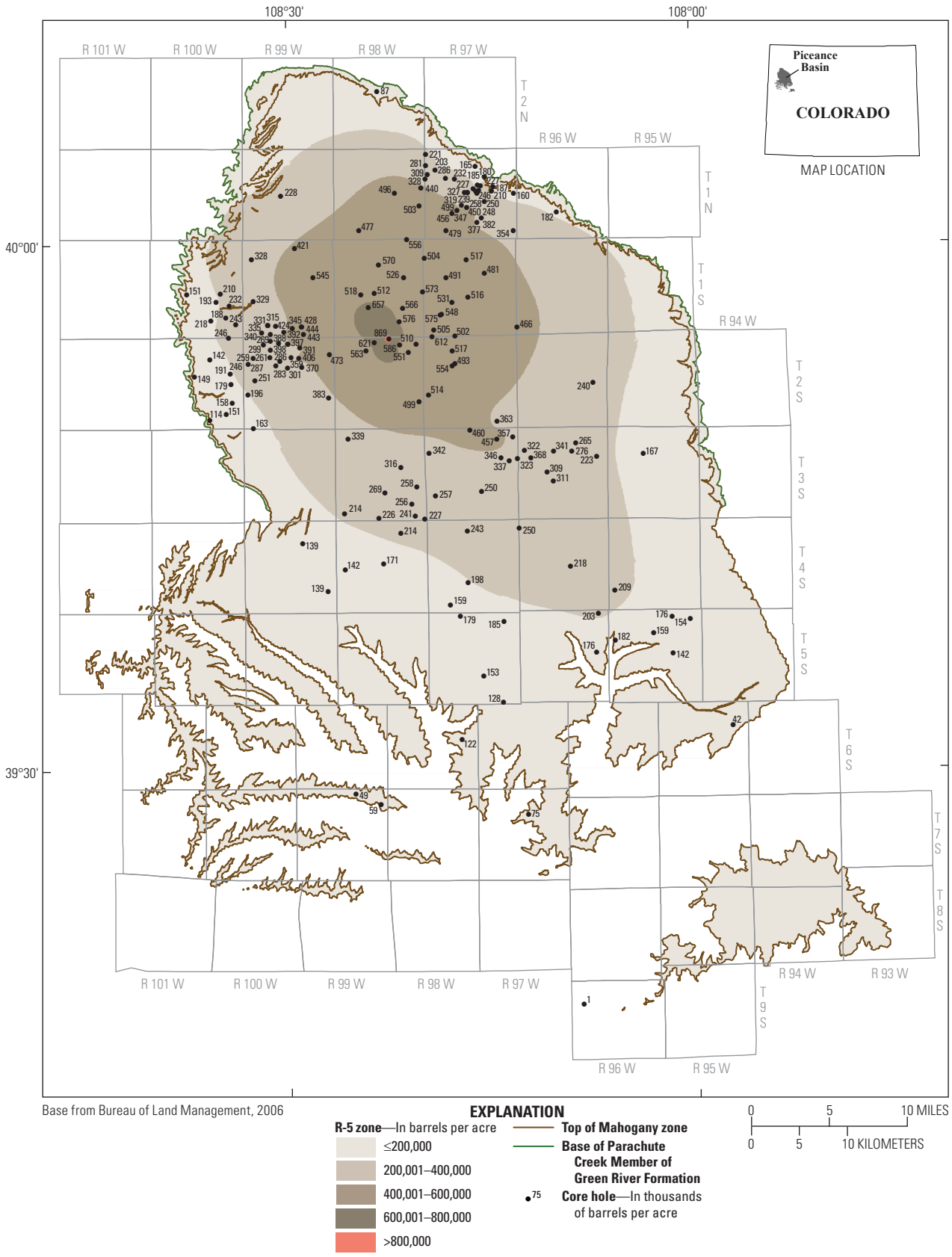

Figure 62. R-5 zone, Piceance Basin, Colo., showing oil yields in barrels per acre (BPA) using only core-hole data. The Radial Basis Function Method (RBF) was used for contouring.

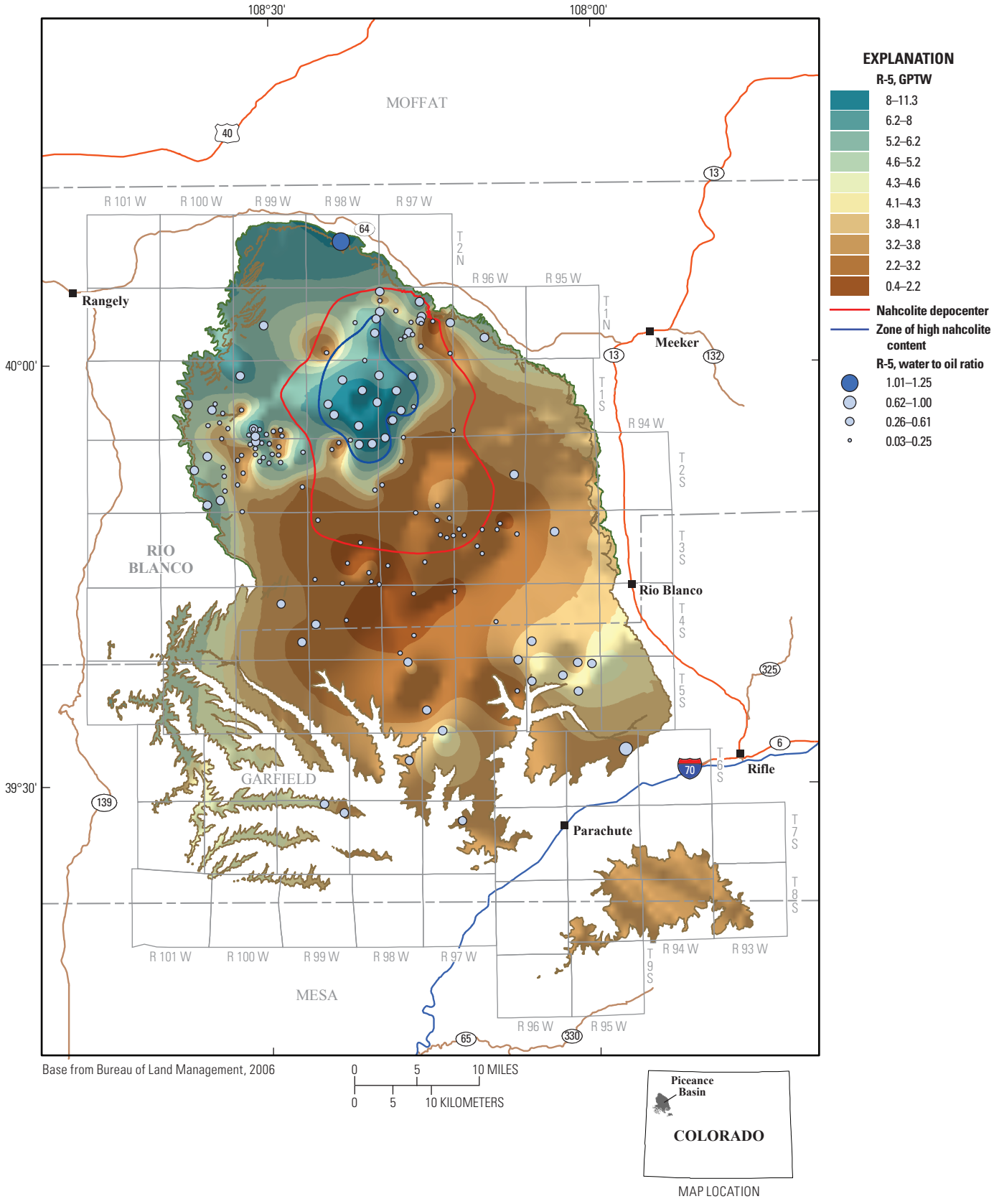

Figure 63. Variation in gallons of water per ton of oil shale (GPTW) for the R-5 oil-shale zone, Piceance Basin, Colo. A hillshade function was applied to visually enhance the displayed contours, creating the illusion that the maps are three dimensional. Bubbles indicate the ratio of water to oil produced for the R-5 zone at each of the control points used.

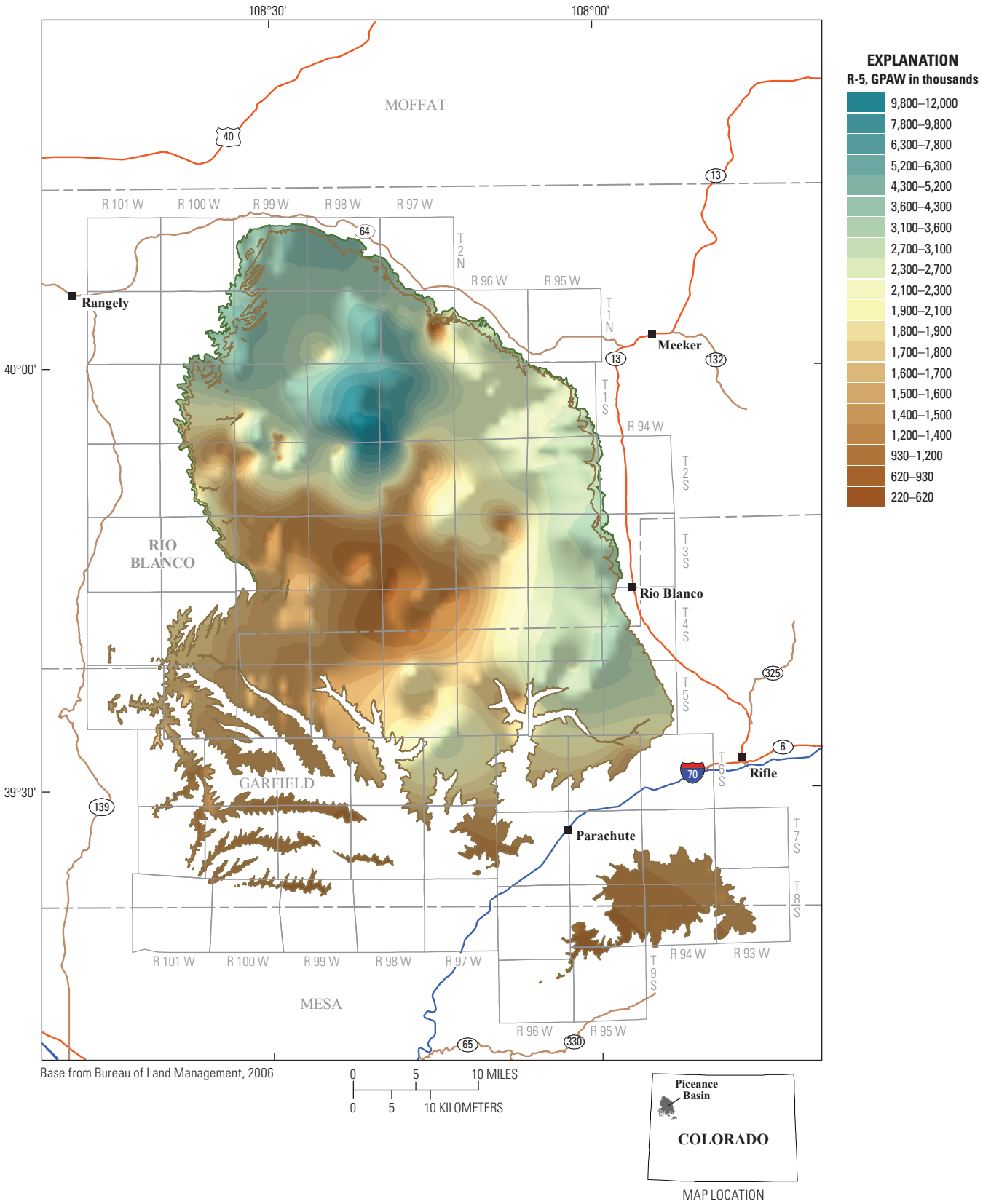

Figure 64. Variations in gallons of water per acre (GPAW) for the R-5 oil-shale zone, Piceance Basin, Colo. A hillshade function was applied to visually enhance the displayed contours, creating the illusion that the maps are three dimensional.

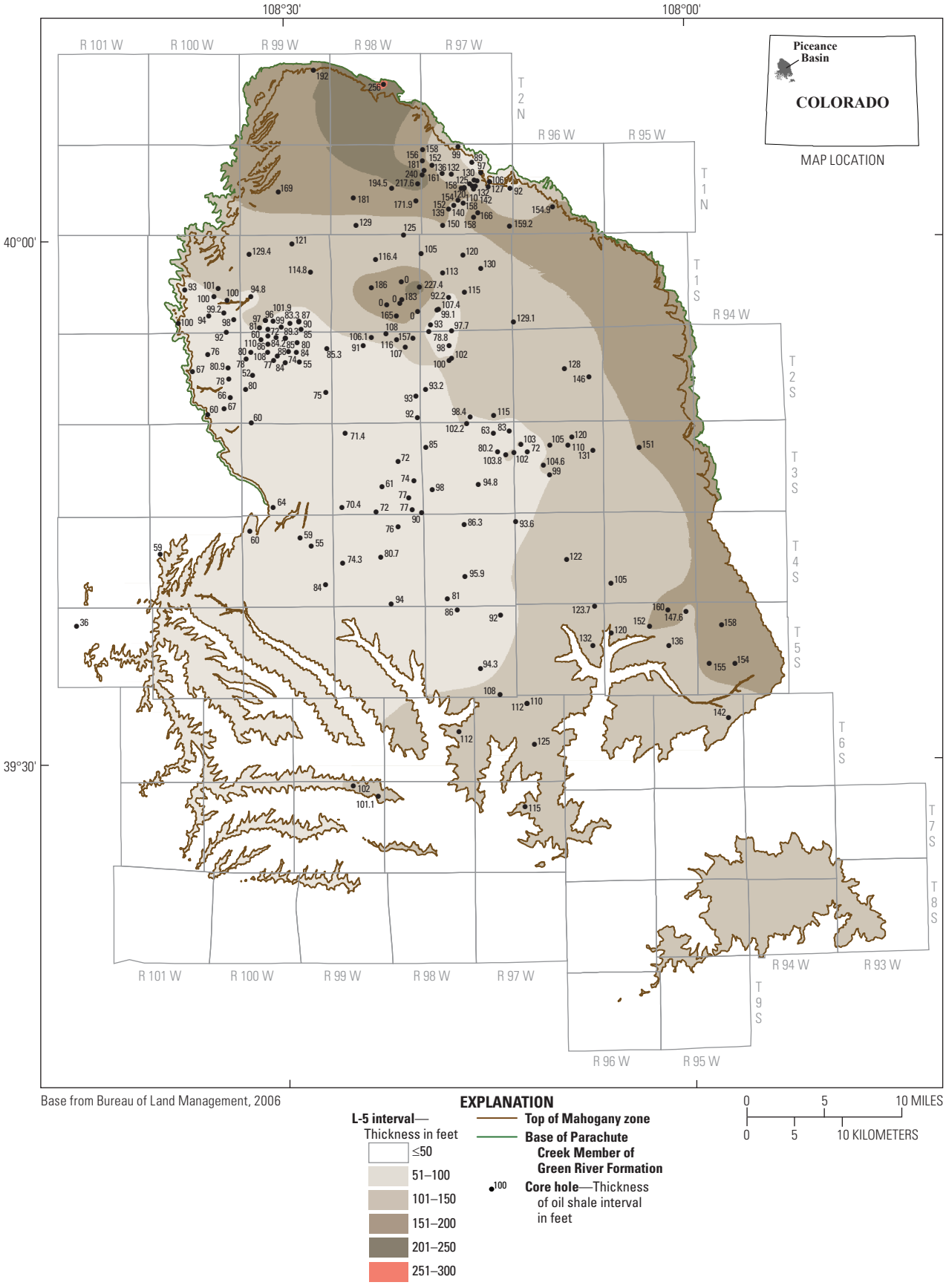

Figure 65. L-5 zone, Piceance Basin, Colo., using both core-hole and rotary-hole data. The Radial Basis Function Method (RBF) was used for contouring.

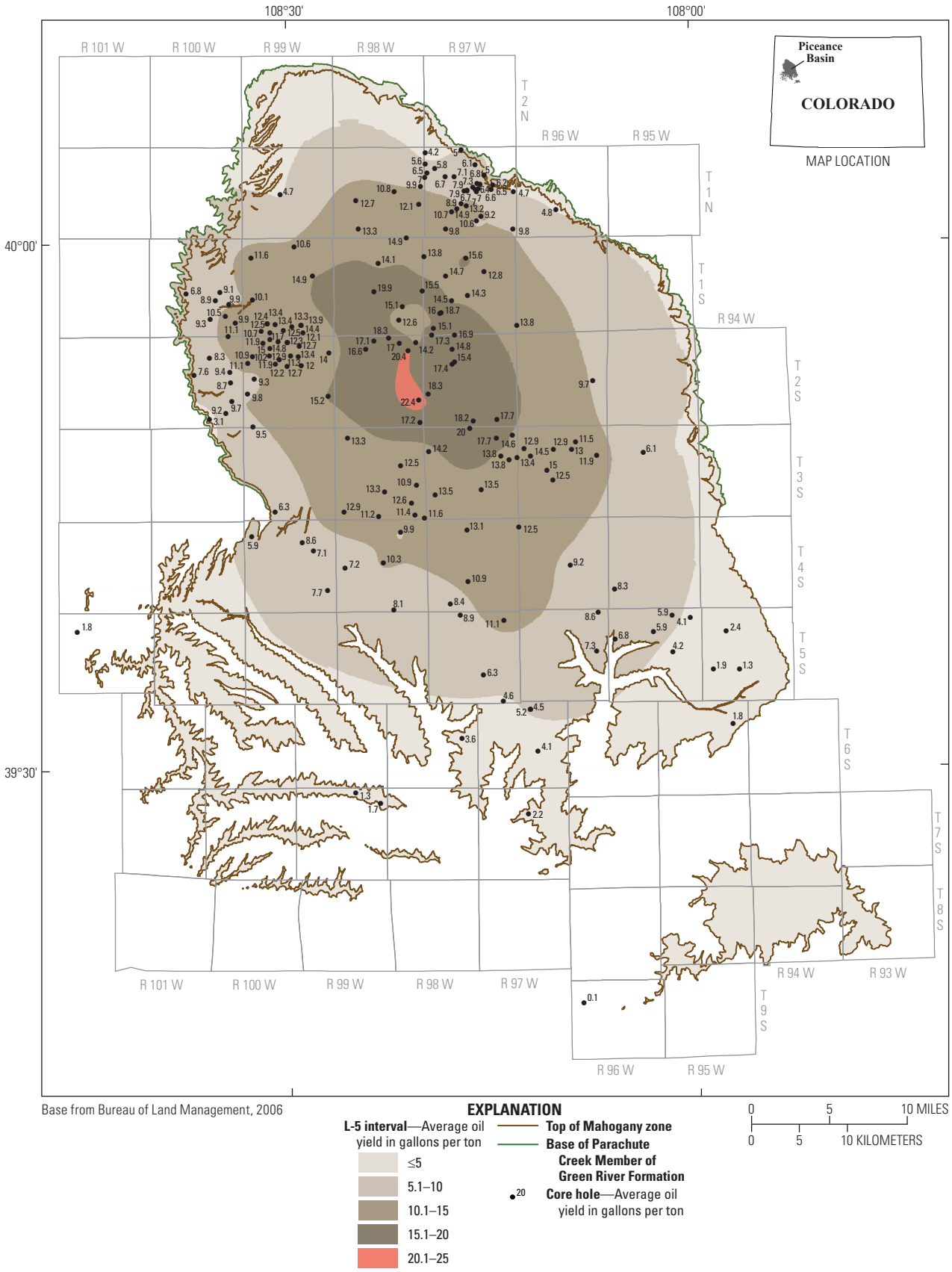

Figure 66. L-5 zone, Piceance Basin, Colo., showing the oil yield in gallons per ton (GPT) using only core-hole data. The Radial Basis Function Method (RBF) was used for contouring.

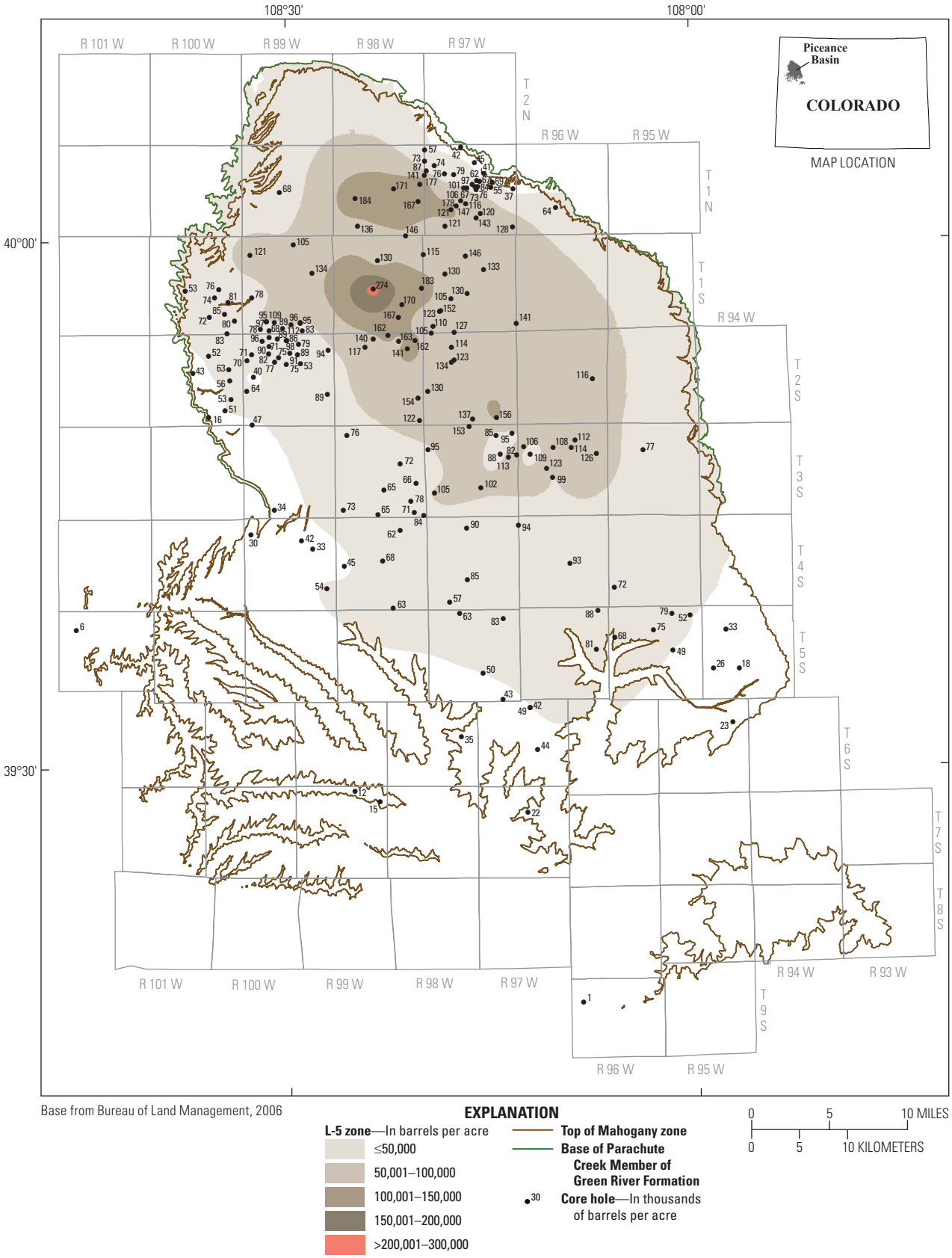

Figure 67. L-5 zone, Piceance Basin, Colo., showing oil yields in barrels per acre (BPA) using only core-hole data. The Radial Basis Function Method (RBF) was used for contouring.

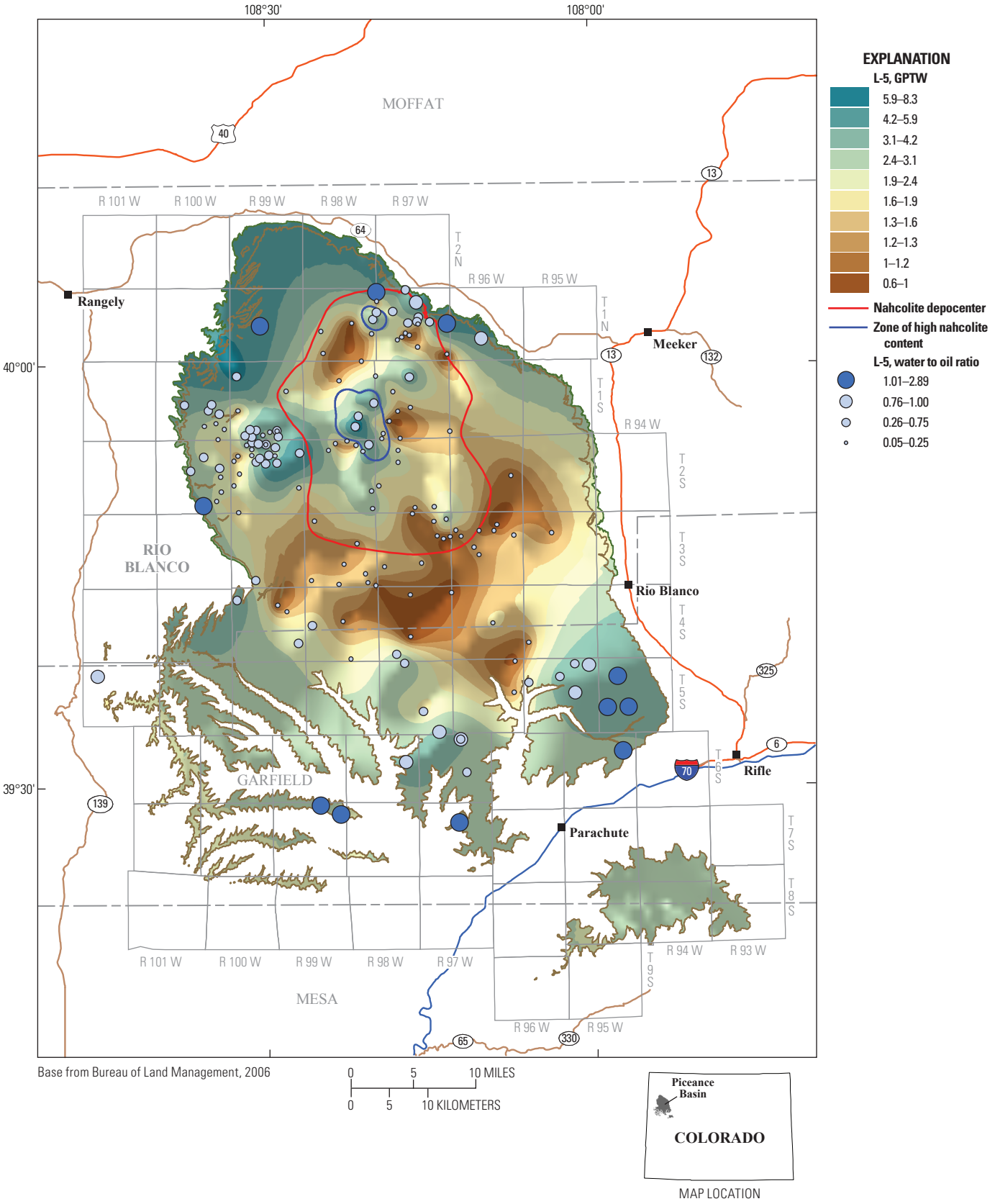

Figure 68. Variation in gallons of water per ton of oil shale (GPTW) for the L-5 oil-shale zone, Piceance Basin, Colo. A hillshade function was applied to visually enhance the displayed contours, creating the illusion that the maps are three dimensional. Bubbles indicate the ratio of water to oil produced for the L-5 zone at each utilized control point.

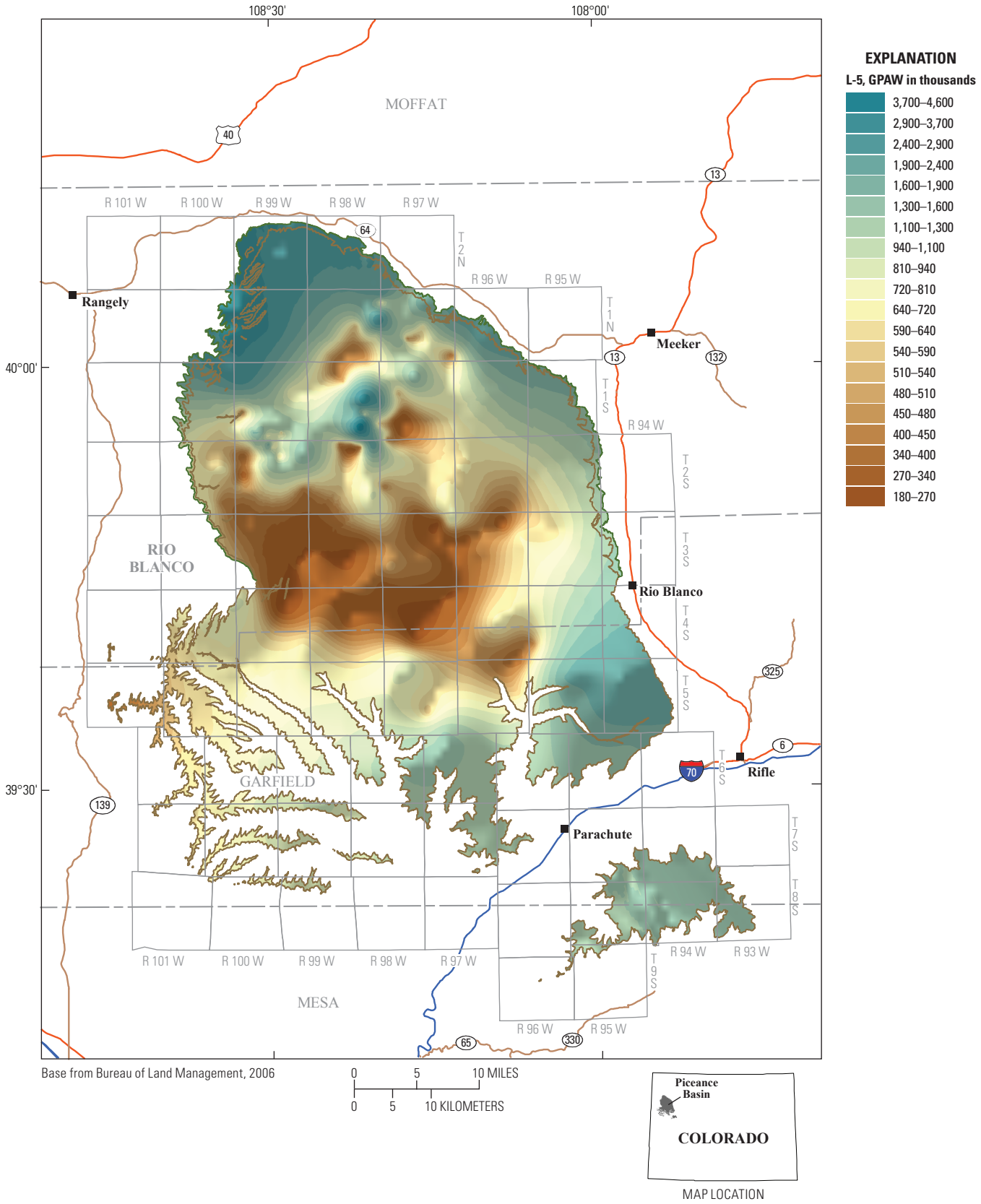

Figure 69. Variations in gallons of water per acre (GPAW) for the L-5 oil-shale zone, Piceance Basin, Colo. A hillshade function was applied to visually enhance the displayed contours, creating the illusion that the maps are three dimensional.

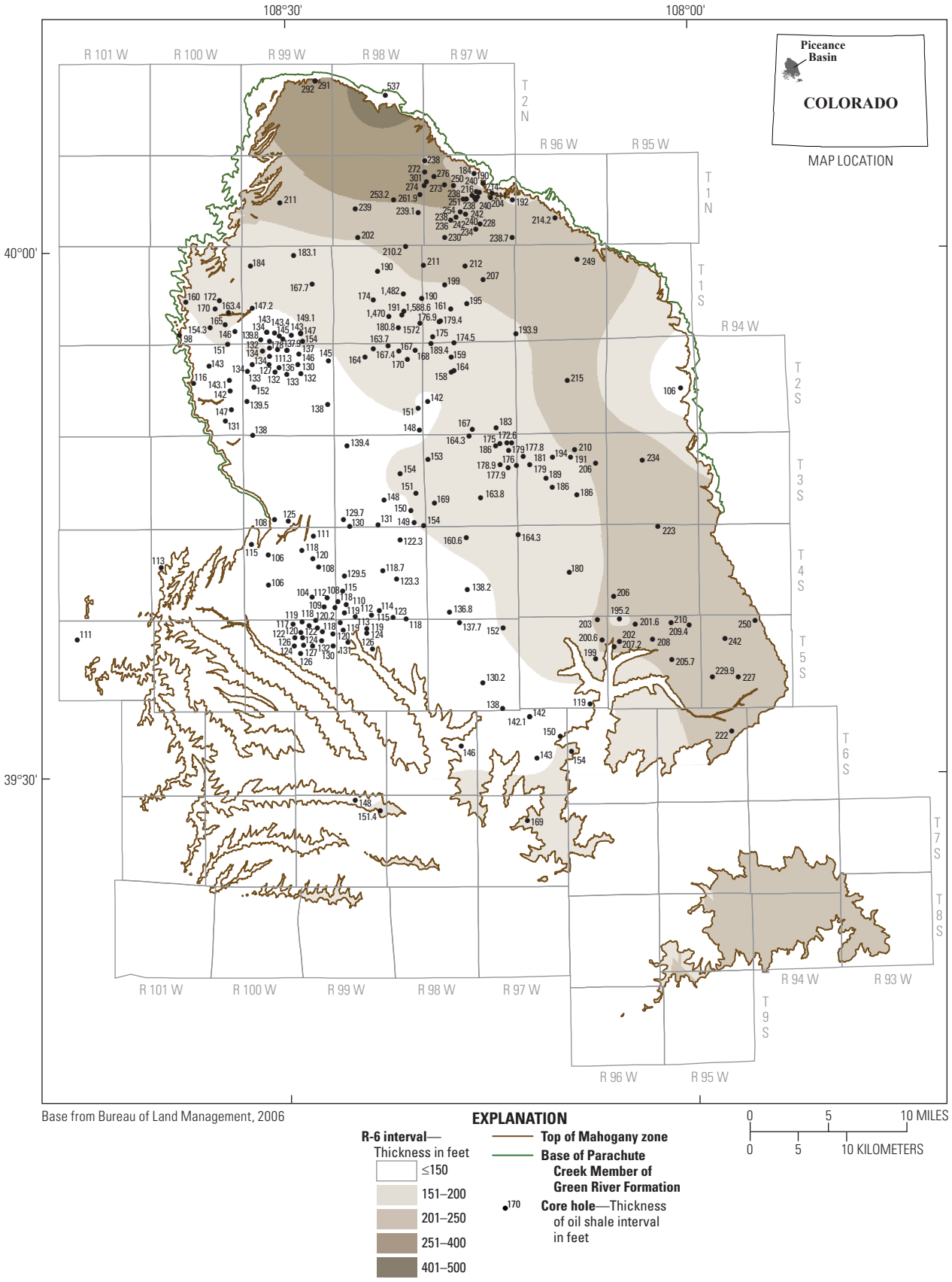

Figure 70. R-6 zone, Piceance Basin, Colo., using both core-hole and rotary-hole data. The Radial Basis Function Method (RBF) was used for contouring.

The R-6 zone is entirely above that dissolution surface, although it originally may have contained some nahcolite prior to leaching. Dawsonite and analcime probably are the major water-bearing minerals in the oil-shale depocenter, with most water tied up in analcime away from the depocenter (pl. 1). The R-6 zone is more than 500 ft thick near the mouth of Yellow Creek in the northern part of the basin and is thinner toward the southwest, to a minimum of 104 ft along the western margin (fig. 70). The area of rich oil-shale deposition expanded greatly during deposition of the R-6 zone, reaching outcrops along Parachute Creek in the southern part of the basin (figs. 71 and 72), where several past oil-shale projects have targeted the R-6 zone and the overlying Mahogany zone. In contrast to the underlying nahcolite-bearing zones, GPTW generally decreases from about 4 to 6 around the basin margins to less than 2 through a broad area in the central part of the basin (fig. 73). The GPAW also decreases from as much as 5,000,000 to less than 1,000,000 in that same central-basin area (fig. 74). Water-to-oil ratios are substantially less than 1:1 in all but four core holes along the basin margins (fig. 73).

The B-groove is a comparatively thin interval varying from 5 to 40 ft thick throughout most of the basin, thickening in the immediate vicinity of the mouth of Yellow Creek in the north to almost 100 ft and toward the extreme eastern basin margin, where it reaches a maximum of 90 ft (fig. 75). The B-groove is characterized by very low oil yields ranging from less than 1 GPT to about 10 GPT throughout most of the basin (fig. 76) and by very low total in-place oil (fig. 77). It is one of the most distinctive and easily recognizable units on geophysical logs and oil-yield histograms in the entire oil-shale interval (fig. 7, pl. 1). The GPTW in B-groove, generally 6 to 9 around the basin margins, decreases to less than 1 in the central part of the basin (fig. 78), and GPAW follows the same general pattern, decreasing from greater than 1,000,000 to less than 100,000 (fig. 79).

The base of the Mahogany zone represents the beginning of a major expansion of Lake Uinta that brought rich oil-shale deposition to much of the broad, marginal shelf that surrounded the oil-shale depocenter (Johnson, 1985). The Mahogany is one of the richest and most extensive oil-shale zones in the basin (fig. 7, pl. 1) and because it crops out along the Colorado River and tributaries in the southern part of the basin, the Mahogany zone has been the target of nearly all projects to extract shale oil in the Piceance Basin. The Mahogany zone exceeds 100 ft in thickness through a broad southeast-trending area that extends to outcrop in the southeastern part of the basin and is more than 200 ft thick in the northern part of the basin near the mouth of Yellow Creek, where the postulated connection with Lake Gosiute existed (Johnson, 1985) to the north (figs. 3 and 80). Although no nahcolite or halite is present, the Mahogany zone does contain scattered nahcolite vugs, indicating that some nahcolite once was present. The Mahogany exceeds 22 GPT in the central part of the basin, extending to outcrop along the Colorado River (fig. 81). Oil yields are low in the northernmost part of the basin near the mouth of Yellow Creek due to the influx of clastic sediments there. Maximum in-place oil in BPA is generally in the area where the Mahogany is thickest (figs. 80 and 82). The GPTW ranges from 5 to 7 in marginal areas and decreases towards the central and south-central parts of the basin to less than 2 (fig. 83). However, water contents are high throughout the north-central part of the basin, an area of high oil yields (figs. 81 and 83). The GPAW decreases from a maximum of more than 3,500,000 along the northern margin of the basin to less than 350,000 in the southwestern part (fig. 84). The water-to-oil ratio is significantly less than 1:1 throughout the basin (fig. 83).

The A-groove is another thin zone similar in thickness to B-groove (fig. 7, pl. 1). It thins in an irregular fashion to the southwest from 25 to 38 ft along the northeastern margin to less than 10 ft in many wells in the southwestern part of the basin (fig. 85), with oil yields of less than 10 GPT throughout most of the basin (fig. 86) and very low amounts of total oil in place (fig. 87). The range of GPTW values is complex but generally decreases from more than 6 in the northern half of the basin and near basin margins to less than 1 in the south-central part (fig. 88). The GPAW range also decreases toward that area in the south-central part of the basin, from more than 300,000 to less than 20,000 (fig. 89). Water-to-oil ratios are less than 1:1 except in some marginal areas (fig. 88).

The interval extending from the top of B-groove to the top of bed 44 of Donnell (2008) is a complex interval deposited during the period when the Piceance Basin part of Lake Uinta was gradually filling with volcaniclastic sediments from Wyoming (fig. 5). Thick wedges of volcaniclastic sediments derived from the Absaroka volcanic field in northwestern Wyoming prograded from north to south across the Piceance Basin starting from a point (fig. 5) near the mouth of Yellow Creek in the north-central part of the basin (Johnson, 1981, 1985). The southward progradation of those volcaniclastic sediments occurred over substantial time, with intervals of oil shale deposited during periods when volcaniclastic sediments supplied to the basin from the north diminished or ceased entirely. The oil-shale intervals coalesce towards the southern end of the basin as the intervening clastic wedges pinch out, creating a nearly continuous interval of oil shale several hundred feet thick in the southern part of the basin (fig. 5). The bed 44 to B-groove interval thickens markedly to the north from less than 150 ft in the southwestern part of the basin to more than 1,500 ft in the north-central part due to insertion of volcaniclastic wedges (fig. 90). Oil yield decreases markedly to the north in the direction of increasing volcaniclastic sedimentary rocks (fig. 91); total oil in place, however, is greatest in the central part of the basin (fig. 92). Many volcaniclastic intervals were not assessed, as they contain little to no oil. That exception does not greatly affect the total-oil-in-place calculation but does affect calculations of water content, as thick, organically lean intervals can contain large amounts of water. As a result, the water GPT and BPA maps for the bed 44 to B-groove interval thus are reliable only in the southern part of the basin, south approximately of the 300-ft isopach line on figure 90, where only minor volcaniclastic sedimentary rocks are present. Both GPTW and GPAW generally decrease southward in that area, but there is a great deal of scatter (figs. 93 and 94). Almost all water-to-oil ratios are significantly less than 1:1 (fig. 93).

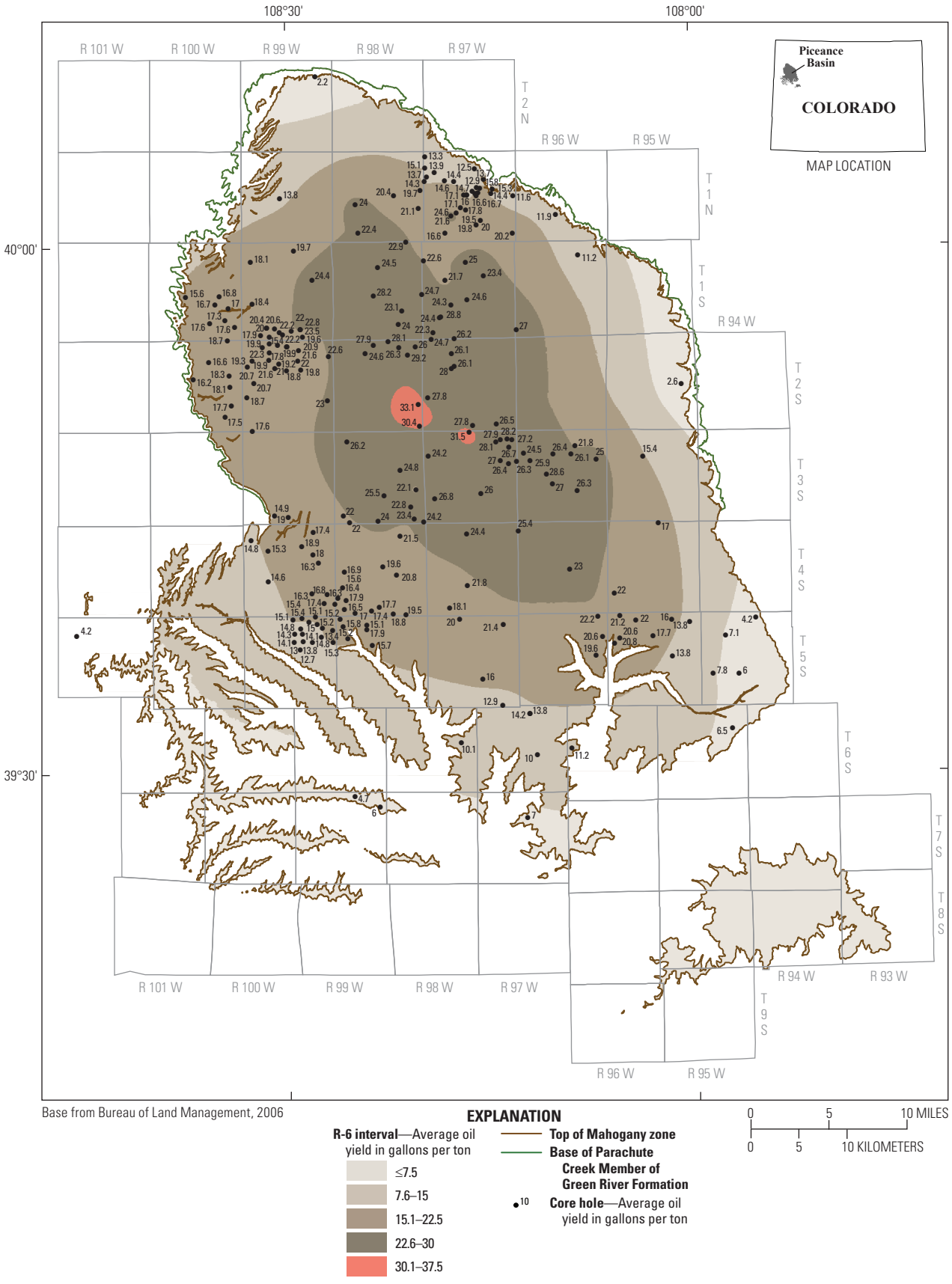

Figure 71. R-6 zone, Piceance Basin, Colo., showing the oil yield in gallons per ton (GPT) using only core-hole data. The Radial Basis Function Method (RBF) was used for contouring.

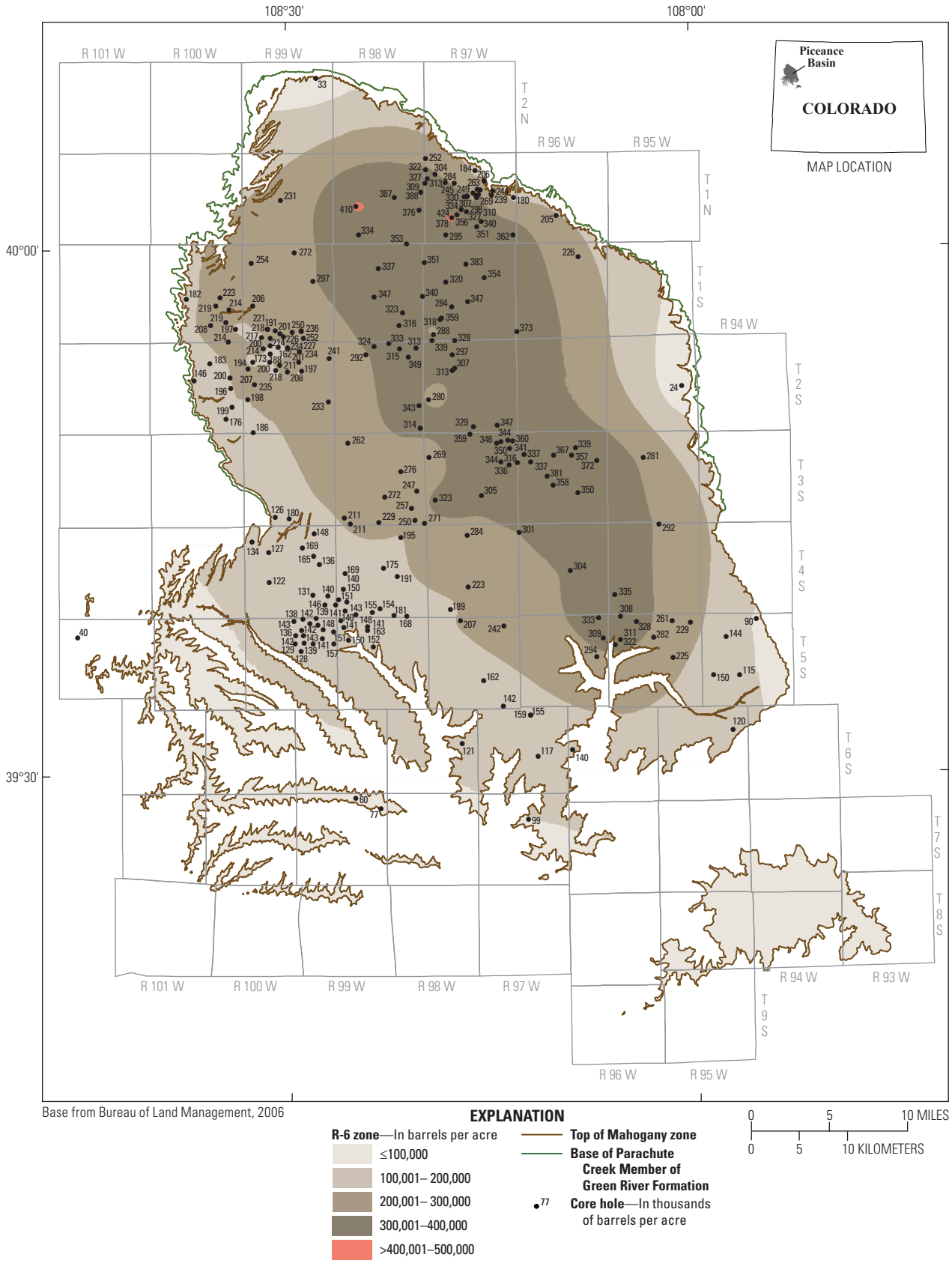

Figure 72. R-6 zone, Piceance Basin, Colo., showing oil yields in barrels per acre (BPA) using only core-hole data. The Radial Basis Function Method (RBF) was used for contouring.

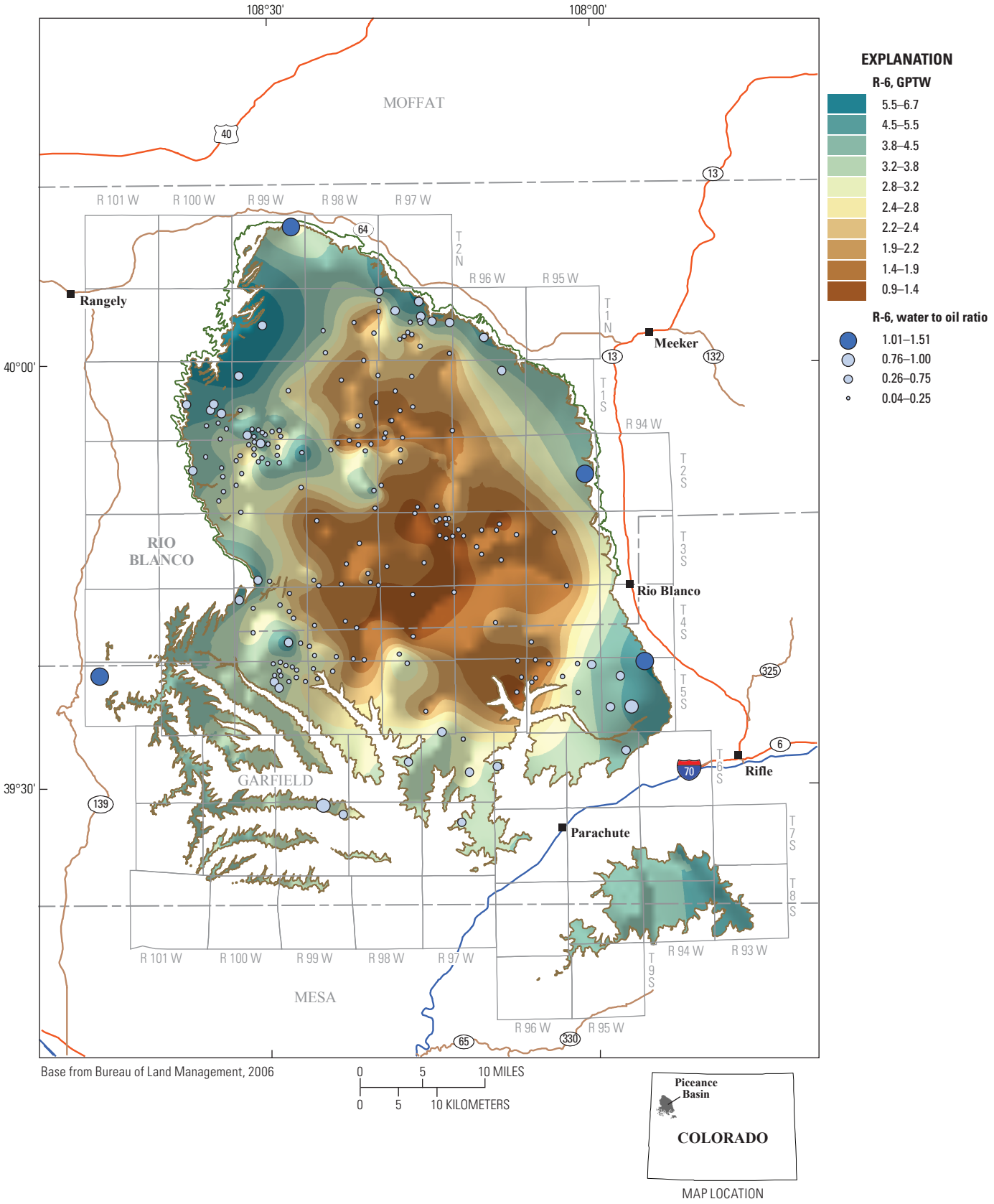

Figure 73. Variation in gallons of water per ton of oil shale (GPTW) for the R-6 oil-shale zone, Piceance Basin, Colo. A hillshade function was applied to visually enhance the displayed contours, creating the illusion that the maps are three dimensional. Bubbles indicate the ratio of water to oil produced for the R-6 zone at each of the control points used.

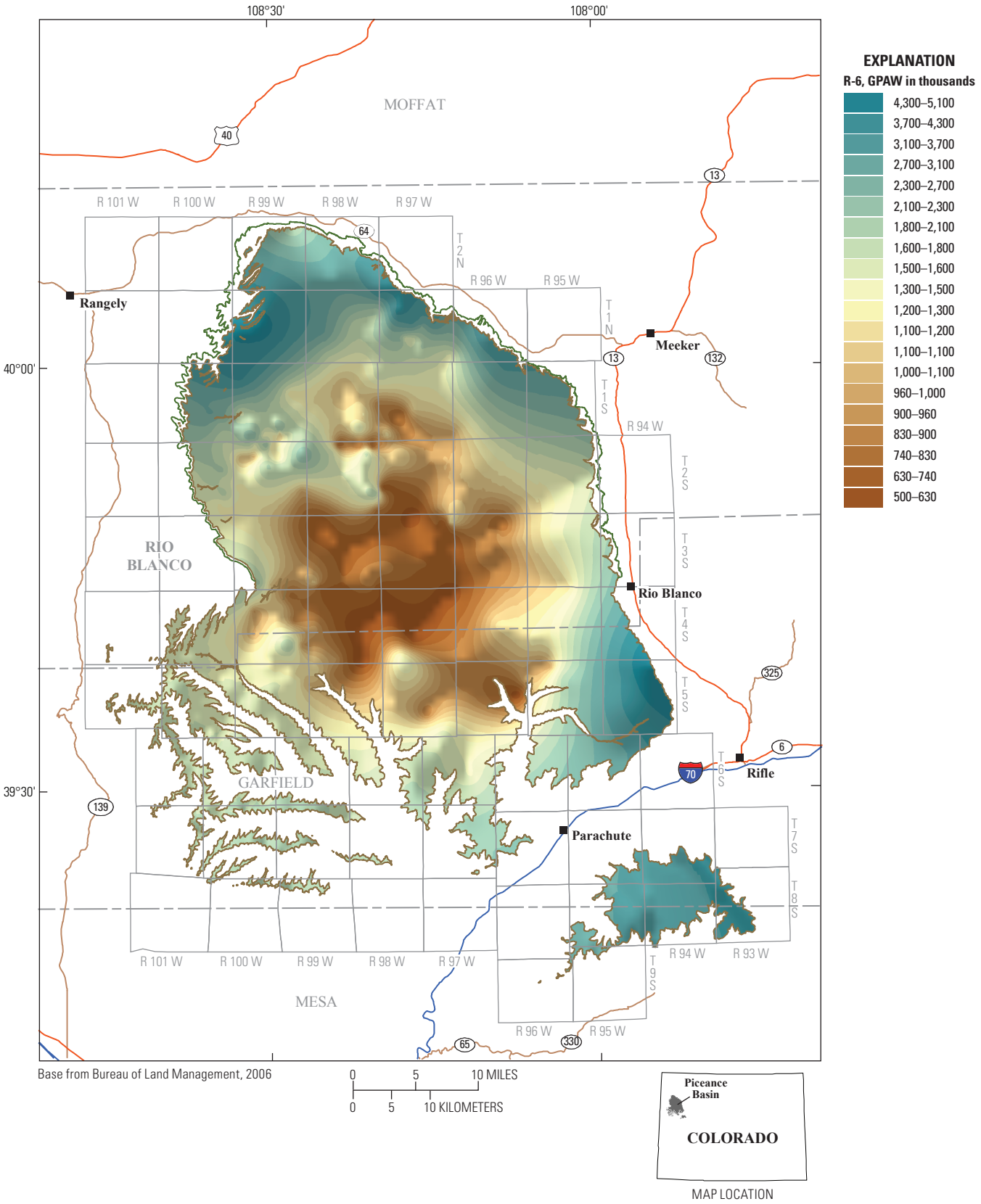

Figure 74. Variations in gallons of water per acre (GPAW) for the R-6 oil shale zone, Piceance Basin, Colo. A hillshade function was applied to visually enhance the displayed contours, creating the illusion that the maps are three dimensional.

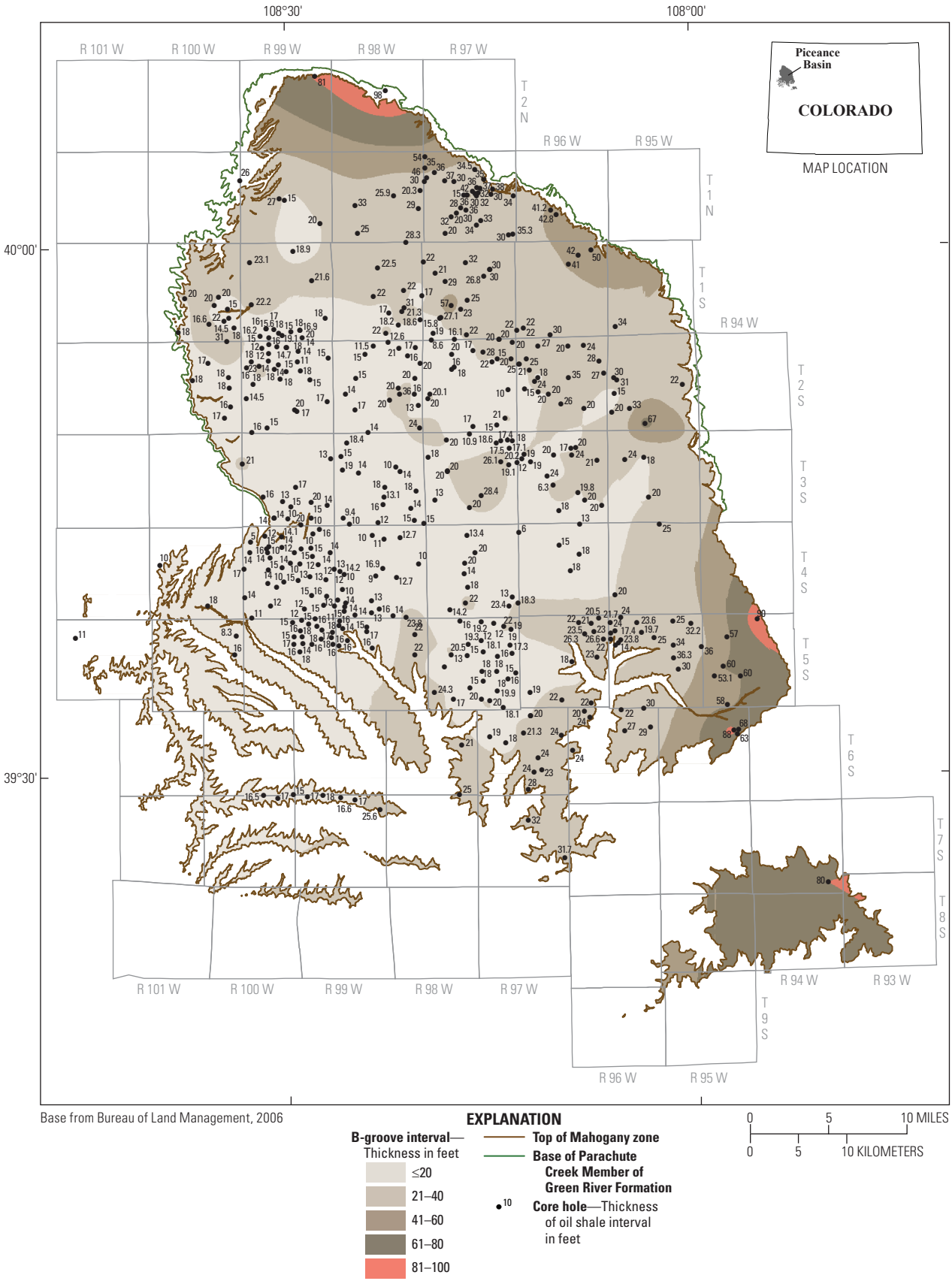

Figure 75. B-groove interval, Piceance Basin, Colo., using both core-hole and rotary-hole data. The Radial Basis Function Method (RBF) was used for contouring.

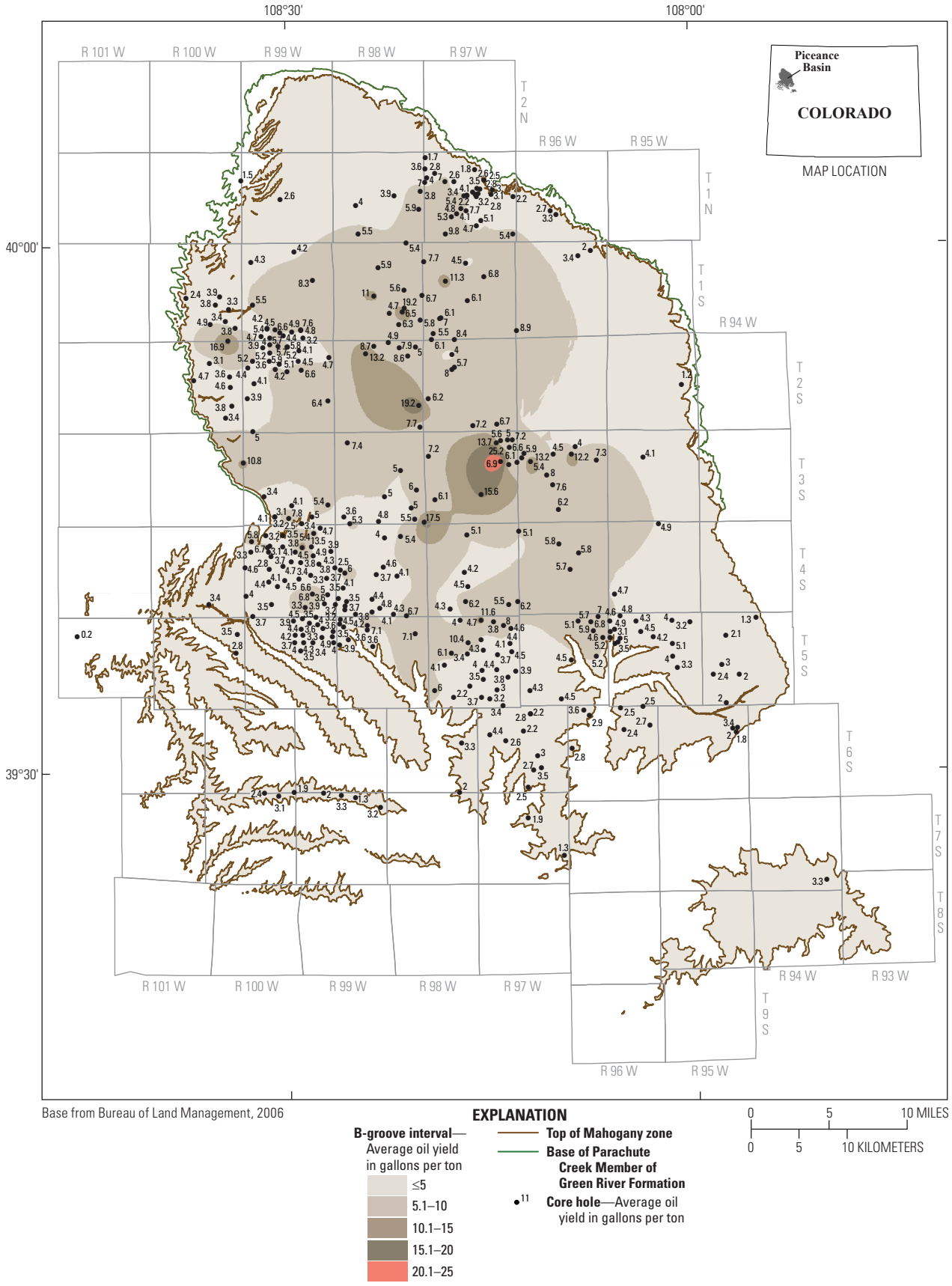

Figure 76. B-groove interval, Piceance Basin, Colo., showing the oil yield in gallons per ton (GPT) using only core-hole data. The Radial Basis Function Method (RBF) was used for contouring.

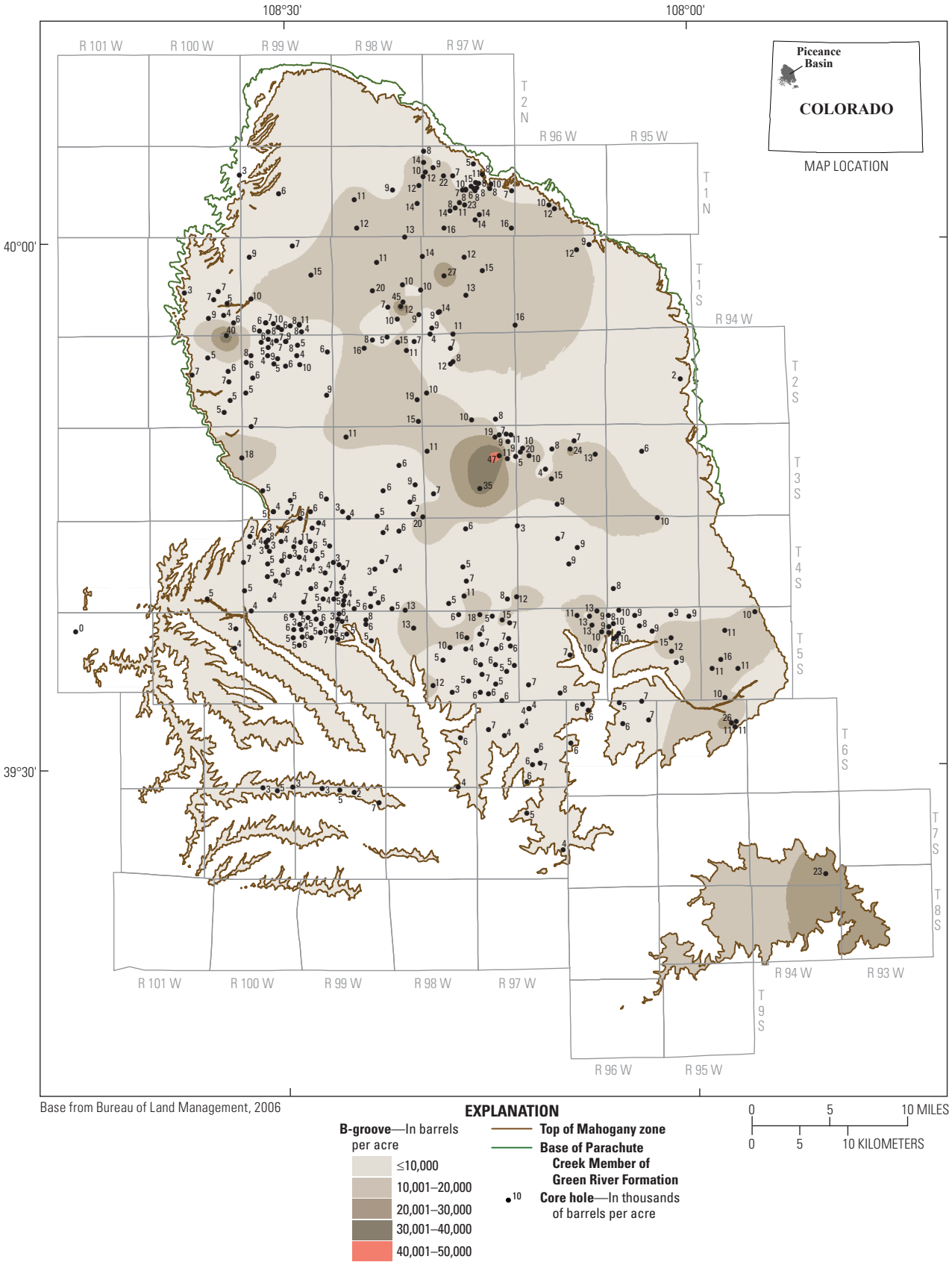

Figure 77. B-groove interval, Piceance Basin, Colo., showing oil yields in barrels per acre (BPA) using only core-hole data. The Radial Basis Function Method (RBF) was used for contouring.

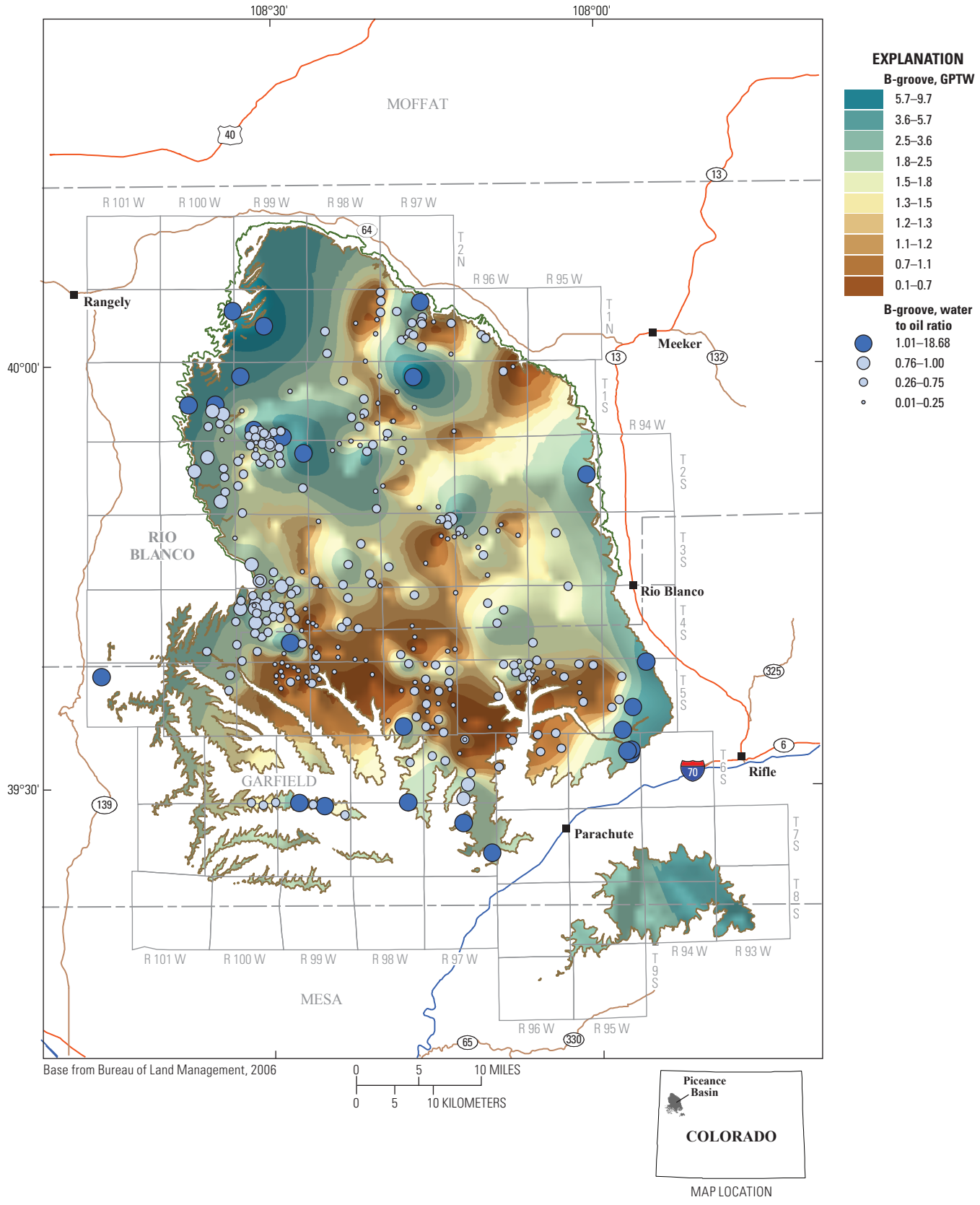

Figure 78. Variation in gallons of water per ton of oil shale (GPTW) for the B-groove interval, Piceance Basin, Colo. A hillshade function was applied to visually enhance the displayed contours, creating the illusion that the maps are three dimensional. Bubbles indicate the ratio of water to oil produced for the B-groove zone at each of the control points used.

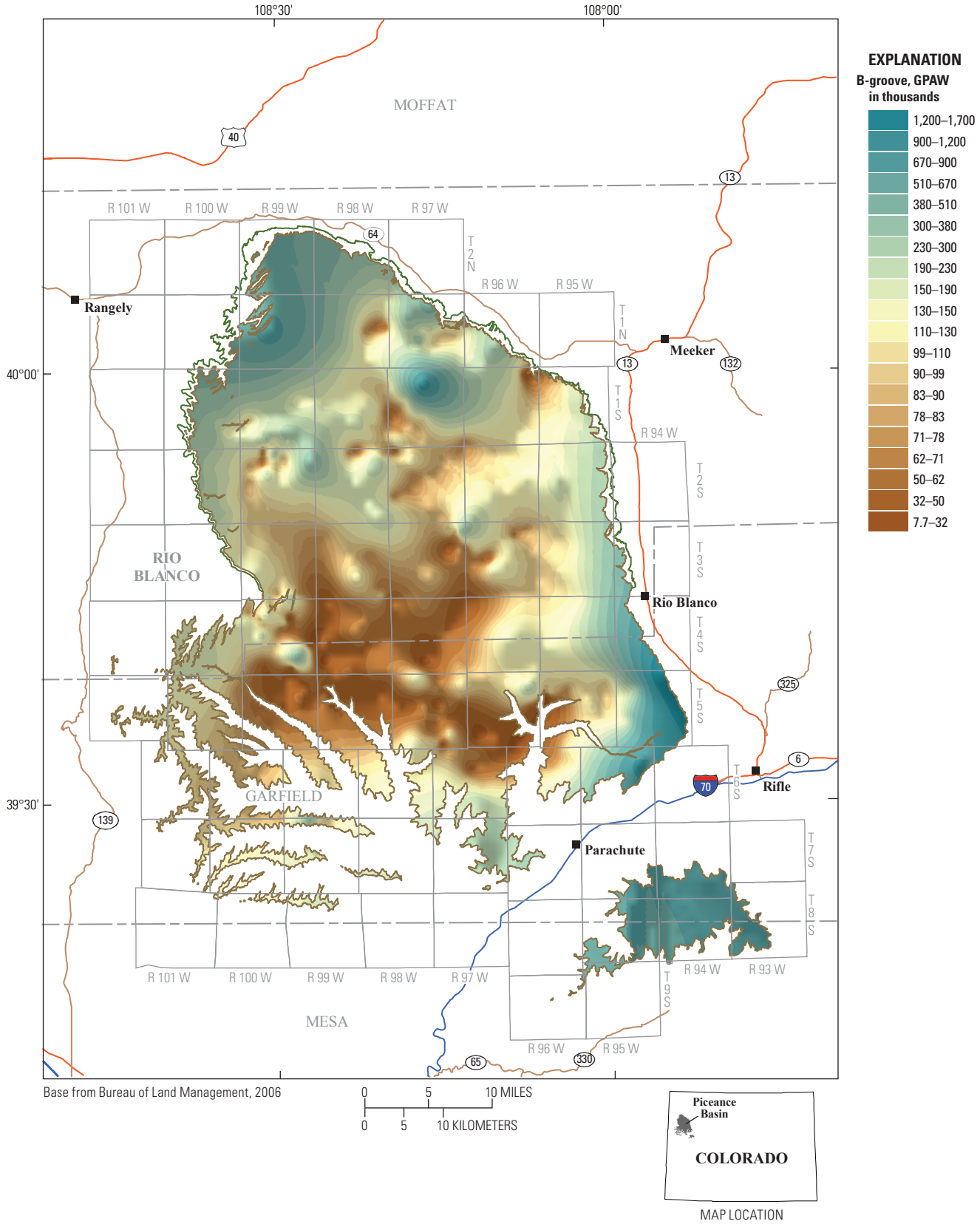

Figure 79. Variations in gallons of water per acre (GPAW) for the B-groove interval, Piceance Basin, Colo. A hillshade function was applied to visually enhance the displayed contours, creating the illusion that the maps are three dimensional.

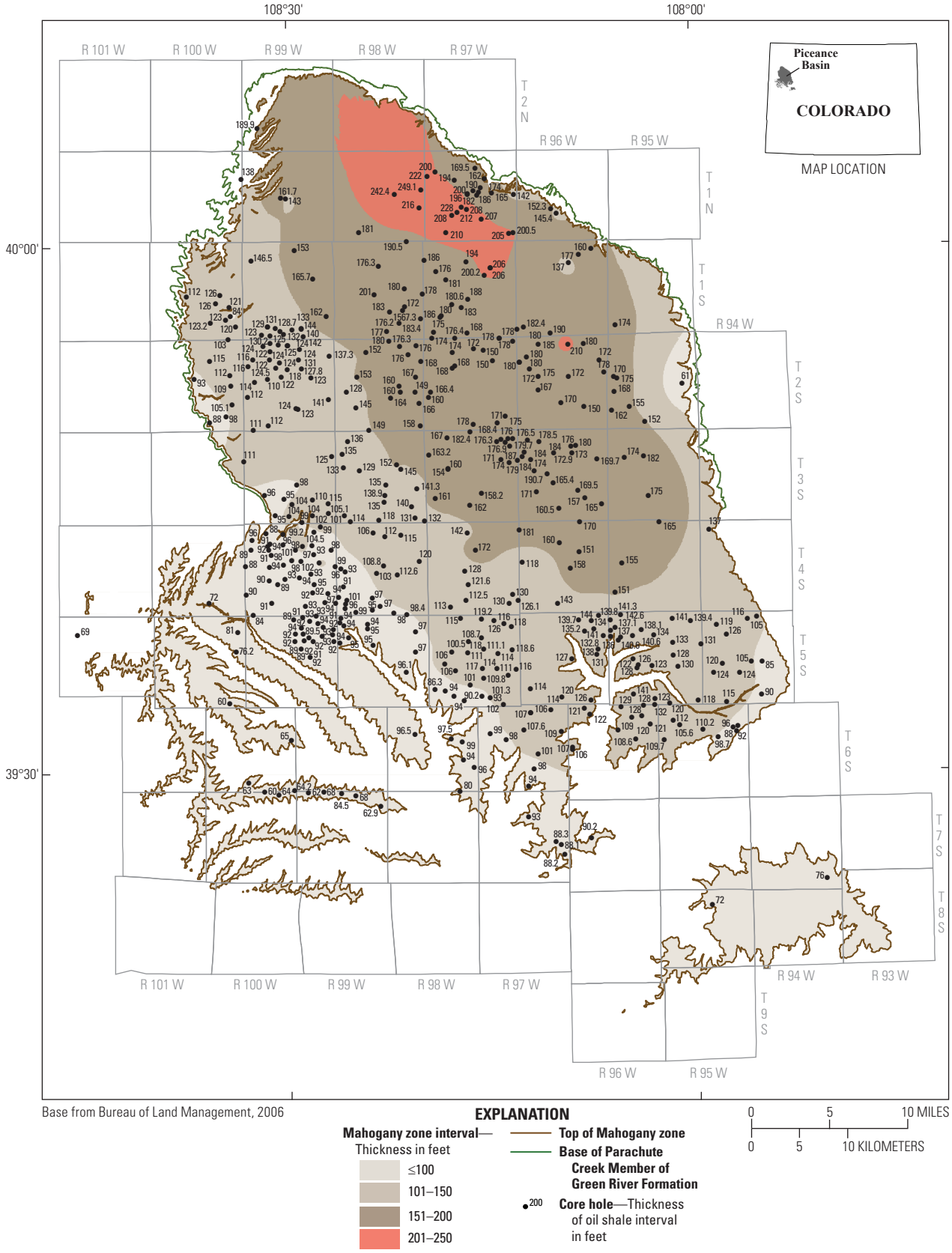

Figure 80. Mahogany oil-shale zone, Piceance Basin, Colo., using both core-hole and rotary-hole data. The Radial Basis Function Method (RBF) was used for contouring.

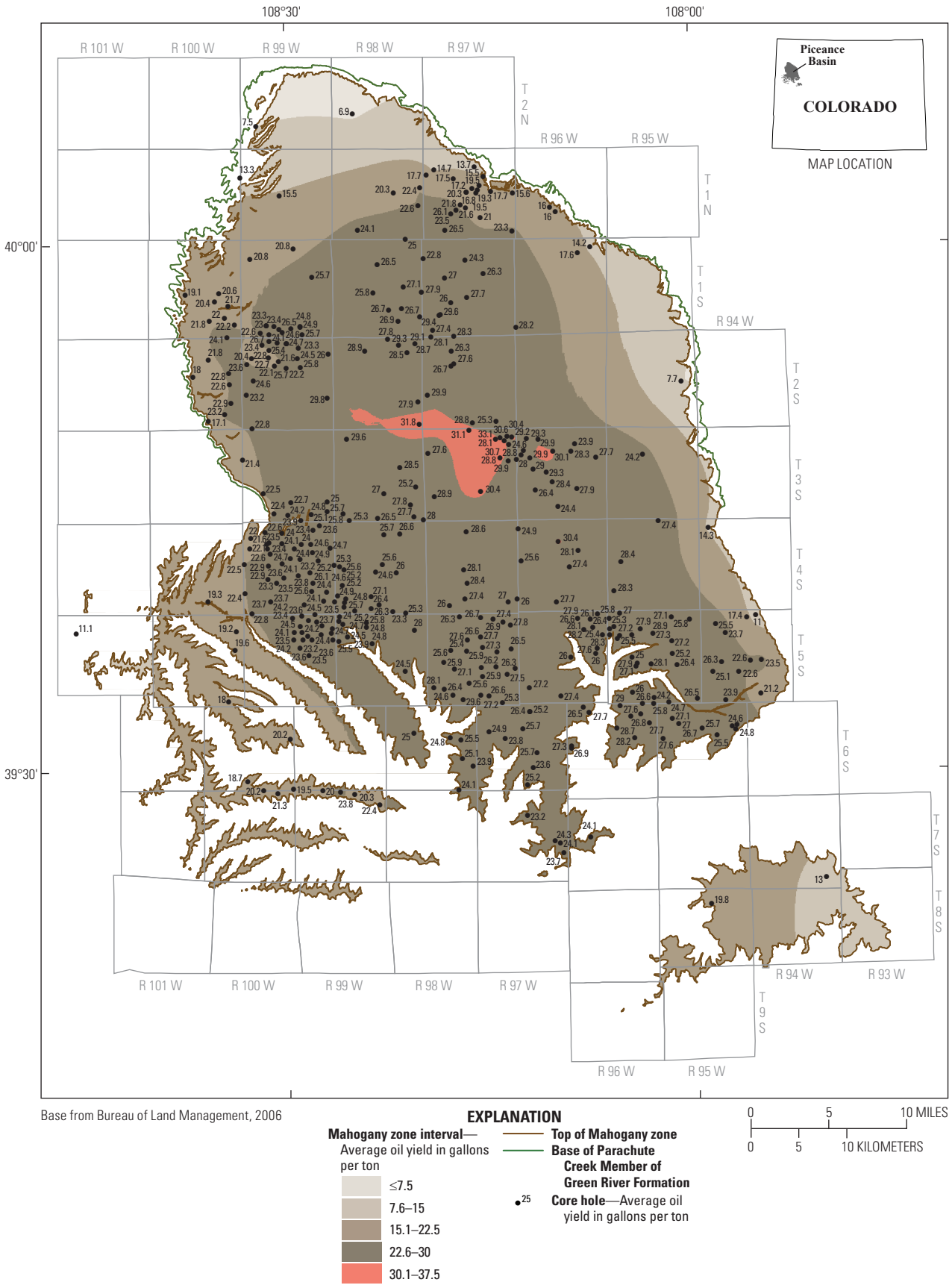

Figure 81. Mahogany oil-shale zone, Piceance Basin, Colo., showing the oil yield in gallons per ton (GPT). The Radial Basis Function Method (RBF) was used for contouring.

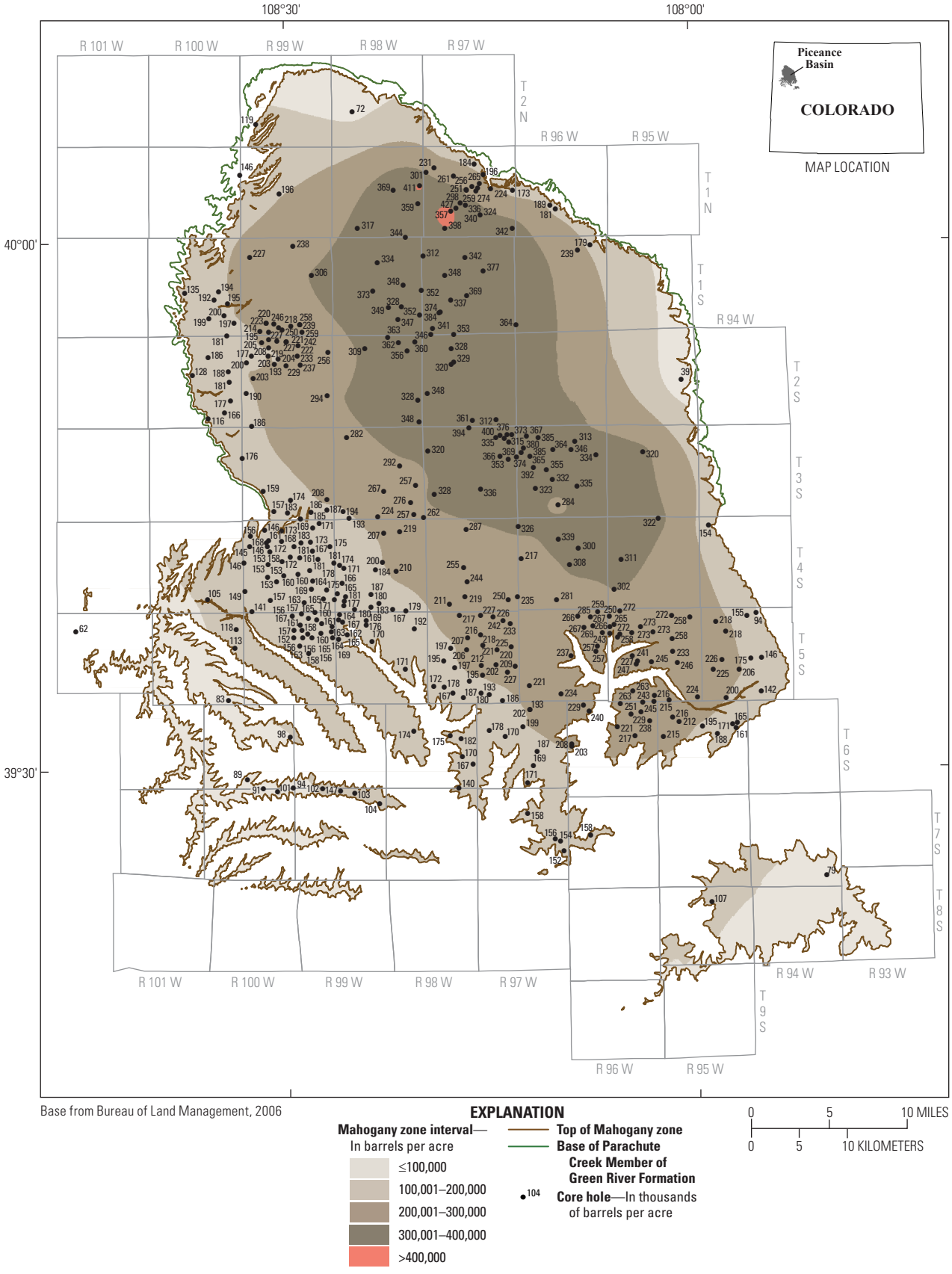

Figure 82. Mahogany oil-shale zone, Piceance Basin, Colo., showing oil yields in barrels per acre (BPA). The Radial Basis Function Method (RBF) was used for contouring.

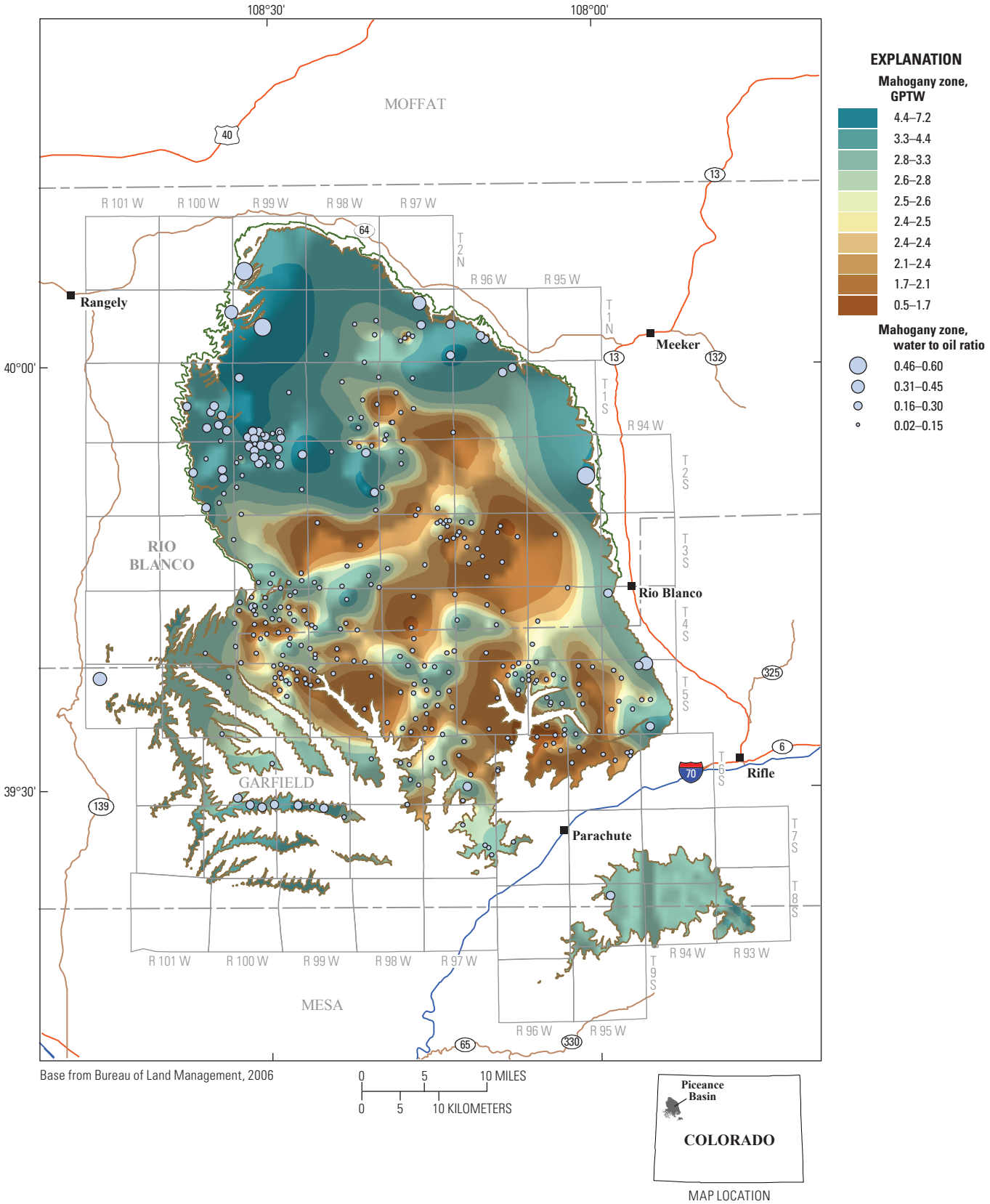

Figure 83. Variation in gallons of water per ton of oil shale (GPTW) for the Mahogany oil-shale zone, Piceance Basin, Colo. A hillshade function was applied to visually enhance the displayed contours, creating the illusion that the maps are three dimensional. Bubbles indicate the ratio of water to oil produced for the Mahogany zone at each of the utilized control points.

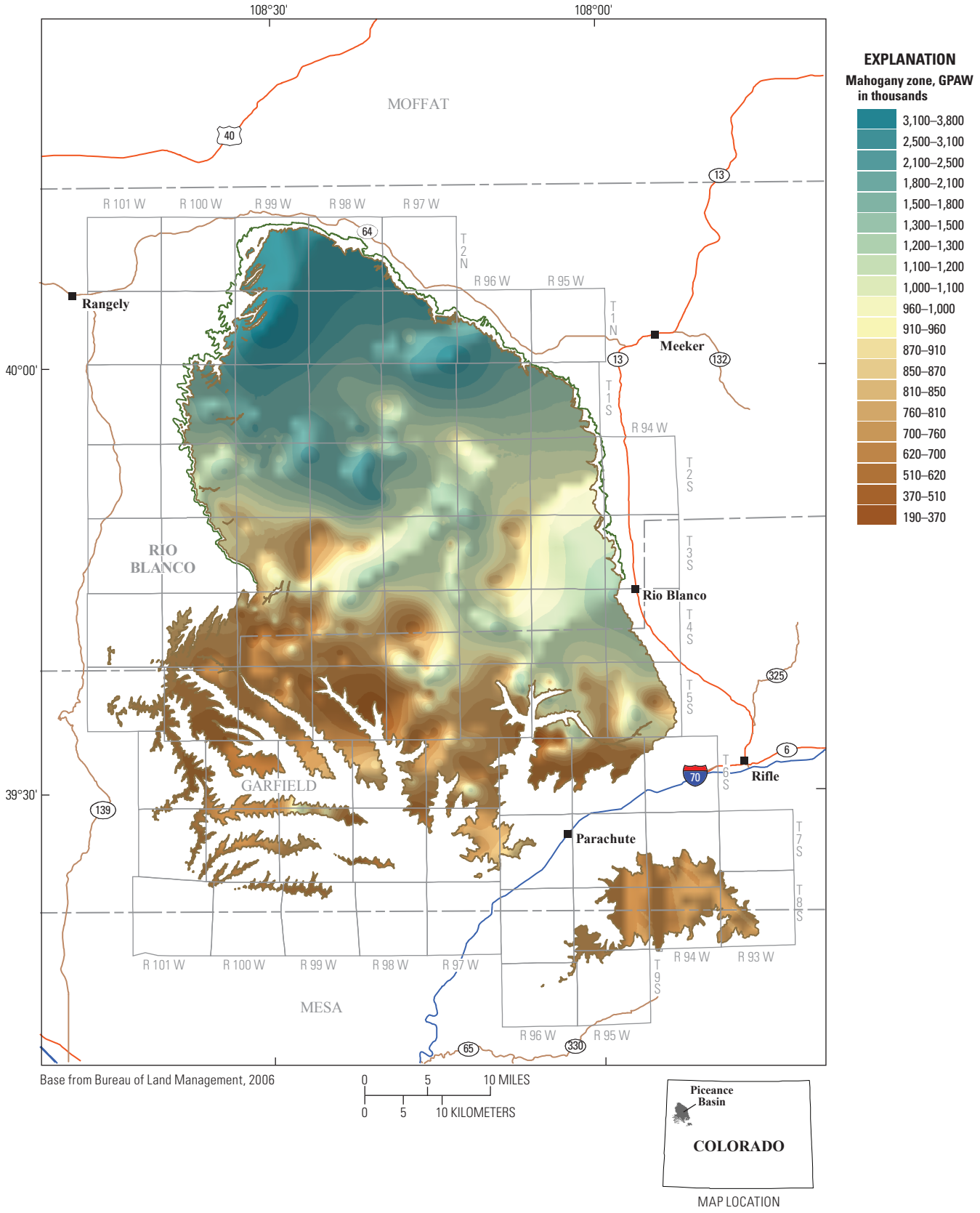

Figure 84. Variations in gallons of water per acre (GPAW) for the Mahogany oil-shale zone, Piceance Basin, Colo. A hillshade function was applied to visually enhance the displayed contours, creating the illusion that the maps are three dimensional.

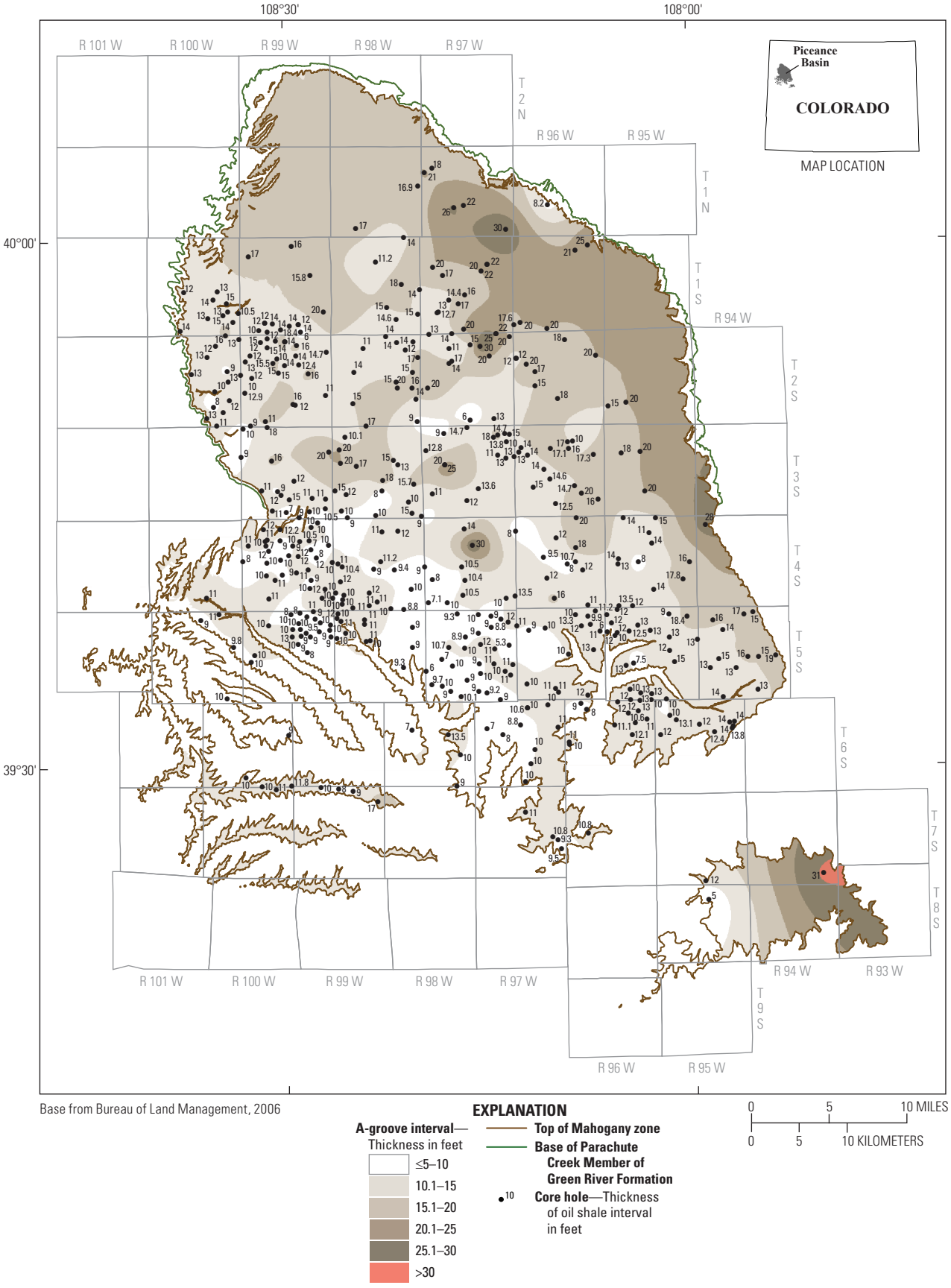

Figure 85. A-groove interval, Piceance Basin, Colo., using both core-hole and rotary-hole data. The Radial Basis Function Method (RBF) was used for contouring.

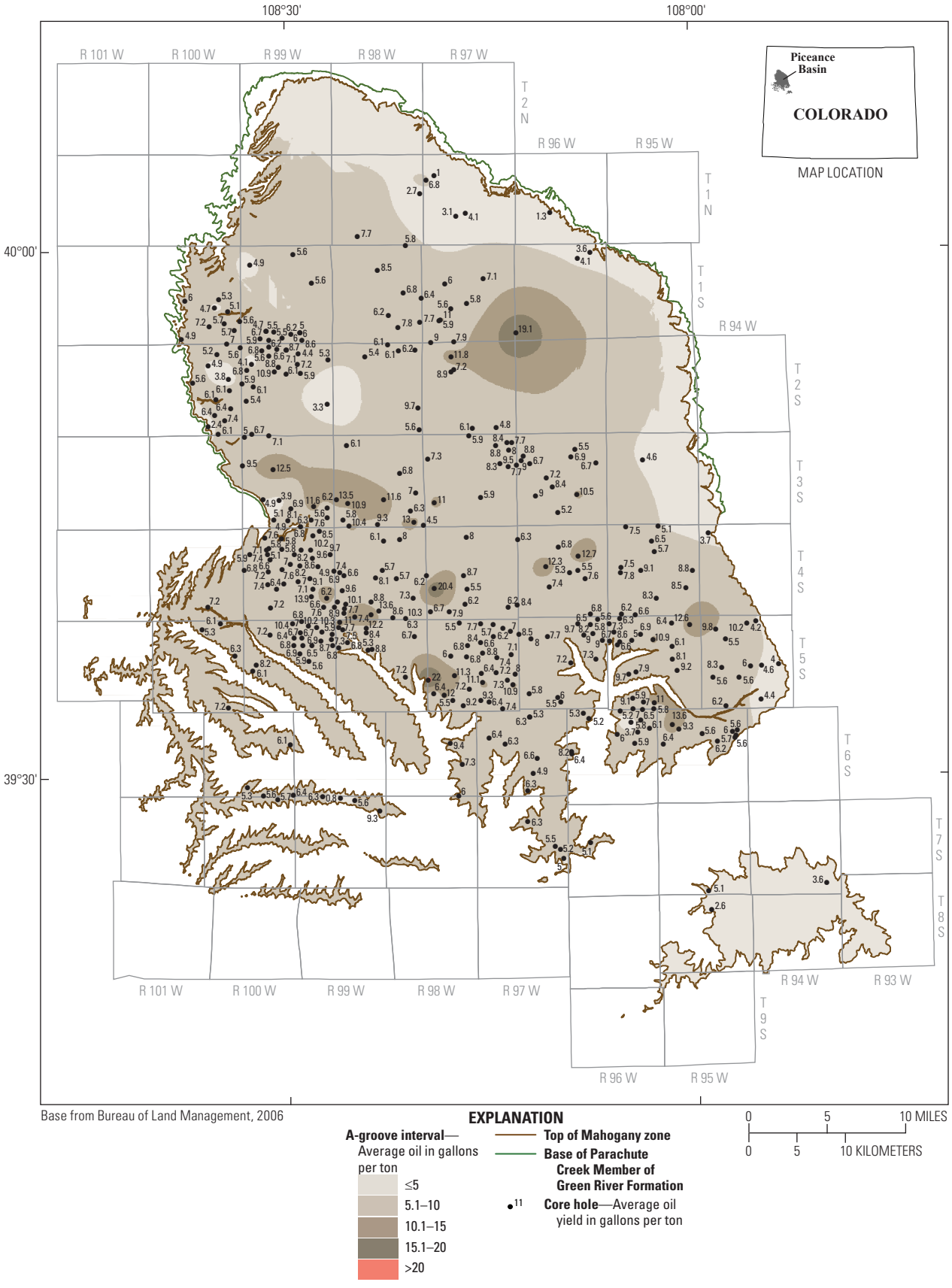

Figure 86. A-groove interval, Piceance Basin, Colo., showing the oil yield in gallons per ton (GPT) using only core-hole data. The Radial Basis Function Method (RBF) was used for contouring.

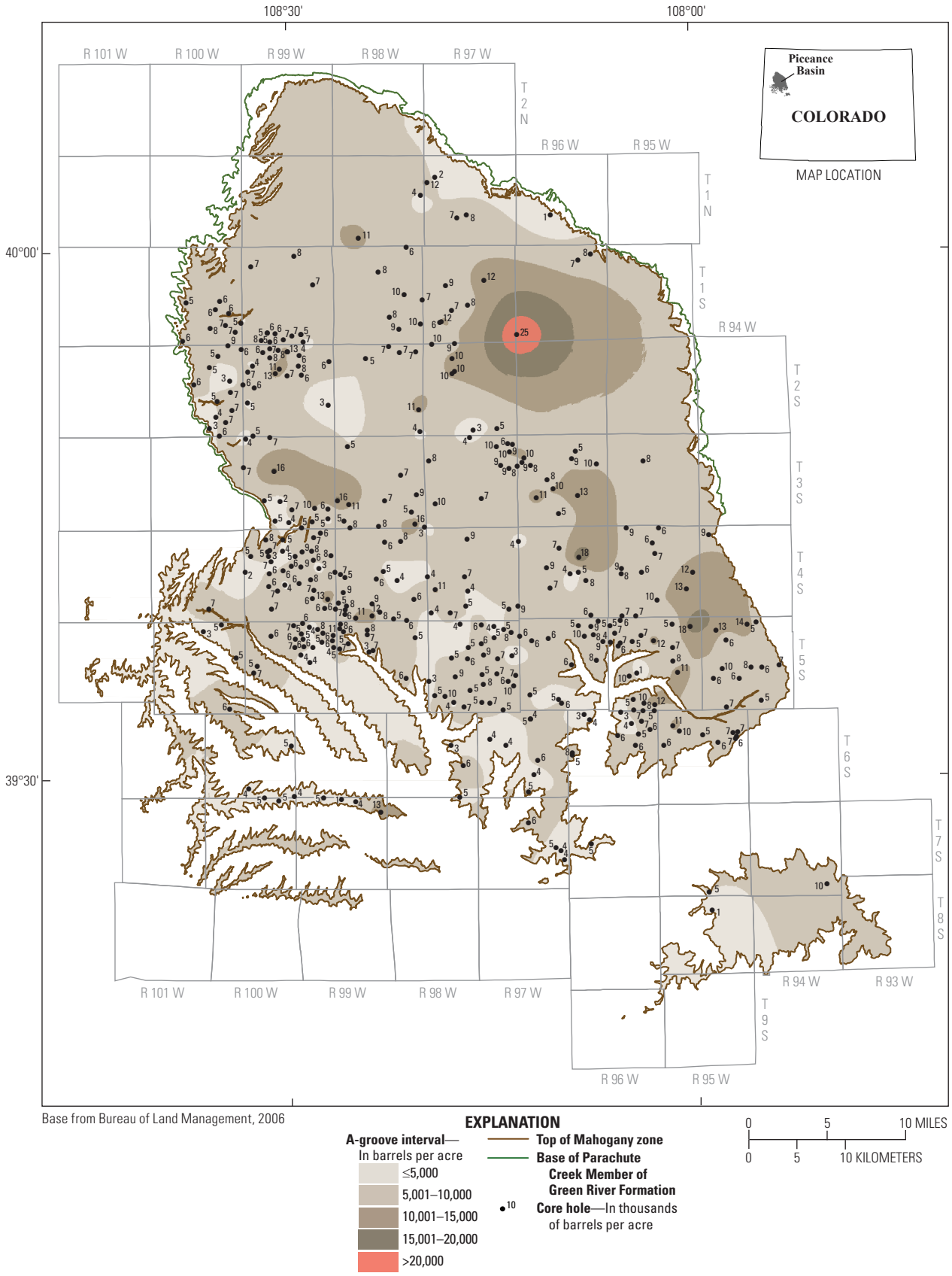

Figure 87. A-groove interval, Piceance Basin, Colo., showing oil yields in barrels per acre (BPA).

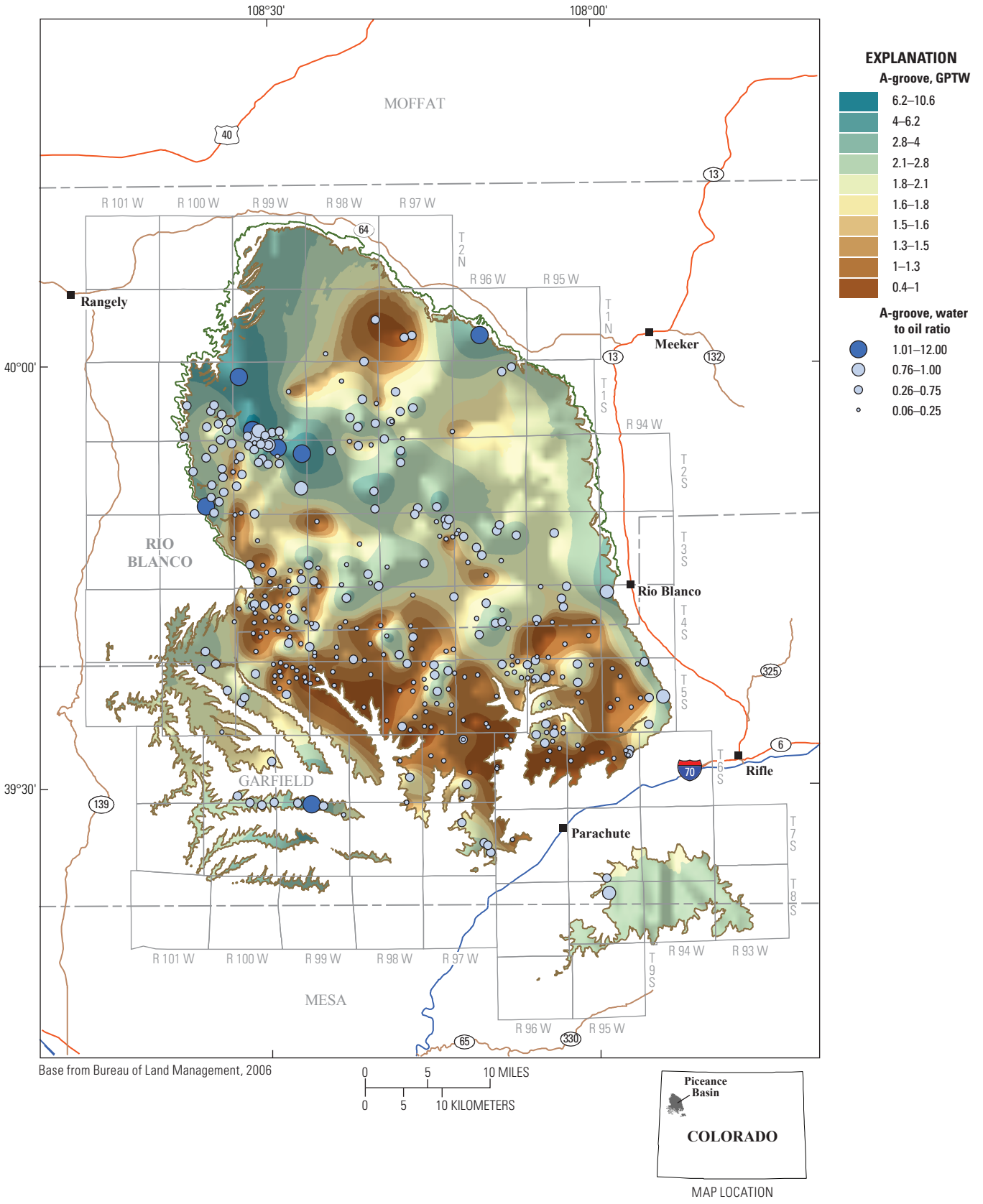

Figure 88. Variation in gallons of water per ton of oil shale (GPTW) for the A-groove interval, Piceance Basin, Colo. A hillshade function was applied to visually enhance displayed contours, creating the illusion that the maps are three dimensional. Bubbles indicate the ratio of water to oil produced for the A-groove interval at each of the control points used.

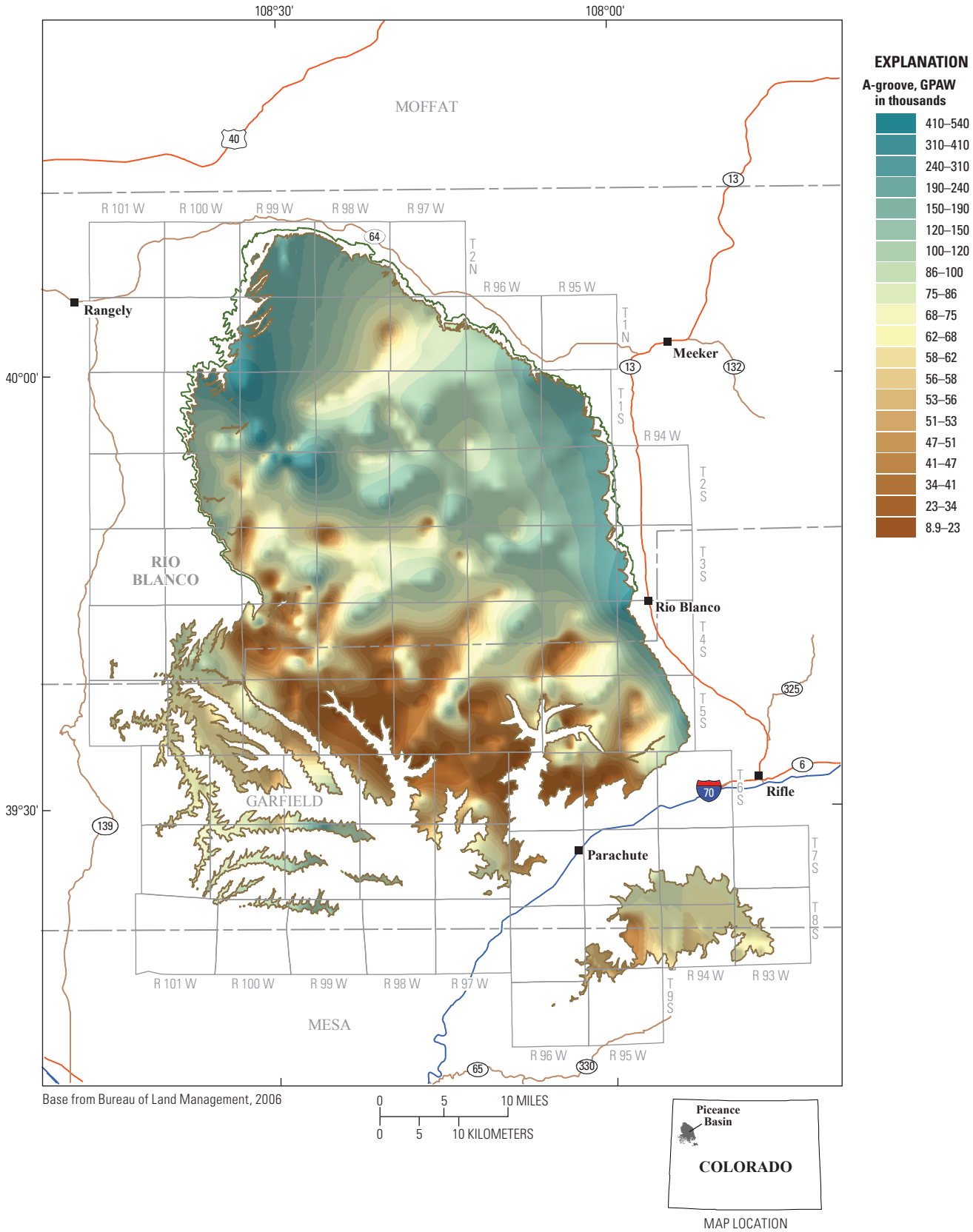

Figure 89. Variations in gallons of water per acre (GPAW) for the A-groove interval, Piceance Basin, Colo. A hillshade function was applied to visually enhance displayed contours, creating the illusion that the maps are three dimensional.

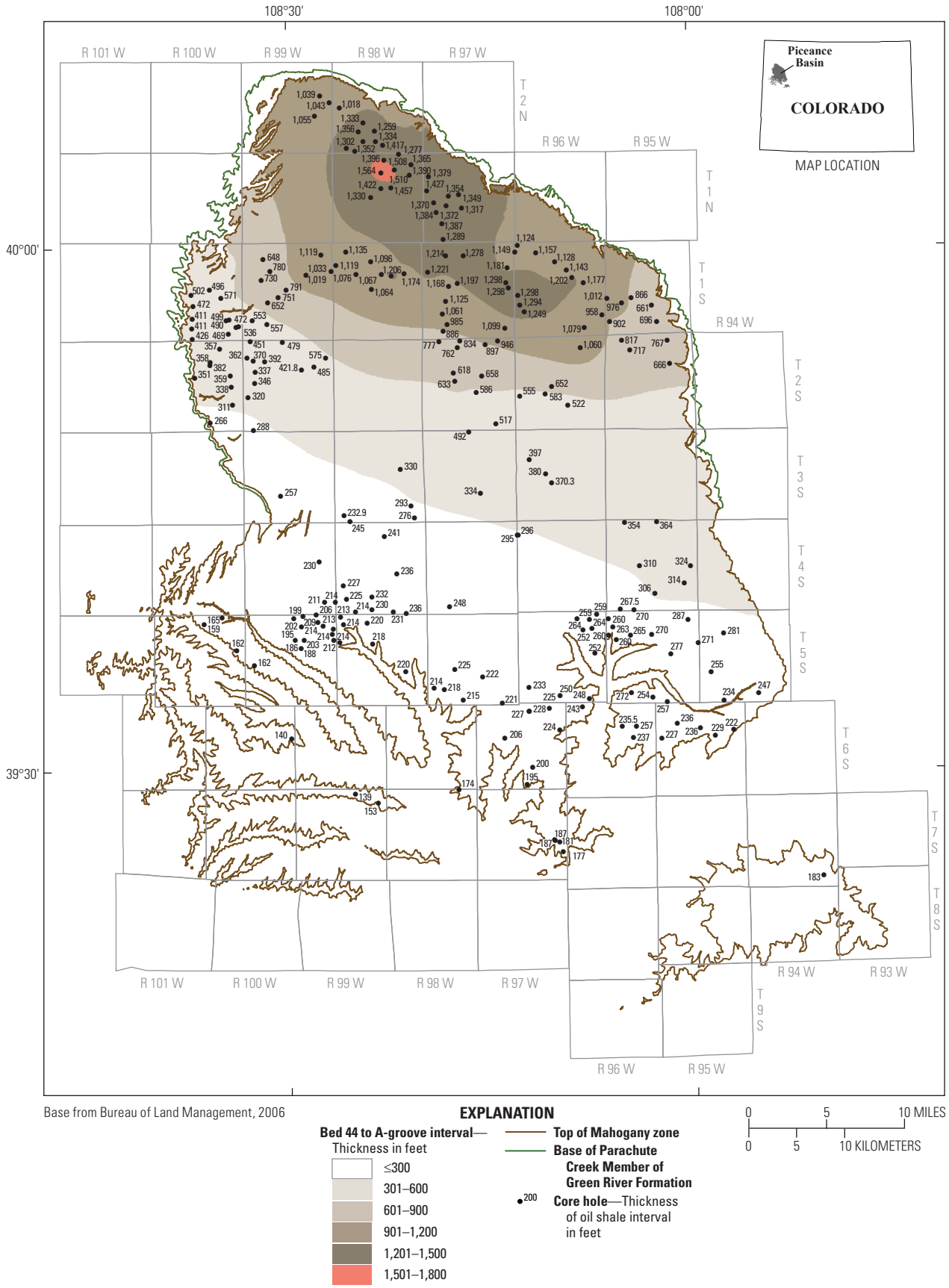

Figure 90. Bed 44 to A-groove interval, Piceance Basin, Colo., using both core-hole and rotary-hole data. The Radial Basis Function Method (RBF) was used for contouring.

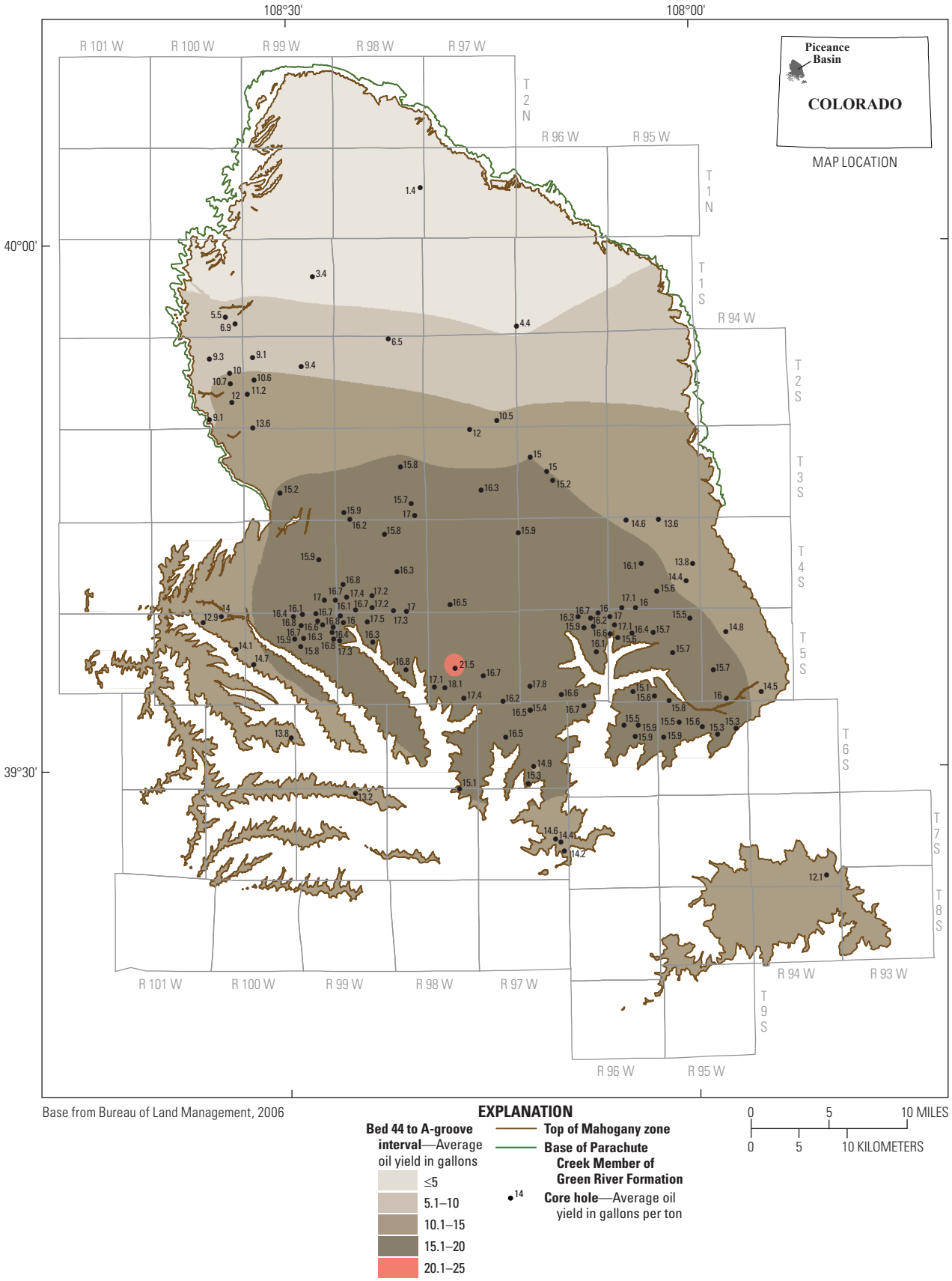

Figure 91. Bed 44 to A-groove interval, Piceance Basin, Colo., showing the oil yield in gallons per ton (GPT), using only core-hole data. The Radial Basis Function Method (RBF) was used to construct the contour map.

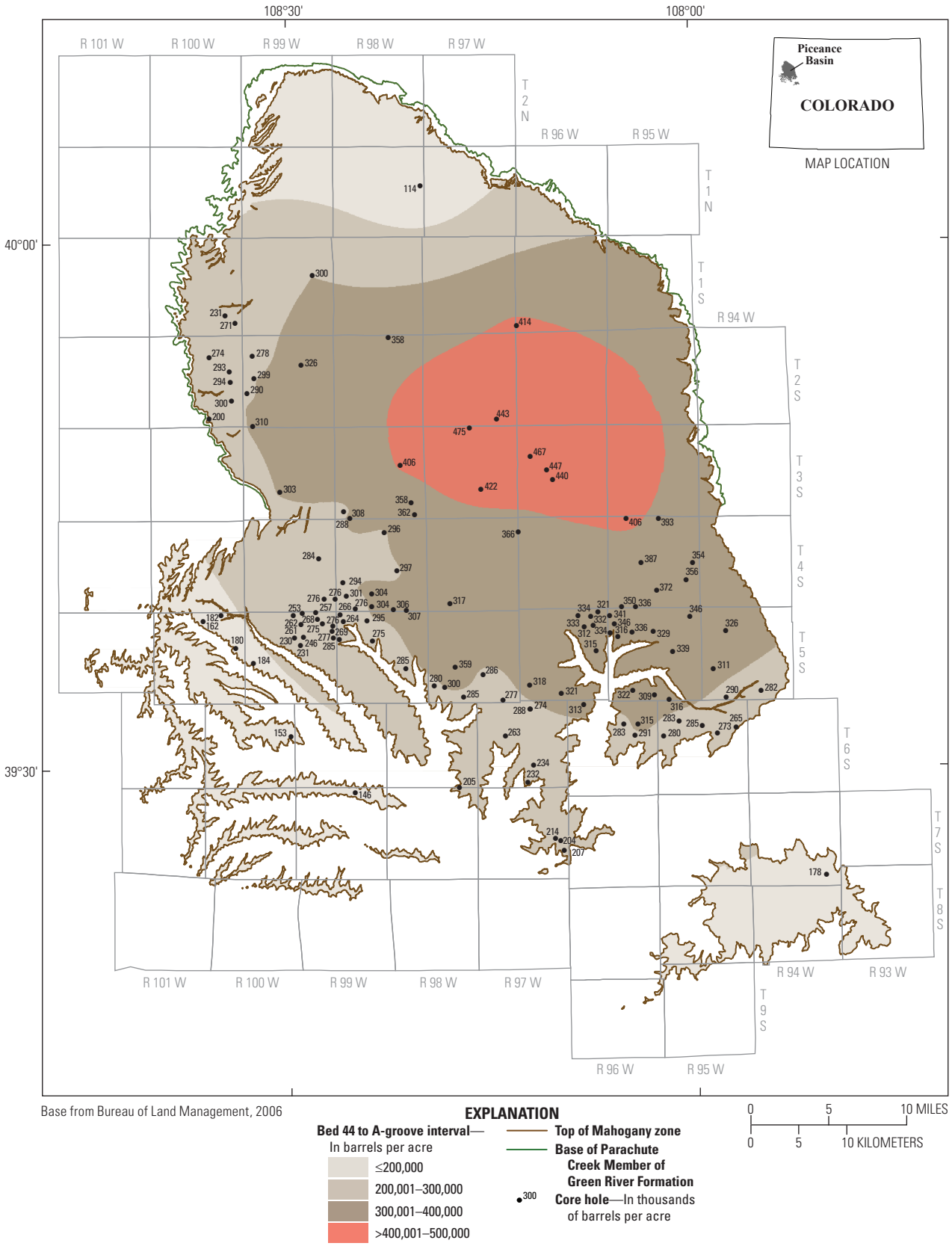

Figure 92. Bed 44 to A-groove interval, Piceance Basin, Colo., showing oil yields in barrels per acre (BPA) using only core-hole data. The Radial Basis Function Method (RBF) was used to construct the map.

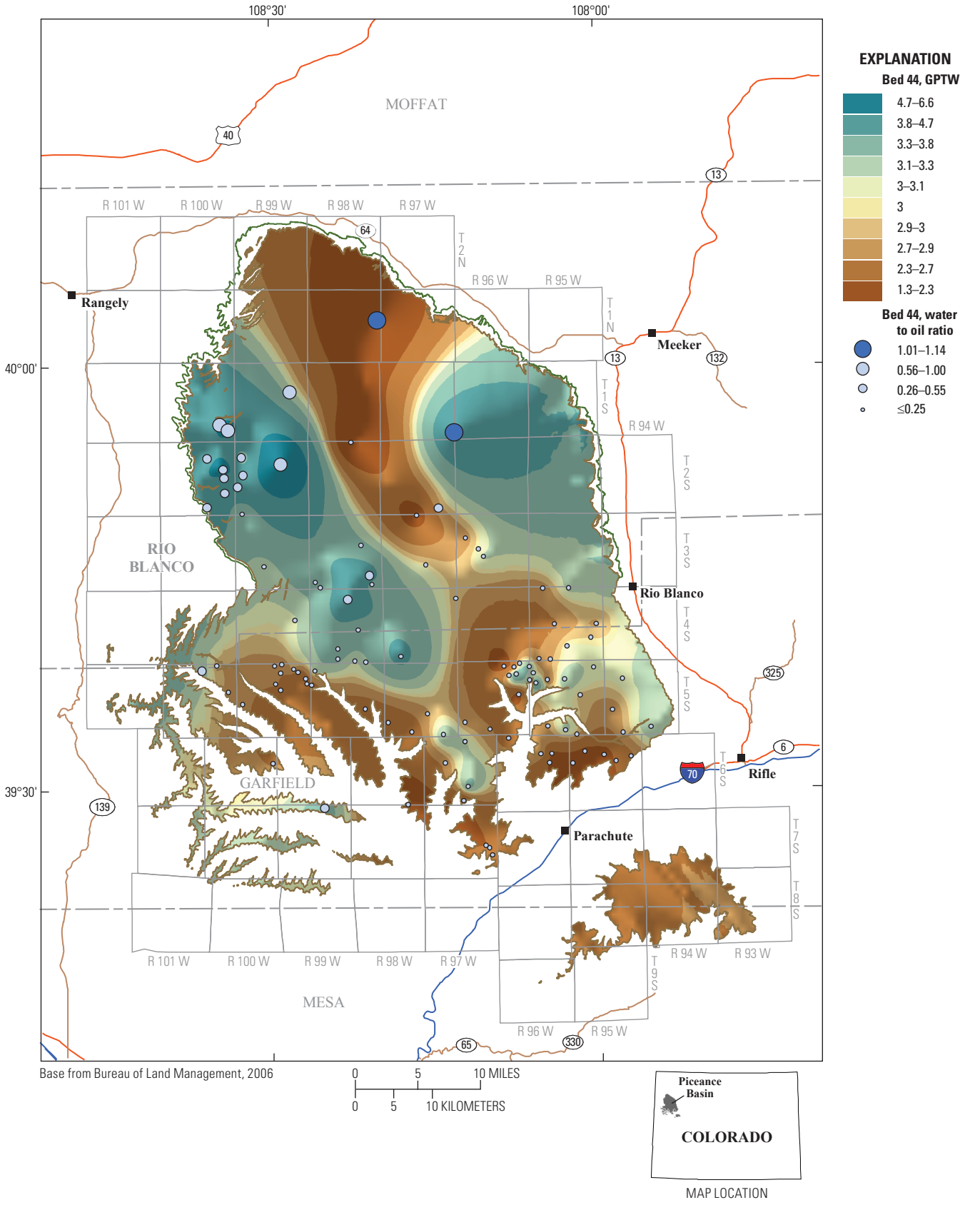

Figure 93. Variation in gallons of water per ton of oil shale (GPTW) for the top of bed 44 to top of A-groove interval, Piceance Basin, Colo. A hillshade function was applied to visually enhance the displayed contours, creating the illusion that the maps are three dimensional. Bubbles indicate the ratio of water to oil produced for the top of bed 44 interval to A-groove interval at each of the control points used.

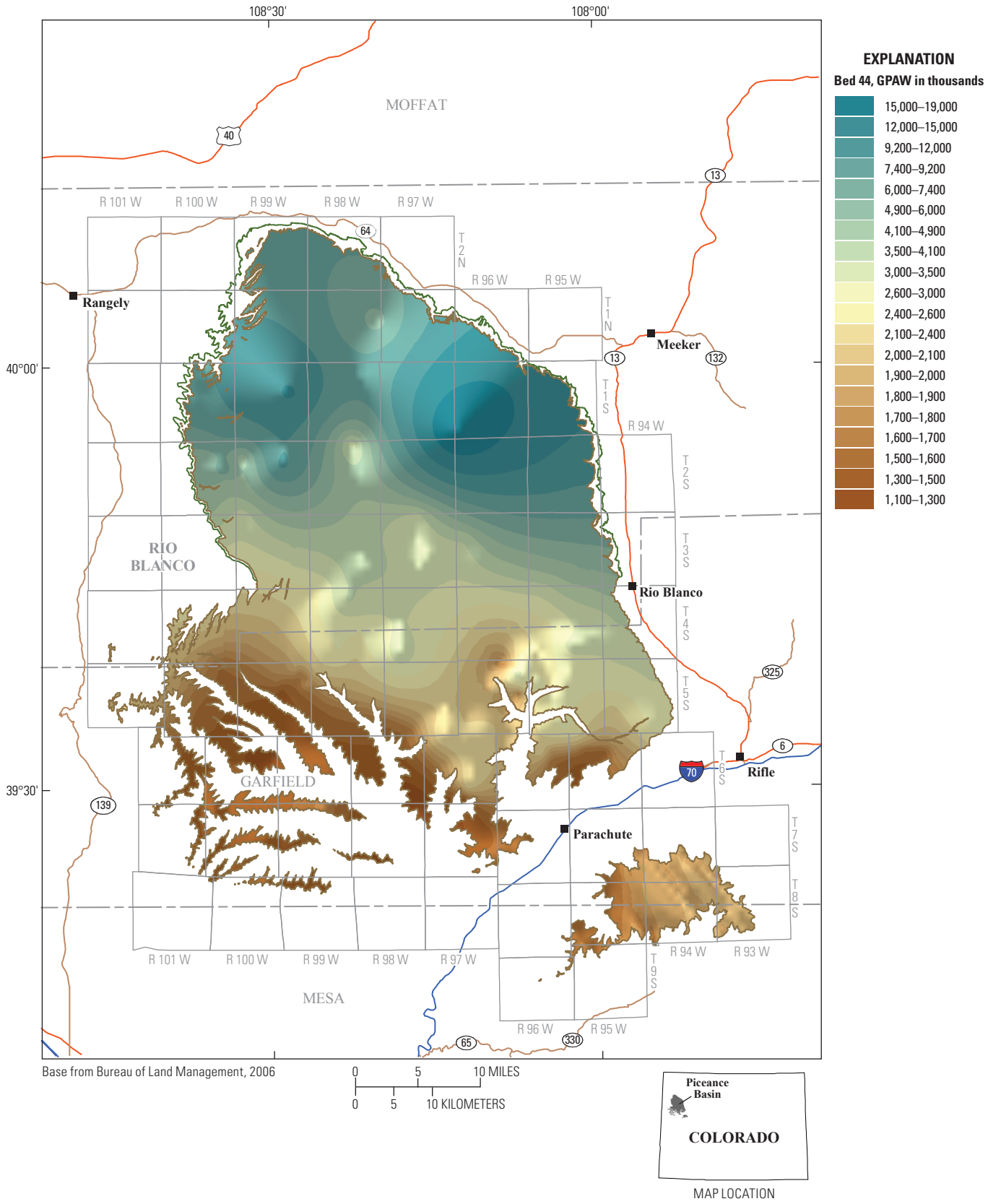

Figure 94. Variations in gallons of water per acre (GPAW) for the top of bed 44 to top of A-groove interval, Piceance Basin, Colo. A hillshade function was applied to visually enhance the displayed contours, creating the illusion that the maps are three dimensional.

Discussion

The maps plotting variations in water content in GPTW and total water in GPAW display complex trends that can be understood only partially at this time due to scarcity of quantitative mineralogical studies of the Green River Formation. Green River oil shale has a complex and highly variable mineralogy. The majority of available studies identifies the major mineral phases present but does not quantify respective amounts of each mineral, and thus we cannot assign percentages of the total measured water to the various water-producing minerals present in the rock. In addition, mineralogy of the various marginal lacustrine facies of the Green River Formation is poorly known. Table 1 lists the overall basin-wide water-to-oil ratios for all 17 oil-shale zones assessed in the basin. With the exception of the L-0 and L-1 zones, which contain very little oil, water-to-oil ratios are significantly less than 1:1, ranging from 0.13:1 for the Mahogany zone to 0.60:1 for the clay-rich R-0 zone. Ratios significantly greater than one locally are found in some marginal areas where oil yields are low, but it is unlikely that those intervals would ever be the target either of above-ground or in situ retorting.

The general decrease in both water content and total water in the illitic interval (R-0 through L-1 zones) toward the structurally deepest part of the basin could have at least two causes, including (1) expulsion of water in illite due to increased burial depth, and (2) dilution of illite due to an increase in kerogen content in that area. Interestingly, for the R-1 zone, both water and kerogen content decrease towards the depocenter (figs. 21 and 23). Total kerogen content in the R-1 zone, in contrast, is highest in an area considerably south of the depocenter, due to pronounced thickening of the R-1 zone in that area combined with relatively high kerogen contents there (fig. 22). A comparison between the isopach map and total water map for the R-1 zone (figs. 20 and 24) indicates that total water is related closely to the thickness of the R-1 zone with total water increasing as the thickness increases, regardless of total kerogen content. The high total kerogen content in the R-1 zone in that area considerably south of the depocenter (fig. 22) is an anomaly that has not yet been explained fully (Johnson and others, 2010). The period when the R-1 zone was deposited was a time of considerable influx of clastic material into the southwestern part of the Piceance Basin from a newly active river system entering the southern part of the Uinta Basin to the west (Johnson, 1985; Johnson and others, 2010).

Nahcolite appears to be the major water-bearing phase in the nahcolite-bearing zones R-2 through L-5 in the saline-mineral depocenter. Brownfield and others (2010) estimated the amount of nahcolite in each of those zones using their nahcolite database. The estimates were used to calculate the amount of water contained in the nahcolite in each zone (table 1). In zones R-2 through L-4, nahcolite occurs as individual nodules or aggregates in oil shale and dispersed within the oil shale. Typically, no attempt is made to separate the nahcolite from the oil shale prior to assessing the sample using Fischer assay, and therefore the amount of water generated with Fischer assay accurately measures the *total* water in the interval. Zones R-5 and L-5, however, contain thick beds of nahcolite and halite that were, as previously mentioned, either not assessed or assessed only partially using Fischer assay. Thus, total water calculated solely from Fischer assay underestimates total water in those two zones. It is therefore not possible to subtract the nahcolite water, calculated from the nahcolite database of Brownfield and others (2010), from total water, calculated from the oil-shale database of Mercier and others (2010), to establish an accurate estimate of water from sources other than nahcolite for those two zones. The calculations that are affected by this problem are shown in red on table 1.

Using the incomplete data in table 1, nahcolite is shown to contribute just 5.51 percent of the total water locked up in the oil-shale interval in the basin. Percentages of water from nahcolite ranges from 1.10 in the R-2 zone to 32.38 for the R-3 zone. These percentages are misleading, however, in that the R-2 through L-5 zones contain nahcolite only in a limited area in the north-central part of the basin, whereas water totals for each zone were calculated to the present-day erosional edge of the basin. The percentages of water from nahcolite for each of the nahcolite-bearing zones within only the saline area would be much higher and would almost certainly be greater than 50 percent for nahcolite-rich zones.

It is unclear if water derived from the breakdown of nahcolite could be used in an oil-shale industry, as nahcolite is a leasable mineral and, under present law, cannot be destroyed or disposed of during the retort process. For conventional mining and above-ground retorting, the nahcolite would simply be removed by water leaching prior to retorting, reconstituted, and sold. For in situ (underground) retorting, nahcolite would have to be solution-mined using hot water prior to retorting or reconstituted at the end of the retort process using water and carbon dioxide. In either case, water in nahcolite likely would not be available for other uses.

The transition from dawsonite to analcime that occurs in the Piceance Creek Member toward the margin of the basin does not noticeably affect the water content (pl. 1). This point is not surprising, as that transition $\{NaAl(CO_3)(OH)_2+SiO_2 \leftrightarrow NaAlSi_2O_6{\cdot}H_2O\}$ does not result in loss of water.

Kerogen in the Piceance Basin also does not appear to be a major source of retort water as Colburn and others (1989) suggested, as there is an extremely poor correlation between oil content and water content for individual core holes. In addition, gallons of water per ton (GPTW) for each of the oil-shale zones generally decreases as gallons per ton of oil increases except in nahcolite-bearing areas. The dilution of water-producing mineral phases by increasing kerogen content in part may explain this trend, but other factors, such as the loss of water from clay minerals towards the deeper, more kerogen-rich part of the basin, probably also play a role.

The ratio of water to oil generated with retorting is significantly less than 1:1 for most areas of the basin and for most stratigraphic intervals, thus water within oil shale can provide only a fraction of the water needed for an oil-shale industry.

Acknowledgments

Krystal Pearson of the U.S. Geological Survey and Wendy Zhou of the Colorado School of Mines reviewed the manuscript and offered many useful comments. Justin Birdwell of the U.S. Geological Survey suggested many publications concerning water in oil shale that proved to be very useful.

References Cited

American Society for Testing Materials [ASTM], 1984, Designation D 388-80, Standard test method for oil from oil shale: West Conshohocken, Pa., Annual Book of ASTM Standards, p. 513–525.

Bartis, J.T., LaTourrette, Tom, Dixon, Lloyd, Peterson, D.J., and Cecchine, Gary, 2005, Oil shale development in the United States—Prospects and policy issues: Santa Monica, Calif., RAND Corporation, ISBN 0-8330-3848-6, 68 p. Also available online (accessed July 25, 2011) at *http://www.rand.org/content/dam/rand/pubs/monographs/2005/RAND_MG414.pdf*.

Beard, T.N., Tait, D.B., and Smith, J.W., 1974, Nahcolite and dawsonite resources in the Green River Formation, Piceance Creek Basin, Colorado, *in* Murray, D. Keith, ed., Guidebook to the Energy Resources of the Piceance Creek Basin, Colorado: Denver, Colo., Rocky Mountain Association of Geologists Field Conference, 25th, p. 101–110.

Boak, J.M., and Mattson, E.D., 2009, Water use for in situ production of oil from oil shale: Oil Shale Symposium, 29th, Golden, Colo., Oct. 19–21, 2009, Colorado School of Mines, abstract and presentation. CD-ROM, unpaginated.

Bradley, W.H., and Eugster, H.P., 1969, Geochemistry and paleolimnology of the trona deposits and associated authigenic minerals of the Green River Formation of Wyoming: U.S. Geological Survey Professional Paper 496–B, 71 p.

Brobst, D.A., and Tucker, J.D., 1973, X-ray mineralogy of the Parachute Creek Member, Green River Formation, in the northern Piceance Creek Basin, Colorado: U.S. Geological Survey Professional Paper 803, 53 p.

Brownfield, M.E., Mercier, T.J., Johnson, R.C., and Self, J.G., 2010, Nahcolite resources in the Green River Formation, Piceance Basin, Colorado: U.S. Geological Survey Digital Data Series DDS–69–Y, chap. 2, 51 p.

Bureau of Land Management, 2006, PLSS township polygons for the Piceance Basin, Colorado: Bureau of Land Management online database.

Cameron, C., Hightower, M., Hoffmann, J., and Wilson, C., 2006, Energy demands on water resources—Report to Congress on the interdependency of energy and water, July 2006: Albuquerque, Sandia National Laboratories, 80 p.

Cashion, W.B., 1973, Geologic and structure map of the Grand Junction Quadrangle, Colorado and Utah: U.S. Geological Survey Miscellaneous Investigations Series Map I–736, scale 1:250,000.

Cashion, W.B., and Donnell, J.R., 1972, Chart showing correlation of selected key units in the organic-rich sequence of the Green River Formation, Piceance Creek Basin, Colorado, and Uinta Basin, Utah: U.S. Geological Survey Oil and Gas Investigations Chart OC–65, one oversized plate.

Chancellor, R.E., Barksdale, W.L., and Dolezal, George, Jr., 1974, Occurrence of oil and gas in the Tertiary system, Rio Blanco unit, Rio Blanco County, Colorado, *in* Murray, D. Keith, ed., Guidebook to the Energy Resources of the Piceance Creek Basin, Colorado: Denver, Colo., Rocky Mountain Association of Geologists Field Conference, 25th, p. 225–233.

Colburn, T.T., Oh, M.S., Crawford, R.W., and Foster, K.G., 1989, Water generation during pyrolysis of oil shales—Sources: Energy and Fuels, vol. 3, chap. 1, p. 216–223.

Crawford, T.A., Sanchez, C.J., and Niemela, D.O., 2009, How does Colorado water rights administration affect oil shale production?: Oil Shale Symposium, 29th, Golden, Colo., Oct. 19–21, 2009, Colorado School of Mines, abstract and presentation. CD-ROM, unpaginated.

Day, R.L., 2009, AMSO's [American Shale Oil Corporation] Colorado oil shale RD&D lease tract—Progress and plans: Oil Shale Symposium, 29th, Golden, Colo., Oct. 19–21, 2009, Colorado School of Mines, abstract and presentation. CD-ROM, unpaginated.

Donnell, J.R., 2008, Intertonguing of the lower part of the Uinta Formation with the upper part of the Green River Formation in the Piceance Creek Basin during the late stages of Lake Uinta: U.S. Geological Survey Scientific Investigation Report 2008–5237, 25 p.

Dyni, J.R., 1974, Stratigraphy and nahcolite resources of the saline facies of the Green River Formation in northwest Colorado, *in* Murray, D. Keith, ed., Guidebook to the Energy Resources of the Piceance Creek Basin, Colorado: Denver, Colo., Rocky Mountain Association of Geologists Field Conference, 25th, p. 111–122.

Dyni, J.R., 1981, Geology of the nahcolite deposits and associated oil shales of the Green River Formation in the Piceance Creek Basin, Colorado: Boulder, University of Colorado, unpublished Ph.D. dissertation, 144 p. Available online at *http://certmapper.cr.usgs.gov/data/oil_shale/Dyni_Thesis_508.pdf*, accessed March 18, 2013.

Dyni, J.R., Hite, R.J., and Raup, O.B., 1970, Lacustrine deposits of bromine-bearing halite, Green River Formation, northwest Colorado, *in* Symposium on Salt, 3rd: Cleveland, Northern Ohio Geological Society, vol. 1, p. 166–180.

Hail, W.J., and Smith, M.C., 1994, Geologic map of the northern part of the Piceance Creek Basin, northwestern Colorado: U.S. Geological Survey Miscellaneous Investigations Series Map I–2400, scale 1:100,000.

Hail, W.J., and Smith, M.C., 1997, Geologic map of the southern part of the Piceance Creek Basin, northwestern Colorado: U.S. Geological Survey Miscellaneous Investigations Series Map I–2529, scale 1:100,000.

Hay, R.L., 1966, Zeolites and zeolitic reactions in sedimentary rocks: Geological Society of America Special Paper 85, 130 p.

Hite, R.J., and Dyni, J.R., 1967, Potential resources of dawsonite and nahcolite in the Piceance Creek Basin, northwest Colorado: Golden, Colo., Colorado School of Mines Quarterly, v. 62, p. 25–38.

Johnson, R.C., 1975, Preliminary geologic map, oil-shale yield histograms and stratigraphic sections, Long Point quadrangle, Garfield County, Colorado: U.S. Geological Survey Miscellaneous Field Studies Map MF–688, scale 1:24,000.

Johnson, R.C., 1981, Stratigraphic evidence for a deep Eocene Lake Uinta, Piceance Creek Basin, Colorado: Geology, v. 9, p. 55–62.

Johnson, R.C., 1985, Early Cenozoic history of the Uinta and Piceance Creek basins, Utah and Colorado, with special reference to the development of Eocene Lake Uinta, *in* Flores, R.M., and Kaplan, S.S., eds., Cenozoic paleogeography of the west-central United States: Rocky Mountain Paleography Symposium, 3rd, 1985, Society of Economic Paleontologists and Mineralogists, Rocky Mountain Section, p. 247–276.

Johnson, R.C., 2007, The outflow of Eocene Lake Gosiute into Lake Uinta and its effects on sedimentation in Lake Uinta in the Piceance Basin of western Colorado: American Association of Petroleum Geologists, Snowbird, Utah, Rocky Mountain Section Meeting, Oct. 7–9, 2007, Meeting Program [abstr.], p. 43.

Johnson, R.C., Nichols, D.J., and Hanley, J.H., 1988, Stratigraphic sections of lower Tertiary strata and charts showing palynomorph and mollusc assemblages, Douglas Creek Arch area, Colorado and Utah: U.S. Geological Survey Miscellaneous Field Investigations Map MF–1997, scale 1:250,000.

Johnson, R.C., and Roberts, L.N., 2003, Depths to selected stratigraphic horizons in oil and gas wells for Upper Cretaceous and Lower Tertiary strata of the Uinta Basin, Utah: U.S. Geological Survey Digital Data Series DDS–69–B, chap. 13, 30 p.

Johnson, R.C., Mercier, T.J., Brownfield, M.E., Pantea, M.P., and Self, J.G., 2010, Assessment of oil shale resources of the Green River Formation, Piceance Basin, Colorado: U.S. Geological Survey Digital Data Series DDS–69–Y, chap. 1, 187 p.

Love, J.D., and Christiansen, A.C., 1985, Geologic map of Wyoming: U.S. Geological Survey and Geological Survey of Wyoming, scale 1:500,000.

Mandarino, J.A., and Back, M.E., 2004, Fleischer's glossary of mineral species 2004: Tucson, The Mineralogical Record, Inc., 309 p.

Mercier, T.J., Brownfield, M.E., and Johnson, R.C., 2010, Methodology for calculating oil shale and nahcolite resources for the Piceance Basin: U.S. Geological Survey Digital Data Series DDS–69–Y, chap. 3, 61 p.

Pipiringos, G.N., and Johnson, R.C., 1976, Preliminary geologic map of the White River City quadrangle, Rio Blanco County, Colorado: U.S. Geological Survey Miscellaneous Field Studies Map MF–736, scale 1:24,000.

Pitman, J.K., 1979, Isopach, structure contour, and resource maps of the R-6 oil shale zone, Green River Formation, Piceance Creek Basin, Colorado: U.S. Geological Survey Miscellaneous Field Investigations Map MF–1069, scale 1:126,720.

Pitman, J.K., and Johnson, R.C., 1978, Isopach, structure contour, and resource maps of the Mahogany oil-shale zone, Green River Formation, Piceance Creek Basin, Colorado: U.S. Geological Survey Miscellaneous Field Investigations Map MF–958, scale 1:126,720.

Pitman, J.K., Pierce, Frances Wahl, and Grundy, W.D., 1989, Thickness, oil-yield, and kriged resource estimates for the Eocene Green River Formation, Piceance Creek Basin, Colorado: U.S. Geological Survey Oil and Gas Investigations, Chart OC–132, 4 p., 6 oversized plates.

Robb, W.A., and Smith, J.W., 1974, Mineral profile of oil shales in Colorado core hole No. 1, Piceance Creek Basin, Colorado, *in* Murray, D. Keith, ed., Guidebook to the Energy Resources of the Piceance Creek Basin, Colorado: Denver, Colo., Rocky Mountain Association of Geologists Field Conference, 25th, p. 81–100.

Rowley, P.D., Hanson, W.R., Tweto, Ogden, and Carrara, P.E., 1985, Geologic map of the Vernal 1-degree × 2-degree quadrangle, Colorado, Utah, and Wyoming: U.S. Geological Survey Miscellaneous Investigations Series Map I–1526, scale 1:250,000.

Ryan, Robert, Patel, Rahul, and Padmasiri, Sudini, 2009, Oil-shale pyrolysis water-treatability study: Oil Shale Symposium, 29th, Golden, Colo., Oct. 19–21, 2009, Colorado School of Mines, abstract and presentation. CD-ROM, unpaginated.

Sheppard, R.L., and Gude, A.J., 3rd, 1968, Distribution and genesis of authigenic silicate minerals in tuffs of Pleistocene Lake Tecopa, Inyo County, California: U.S. Geological Survey Professional Paper 597, 38 p.

Sheppard, R.L., and Gude A.J., 3rd, 1969, Diagenesis of tuffs in the Barstow Formation, Mud Hills, San Bernardino County, California: U.S. Geological Survey Professional Paper 634, 35 p.

Smith, J.W., 1974, Geochemistry of oil-shale genesis in Colorado's Piceance Creek Basin, *in* Murray, D. Keith, ed., Energy Resources of the Piceance Creek Basin, Colorado: Denver, Colo., Rocky Mountain Association of Geologists Field Conference, 25th, p. 71–79.

Southwest Wyoming Province Assessment Team, 2005, Petroleum Systems and Geologic Assessment of Oil and Gas in the Southwestern Wyoming Province, Wyoming, Colorado, and Utah: U.S. Geological Survey Digital Data Series DDS–69–D.

Smith, J.W., and Milton, C., 1966, Dawsonite in the Green River Formation of Colorado: Economic Geology, v. 61, p. 1029–1042.

Stanfield, K.E., Frost, I.C., 1949, Method of assaying oil shale by a modified Fischer retort: U.S. Bureau of Mines Report of Investigation RI–4477, 13 p.

Stanfield, K.E., Rose, C.K., McAuley, W.S., and Tesch, W.J., Jr., 1954, Oil yields of sections of Green River oil shale in Colorado, Utah, and Wyoming, 1945–52: U.S. Bureau of Mines Report of Investigation RI–5081, 153 p.

Tweto, Ogden, 1979, Geologic map of Colorado: U.S. Geological Survey and the Colorado Geological Survey, scale 1:500,000.

Uinta-Piceance Assessment Team, 2003, Petroleum Systems and Geologic Assessment of Oil and Gas in the Uinta-Piceance Province, Utah and Colorado: U.S Geological Survey Digital Data Series DDS–69–B.

Witkind, I.J., 1995, Geologic map of the Price 1-degree × 2-degree quadrangle, Utah: U.S. Geological Survey Miscellaneous Investigations Series Map I–2462, scale 1:250,000.

Young, N.B., and Smith, J.W., 1970, Dawsonite and nahcolite analyses of the Green River Formation oil-shale section, Piceance Creek Basin, Colorado: U.S. Bureau of Mines Report of Investigation RI–7445, 22 p.

Ziemba, E.A., 1974, Oil shale geology, Federal Tract C-a, Rio Blanco County, Colorado, *in* Murray, D. Keith, ed., Guidebook to the Energy Resources of the Piceance Creek Basin, Colorado: Denver, Colo., Rocky Mountain Association of Geologists Field Conference, 25th, p. 123–129.

Publishing support provided by:
Denver Publishing Service Center, Denver, Colorado

For more information concerning this publication, contact:
Center Director, USGS Central Energy Resources Science Center
Science Center
Box 25046, Mail Stop 939
Denver, CO 80225
(303) 236-1647
Or visit the Central Energy Resources Science Center Web site at:
http://energy.usgs.gov/

This publication is available online at:
http://dx.doi.org/10.3133/sir20135241

ISSN 2329-132X (online)
http://dx.doi.org/10.3133/sir20135241